CHARACTERISATIONS THE BIO-ACTIVE COMPOUNDS OF BIO-OIL EXTRACTED FROM RED MERANTI SAWDUST BY FAST PYROLYSIS

NOR WAHIDATUL AZURA BINTI ZAINON NAJIB

DOCTOR OF PHILOSOPHY

UNIVERSITI MALAYSIA PAHANG

UNIVERSITI MALAYSIA PAHANG

DECLARATION OF THESIS AND COPYRIGHT

Author's Full Name : Nor Wahidatul Azura binti Zainon Najib

Date of Birth : 26 September 1981

Title : Characterisations the Bio-active Compounds of Bio-oil Extracted from Red Meranti Sawdust by Fast Pyrolysis

Academic Session : Sem 2 2017/2018

I declare that this thesis is classified as:

☐ CONFIDENTIAL (Contains confidential information under the Official Secret Act 1997)*

☐ RESTRICTED (Contains restricted information as specified by the organization where research was done)*

☑ OPEN ACCESS I agree that my thesis to be published as online open access (Full Text)

I acknowledge that Universiti Malaysia Pahang reserves the following rights:

1. The Thesis is the Property of Universiti Malaysia Pahang
2. The Library of Universiti Malaysia Pahang has the right to make copies of the thesis for the purpose of research only.
3. The Library has the right to make copies of the thesis for academic exchange.

Certified by:

_____   _____
(Student's Signature)   (Supervisor's Signature)

810926-08-6640   Professor Dato' Dr. Zularisam Ab.
New IC/Passport Number   Wahid
Date: 10 August 2018   Name of Supervisor
                                  Date: 10 August 2018

SUPERVISOR'S DECLARATION

We hereby declare that we have checked this thesis and in our opinion, this thesis is adequate in terms of scope and quality for the award of the degree of Doctor of Philosophy.

_____

(Supervisor's Signature)

Full Name   : PROFESSOR DATO' DR. ZULARISAM BIN AB WAHID

Position   : PROFESSOR

Date   : 10 AUGUST 2018

_____

(Co-supervisor's Signature)

Full Name   : PROFESSOR DATIN DR. MIMI SAKINAH BINTI ABDUL
MUNAIM

Position   : PROFESSOR

Date   : 10 AUGUST 2018

STUDENT'S DECLARATION

I hereby declare that the work in this thesis is based on my original work except for quotations and citations which have been duly acknowledged. I also declare that it has not been previously or concurrently submitted for any other degree at Universiti Malaysia Pahang or any other institutions.

_____

(Student's Signature)

Full Name   : Nor Wahidatul Azura binti Zainon Najib

ID Number   : PKE 13003

Date   : August 2018

CHARACTERISATIONS THE BIO-ACTIVE COMPOUNDS OF BIO-OIL EXTRACTED FROM RED MERANTI SAWDUST BY FAST PYROLYSIS

NOR WAHIDATUL AZURA BINTI ZAINON NAJIB

Thesis submitted in fulfillment of the requirements

for the award of the degree of

Doctor of Philosophy

Faculty of Engineering Technology

UNIVERSITI MALAYSIA PAHANG

AUGUST 2018

ACKNOWLEDGEMENTS

ABSTRAK

Pirolisis pantas ialah satu teknologi penukaran habakimia untuk menukar biojisim kepada produk bio-minyak. Dalam kajian ini, habuk meranti merah (RMS) dipilih sebagai biojisim suapan untuk menilai potensinya menghasilkan bio-minyak melalui pirolisis pantas. Kajian ini merangkumi objektif untuk menyiasat kesan parameter proses dalam mengoptimumkan penghasilan bio-minyak dan mencirikan bio-minyak yang diekstrak. Pirolisis cepat dijalankan dalam skala-makmal reaktor lapisan terbendalir, bersama sistem yang terdiri dari pengawal suhu, siklon, pemeluwap, gas nitrogen, meter alir and pengumpul arang dan bio-minyak. Dalam mengkaji kesan keadaan pirolisis, eksperimen dijalankan mengikut pendekatan satu-faktor-pada-satu-masa (OFAT) dengan parameter yng terlibat ialah suhu, kadar alir N_2, masa tahanan dan saiz partikel suapan. Keputusan menunjukkan bio-oil mencapai hasil maksimum sekitar 56.3 % pada suhu 450 °C, kadar alir N_2 25 L/min dan masa tahanan 20 min. untuk saiz partikel suapan 0.3 mm. Dapat disimpulkan bahawa suhu adalah parameter yang paling berpengaruh untuk hasilan bio-minyak. Pencirian fizikokimia bio-minyak menunjukkan bio-minyak tidak sesuai untuk bahan bakar pengangkutan kerana tinggi kandungan oksigen. Melalui analisis spektrometri kromatografi gas (GC-MS), fenolik adalah sebatian dominan yang dikenalpasti dalam bio-minyak. Jumlah gula dalam bio-minyak ialah 12.82 % luas termasuk hasil levoglucosan adalah 8.97 % luas. Dalam menentukan kesan rawatan basuhan biojisim, RMS dibasuh dengan air dinyahion (DI) atau asid hidroklorik (HCl) cair. Kecekapan penyingkiran AAEM dengan air DI, 1.0M HCl dan 2.0 M HCl adalah 66.39%, 93.32% dan 97.28%, masing-masing. Dari analisis FTIR, rawatan basuhan telah menguatkan ikatan kimia RMS. Untuk pengeluaran bio-minyak, bio-minyak yang diekstrak dari RMS - air DI mencapai hasil maksimum kira-kira 57.2 % pada 450 °C suhu optimum. Dalam bio-minyak yang diekstrak, RMS yang dibasuh menghasilkan lebih banyak kompaun berat dan lebih banyak levoglucosan daripada RMS mentah. Dalam kajian pyrolysis RMS yang diresapi, RMS diresapkan dengan $CaCl_2$, $CaSO_4$, $FeCl_2$ atau $FeSO_4$. Antara suapan ini, RMS - $FeSO_4$ meningkatkan proses penguraian pada suhu yang lebih rendah dengan suhu penguraian maksimum telah beralih dari 361 °C bagi RMS kawalan kepada 314 °C bagi RMS - $FeSO_4$. Melalui FTIR, resapan RMS dengan $FeSO_4$ telah melemahkan ikatan kimia dalam RMS. Dalam bio-minyak yang diekstrak, ia mengandungi sebatian berat molekul berjulat besar dan menunjukkan peningkatan dalam hasil levoglucosan. Levoglucosan adalah tertinggi dalam RMS - $FeSO_4$ iaitu 40.23 % luas, dengan hasil gula sebanyak 42.24 % luas. Dalam mengoptimumkan hasil bio-minyak, rekabentuk komposit pusat (CCD) daripada kaedah pemodelan permukaan respon (RSM) digunakan untuk membangunkan model matematik dan mengoptimumkan parameter proses. Melalui model yang diramalkan, keputusan menunjukkan keadaan proses pirolysis optimum diperoleh pada suhu 480 °C, 25 L/min kadar aliran N_2 dan 24 min masa tahanan dengan 56.5 % hasil bio-minyak dan 2.11 % ralat oleh eksperimen. Kesimpulannya, RMS mempunyai potensi untuk menghasilkan bio-minyak. Dengan rawatan lanjut ke atas bio-oil untuk menyingkirkan kandungan oksigen, bio-minyak ini boleh digunakan untuk menggantikan bahan api konvensional. Rawatan terapi RMS dengan $FeSO_4$ mendedahkan bahawa proses penguraian dapat ditingkatkan pada suhu yang lebih rendah dan meningkatkan levoglucosan dalam bio-minyak. Penemuan-penemuan ini dijangka menyediakan beberapa garis panduan dalam kajian masa depan untuk menghasilkan produk tambah nilai dari sisa lignoselulosa yang lain dan seterusnya, konsep kerajaan untuk mengalihkan sisa kepada produk-kekayaan dapat dicapai.

ABSTRACT

Fast pyrolysis is a thermochemical conversion technology to convert biomass into bio-oil product. In this study, red meranti sawdust (RMS) was selected as biomass as feedstock to evaluate its potential to produce bio-oil by fast pyrolysis. The study covers the objective to investigate the parameters effect of process in optimising the bio-oil production and characterise the extracted bio-oil. Fast pyrolysis process was conducted in a bench-scale fluidized bed reactor, with the system consist of temperature controller, cyclone, condensers, nitrogen gas, flow meter, char and bio-oil collectors. In investigating the effect of pyrolysis condition, the experiments were run according to one-factor-at-a-time (OFAT) approach with the parameters involved were temperature, N_2 flow rate, retention time and feed particles size. Results showed that bio-oil achieved maximum yield about 56.3 % at 450 °C of temperature, 25 L/min of N_2 flow rate and 20 min of retention time for 0.3 mm of feed particles size. It can be concluded that the temperature was the most influential parameter for bio-oil yield. Physicochemical characterisation of bio-oil indicated bio-oil not suitable for transportation fuel due to high oxygen content. Through gas chromatography–mass spectrometry (GC-MS) analysis, phenolic was the dominant compound identified in bio-oil. Total sugars in bio-oil was 12.82 % area including levoglucosan yield was 8.97 % area. In determining the effect of washing treatment, RMS was washed with deionised (DI) water or diluted hydrochloric (HCl) acid. The efficiency of AAEM removal by DI water, 1.0M HCl and 2.0 M HCl were 66.39 %, 93.32 %, and 97.28 %, respectively. From FTIR analysis, washing treatment had strengthened the RMS chemical bonds. For bio-oil production, bio-oil extracted from RMS - DI water achieved maximum yield about 57.2 % at 450 °C of optimum temperature. In extracted bio-oil, washed RMS produced higher heavier compound and higher levoglucosan than raw RMS. In pyrolysis of impregnated RMS study, RMS was impregnated with $CaCl_2$, $CaSO_4$, $FeCl_2$ or $FeSO_4$. Among these feedstocks, RMS - $FeSO_4$ enhanced the degradation process at lower temperatures with the maximum degradation of temperature has been shifted from 361 °C for RMS control to 314 °C for RMS - $FeSO_4$. Through FTIR analysis, impregnated RMS with $FeSO_4$ has weakened the RMS chemical bond. In extracted bio-oil, it consisted large range of molecular weight compounds and showed an increasing in levoglucosan yield. Levoglucosan was the highest in RMS - $FeSO_4$ about 40.23 % area, with 42.24 % area of total anhydrosugars yield. In optimising bio-oil yield, central composite design (CCD) of response surface methodology (RSM) modelling was employed to develop mathematical model and optimise the process parameters. Through predicted model, results showed that the optimal pyrolysis process condition was obtained at 480 °C of temperature, 25 L/min of N_2 flow rate and 24 min of retention time with 56.5 % of bio-oil yield and 2.11 % of error by experiment. Conclusion, RMS has a potential to produce bio-oil. With further treatment on bio-oil to remove oxygen content, this bio-oil can be applied to substitute conventional fuel. Impregnated treatment of RMS with $FeSO_4$ reveals degradation process can be enhanced at lower temperature and increases levoglucosan in bio-oil. These findings are expected to provide some guidelines in future study to produce value-added product from other lignocellulose waste and further, the government concept of divert waste to wealth-product can be achieved.

TABLE OF CONTENT

LIST OF TABLES

LIST OF FIGURES

LIST OF SYMBOLS

°C	degree Celsius
°C/s	degree Celsius per Second
cSt	centistokes
g/mol	gram/mol
kJ/kg	Kilojoule/kilogram
L/min	Litre per minute
m^3	cubic meter
min	minute
mL	mililitre
mm	millimetre
MJ/kg	Megajoule/kilogram
Mtoe	Million tons of oil equivalent
rpm	Rotation per Minute
wt. %	percentage by weight
W/mK	Watts per meter Kelvin
µm	micrometre
Y_b	bio-oil yield

LIST OF ABBREVIATIONS

AAEM	Alkali and Alkaline Earth Metal
ASEAN	Association of Southeast Asian Nations
ASTM	American Society for Testing and Materials
BC	Bio-oil Collector
C	Carbon
Ca	Calcium
$CaCl_2$	Calcium Chloride
$CaSO_4$	Calcium Sulphate
CC	Char Collector
CCD	Central Composite Design
CO	Carbon Monoxide
CO_2	Carbon Dioxide
DI	Deionised
DTG	Differential Thermogravimetric
ENSYN	Renewable Fuels and Chemical from Non-Food Biomass
$FeCl_2$	Iron (II) Chloride
$FeSO_4$	Iron (II) Sulphate
FTeK	Fakulti Teknologi Kejuruteraan
FTIR	Fourier Transform Infrared Spectroscopy
GC-MS	Gas Chromatography – Mass Spectrometry
H^+	Hydrogen Ion
H_2	Hydrogen Gas
H_2O	Water
HAA	Hydroxyacetaldehyde
HCl	Hydrochloride Acid
HHV	Higher Heating Value
ICP-OES	Inductively Coupled Plasma – Optical Emission Spectroscopy
K	Potassium
LHV	Lower heating value
Mg	Magnesium
N_2	Nitrogen Gas
Na	Sodium
NCG	Non-Condensable Gases
NO_x	Nitric Oxide and Nitrogen Dioxide

NREL	National Renewable Energy Laboratory
O	Oxygen
OFAT	One Factor at a Time
PAH	Polycyclic Aromatic Hydrocarbon
pH	Potential of Hydrogen
RMS	Red Meranti Sawdust
RSM	Response Surface Methodology
TGA	Thermogravimetric Analysis
UMP	Universiti Malaysia Pahang
Zn	Zink
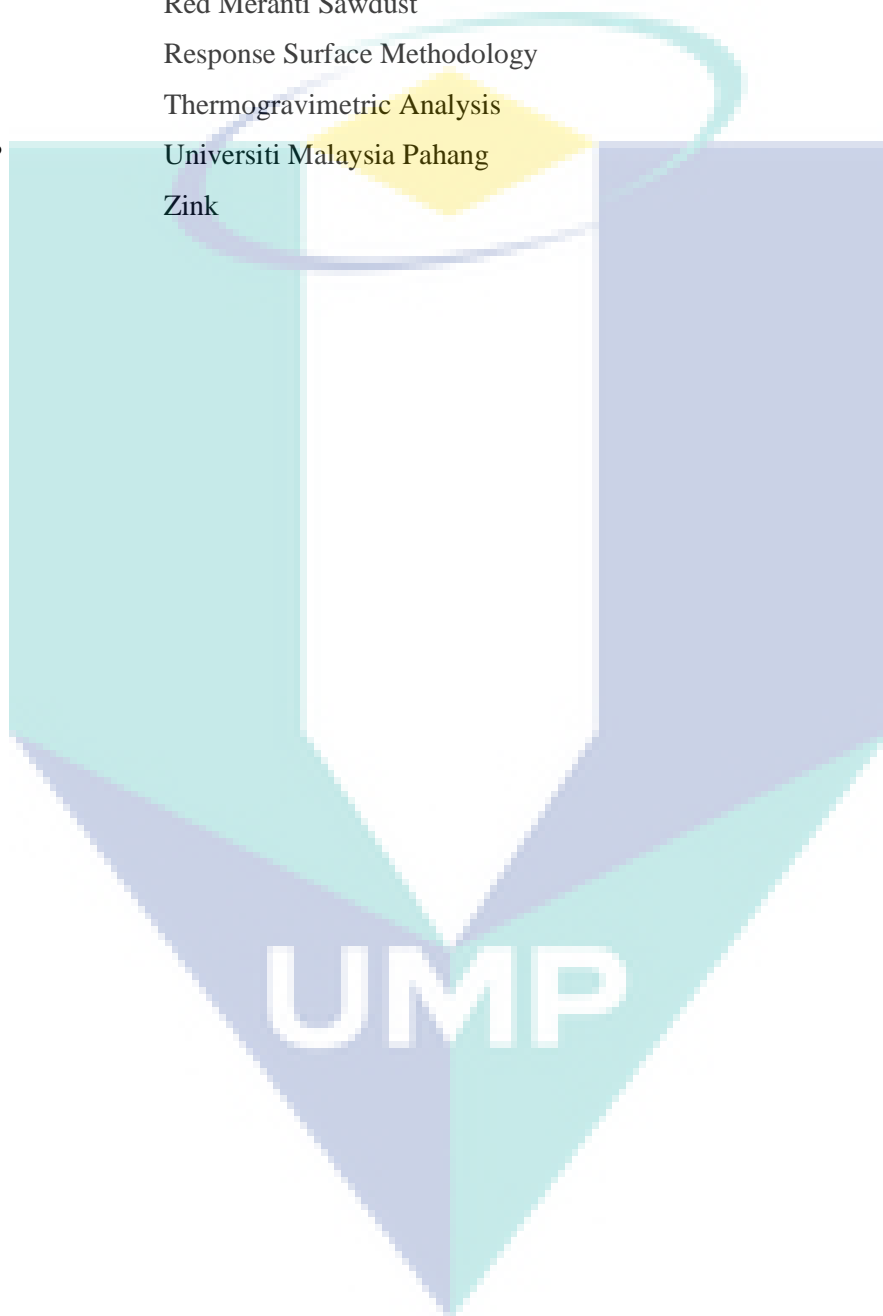
CHAPTER 1

INTRODUCTION

1.1 Introduction

This chapter briefly introduces about the emergence of bio-fuel as renewable energy, identification of the problem related to the production of bio-oil from lignocellulose biomass by fast pyrolysis process and the objective studies involved in this research. Scope and significant studies related to this research also is included in this chapter.

1.1.1 The Emergence of Biofuel

Since 1970s, global energy crisis has begun due to the shortages of petroleum resources. This issue is getting worse due to rapid increase in world's population, industrialization and motorization which lead to a steep rise of petroleum fuel demand. According to Mofijur, Masjuki, Kalam, Hazrat, Liaquat, Shahabuddin and Varman, (2012), the global primary fuel consumption in 1980 was 6,630 million tonnes of oil equivalent (Mtoe) which grown almost double in 2010 with the consumption was 12,004.4 Mtoe. Based on the estimation done by International Energy Agency, the global energy consumption is foreseen to increase about 53 % in 2030 (Ong, Mahlia & Masjuki, 2011). Therefore, other renewable fossil fuel-derived should be revealed as a backup energy and this scenario develops a new interest in exploring new alternative energy sources. Furthermore, issue on environmental concerns also increase which lead to the research and development of new resources for fossil fuel substitution. Fossil fuel is regards as a major contribution on greenhouse gas emission, which leads to numerous adverse effects including climate change (Nigam & Singh, 2011).

The increase of these major issues have led to a move towards alternative, renewable, sustainable, efficient and cost effective energy sources with lesser gases emissions (Nigam & Singh, 2011). Among alternative energy that has been studied and developed, biofuel, hydrogen, natural gas and syngas have emerged as the four strategically important sustainable fuel sources. Within these four, biofuel is the most environmentally friendly energy source (Nigam & Singh, 2011) and has been recognized as major world renewable energy sources to support the declining of fossil fuel resources (Isahak, Hisham, Yarmo & Yun Hin, 2012). Apart of these points, biofuel is derived from biomass, and biomass energy sources are recognised having most similar end products characteristics to that fossil fuel-derived products (Mekhilef, Saidur, Safari & Mustaffa, 2011). Figure 1.1 shows the similarity of both petroleum and biomass end products, and comparison routes of technology for end-products production.
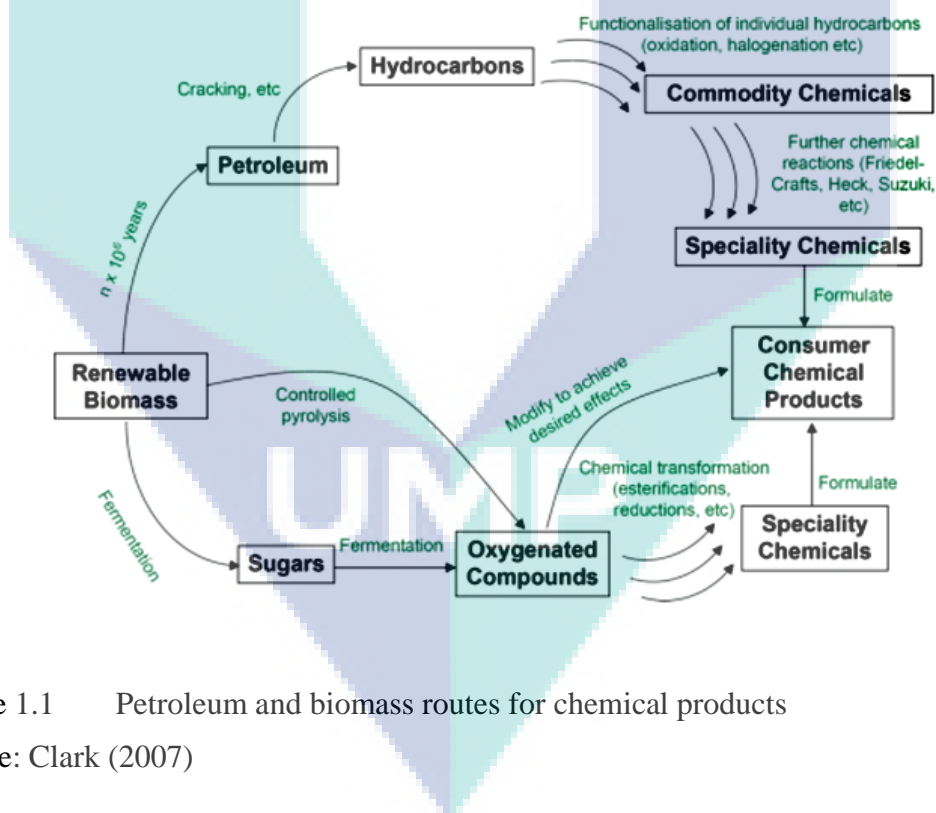
Figure 1.1   Petroleum and biomass routes for chemical products
Source: Clark (2007)

As compared to fossil fuel, biofuel energy has a great potential due to its advantages as sustainable energy sources on resources biodegradability, universality and reproducibility (with a potential to provide 11 %) of the world's total primary energy supplies (Ong et al., 2011), as well as, promising with the environmental protection

(Zhang, Liu, Yin & Mei, 2013) and preservation by emitting acceptable quality exhaust gases with CO_2 are nearly neutral (Ortega, Renehan, Liberatore & Herring, 2011).

There are four classes of biofuel resources, as listed in Table 1.1. At present, second generation biofuel has emerged a great interest and is seen as a sustainable energy resources since the source of biomass such as plant forestry, plant residue, agriculture residue etcetera, representing the most abundant and underutilised biological resources as compared to resources of both first and third generation bio-fuels (Naik, Goud, Rout & Dalai, 2010).

Though so, it appears in literature (Nigam & Singh, 2011) that the process of second generation biomass conversion to biofuel requires sophisticated equipment for bio-refineries, involves complex conversion processes for different type and composition of biomass, and long-time needed for the conversion, which all these barriers incur high capital cost. In spite of that, as stated by Larson (2008), it is believed that basic characteristics of feedstock hold potential for lower cost, and significant energy and environmental benefits for the second generation biofuel. Thus, to achieve the potential energy and economic outcome, lots of studies and researches is still been carried out, and working on the development, globally, in order to improve the processes and technologies of conversion biomass to biofuel.

With regards to this point, this research has been conducted to provide some input related to renewable energy of second generation biofuel with focussing on the bio-oil production via fast pyrolysis process of thermo-chemical approach. Studied biomass in this research is red meranti wood, one of native plant species in Southeast Asia.

Table 1.1   Biofuels classification

Classification	Primary	Secondary		
		First generation	Second generation	Third generation
Substrate or feedstock	Natural and unprocessed biomass such as fire wood, wood chips and pellets.	Vegetable oils, seeds, grains or sugars.	Non-edible sources, lignocellulose biomass.	Algae, sea weeds.
Product	Cooking fuel Heating and electricity production for industrial application.	Bioethanol or butanol by fermentation of starch (wheat, barley, corn, potato) or sugars (sugar cane, sugar beet etc.). Biodiesel by transesterification of plant oils (rapeseed, soybeans, sunflower, palm, coconut etc.).	Bioethanol or butanol by enzymatic hydrolysis. Methanol, Fisher-Tropsch gasoline and diesel, mixed alcohol, dimethyl ether and green diesel by thermo-chemical processes. Biomethane by anaerobic digestion.	Biodiesel from algae. Bioethanol from algae and sea weeds. Hydrogen from green algae and microbes.
Advantage	Directly combusted.	Biodegradable. Environmentally friendly. Energy security	No food competition. Environmentally friendly. Production of high value-added product. Energy security. Feedstock can be planted specifically for energy purpose – enabling higher production per unit land area-increase land efficiency.	High oil (biodiesel) yield. No food and land competition. No toxic content. Energy security.
Disadvantage		Limited feedstock with high production cost due to competition with food. Utilisation only small fraction of biomass reduces land use efficiency. Blended partly with conventional fuel. Highest carbon footprint compared with other generations of biofuel.	Requires complex processes. Requires more sophisticated equipment – incurred high cost of conversion technology. Still under development to reduce cost of conversion – need further research.	High processing cost. Production technology is under development. Difficult to harvest and process.

Source: Nigam and Singh (2011), Naik et al. (2010) and Liew, Hassim and Ng (2014)

1.1.2   Lignocellulose Biomass Production and Conversion in Malaysia

Being a major agriculture and forestry commodity producer amongst the ASEAN countries, Malaysia is well positioned to promote the use of biomass as renewable energy resources (Zafar, 2015). In 2009, Malaysia produces at least 168 million tons of lignocellulose biomass residue annually (Zafar, 2011), generated from agriculture wastes, forest residues and municipal solid wastes (Goh, Tan, Lee & Bhatia, 2010). Therefore, it is crucially important to exploit the wastes by converting it to biofuel energy and to preserve the environment by diverting biomass from waste disposal, as well as, lessen the adverse effect due to greenhouse gas emission resulted by conventional fuel. Table 1.2 shows the biomass residues generated for every sector in Malaysia.

Table 1.2   Quantity of lignocellulosic biomass produced in Malaysia in 2007

Type	Source	Source (Ktonnes)	Quantity (Ktonnes)	MC (wt. %)	DW (Ktonnes)
Agriculture waste:					
Oil palm fronds			46,837	60.0	18, 735
EPFB			18,022	65.0	6,308
Oil palm fibers	Oil palm FFB	81,920	11,059	42.0	6,414
Oil palm shells			4,506	7.0	4,190
Oil palm trunks			10,827	75.9	2,609
Paddy straw	Replanting paddy	-	880	11.0	783
Rice husk		2375	484	9.0	440
Banana residues	Banana	265	530	10.7	473
Sugarcane bagasse	Sugarcane	730	234	50.0	117
Coconut husk	Coconut	505	171	11.5	151
Pineapple waste	Pineapple industries	69	48	61.2	19
Forest residues:					
Logging residues	Logs	2649	2649	12.0	2,331
Playwood residues	Plywood	2492	2492	12.0	2,193
Sawmill residues	Sawn timber	1418	1160	12.0	1,021
Municipal solid waste:	MSW	6744	4653	57.5	1,978

Source: Mekhilef et al. (2011)

Although Malaysia has adopted the concept of waste-to-wealth since late 1990 (Mekhilef, et al., 2011), the energy potential of lignocellulose biomass is still yet to be exploited properly in the country and it is estimated about 75.5 % of potential biomass is wasted (The Japan Institute of Energy, 2010). Forestry industries contribute to second

largest biomass waste producer in Malaysia after palm oil industries. This waste has a huge renewable energy potential to be exploited, in which however, only 60 – 65 % of the residues have been harvested for energy ("Malaysia Energy Centre," 2002) and remaining is left to rot or burned as waste (Mekhilef et al., 2011).

In Malaysia, currently, the study of liquid biofuel production from palm oil biomass residue induce widespread attention among researchers, since this residue is abundantly available as compared to other types of biomass wastes. Although forestry industries generate second largest lignocellulose biomass wastes, the comprehensive study on forestry wastes conversion into biofuel is still getting less attention and purely reported, especially related to bio-oil production from particular wood biomass using fast pyrolysis technology. Therefore, this study was conducted to gain and disseminate some knowledge regarding conversion of red meranti wood as biomass feedstock in fast pyrolysis process in evaluating its potential to produce bio-oil.

1.1.3 Red Meranti Wood

Red meranti is meranti wood typed, light hardwood with scientific name is *Shorea Curtisii*. Red meranti is a large tree native to Southeast Asia, which commonly found from Northern India to Malaysia, Indonesia and Philippines (Eric Meier, 2015). In Malaysia, red meranti is one of the most popular timber as it is perfect for producing any light duty wooden products ("Timber Wood Supply," 2017).

In this study, red meranti was chosen because red meranti is one of the most abundant forestry waste generated in Malaysia, in which, its potential is still not fully exploited for the purpose of energy recovery (The Japan Institute of Energy, 2010). Red meranti is a lignocellulosic biomass, chemically composed of cellulose, hemicellulose and lignin components with small amount of extractive. Based on its nature as lignocellulosic biomass, red meranti has a great potential to be transformed into energy dense-components for use as fuels or chemicals via conversion technologies (Nanda, Kozinski & Dalai, 2016).

In general, liquid biofuel is produced by two fundamentally different processes, either by bio-chemical or thermo-chemical processing of biomass with the route of conversion is shown in Figure 1.2. Since the purpose of this study is to produce bio-oil, there are two possible conversion technologies considered; (i) pyrolysis, and (ii)

liquefaction. Comparing these two processes, pyrolysis process is more favourable by considering the process can be carried out at atmospheric pressure (0.1 – 0.5 MPa) as compared to liquefaction (5 – 20 MPa) (Demirbaş, 2000) which requires higher operating cost (Nanda et al., 2016). Thus, the pyrolysis process, specifically fast pyrolysis was selected and considered as a good method for converting red meranti wood to valuable products, namely bio-oil.
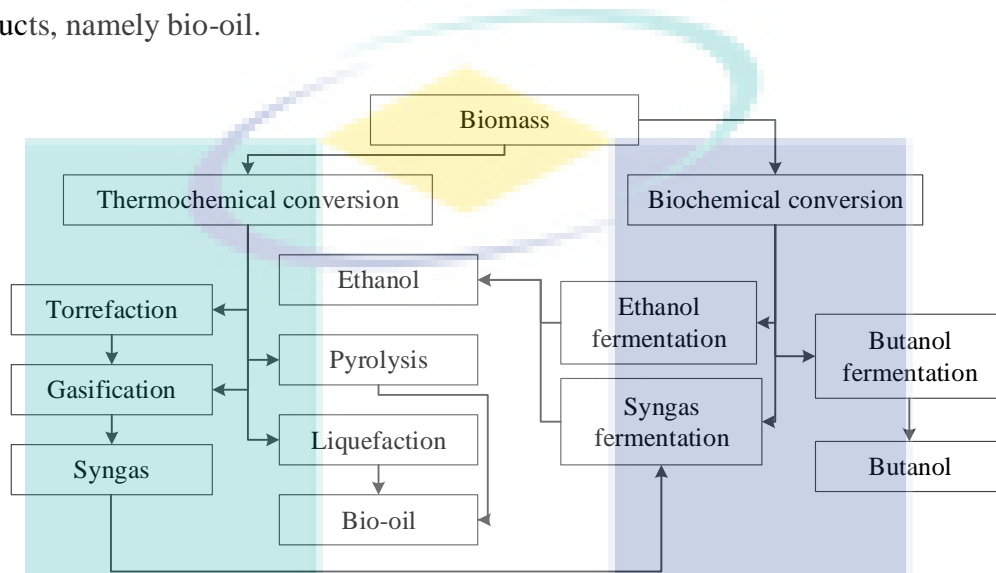
Figure 1.2   Thermochemical and biochemical conversion of lignocellulosic biomass
Source: Nanda et al. (2016)

1.2   Problem Statement

Fast pyrolysis process is a thermochemical process technology to convert biomass into liquid bio-oil as a main product, with solid and non-condensable gases (NCG) as the by-products. Numerous pyrolysis studies have been conducted to various types of biomass in different pyrolysis reactors with concern to optimise the production of bio-oil. Among of these biomass, the utilisation of red meranti as feedstock is rarely reported, unless the study investigated by Mazlan, Uemura, Osman and Yusup (2015). Mazlan et al. carried out the pyrolysis study of meranti wood sawdust and rubber wood sawdust in fixed bed drop-type pyrolyser. Their scope of study covered investigating the effect of temperature and biomass type on the properties of pyrolysis product. However, for optimisation of bio-oil production, beside temperature, there is a need to investigate and optimise the whole influential parameter process including N_2 flow rate, feed particles size and retention time of biomass in pyrolysis reactor. In addition, the characteristic and suitability of bio-oil produced from red meranti wood as transportation fuel never been reported. Therefore, this study is conducted and limited to evaluate the effect of these

above-mentioned pyrolysis process parameters to bio-oil production and characterise bio-oil produced in term of chemical composition and compound.

Previous research studies such as Eom, Kim, Kim, Lee, Yeo, Choi and Choi (2011), Mourant, Wang, He, Wang, Garcia-Perez, Ling and Li (2011), Lv, Xu, Liu, Zhan, Li and Yao (2010) and Jendoubi, Broust, Commandre, Mauviel, Sardin and Lédé (2011) reported that alkali and alkaline earth metals (AAEM) presence in biomass has significant effect on bio-oil yield and compound. Some of them conducted washing treatment on biomass and evaluate the effect of AAEM concentration to bio-oil yield and composition. However, the investigation on the effect of washing treatment on biomass structures itself, and further to thermal decomposition behaviour is purely reported. Thus, this study is performed and limited to evaluate the influence of washing treatment on AAEM concentration and RMS structures to bio-oil production and bio-oil compounds.

Catalytic pyrolysis is a promising way to improve bio-oil compound (Eibner, Broust, Blin & Julbe, 2015). One of catalytic pyrolysis is impregnated method, by which, metal salt solution is directly impregnated into biomass to generate in-situ catalyst. Eibner et al. (2015) focussed on anhydrosugars production and reported that the presence of metal salt catalyst improves anhydrosugars yield. Richards and Zheng (1991) revealed that impregnated biomass with a few metal salt solutions such as transition metal or alkali metal salt solutions increased the yield of levoglucosan in bio-oil. However, no explanations were given to explain the effect of impregnated method to biomass itself, since levoglucosan is the product of cellulose component in biomass. In addition, the catalytic effect of metal salts towards thermal decomposition behaviour of biomass also never been reported in literatures. Thus, the effect of impregnated is studied with limited to evaluate the effect of impregnated treatment to RMS chemical bond strength, thermal decomposition process and levoglucosan production in bio-oil.

There are several studies been reported on optimisation of pyrolysis process parameter for bio-oil production according to central composite design (CCD) in response surface methodology (RSM) such as the production of bio-oil from palm shell in tabular tube furnace (Abnisa, Wan Daud & Sahu, 2011) and bio-oil production from pyrolysis of red oak in free fall reactor (Ellens & Brown, 2012). However, the optimisation of bio-oil production from red meranti as biomass feedstock using CCD of RSM approach has not yet been reported. With regards to this point, in this study, optimisation model for bio-oil

production from RMS as a function of specific close range operating parameters as variables is developed using CCD in RSM approach.

1.3   Research Objective

This research has been performed to gain comprehensive understanding of fast pyrolysis process for bio-oil production from red meranti sawdust (RMS). The study covers the objective as following:

1) To evaluate the effect of fast pyrolysis process parameters of RMS feedstock to bio-oil production and characterise the extracted bio-oil in term of its composition and bio-active compounds.

2) To investigate the influence of washing treatment on AAEM concentration and RMS structures to bio-oil production and characterise the bio-active compounds in extracted bio-oil.

3) To evaluate how far the impregnated treatment affecting RMS structures and enhancing the decomposition process at lower temperatures, as well as, improving levoglucosan yield in extracted bio-oil.

4) To develop an optimisation model for bio-oil production from RMS as a function of specific close-range operating parameters as variables using RSM approach by CCD to generate results.

1.4   Scope of Study

The study of fast pyrolysis process of RMS for bio-oil production was carried out using pyrolysis system consisting a vertical tube furnace as pyrolysis reactor, a temperature controller, a cyclone to separate solid char from volatiles, two unit condensers to cool pyrolysis vapour, nitrogen gas (N_2) to provide inert gas as pyrolysis atmosphere and sweep vapour out from pyrolysis reactor, a char collector and three unit bio-oil collectors. All the experiments were conducted at Faculty of Engineering Technology (FTeK), University Malaysia Pahang (UMP). In this study, RMS was used as pyrolysis feedstock. RMS was collected from Sen Peng Sawmill, Gambang. Prior to pyrolysis process, the RMS was pre-dried under the sun and separated by sieve shaker using four mesh sieves with mesh size of 0.60, 1.18, 2.00 and 4.00 mm. After separated,

the RMS was treated according to the objective of study. Before pyrolysis process, sample of RMS feedstock was taken for a few analyses to determine its physicochemical properties, TGA and DTG to assess its degradation behaviour and FTIR to examine its functional group.

There were four objectives studies involved in this research. The first objective was conducted to study the effect of fast pyrolysis conditions to products distribution, especially bio-oil production. In this study, raw RMS was used as feedstock and parameters process studied were temperature (350 – 600 °C), N_2 flow rate (5 – 30 L/min), retention time of RMS in furnace (10 – 40 min) and particles size of RMS (0.30, 0.89 and 1.59). This study was conducted by using one-factor-at-a-time (OFAT) approach.

For the second objective, raw and washed RMS were used as feedstock in order to investigate the influence of washing treatment to RMS chemical bond strength and AAEM concentrations on bio-oil production. Extracted bio-oils from different washing treatment also had been characterised to determine its compound. In this study, RMS was treated by washing it using either one of the following solutions; (i) water wash by DI water, or (ii) acid wash by 1.0 M or 2.0 M HCl. After washing, beside TGA and FTIR analyses, samples of raw- and demineralised RMS also were subjected to ICP-OES analysis to determine the concentration of AAEM in feedstock. All the feedstock excluding demineralised RMS - 2.0 M HCl were subjected to fast pyrolysis experiment. In this experimental study, only temperature process was varied, from 350 to 600 °C, while three other parameters which are N_2 flow rate, retention time and feed particles size were maintained (constant) at specific value. The trend of thermal degradations was observed and the amount of bio-oils yield were compared. The bio-oils compounds, then, were analysed using GC-MS to characterise the bio-active compounds in extracted bio-oils.

In the third objective, 0.1 M of metal salt ($CaCl_2$, $CaSO_4$, $FeCl_2$ or $FeSO_4$) solution was added to raw RMS prior to pyrolysis. This study was carried out to examine the influences of metal salt solution addition in RMS, in order to observe whether its presence was capable to enhance degradation process at lower temperature or otherwise. Furthermore, the amount of bio-oils yield also were compared and its components were analysed by GC-MS to determine whether the presence of metal salt was capable to improve levoglucosan compound in bio-oil or not. The pyrolysis work in this study also

was run by varying temperature process from 350 to 600 °C and three other parameters were constant at specific value.

In the last objective, optimisation of bio-oil production from RMS was developed using RSM under CCD approach. In this study, three operating parameters were considered as independent variables (factors); temperature (A), N_2 flow rate (B) and retention time (C). The bio-oil yield (Y_B) was considered as the dependent factor (process response). The fast pyrolysis experiment was conducted based on design matrix which the range of parameter was 400 – 520 °C of temperature, 20 – 30 L/min of N_2 flow rate and 15 – 25 min of retention time. Particles size of RMS used as feedstock was less than 2.00 mm.

1.5 Significance of the Study

Pyrolysis process is an alternative thermochemical technology to convert biomass into renewable energy. In this study, fast pyrolysis process was applied to extract valuable product, which is bio-oil from RMS. RMS is one of the renewable energy resources that can be easily obtained at low cost as it is abundantly generated from forestry and industrial wood wastes. According to "Malaysia Energy Centre," (2002) and Water and Energy Consumer Association of Malaysia [WECAM] (2009), residues from timber industry generated about 9.83 m^3 of waste, in which however, only 60 – 65 % of the residues have been harvested for energy and remaining was dumped or burned as waste. This situation is a huge loss to Malaysia since these residues can be pyrolyzed to make a pyrolysis oil, or bio-oil.

Bio-oil product has a potential application which can be used directly for heat and power generation in burner, furnace or boiler systems where several companies have been interested in using bio-oil, especially for district heating to replace heavy fuel oil. Bio-oil also widely been extracted to recover useful chemical by taking advantage of its most abundant functional groups: sugar, carbonyl, carboxyl, and phenolic. In addition, by upgrading process using physical and chemical processing, bio-oil has a potential to substitute conventional transportation fuel. Although production of bio-oil is a main concern product in fast pyrolysis process, the char and gases by-products from this process also have a significant value in commercial sector.

Therefore, the pyrolysis study of red meranti is performed to evaluate its potential as a sustainable renewable energy resource for the production of bio-oil through fast pyrolysis technology. Outcomes and findings from this research are expected to provide some knowledges and guidelines related to 'waste to energy' conversion by diverting lignocellulose waste to wealth product, namely bio-oil as new alternative energy for petroleum based-product replacement. This study, in the meantime, perhaps can conserve the environment in aspect of preserving environment by reducing greenhouse gas emission and reducing solid waste disposal. Therefore, the concept of 'waste-to-wealth' as campaigning by Malaysia government can be achieved.
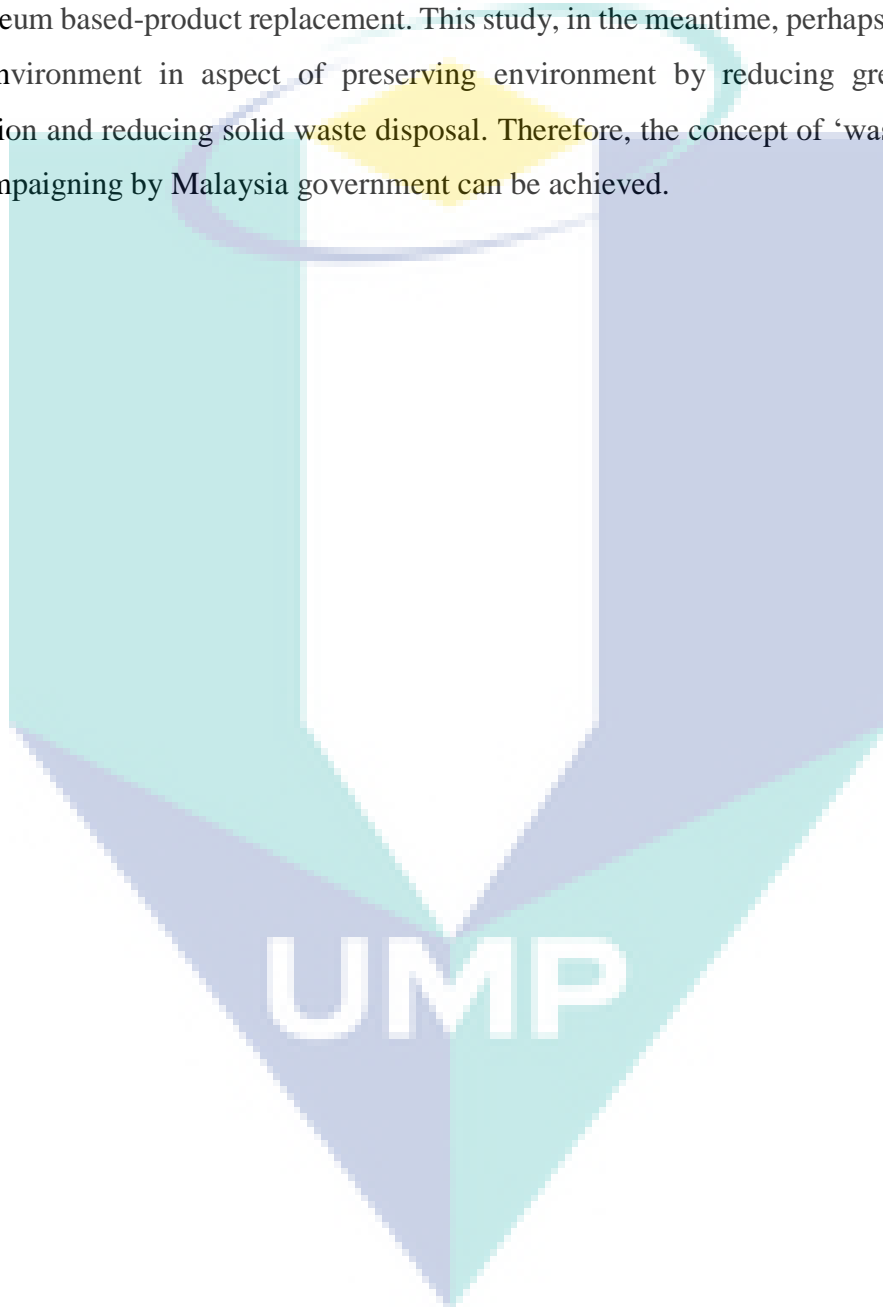
CHAPTER 2

LITERATURE REVIEW

2.1   Pyrolysis

Pyrolysis process is a thermal degradation process of biomass, which carried out in the absence of oxygen, at atmospheric pressure, and at the temperature ranging from 300 to 600 °C (Venderbosch & Prins, 2011). Generally, pyrolysis products of biomass include solid (charcoal), liquid (tar, high molecular hydrocarbons and water) and combustible gas products (mainly CO_2, H_2, CO, CH_4, C_2H_2, C_2H_4 and C_6H_6) (Naik et al., 2010) which the distribution of each product produced can be varied over a wide range of process parameter adjustment (Bridgwater, 2012), feedstock's types and type of pyrolysis process (Akhtar & NorAishah, 2012). Lower temperature below than 400 °C with longer vapour residence time favour for the production of charcoal, moderated temperature approximately around 450 to 550 °C with short vapour residence time are the optimum operating process for liquid production and high temperature together with longer residence time lead to the conversion of biomass to NCG product (Larson, 2008).

Charcoal, the solid product consist carbon and ash remaining after pyrolysis, which this product has a potential as absorbent material for catalyst or fertilizer support (Ran Xu, 2010). In addition, solid char product also can be used in chemical, pharmaceutical and food industries due to its low sulphur and phosphorus content, as well as, its structural and reactivity properties (Ran Xu, 2010). The liquid product contains valuable organic compounds that can be used as a fuel and can be extracted for other uses (Ran Xu, 2010). NCG products from pyrolysis, at the same time can be combusted to provide the energy required for the further endothermic pyrolysis process (Ran Xu, 2010).

In general, the changes that occur during pyrolysis are enumerated below (Bridgwater, 2012):

1)   Heat transfer from a heat source, to increase the temperature inside the fuel,

2)   The initiation of primary pyrolysis reactions at this higher temperature releases volatiles and forms char,

3)   The flow of hot volatiles toward cooler solids results in heat transfer between hot volatiles and cooler unpyrolysed fuel,

4)   Condensation of some of the volatiles in the cooler parts of the fuel, followed by secondary reactions, can produce tar,

5)   Autocatalytic secondary pyrolysis reactions proceed while primary pyrolytic reactions (item 2, above) simultaneously occur in competition, and

6)   Further thermal decomposition, reforming, water gas shift reactions, radicals recombination, and dehydrations can also occur, which are a function of the process's residence time/ temperature/pressure profile.

Pyrolysis process can be divided into three subclasses by depending upon the operating conditions; conventional pyrolysis, fast pyrolysis and flash pyrolysis (Naik et al., 2010). The optimal range of main operating parameters, product yields distribution and reactors configuration for each process are summarised in Table 2.1. Recent years, interest towards the use of catalysts during pyrolysis is growing with the aim of improving the quality of yielded bio-oil (Wang, Zhan, Yu, Xue & Hong, 2010).

2.1.1   Conventional Pyrolysis

Conventional pyrolysis, also known as slow pyrolysis or carbonisation is conducted on massive pieces of wood with a particle sizes of 5 to 50 mm, under a very low heating rate (0.1 – 1 °C/s), with the temperature ranging from ~ 300 to 700 °C and long residence time lasting from hours to days (Kan, Strezov & Evans, 2016). Conventional pyrolysis is targeted for the production of solid char (Ran Xu, 2010). First stage of biomass decomposition, called pre-pyrolysis occurs in the temperature between 277 and 677 °C (Naik et al., 2010). During pre-pyrolysis, some internal rearrangement

such as water elimination, bond breakage, appearance of free radicals, formation of carbonyl, carboxyl and hydroperoxide group take place (Shafizadeh, 1982). The second stage process corresponds to the main pyrolysis process which proceeds with a high rate and leads to the formation of pyrolysis products. The last stage, the char decomposes at a very slow rate and it forms carbon rich solid residues, charcoal (Naik et al., 2010).

Table 2.1   Main operating parameter and product distribution for pyrolysis process

	Conventional Pyrolysis	Fast Pyrolysis	Flash Pyrolysis
Operating Conditions:			
Temperature (°C)	300 – 700	400 – 650	
Heating Rate (°C/s)	0.1 – 10	10 – 200	>1000
Particle Size (mm)	5 – 50	< 1 to 3	< 0.2
Vapour Residence Time (s)	450 – 500	0.5 – 10	< 0.5
Product Yield, wt. %:			
Liquid	~ 30	60 – 75	~ 80
Char	~ 35	15 – 25	~ 15
Gas	~ 35	15	~ 5
Reactor Configurations		Ablative reactors, rotational cone reactors, circulating fluidised beds, auger reactors, etc.	Fluidised bed, circulating fluidised beds, vacuum flash pyrolysis

Source: Demirbas and Arin (2002)

2.1.2   Fast Pyrolysis

Fast pyrolysis involves the process on fine particle's biomass (< 1 to 3 mm), occurs in high temperature around 400 to 650 °C, with very high heating rate (> 10 – 200 °C/min) (Demirbas & Arin, 2002) and short vapour residence time (< 2 s) and rapid quenching of hot pyrolysis vapours (Ingram, Mohan, Bricka, Steele, Strobel, Crocker, Mitchell, Mohammad, Cantrell & Pittman, 2008; Lu, Li & Zhu, 2009; Heo, Park, Park, Ryu, Suh, Suh, Yim & Kim, 2010) to suppress secondary reactions (Bridgwater, 1999; Bridgwater & Peacocke, 2000; Balat, Balat, Kirtay, & Balat, 2009; Bridgwater, 2012). The process is recommended for the aim to produce maximum quantity of liquids product (Venderbosch & Prins, 2011) by shift the product distribution primarily to liquid bio-oil through minimising the secondary cracking reactions (Ran Xu, 2010). Final products of fast pyrolysis is estimated around 60 – 75 % of bio-oil, 15 – 25 % of solid char, and 10 –

20 % of non-condensed gases, which depending upon the feedstock used (Mohan, Pittman & Steele, 2006).

2.1.3 Flash Pyrolysis

Flash pyrolysis is characterised by a higher heating rate, >1000 °C/s (Ran Xu, 2010). It is performed slowly on fine pieces of wood with the size smaller than 0.2 mm (Naik et al., 2010) in order to achieve rapid heating (Ran Xu, 2010), with the temperature range of 1323 – 1573 °C and short vapour residence time, less than 0.5 s (Naik et al., 2010). The conversion of biomass to crude oil can have an efficiency of up to 70%.

2.2 Fast Pyrolysis Principle

Fast pyrolysis occurs in very high heating rates (> 10 – 200 °C/s) in the absence of oxygen, at the temperature around 500 °C, followed by rapid cooling and condensation of the hot vapours produced during pyrolysis. This such process produces a maximum volume of liquid product, which has a heating value approximately equal to the feedstock and roughly half the heating value of conventional fuel (Venderbosch & Prins, 2011), together with char and gas as by-product, which commonly circulated within the process to provide heat requirements for pyrolysis reaction and hence, there are no waste streams other than ash and flue gas (Bridgwater, 2012).

Pyrolysis is realised by rapid heat transfer, primarily by radiation or convection from gas to the surface particle of biomass, and subsequently, conduction by heat penetration from surface into the inner particles (Venderbosch & Prins, 2011). During fast pyrolysis process, the heat develop inside the biomass particle and the corresponding intrinsic reaction kinetics contribute to the decomposition rate and product distribution (Venderbosch & Prins, 2011). During fast pyrolysis process, to produce as much as possible condensable vapour, two following conditions should be avoided; (i) primary decomposition products being cracked thermally or naturally catalysed (due to already char formation) to noncondensable gas molecules, and (ii) primary pyrolysed products recombined or repolymerised to form char (Venderbosch & Prins, 2011).

Figure 2.1 shows possible reaction scheme for biomass pyrolysis, although other mechanism also have been proposed (Venderbosch & Prins, 2011). Upon sufficiently fast heating, first stage of biomass pyrolysis involved decomposition of biomass to char (10

– 15 wt. %) and pyrolysis vapours, which consisting both gases (CO, CO_2, CH_4) and condensable liquids (organics fraction, biomass moisture and water produced during decomposition). The primary reactions depend only on the local solid temperature (Sinha, Jhalani, Ravi & Ray, 2000). The large organic molecules (molecular weight up to 20 000) in vapour are subject to secondary thermal cracking which may be enhanced by direct contact with the pyrolysis fine char. For this reaction, fine char in condensable vapour react as catalyse for the reaction. Fine char particles are readily entrained from the pyrolysis reactor and carried by the vapour stream to the condenser and is collected with the bio-oil. During storage of condensed bio-oil over a longer period, repolymerisation reactions could occur, which is often suggested to be accompanied by production of water and possibly CO_2.
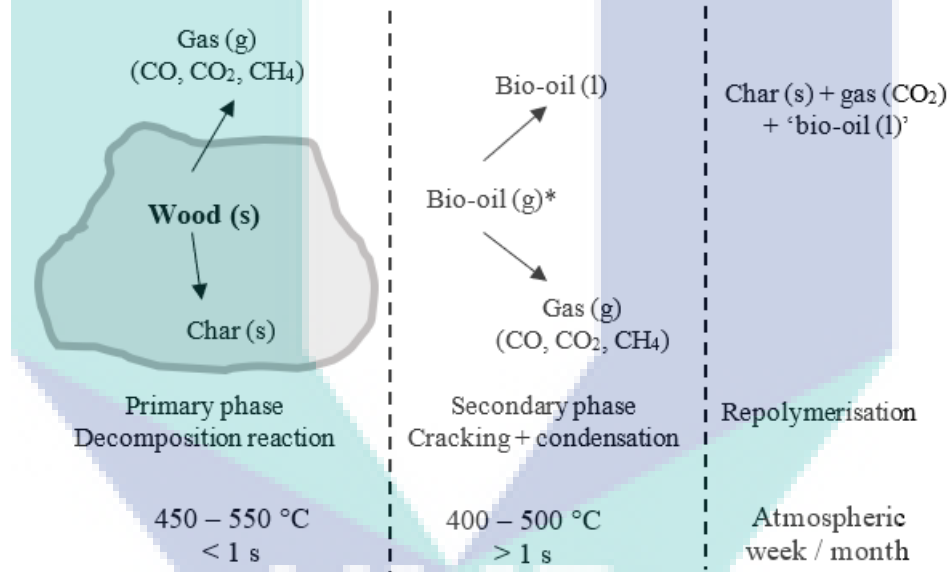
Figure 2.1   Representation of reaction path for wood fast pyrolysis

Source: Venderbosch and Prins (2011)

The pyrolysis of biomass can be endothermic or exothermic, depending on the feedstock component and pyrolysis reaction temperature. Yang, Yan, Chen, Lee and Zheng (2007) reported in their literature, at temperature around 100 °C, all of the individual component of cellulose, hemicellulose and lignin behaved a similar tendency for endothermic reaction. This was attributed to moisture removal when these components were heated up. According to Rath, Wolfinger and Stainer (2003), pyrolysis of holocellulosic (sum of hemicellulose and cellulose) component experienced endothermic reaction at temperature below than 450 °C and at higher temperature an

exothermic reaction took place. In pyrolysis process, vapours formed inside the pores of a decomposing biomass particle are subject to further cracking, leading to the formation of additional gas and/or stabilised tar. In particular, the sugar like fractions can be readily repolymerised, increasing the overall char yield. This may be desired for slow pyrolysis, but it should be avoided in fast pyrolysis. For the small particles used in fast pyrolysis, secondary cracking inside the particles is relatively unimportant due to a lack of residence time. However, when the vapour products enter the surrounding gas phase, they will still decompose further, if they are not condensed quickly enough ("Part 1: Literature Review and Model Simulations," 2005).

There are five essential features of a fast pyrolysis process for producing liquids; (i) very high heating rates and very high heat transfer rates are used, which require a finely ground biomass feed of typically less than 3 mm sizes as biomass generally has a low thermal conductivity, (ii) carefully control pyrolysis reaction temperature between the range 425 and 500 °C, (iii) short vapour residence times are used, typically less than 2 s to minimise secondary reactions, (iv) pyrolysis vapour and aerosol are rapidly cooled to give bio-oil product, and (v) remove char rapidly to minimise cracking of vapours (Mohan et al., 2006; Bridgwater, 2012).

A fast pyrolysis process includes drying the feed to typically less than 10 wt. % water in order to minimise the water in the product liquid oil, grinding the feed to give sufficiently small particles to ensure rapid reaction, fast pyrolysis, rapid and efficient separation of solids (char), and rapid quenching and collection of the liquid product (Bridgwater, 2012).

2.2.1   Reaction Mechanism

The mechanism by which biomass thermally decomposes to bio-oil is not fully understood but the overall pyrolysis process of biomass is believed to proceed as presented in Figure 2.2 where TGA curve of reed is taken as an example (Venderbosch & Prins, 2011). At temperature around 160 °C, all moisture in surface and pores of wood is completely evaporated (dehydration) (Park, Dong, Jeon, Park, Yoo, Kim, Kim & Kim, 2008), which give the initial moisture content of biomass (Uzun, Pütün, & Pütün, 2007). As temperature reaction rises, hemicellulose is the first to be decomposed, starting at 220 °C and completed around 400 °C (Venderbosch & Prins, 2011), predominantly volatile

products such as CO_2, CO and condensable organic vapours, and some of solid residue. At temperature around 300 to 450°C, the decomposition of cellulose picks up and reaches a peak around 320 °C which almost all cellulose is converted to noncondensable gas and condensable organic vapour. Lignin may begin to decompose at temperatures as low as 160 °C, slow and steady process extending up to 800 to 900 °C with accompanied by a comparatively rapid increase in the carbon content of the residual solid material.

From these TGA data, it can be concluded that most of the cellulose is converted to bio-oil, while hemicellulose and lignin also yield substantial quantities of gas, tar and char. The result can be explained by the linkage of lignin and hemicelluloses through covalent bonds, which prevent their ready release during pyrolysis. For cellulose and hemicellulose, there have a link namely hydrogen bonds which the bonder are much weaker than lignin (Vaca Garcia, 2008).
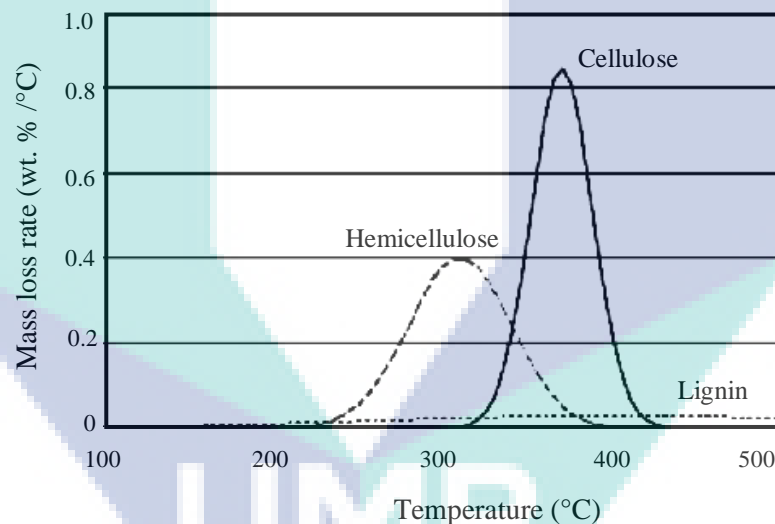
Figure 2.2   TGA curve for reed in terms of cellulose, hemicellulose and lignin
Source: Venderbosch and Prins (2011).

During biomass pyrolysis, a large number of reactions occur throughout the process in which these reactions taking place in parallel and series, involving dehydration, depolymerisation, isomerisation, aromatisation, decarboxylation and charring reactions (Vamvuka, 2011; Collard & Blin, 2014). The reaction mechanisms of pyrolysis generally consisted as three main stages; (i) initial evaporation of free moisture, (ii) primary decomposition, and (iii) secondary reactions (Collard & Blin, 2014).

2.2.1.1   Primary Mechanism

Primary decomposition mechanism of biomass generally occurs at the temperature of 200 – 600 °C (Collard & Blin, 2014; Kan et al., 2016). During this range of temperature, various polymeric chemical bonding within biomass are broken, resulted in releasing of volatile compounds and rearrangement of matrix biomass residue (Collard & Blin, 2014). This primary thermal reactions are responsible for the largest conversion of biomass (Fisher, Hajaligol, Waymack & Kellogg, 2002). During primary decomposition, there are three main pathways mechanism involved in the process, which are char formation, depolymerisation and fragmentation. These mechanisms occur and take place depends on the nature of chemical bonds that are broken. Figure 2.3 illustrates the pathway mechanisms involve within the biomass matrix during the conversion.
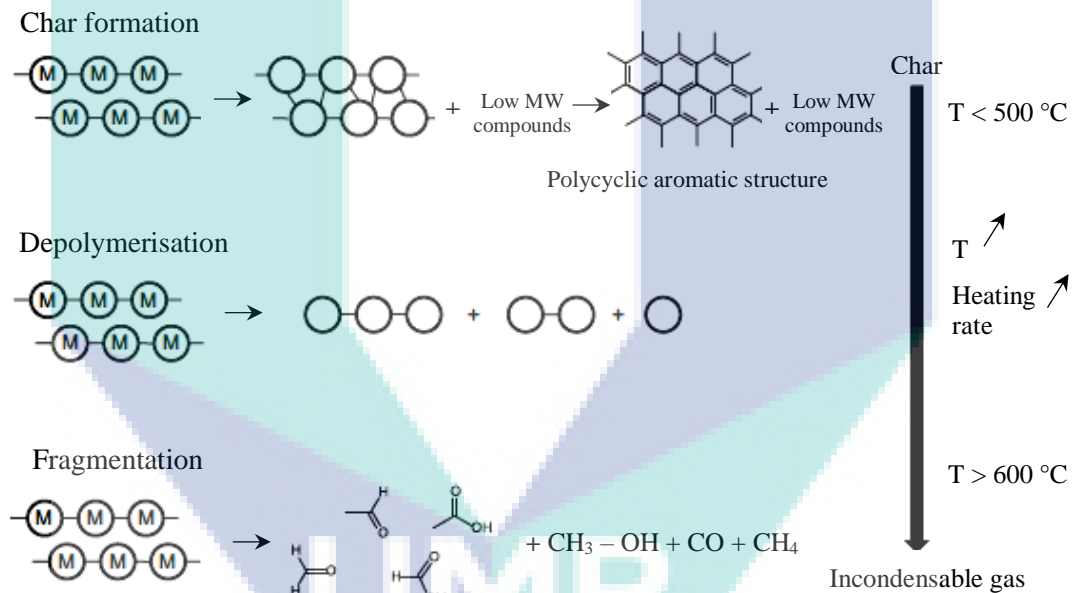
Figure 2.3   Mechanism involved in primary decomposition of biomass constituent
Source: Collard and Blin (2014)

Char Formation

Char formation refer to the conversion of biomass into a solid residue, named char, consisting of aromatic polyclinic structure (McGrath, Chan & Hajaligol, 2003). The pathway of char formation is generally realised by intra- and inter-molecular rearrangement reactions, resulting in the production of solid product with higher degree of network chemical bonding and higher thermal stability (Scheirs, Camino & Tumiatti,

2001; McGrath et al., 2003). The principal steps of this pathway are the formation, combination and rearrangement of benzene rings in polyclinic structure. All these reactions are commonly accompanied with the releasing of water and incondensable gases (Scheirs et al., 2001; Collard, Blin, Bensakhria & Valette, 2012).

Depolymerisation

Depolymerisation essentially occurs at the temperature in range from 250 to 500 °C (Van de Velden, Baeyens, Brems, Janssens & Dewil, 2010; Neves, Thunman, Matos, Tarelho & Gómez-Barea, 2011). Depolymerisation involves dissociation of bonds between monomer units of the polymers under thermal condition, resulting in lower degree of polymerisation of the chains (Mamleeva, Bourbigot, Le Bras & Yvon, 2009). After rupture, new end developed chains would achieve stabilisation reaction (Scheirs et al., 2001; Mamleeva et al., 2009). The continuity of this depolymerisation mechanism reaction finally produces hot volatile molecules and when introduced to rapid quenching, these molecules are condensable and forming liquid fraction, known as bio-oil. Most frequent fractions found in bio-oil are in the form of derived-monomer, dimer or trimer (Garcia-Perez, Chaala, Pakdel, Kretschmer & Roy, 2007; Mullen & Boateng, 2011).

Fragmentation

Pyrolysis thermal fragmentation is the process of breaking up the polymeric chemical bonds into smaller unit, in which this reaction typically take place at the temperature range higher than 550 °C by taking into account a few types of chemical bonds (Van de Velden et al., 2010). As temperature rise, more and more fragmentation happen, resulting in the formation of incondensable gases and some amount of condensable smaller chain of various organic compounds when subjected to rapid cooling at ambient temperature (Van de Velden et al., 2010). Fragmentation comprises the linkage of many polymeric covalent bonds, even within the monomer units (Van de Velden et al., 2010; Lu, Yang, Dong, Zhang, Zhang & Zhu, 2011).

2.2.1.2   Secondary Mechanism

Secondary mechanisms occur on the released volatile compounds that are not stable under the reactor temperatures. These unstable volatiles will undergo secondary reactions such as cracking (Di Blasi, 2002; Morf, Hasler & Nussbaumer, 2002) and

repolymerisation (Morf et al., 2002; Wei, Xu, Zhang, Zhang, Liu, Zhu & Liu, 2006). Cracking reaction refer to the breaking of chemical bonds in volatile compounds, which the reaction results in the formation of lower molecular weight molecules (Neves et al., 2011). This reaction started to begin at the temperature above 600 °C (Collard & Blin, 2014). The products of cracking reaction has similarities with those in fragmentation reaction (Blanco López, Blanco, Martínez-Alonso & Tascón, 2002), thus, sometimes it is difficult to differentiate and determine which pathway is mainly responsible for the formation of lower molecular weight compounds (Collard & Blin, 2014). Repolymerisation (or recombination) reaction, on the other hand, is the combination of volatile compounds to produce higher molecular weight products, in which this product, sometimes is no longer volatile under the conditions of temperature of the reactor (Morf et al., 2002). If repolymerisation occurs inside the pores of the polymer, this reaction would be favour for the formation of secondary char (Wei et al., 2006; Neves et al., 2011). In gas phase, the existence of repolymerisation reaction can be traced by the presence of PAH, which typically observed when the pyrolysis works conducted higher than 800 °C (Morf et al., 2002). Besides the factor of temperature reactions, secondary mechanisms also could be happened if residence time of volatile compounds is long (Wei et al., 2006).

2.2.2 Fast Pyrolysis System

Fast pyrolysis system consists of an integrated series of operations starting with a roughly prepared feedstock until the collection of bio-oil. A conceptual fluidised bed fast pyrolysis system as shown in Figure 2.4 is used as indication for the main components that are explained as following subsection.

2.2.2.1 Reactor Configuration

The core part of a fast pyrolysis process is the reactor. A wide range of reactor configurations have been investigated that show considerable diversity and innovation in meeting the basic requirements of fast pyrolysis. The best method is not yet established with most processes giving between 65 – 75 % liquids based on dry wood input. The essential features of a fast pyrolysis reactor are very high heating and heat transfer rates, moderate and carefully controlled temperature, and rapid cooling or quenching of the pyrolysis vapours (Bridgwater & Peacocke, 1994; Diebold & Bridgwater, 1997).
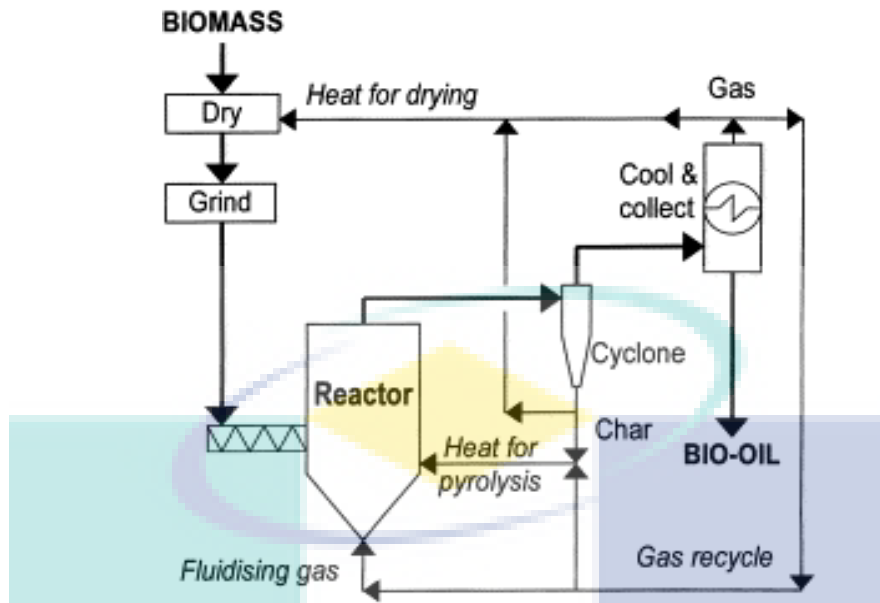
Figure 2.4   Fast pyrolysis system configuration

Source: Bridgwater and Peacocke (1994)

2.2.2.2   Heat Supply

Char and gas are by-products of fast pyrolysis process. Typically, char and gas containing about 20 % and 5 % of the energy in the feed material respectively (Bridgwater, 2012). The pyrolysis process itself requires about 15 % of the energy of in the feed, and of the by-product, only the char has sufficient energy to provide the heat. The heat can be derived by burning char in reaction system design, which makes the process energy self-sufficient (Bridgwater, 2012). The heat waste from char combustion and any heat from surplus gas or by-product gas can be used for feed drying. In large scale installations, the gas also could be used for power generation (Bridgwater, 2012).

2.2.2.3   Heat Transfer

Pyrolysis is an endothermic process which require a substantial heat input to heat the biomass to reaction temperature, even though reaction heat is insignificant (Bridgwater, 2012). The char typically contains about 25 % of the energy of feedstock, and about 75 % of this energy is required to drive the process. The by-product gases is only containing about 5 % of the energy and utilization of gas itself needs supplementation to support the process.

The possible ways to utilize the heat from by-product char and gas, or other sources to the reactor are (Bridgwater, 2012):

i)   Combustion of by-product char, all or part char produced,

ii)   Combustion of by-product gas, together with supplementation,

iii)   Combustion of other biomass, particularly if there is a lucrative market for the char,

iv)   Gasification of char to a LHV gas, then burning the resultant gas to provide greater temperature control with the advantage to avoid alkali metal problems such as slagging in the char combustor,

v)   Use of bio-oil product,

vi)   Use of fossil fuel if they are available at low cost and do not affect the process and product. This point only applicable if the bio-oil or by-product has a sufficiently high value.

The high heat transfer rate that is necessary to heat the particles sufficiently quickly imposes a major design requirement on achieving the high heat fluxes required to match the high heating rates and endothermic pyrolysis reaction (Bridgwater, 2012). There are two important requirements that must be achieved to transfer the heat during pyrolysis process; (i) from the heat supply to the reactor heat transfer medium (solid reactor wall in ablative reactors, gas and solid in fluid and transport bed reactors, gas in entrained flow reactors), and (ii) from the heat transfer medium to the pyrolysing biomass (Bridgwater, Meier & Radlein, 1999).

Two possible ways transfer the heat to biomass particles in a fast pyrolysis system; (i) gas-solid heat transfer as in an entrained flow reactor where heat is transferred from the hot gas to the pyrolysing biomass particles by primarily convection, and (ii) solid-solid heat transfer with mostly conductive heat transfer (Bridgwater et al., 1999). Fluidised bed pyrolysis utilises inherently the good solids material, for instant hot sand (Venderbosch & Prins, 2011) for mixing the cold biomass feed and heat transfer achieved by solid-solid conductive heat transfer approximately up to 90 % with a probable small contribution from gas-solid convective heat transfer of up to 10 % (Bridgwater et al., 1999). For more an efficient heat transfer into the biomass particle, small heat penetration depth is required, which the size particle's limit must be less than 2 mm (Venderbosch & Prins, 2011). For circulating fluid bed and transport bed reactors, these reactors rely on

both gas-solid convection heat transfer from the fluidizing gas and solid-solid conductive heat transfer from the hot fluidising solid although the latter maybe less significant due to the lower solids bulk density. Some radiation effects occur in all reactors.

Attrition of the char from the pyrolysing can also occur in both fluid and circulating fluid beds, due to contact of the biomass with in-bed solids where solid mixing occurs. In fluid bed reactors, however, attrition of the product char is relatively low and it has been observed that the chars particles have the original particle shape, but are slightly reduced in size by char layer shrinkage and attrition (Bridgwater et al., 1999).

Thermal conductivity of biomass is very poor (0.1 W/mK along the grain, ca 0.05 W/mK cross grain), and by reliance on gas-solid heat transfer means that biomass particles have to be very small to fulfil the requirements of rapid heating to achieve high liquid yields (Bridgwater et al., 1999). As particles size increases, liquid yields reduce as secondary reactions within the particles become increasingly significant (Scott & Piskorz, 1984).

2.2.2.4   Char and Ash Separation

Char acts as a vapour cracking catalyst and cyclones are the usual method to remove char. However, some fine char is inevitably always pass through the cyclones and will collected it with liquid product (Bridgwater & Peacocke, 2000). Char contributes to secondary cracking by catalysing secondary cracking in the organic vapour and forms secondary char, water and gas both during primary vapour formation and in the reactor gas environment (Bridgwater et al., 1999). Therefore, rapid removal of char from the hot reactor environment and complete char separation is desirable (Bridgwater et al, 1999; Bridgwater, 2012). Fine char present in cooled collected liquid product also contributes to instability problems where it would accelerate the slow polymerisation process which manifests as increasing viscosity (Bridgwater & Peacocke, 2000). Some success of char removal has been achieved with hot vapour filtration which is analogous to hot gas cleaning in gasification systems, however problems are arise with the sticky nature of fine char and disengagement of the filter cake from the filter (Bridgwater, 2012). Pressure filtration of the liquid for particulate removal (smaller than 5 µm) is very difficult to conduct as well because of the complex interaction of the char and pyrolytic lignin which appears to form a gel-like phase that rapidly block the filter (Bridgwater, 2012).

Modification of the liquid microstructure by addition of solvent such as methanol or ethanol that solubilise the less soluble constituents has been proven can improve this problem and contribute to the improvement in liquid stability (Bridgwater, 2012).

Almost all of the ash containing alkali metals in the biomass is retained in the char, so successful char removal gives successful ash removal. Due to the difficulty of char separation, the removal of char may not be necessary for all applications (Bridgwater & Peacocke, 2000).

2.2.2.5   Condenser

The bio-oil aerosols are submicron droplets which are typically present in product gases and in some pyrolysis systems (fluidised bed etcetera). The aerosols also present in carrier or fluidisation gas in a relatively low concentration. These factors need to the specific requirements for the design of condensation systems that can provide simultaneously; (i) effective cooling, (ii) relatively long residence time, (iii) prevention of blockage due to the differential condensation of heavy ends.

At both the bench and pilot scales, quenching of the bio-oil vapours is commonly achieved by immersing condenser containers into a refrigerated fluid (ethylene glycol or chilled water) (Ran Xu, 2010). Commercial scale processing mostly use direct by counter-current contacting of bio-oil vapours with the cooling media such as scrubber (Ran Xu, 2010). In all the processes, rapid cooling rate is essential to avoid further cracking of bio-oil. Other than quenching, the applications of the condensation on pyrolysis process have been further extended to the minimisation of the bio-oil water content and separating certain compounds from the bio-oil under selective operating conditions (Ran Xu, 2010).

2.2.2.6   Liquids Collection

The collection of liquids has long been a major difficulty in the operation of fast pyrolysis processes due to the nature of the liquid product which is mostly in the form of aerosols rather than a true vapour (Bridgwater & Peacocke, 2000). Once the pyrolysis reaction takes place, the condensable vapours which form the bio-oil, together with the non-condensable product gases, exit from the reactor and form aerosols (Ran Xu, 2010). In fluidised bed systems, these aerosols are typically diluted in carrier gas either or both in atomisation or/and fluidisation gas. Due to the nature of the liquid bio-oil, Bridgwater

(1999) and Bridgwater and Peacocke (2000) concluded that pyrolysis aerosols can be characterized as a combination of true vapours, micron sized droplets and polar molecules bonded with water vapour molecules. Liquid product of fast pyrolysis can be recovered by quenching process by contact the vapours with cooled liquid but control design and temperature control is needed to avoid blockage from the differential condensation of heavy ends. Light ends collection is important in reducing liquid viscosity (Bridgwater & Peacocke, 2000).

2.3   Factor Influencing Fast Pyrolysis Product

In fast pyrolysis process, there are several factors affecting fast pyrolysis products where both quantity and quality of products yield are strongly sensitive to pyrolysis operating condition and type of biomass feedstock.

2.3.1   Effect of Pyrolysis Operating Condition

Pyrolysis reaction environments play a major role to define products yield and products distribution. In fast pyrolysis, which regards to process conditions, pyrolytic product yields are very sensitive to temperature reaction, heating rate, residence times, feed particles sizes (Akhtar & NorAishah, 2012) and pyrolysis medium. Therefore, by changing or modify one of these parameters, it is quite enough to change and give different significant results on products distribution and nature.

2.3.1.1   Temperature

Reactor temperature is different with the temperature of reaction. In pyrolysis process, the reactor temperature must be higher to provide adequate temperature to support temperature gradient due to heat transfer effect during biomass decomposition into fragment linkages (Akhtar & NorAishah, 2012; Bridgwater, 1999).

Among of all fast pyrolysis process parameters, temperature is the most influential process variable upon the yield and properties of pyrolysis products. Pyrolysis products is always changing at a wide range of temperature, and this closely related to thermal decomposition of components in feedstock as well as the reaction occurs within feed particles and products in pyrolysis reactor.

Generally, at lower temperature than 300 °C, thermal decomposition of biomass is started slowly due to lower heat transfer rate. Such condition leads to the production of high quantity of char, while liquid and gas yields are still low. Dominant gas released at this temperature was CO_2, attributed to the fact that carboxyl release CO_2 at low temperature (Boroson, Howard, Longwell & Peters, 1989).

When the reactor temperature is increased in the range up to 450 to 550 °C, the char yield decreased and released more pyrolysis vapours containing bio-oil and gases. Many studies reported highest bio-oil yield at this range of temperature when pyrolysed various type of biomass in different pyrolysis reactor such as Garcia-Perez, Wang, Shen, Rhodes, Tian, Lee, Wu and Li (2008), Heo, Park, Park, et al. (2010), Heo, Park, Yim, Sohn, Park, Kim, Ryu, Jeon and Park (2010), Heidari, Stahl, Younesi, Rashidi, Troeger and Ghoreyshi (2014) and many more. This typical result can be described by decomposition of fraction components in biomass feedstock containing holocellulosic (sum of cellulose and hemicelluloses) and lignin. Incorporated with the optimum biomass particle size, the thermal degradation of holocellulosic fraction in biomass started to degrade at 200 °C and ended at 350 °C, with degradation mainly contribute to liquid product (Butler, Devlin, Meier & McDonnell, 2011).

However, as the temperature increased higher than 550 °C, the pyrolysis reaction continue to produce highest gas volume, while liquid and char yield gradually decreased (Vigouroux, 2001). Around this temperature, CO_2 was still the main component gases released along with CO and light hydrocarbon (C_1 – C_4) and in spite of that, CO_2 concentration became decreasing, contrary with CO and those light hydrocarbons (Heo, Park, Park, et al., 2010). Such result is obtained due to the higher heat transfer rate, which lead to the secondary cracking conversion of heavy-molecular-weight product in pyrolysis vapour to gases product (Heidari et al., 2014) and further pyrolysis reaction on solid fuel (Heo, Park, Park, et al., 2010). Even though decomposition of lignin is still occur at this temperature, the volatile product of lignin is still not significant (Heo, Park, Yim, et al., 2010), and lignin itself mostly yield char.

In term of bio-oil properties, temperature is the major operating parameter that is responsible in determining the characteristics of the recovered bio-oil. According to previous research, other pyrolysis operation conditions can be ignored due to their less influence in affecting the bio-oil quality (Wang et al., 2010). During pyrolysis, pyrolytic

water and reaction water are produced in which the amount of water produced was varies depending on the temperature and the reactions occurred at certain particular temperature. Pyrolytic water is resulted mainly from dehydration of hemicellulosic component (Azeez, Meier, Odermatt & Willner, 2010), and reaction water is generated due to catalytic cracking reaction (Fahmi, Bridgwater, Donnison, Yates & Jones, 2008) occurs throughout pyrolysis process.

2.3.1.2   Vapour Residence Time and Sweeping Gas Flow rate

It is well known that the short vapour residence time also an important criterion that should be consider while designing fast pyrolysis reaction and process. For the production of liquid, pyrolysis process needs very short vapour residence time (Akhtar & NorAishah, 2012), with the aim to minimise secondary reactions react on produced volatiles (Boroson et al., 1989). The short vapour residence time in fast pyrolysis is realised by introducing rapid purging of pyrolysis vapour, or inert gas (such as N_2, Argon or water vapour) at particular flow rate to pyrolysis reactor, by ensuring that residence times for biomass decomposition must be longer than vapour residence times (Scott, Majerski, Piskorz & Radlein, 1999).

Vapour residence time is defined as the empty reactor volume divided by the volumetric gas flow rate taken at reactor outlet conditions. Since pyrolysis reactor was fixed, then vapour residence time was measured by sweeping gas flow rate. The gas flow rate determines fluidisation condition, residence time of the products and consequently, heat transfer characteristics and the extent of the secondary reactions (whether thermal cracking, recondensation or repolymerisation of tar) (Vigouroux, 2001; Heo, Park, Yim, et al, 2010; Heidari et al., 2014), which eventually affect gaseous and liquid products (Heo, Park, Yim, et al., 2010).

When gas flow rate increased, mixing between feed particles will be enhanced due to vigorous bubbling motion, and in the meantime, short residence time was achieved, in which probability for secondary cracking reaction on tar occurs was low. However, when gas flow rate is increased highly, bubbling motion becomes larger which lead to lower both solid mixing and heat transfer efficiency, which eventually, results in decreasing bio-oil yield (Heidari et al., 2014). On the other hand, when the flow rate is too low, vapour residence time will be longer than needed, which finally results in

secondary reaction (cracking, repolymerisation and recondensation) of the primary product which contribute to lessen yield of bio-oil (Heo, Park, Park, 2010) and affecting it properties, as well as, provokes char formation (Akhtar & NorAishah, 2012).

Unlike temperature and particle size parameters, the optimum range of gas flow rate is undetermined specifically and it might closely have related to pyrolysis operating temperature, and pyrolysis reactor type and size. Most of the researchers reported the differences of gas flow rate in their experiments. Heidari et al. (2014) conducted fast pyrolysis experiment of eucalyptus grandis in fluidised bed reactor and obtained the highest bio-oil derived yield at 12.6 L/min. Heo, Park, Park, et al. (2010) also carried out the experiments in fluidised bed reactor and they gained maximum yield of bio-oil at 5 L/min. In term of vapour residence time, optimum range for highest bio-oil yield is always estimated less than 2 s (Ingram et al., 2008; Heo, Park, Park, et al., 2010; Lu et al., 2009). However, Scott et al. (1999) had proven the evidence through experimental works, that maximum bio-oil yield can be obtained at vapour residence times up to 10 s if the reactor temperature not over than 500 °C.

The time and temperature profile between formation of pyrolysis vapour and their quenching influences the composition and quality of the liquid product (Bridgwater & Peacocke, 2000). High temperature will continue to crack the vapours and the longer the vapours at higher temperatures, lead to the greater extent of cracking which result to the reducing yields of specific products and organics liquids (Bridgwater, 1999). Vapour residence times of a few hundred milliseconds are necessary for optimum yields of chemicals and food additives, while fuels can tolerate vapour residence times of up to around 2 seconds (Bridgwater & Peacocke, 2000).

2.3.1.3 Residence Time

The effect of retention time towards bio-oil yield is seldom reported. Ngo, Kim, and Kim (2013) reported in their experiments, at low temperature of 400 °C, receiving energy not enough to decompose biomass completely especially in limited time available for the reaction. However, at high temperature of 500 °C, biomass can be completely decomposed, and retention time of biomass is decreased. Furthermore, according to Boroson et al. (1989), bio-oil yield also can be decreased attributed to secondary cracking

and repolymerisation reactions occurred on unstable pyrolysis vapour, leading to releasing more gases and forming more char.

2.3.1.4   Feed Particle Size

Particle size of biomass feedstock has a major implication where it is closely related to transfer heating rate within the particle in reactor during both particle drying and primary pyrolysis reaction, making it an important parameter to be controlled (Isahak et al., 2012). Biomass has a poor thermal conductivity which often poses difficulty in heat transfer during pyrolysis, thus smaller feed biomass particle size is much needed in order to provide higher surface area per unit weight for better heat transfer. Previous experiments have demonstrated that, the smaller the particle size, particularly for fine particles less than 1 mm, the higher the yield of volatiles (Neves et al., 2011).

Larger particle sizes prefer to heat up more slowly due to heat transfer challenging within the feed particle where heat residence distance from the surface to centre of particles is longer. This is the drawback for rapid transfer heat from hot to cool part, resulting in imperfect pyrolysis reaction which can cause incomplete thermal decomposition, eventually leading to char production. Smaller particles, on the other hand, desire more expenses which make it less profitable for feedstock preparation. Estimated cost for reducing biomass particle with range of 2.5 to 0.25 mm incurred added expenses about $ 1.80/tonnes to $ 5.60/tonnes, respectively (Isahak et al., 2012).

Particle size distribution of biomass feedstock also needs thorough study. Wide ranges of particle size tend to undergo different thermal decomposition behaviour, and consequently, cross-reactions prefer to occur involving incomplete feed particle and primary pyrolysis products. Wang, Kersten, Prins and Van Swaaij (2005) carried out the fast pyrolysis experiments in fluidised bed at the temperature of 500 °C, and the results shown that secondary reaction of tar, which is product of pyrolysed fine particles was suspected to occur due to the effect of particle size distribution (3 – 12 mm), and consequently lead to declining in bio-oil yield (Park, Park, Dong, Kim, Jeon, Kim, Kim, Song, Park & Lee, 2009). Smaller particle present converts the vapour to gas and thus, increases the gas yield due to heat transfer coefficient much larger for this smaller particle (Islam & Ani, 1998).

In term of bio-oil quality, in addition of temperature, previous literatures have reported that feed particle size also affect pyrolytic water produced during pyrolysis as well. Garcia-Perez et al., (2008) had compiled the data taken from other literatures and this compilation is presented in Figure 2.5. As illustrated in figure, pyrolytic water yield shows an increasing as feed particle size increased while pyrolysis was operated at similar temperature. This is due to progressive thermal scission of chemical bonds in biomass components when heated. During primary thermal decomposition, initial depolymerisation product could undergo additional cracking to form volatiles, and some may undergo condensation/polymerisation to form part of char. These released volatiles, then, have to travel through the porous of the formed char around biomass particle. This circumstance would encourage catalysing of dehydration reaction by char towards some primary products (Garcia-Perez et al., 2008)..
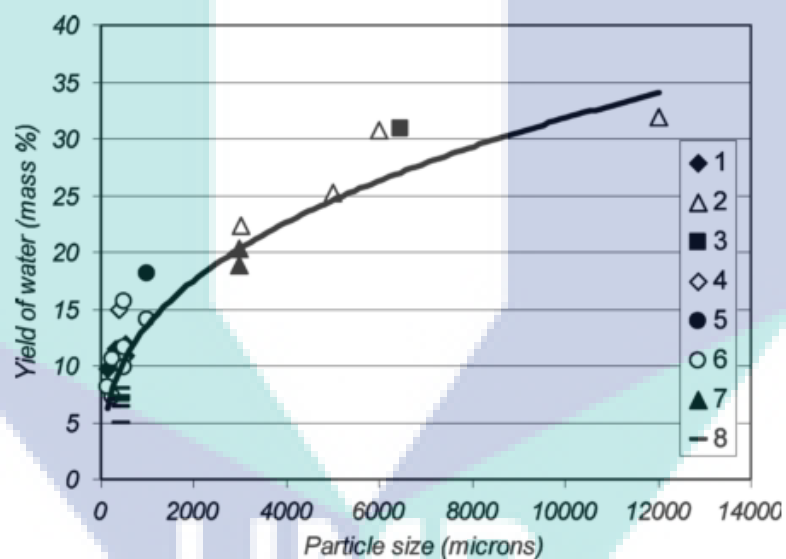
Figure 2.5   Relationship between biomass particles size and pyrolytic water yield at pyrolysis temperature ~ 500 °C; (1) (Garcia-Perez et al., 2008), (2) (Wang et al., 2005), (3) (Garcia-Perez, Adams, Goodrum, Geller & Das, 2007), (4) (Lédé, Broust, Ndiaye & Ferrer, 2007), (5) (Kang, Lee, Park, Park & Kim, 2006), (6) (Scott et al., 1999), (7) (Garcia-Pèrez, Chaala & Roy, 2002) and (8) (Agblevor, Besler & Wiselogel, 1995)

Source: Garcia-Perez et al., (2008)

Therefore, understanding the behaviour of particle size distributions in feedstock during thermal decomposition towards pyrolytic products yields and quality may help to optimise other pyrolysis operating parameters (Açıkalın, Karaca & Bolat, 2012). Based on previous report, the optimum feed particle size for more efficient heating transfer rate

is smaller than 2 mm (Garcia-Perez et al., 2008), while larger than 2 mm, the production of char is more favourable (Shen, Wang, Garcia-Perez, Mourant, Rhodes & Li, 2009).

2.3.2 Feedstock's Composition

Generally, common biomass feedstock for pyrolysis conversion systems is forestry and agriculture residues. These types of biomass are categorised in lignocellulosic biomass type. As natural materials, these biomass are heterogeneous and show great variations in physical and chemical structures, even in a single species (Zaror & Pyle, 1982). Plant biomass essentially has a fibrous structure, constructed from oxygen-containing organics polymers with an empirical chemical formula according to $C_{3.3 - 4.9}H_{5.1 - 7.2}O_{2.0 - 3.1}$ (Tillman, 1991), and made up of various types of small cells, where all the tissue perform different physiology functions, as well as, providing mechanical support (Zaror & Pyle, 1982). Molecular structure of wood are connected by physical forces of attraction; (i) the Van Der Waal's bonds which include dipole-dipole bonds (positively and negatively charged polar molecules that have strong attraction for other polar molecules), (ii) London bonds (weaker bond of attraction between nonpolar molecules) and (iii) hydrogen bonds (special type of dipole-dipole force for strong attraction between positively charged hydrogen atom of one polar molecule and other electronegative atom of another molecule) (Vick, 2007).

The general structure of plant components is shown in Figure 2.6, with the major structure chemical components are carbohydrate polymers and oligomers (65 – 75 %), lignin (18 – 35 %), and minor components are extraneous materials which mostly organics extractives and inorganics materials (4 – 10 %) (Mohan et al., 2006).

The weight percentage of these components varies in different biomass type (Ran Xu, 2010) and these relative portions significantly influence the pyrolysis' products quality and yield (Butler et al., 2011), as well as, the trend of biomass thermal decomposition during thermo-chemical conversion with regards to different kinetic characteristics behaviour of structural individual stability at particular reaction temperature and the presence of contaminants (Zaror & Pyle, 1982; Gupta & Lilley, 2003). Furthermore, at higher reaction temperature, some amount of primary products experienced secondary reaction which lead in cross-reactions of primary pyrolysis

products and between pyrolysis products and the original feedstock molecules (Mohan et al., 2006), resulting in uncertainty amount of product yield.
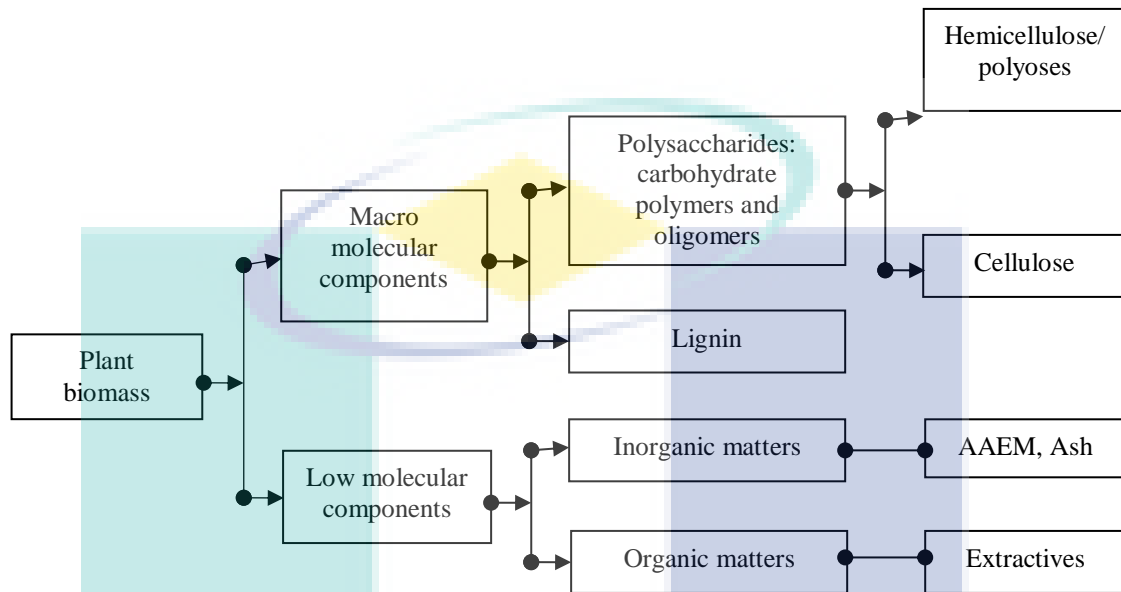
Figure 2.6   General components in lignocellulosic biomass
Source: Mohan et al. (2006)

As the individual components of plant biomass have their own thermo-chemical characteristics and behaviour, as well as the effect towards products yield, the features of these components are discussed in the next subchapter.

2.3.2.1   Major Molecular Component

Major structures of plant are made up of cellulose and hemicelluloses (65 – 75 %) and lignin (18 – 35 %), which composed of carbon, hydrogen and oxygen. Cellulose and hemicelluloses comprises the fibres which are bound together by lignin (Vigouroux, 2001). Each component has different characteristics and thermal behaviour, and eventually influence products yield. General features of these components are explained below.

Hemicelluloses

Hemicelluloses or polyose is a second major wood constituent, also known as polysaccharide which consist of various polymerised monosaccharide with five carbon of D-xylose, D-arabinose, and six carbon of D-mannose, D-galactose and D-glucose, as

well as other mixture of several types 4-*0*-methyl glucuronic acid and galacturonic acid residues (Mohan et al., 2006). Chemical structures of hemicelluloses are illustrated in Figure 2.7.
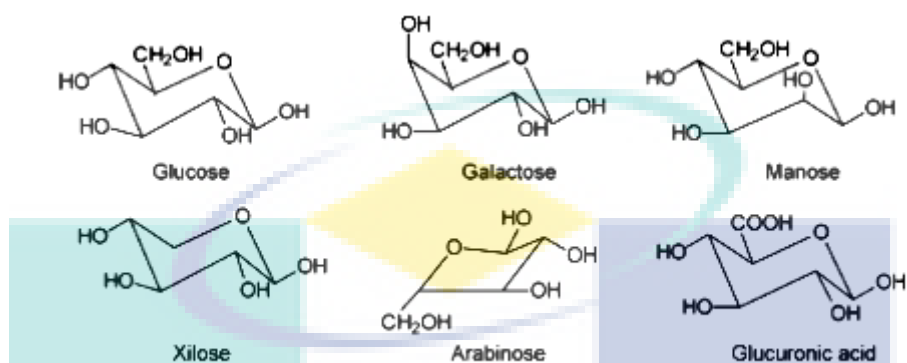
Figure 2.7   The chemical structure of hemicelluloses
Source: Mohan et al. (2006)

Typically, hemicelluloses possess lower molecular weight than cellulose (Sinha et al., 2000). Hemicelluloses in hardwood are rich in xylan and contain small amounts of glucomannan, whereas hemicelluloses in softwood contain a small amount of xylan and they are rich in galactoglucomannan. Hemicelluloses has an average chemical formula according to (C5H8O4)n, where n = 50 – 200. Hemicelluloses is amorphous and its average molecular weight is less than 30 000 (Zhang, 1996). It's content varies from 25 – 35 wt. % of dry wood, 28 wt. % in softwoods and 35 wt. % in hardwoods (Rowell, 1984). Unlike cellulose, hemicelluloses contains several short side-chain "branches" pendent along the main polymeric chain, which enables its less thermal decomposition resistance and hence, possess lower decomposition temperatures started at 220 °C and ended at 400 °C (Venderbosch & Prins, 2011).

During pyrolysis, the decomposition of hemicelluloses may experience two stages; (i) decomposition of the polymer into soluble fragments and/or conversion into monomer units, (ii) products of decomposed polymer further decomposes into volatile products. As compared to cellulose, hemicelluloses derived bio-oil yields are much lower (45 wt. %) and produces significant quantities of char (25 wt. %) (Sinha et al., 2000; Butler et al., 2011) and gases. Thermal decomposition of hemicelluloses results in bio-oil containing organics acid such as acetic, formic and propionic acids attributed to deacetylation of hemicelluloses, water due to dehydration during pyrolysis, methanol,

hydroxyl-1-propanone, hydroxyl-1-butanone and few furfural derivatives (Azeez et al., 2010). At lower temperature, CO_2 and CO are dominant gas released attributed to cracking and reforming of functional groups of carboxyl (C=O) and COOH, and cracking of carbonyl (C-O-C) and carboxyl (C=O), respectively (Yang et al., 2007). In addition of these gases, CH_4 and some organics of a mixture of acids, aldehydes (C=O), alkanes (C-C), ethers (C-O-C) also significantly released during pyrolysis reaction (Yang et al., 2007).

Cellulose

Cellulose is a polysaccharide where D-glucose is connected in uniform by β-glycoside bonds. Cellulose exhibits a crystalline structure that gives mechanical strength to the wood (Vigouroux, 2001). Cellulose has high-molecular weight of long linear polymer without branches, in a good order with the empirical formula is $(C_6H_{10}O_5)n$, where n is the degree of polymerisation range of 500 – 4000 (Venderbosch & Prins, 2011; Vigouroux, 2001). The average molecular weight of cellulose is 100 000 (Vigouroux, 2001). Chemical structure of cellulose is shown in Figure 2.8.
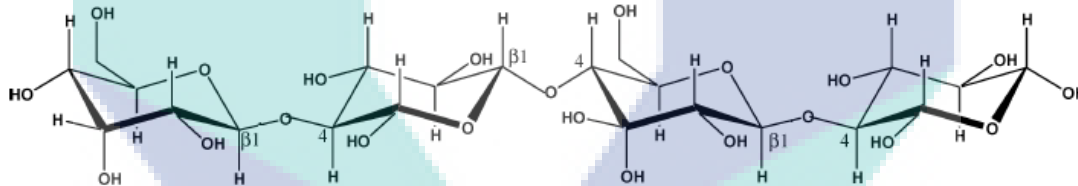
Figure 2.8　　The chemical structure of cellulose
Source: Mohan et al. (2006)

Cellulose when hydrolysed will yield molecules of glucose $(C_6H_{10}O_5)$. Cellulose component is made up normally 40 – 50 wt. % of the dry wood (Venderbosch & Prins, 2011). Gani & Naruse (2007) observed that the biomass with higher cellulose content speed up the pyrolysis reaction rate. Lv et al. (2010) concluded that the pyrolysis of biomass can be divided into two stages; (i) rapid mass decrease attributed to cellulose volatilization at low temperatures and within a narrow temperature range, and (ii) slow mass decrease due to lignin degradation at higher temperatures with the total decomposition rate becomes slower.

The degradation of the cellulose takes place at 300 to 450 °C (Venderbosch & Prins, 2011), contributes notably to bio-oil production (about 72 % at 580 °C) containing levoglucosan and anhydrocellulose (Butler et al., 2011). Decomposition of cellulose occurred at low temperature is supported by the fact that cellulose compounds have the structure of long polymer without branches of polysaccharides and no aromatic compounds which make the bonding easily to break up and volatiles (Lv et al., 2010). Shafizadeh (1982) studied the pyrolysis of cellulose as the temperature is increased. At temperatures up to 300 °C, the dominant process is the reduction in degree of polymerisation. At this point, the most important primary product of cellulose is levoglucosan which is formed through transglycosylation (Azeez et al., 2010). In the second step, at temperatures above 300 °C, there is formation of char, tar and gaseous products. The major component of tar, which is levoglucosan will vaporizes and then decomposes with increasing temperature (Sinha et al., 2000), ultimately lead to the formation of furans and acids via fission and disproportionation, and other significant sugar product via dehydrated form of levoglucosan (Azeez et al., 2010). Uzun et al. (2007) concluded during pyrolysis, biomass with higher cellulose and hemicellulose content increases the release of volatiles, whereas higher in lignin increases the char yield. With regards to the relationship of levoglucosan yield versus temperature, Shafizadeh, Furneaux, Cochran, Scholl and Sakai (1979) reported that the lower temperatures correspond with increased levoglucosan production. In term of gases products, cellulose produces higher CO_2 yield and as the temperature increased, the concentration of CO_2 will be diminished (Uzun et al., 2007).

Lignin

Lignin is the third most important component in plant (Mohan et al., 2006). Lignin is amorphous cross-linked resin with a random polymer of substituted phenyl propane units and highly branched of full aromatic rings which act as a main binder for the agglomeration of cellulosic fibrous components (Vigouroux, 2001). Chemical structure of lignin is shown in Figure 2.9. Lignin has a chemical composition as $[C_9H_{10}(OCH_3)_{0.9 - 1.7}]n$ (Tillman, 1991). The lignin component in biomass varies between 23 – 33 % in softwoods and 16 – 25 % in hardwoods (Mohan et al., 2006). Lignin solely, has different physicochemical properties which depending upon the isolation and extraction method used to segregate them, and when subjected to thermal decomposition studies, this

isolated lignin will not necessarily give equivalent characteristics of pyrolysis behaviour when it is present in the original biomass (Mohan et al., 2006).
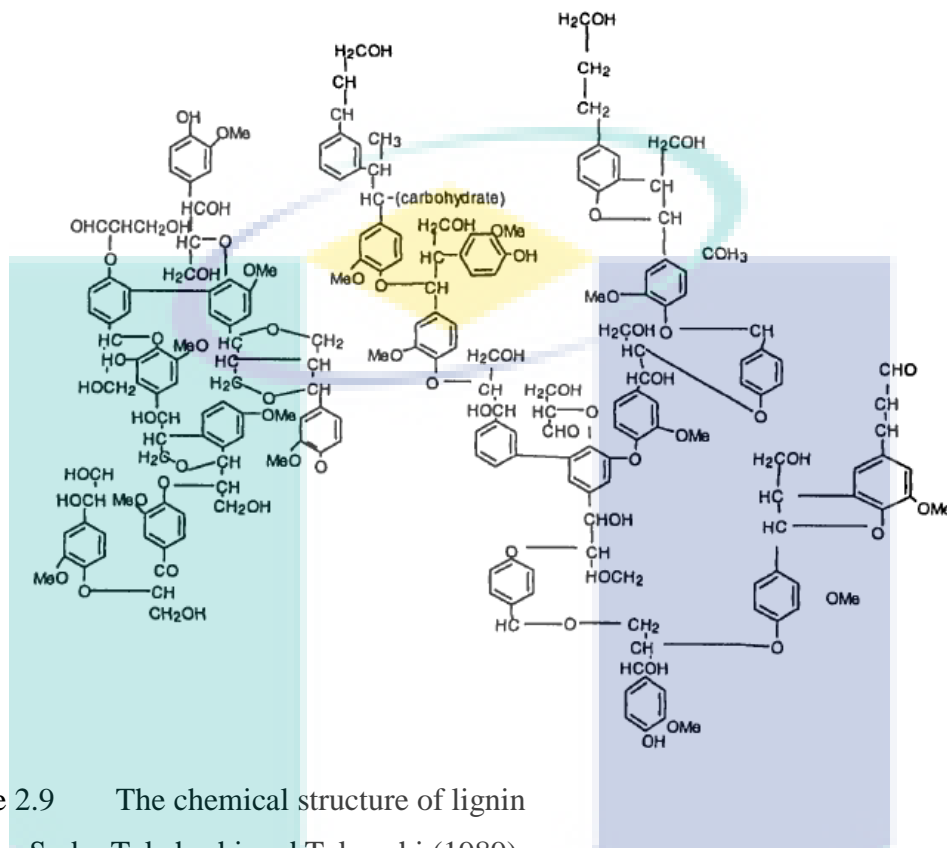
Figure 2.9   The chemical structure of lignin
Source: Sudo, Takahashi and Tekeuchi (1989)

Lignin is observed to decompose slowly at wide range starting at the temperature of 160 to 900 °C, with a maximum rate being observed at 350 – 450 °C (Venderbosch & Prins, 2011). As compared to holocellulosic component, lignin is more difficult to decompose (Mohan et al., 2006), attributed to chemical bonding of various -C-, C-O-C- and =C= containing functional groups and aromatic structural units (Yang et al., 2007; Sharma, Wooten, Baliga, Lin, Geoffrey Chan & Hajaligol, 2004), resulted in slower pyrolysis rate especially for biomass with higher lignin content (Gani & Naruse, 2007).

For agricultural biomass, lignin in feedstock is cracked better than woody feedstock, likely due to the catalysing effect by the presence of significant alkali metals (Butler et al., 2011). Pyrolysed lignin yields char as a more abundant constituent product, contributing about 55 wt. % of total dry lignin. However, according to Fahmi, Bridgwater, Darvell, Jones, Yates, Thain and Donnison (2007) and Tröger, Richter and Stahl (2013), total liquid yield (containing light organic composition) can be increased if the lignin amount increased, provided ash and AAEM level decreased, so that cracking of lighter

fraction was reduced. Liquid product of lignin known as pyroligneous acid and typically contains about 20 wt. % aqueous components and 15 wt. % tar residue on dry lignin basis. Aqueous portion in liquid is composed of methanol, acetic acid, acetone and water, whereas tar residue consists mostly of homologous phenolic compounds which yield through the dissociation of ether and C=C linkages. The 10 wt. % rest of pyrolysed lignin products is represented by gaseous product which released especially at higher reaction temperature (over 500 °C), with composting mainly of H_2 gas, estimated about 1/3 of gas mixture. The production of H_2 is attributed to the rearranging and condensing of aromatics rings during secondary reaction (Uzun et al., 2007). In addition of H_2, lignin also releases CO, CH_4 and other light hydrocarbons where their concentration increases with the increasing pyrolysis temperature (Uzun et al., 2007). CO released is highest in lignin possibly due to thermal cracking of primary product. The formation of methane is attributed to the releasing of methoxyl–O–CH_3 groups (Yang et al., 2007), involving C-C rupture, and it is controlled by hydrogen transfer reactions (Uzun et al., 2007).

Agricultural residues generally contain more hemicelluloses and ash/alkali metals, and less lignin than wood biomass, so that gas formation is more significant with resulting in higher O/C molar ratio for agricultural biomass as compare to woody biomass (Butler et al., 2011). Bio-oil product from lignin component has lower oxygen content, thus it gives higher energy density. Therefore, it can be concluded that agricultural feedstock with less lignin have lower heating values than those from woody feedstock (with a comparatively higher lignin content) (Nowakowski, Bridgwater, Elliott, Meier & de Wild, 2010).

2.3.2.2   Minor Molecular Components

As mention earlier, minor molecular components consist of inorganic (AAEM) and extractive materials, which are presented about 4 – 10 wt. % in lignocellulosic biomass.

Alkali and alkaline earth metal (AAEM)

AAEM are the essential nutrients present in plant to support plant growth. Generally, harvested plant contains these trace elements less than 1 wt. % and their present can exist up to 15 % depending on the biomass species (Eom et al., 2012), composting of K, Na, P, Ca, Mg and so forth, with the greatest contribution are Na and P

(Fahmi et al., 2008). Although their present is relatively low, yet, it still had a decisive influence on thermal decomposition behaviour of biomass during fast pyrolysis process (Mohan et al., 2006; Akhtar & NorAishah, 2012). During pyrolysis, high levels of AAEM in feedstock catalyst primary fragmentation of the monomers, which favour in producing liquid containing considerable amount of small highly oxygenated carbonyls or hydroxyl compounds (HAA, acetic acid and so on) due to fragmentation of the monomers (Scott, Paterson, Piskorz & Radlein, 2001), while lower levels predominates depolymerisation resulting in higher molecular weight compounds (anhydrosugar derivatives) (Fahmi et al., 2007). These reactions mechanism results in different liquid compositional (Scott et al., 2000) and significantly determine product distribution (Wang, Zhang, Shanks & Brown, 2015). These are the mineral matters or AAEM in biomass, in which based on previous literatures, their presence lead to undesired effect on thermal degradation mechanism and result in

The higher the content of AAEM in the biomass, the lower the bio-oil produced and the higher the char formation (Nik-Azar, Hajaligol & Sorahbi, 1996). AAEM elements are appeared in pyrolysis ash. As stated in literatures, AAEM species present in feedstock can lead to decreasing in liquid yield, and tend to promote char and gaseous formation (Akhtar & NorAishah, 2012). Therefore, for the purpose of char production, mineral matters (mainly K and Na) (Jendoubi et al., 2011) presence in biomass is part an important characteristics for secondary pyrolysis reactions and influence in the reactivity of pyrolysis char by accelerating the charring and dehydration reactions of primary product during both primary and secondary pyrolysis (Akhtar & NorAishah, 2012) and indirectly, it have the ability to lower temperatures of degradation reaction (Fahmi et al., 2008). Besides that, alkali metals also possess as a natural catalyst where it catalyse the effect on the thermal degradation towards cracking of heavier compounds of volatiles during pyrolysis (Fahmi et al., 2008; Akhtar & NorAishah, 2012).

In contrast, for the aim of bio-oil production, the presence of high amounts of AAEM (especially K) (Jendoubi et al., 2011) are substantially drawbacks for maximum heavy molecular weight of bio-oil, by which it suppress the formation of levoglucosan (Eom et al., 2012) and stimulates the catalysing effect towards secondary cracking of vapours (Nik-Azar et al., 1996). This condition ultimately leads to increase in lower molecular weight compounds with lower heating value attributed to high yield of reaction

water (Fahmi et al., 2008; Lehto, Oasmaa, Solantausta, Kytö & Chiaramonti, 2013), and increasing in the production of gases. Furthermore, Mourant et al., (2011) also explained that during pyrolysis, bonding between AAEM and lignin-originated fragments would be continuously broken and reformed during pyrolysis. This reaction leads to extended 'holding time' for large organic fragments cracking within the biomass. However, further cracking still occurs which involve breaking down of weaker bonds of larger fragments into smaller ones. These reactions ultimately cause the increasing in lighter lignin derivatives, and decreasing in heavier components derived from lignin, as well as, increasing in water formation in bio-oil resulting from intra-particle cracking and/or condensation reactions.

Raveendran, Ganesh and Khilart (1995) proposed a correlation in Equation 2.1 for determining the change in volatiles yields related to the present of inorganic mineral matters elements (K, Zn) and amount of lignin in biomass feedstock of pyrolysis.

$$\Delta V = -0.964 \left(L^{1.0952} \times X_k^{1.3727} \times X_z^{0.0996} \right) + 7.192 \qquad \text{2. 1}$$

Where ΔV is the change in the volatiles volume, L is the amount of lignin, X_k and X_z are the fractions of K and Zn in the mineral matter, respectively.

Based on Equation 2.1, it is apparent indicating that either greater amount of lignin and/or corresponding metals in mineral matter of feedstock will lessen the volume of volatiles yield (Raveendran et al., 1995). This equation, on the other hand, contrary with the finding by Fahmi et al. (2008) where their report stated that as the lignin content increase in washed feedstock, the total organics (volatiles) yield also increased. This contradicting result might be affected by washed feedstock behaviour during thermal decomposition. In addition, their experiments also did not consider the total of cellulose content in which it could affect the results, as well.

Fahmi et al. (2007; 2008) reported in their experimental studies that total AAEM concentration in biomass was inversely proportional to lignin content, in which as AAEM content increased, the lignin content decreased as shown in Figure 2.10(a). On the other hand, Lv et al. (2010) reported based on experiment conducted that total AAEM species in biomass was directly proportional to cellulose content, given by the correlation as shown in Figure 2.10(b).
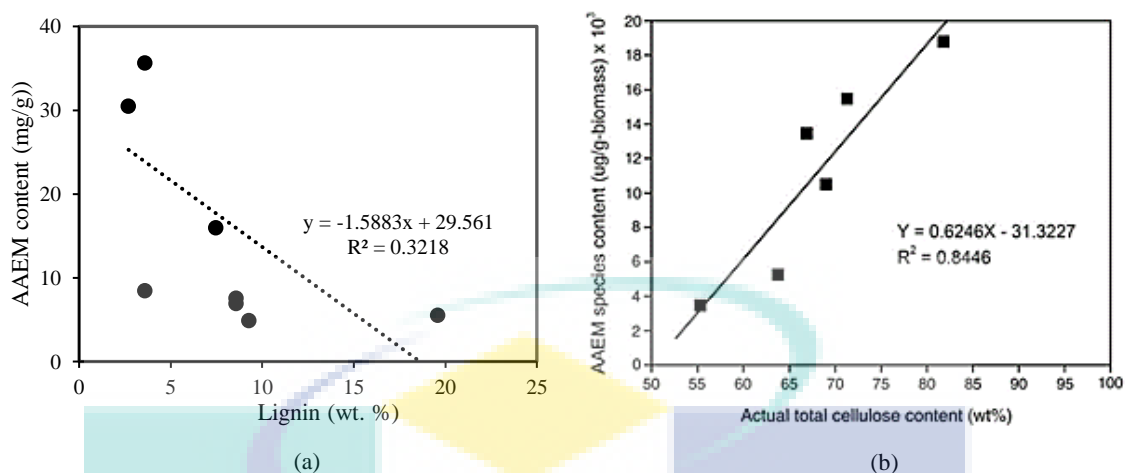
Figure 2.10   A correlation between total AAEM content to (a) lignin and (b) cellulose content in biomass

Source: (a) Fahmi et al. (2007; 2008) and (b) Lv et al. (2010)

Ash content

Apart from the main feedstock compositions as mentioned above, ash presences in feedstock also contribute to different pattern of pyrolysis products and thermal decomposition behaviour. Ash consisted commonly in the range of 0.2 – 1 % (Vigouroux, 2001). Ash content of biomass consist of mineral and alkali matters, with the major elements of alkali metals are Na and K. Ash in biomass having the greatest contribution in inhibiting the bio-oil production. Thus, if the ash content decreased, the total amount of liquid yields would be increased as shown in Figure 2.11 (Fahmi et al., 2008). As indicated in Figure 2.11, the oil yields can drop to below 50 wt. % if the feedstock has high ash. This is due to the undesirable reaction where ash catalyses reactions compete with biomass pyrolysis, leading to increasing formation of water and gas at the expense of liquid organics (Butler et al., 2011). Raveendran et al. (1995) investigated the influence of ash in biomass and he suggested that deashing of biomass can increase the volatile yield, initial decomposition temperature and pyrolysis rate, as well as results in a better quality of bio-oil. To slow down ageing and prevent phase separation of bio-oil during storage, maximum level of 3 % ash in feedstock are recommended (Abdullah & Gerhauser, 2008). One suggested way to prevail over the problem for feedstock with high ash content is pre-treatment washing the feedstock with acid or water prior to pyrolysis experiment (Butler et al., 2011).
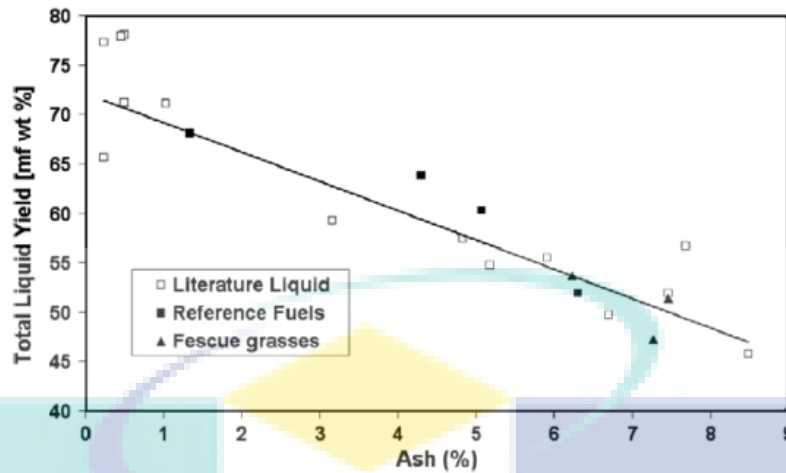
Figure 2.11   Relationship between total liquid yield (mf %) against ash content

Source: Fahmi et al. (2008)

Extractive

Extractives are the organic matters which present substantially in forestry and agriculture biomass. Extractives include essential oil, fat, waxes, phenolic, protein alkaloid, simple sugars, pectines, mucilages, terpenes, gums, resins, starches, glycosides and saponins (Mohan et al., 2006). The amount and composition of extractives in plant biomass vary greatly, relying upon the geographic and plant species (Ballesteros, Ballesteros, Cara, Saez, Castro, Manzanares, Negro & Oliva, 2011). Pyrolysis of biomass containing varying percentage of extractive content results in different degree of solubility, polarity and density which ultimately lead to inhomogeneity of resulting bio-oil product.

2.3.2.3   Moisture Content

Moisture in wood exists in three forms; (i) free water, which is mechanically held to the walls of the cell cavities in the structure of wood. The energy needed to release this water is slightly greater than the latent heat of vaporisation; (ii) bound water, which is approximately 30 % of the oven-dry weight of the wood. In this case, the water molecules are attached to the cell walls via hydrogen bonds, so energy in excess of the latent heat is required to release this water; (iii) constitution water, which is part of the wood polymer molecules. It is formed during pyrolysis and liberated along with the other pyrolysis products (Nurbakhsh Said, 1989).

Feedstock moisture has a direct effect on the reactions that occur during pyrolysis (Vigouroux, 2001) by affecting both the solid internal temperature history (due to the endothermic evaporation) and the total energy required to bring the charge to the pyrolysis temperature (Zaror & Pyle, 1982). The rate of moisture removal depends upon the rate of biomass heating rate and final pyrolysis temperature (Akhtar & NorAishah, 2012). Too high moisture content in biomass slowdown the biomass heating rate and need more energy which the biomass with 40% initial moisture content required extra energy of 1120 kJ/kg dry wood energy to commence pyrolysis reaction as compared to dry wood sample (Zaror & Pyle, 1982). Thus, the rate of biomass heating and final pyrolysis temperature show a significant dependence on initial moisture present in biomass (Demirbas, 2004). Moreover, initial moisture content in biomass also contribute to the amount of water content in total bio-oil yield due to moisture present directly added into aqueous oil product. Demirbaş (2005) conducted the experiment of relationship between initial moisture content and the liquid yield from pyrolysis of sawdust and the results showed the increasing in water content approximately 3 % for spruce biomass sample with the variations in initial moisture. He also observed approximately 6 % higher in liquid yields with 11.5 % initial moisture contents in spruce biomass pyrolysis compared to dry spruce sample. This is due to better stabilisation of biomass fragment and enhancement in water content of oil. Hence, for the purpose of the liquid bio-oil yield, the role of initial moisture seems beneficial and helpful to achieve high liquid yield through both stabilisation of the pyrolysis fragments and dissolution of soluble fragments (Akhtar & NorAishah, 2012).

On the other hand, in term of composition and physical properties of pyrolytic bio-oil produced, initial moisture of biomass is significantly sensitive especially to prepare the oil for the purpose of transportation fuel. During pyrolysis, almost all of the initial moisture contents appear in the aqueous product fraction. Typically, when the feed moisture content is less than 10 %, water content in liquid yield usually lie within the range of 18 – 25 % (Scott et al., 1999). Besides contributed from biomass initial moisture, the water in oil also originate from dehydration reactions (Azeez et al., 2010), and catalytic cracking (Fahmi et al., 2008), as well as, decomposition of oxygenates present in solid feed and water-gas shift reactions during pyrolysis process. High water content in oil lowers the fuel value of bio-oil by affecting the physical properties of oil such as chemical stability, viscosity, corrosiveness and pH (Venderbosch & Prins, 2011). Therefore, to avoid misconception in respect of aqueous product yield, the actual amount

of aqueous product should only takes into account the amount of water produced during pyrolysis, regardless of the initial moisture content (Akhtar & NorAishah, 2012).

For the bio-oil production with the objective of fuel transportation utilisation, the low initial moisture contents in biomass are advisable prior to pyrolysis process. The advantages getting from low initial moisture content include; (i) low heat energy requirements for vaporisation and commencement of pyrolysis reaction, (ii) reduction in residence time, and (iii) better oil quality (Akhtar & NorAishah, 2012). However, completely dried biomass feedstock suffers heat transfer limitations due to its low heat conductivity. Thus, minimum amount of initial moisture is still needed because water acts as reactant for biomass species and as heat transfer medium, which enhances pyrolysis (Akhtar & NorAishah, 2012).

2.4   Feedstock Treatment

Biomass contains very actives natural catalysts within its structure, called AAEM. Previous literatures have demonstrated that, if AAEM in biomass are removed before pyrolysis, mechanism of thermal decomposition is markedly affected and only depolymerisation reaction is predominated, rather than fragmentation (Scott et al., 2000). There are two ways to remove AAEM in bio-oil, either using hot filtration technique before condensation or remove AAEM from biomass itself via washing technique prior to pyrolysis process. The latter seems to be more effective way to achieves substantial AAEM removal from bio-oil (Scott et al., 2001; Várhegyi, Grønli & Di Blasi, 2004; Fahmi et al., 2008). Apart of washing, impregnated and ion-exchange methods also have been practiced in fast pyrolysis studies. Both methods are applied mainly to investigate the changes in inorganic metals behaviour in biomass, and so forth to propose the best practice for bio-oil production.

2.4.1   Washing Method

Washing of mineral matter is one of the best practice options to remove cation elements in wood prior to pyrolysis process. This method is principally conducted to minimise the effect of AAEM during thermal conversion by producing liquid rich in anhydrosugars (especially anhydroglucose and anhydropentoses). Washing include dilute acid (or ion exchange), hot and cold water washing (Akhtar & NorAishah, 2012). For comparison, acid washing is more applicable to remove acid soluble or alkaline species

present in wood. This method also leads to the partial hydrolysis of biomass components, as well (Akhtar & NorAishah, 2012). While, the hot water washing is capable of removing major components of mineral matter from wood (Scott et al., 2000). According to previous studies, washing with hot water washing technique alone was able to remove a major portion of alkaline cations and mineral matter for wide range of biomass species (Mszros, Vrhegyi, Jakab & Marosvlgyi, 2004). For commercial scales, the application of rain leaching of feedstock in the field after harvesting could be considered for pretreatment (Coulson, 2006). For the purpose of thermal conversion of cellulose and hemicellulose to anhydrosugars, deionised washing technic is more than sufficient to be used (Scott et al., 2000).

Mourant et al. (2011) reported in their study on malle wood that AAEM species are presence in different form, with numerous location which bound at different degree to cell constituent and at different depth from the cell lumen. These AAEM sometime easy to remove by water washing, and to what extent, it's difficult to remove and need acid washing technique. This is attributed to AAEM bonding which appear to act as 3-D cross-linking point within biomass structure, and so forth, played an important role during pyrolysis reaction. Mourant et al. also reported that washing treatment, regardless of their length of treatment, were generally quite successful at removing large fraction of AAEM species. Based on the report of Eom et al. (2011), pre-treatment washing on biomass indicated the thermal decomposition at different rates which increased in the order of HF-treated biomass (1.15 %/°C) < tap H_2O-treated biomass (1.19 %/°C) < deionised H_2O-treated biomass (1.23 %/°C) < HCl-treated biomass (1.55 %/°C).

Many studies suggested that washing treatment can improve thermal decomposition reaction by reducing catalysing effect of natural catalyst and thus, improve bio-oil quality by increase anhydrosugars and minimising ash content. However, pyrolysis experiments conducted by Fahmi et al. (2008) on washed *Festuca Arundinace* had proven that lower AAEM concentration results in less cracking of volatile and further produce less reaction water in liquid oil, which finally lead to the increasing in higher heavy molecular weight concentration. This resulting liquid has a higher viscosity and lower stability as compared to bio-oil derived natural feedstock. On the other hand, in the aspect of heating value and water content, washed feedstock provides better quality. The experiment also indicated that the molecular weight and viscosity of pyrolytic oil would

be higher if lignin content in washed feedstock also higher attributed to lower reaction water produced during pyrolysis and the increase in heavier lignin derivatives.

Mourant et al. (2011) in their experimental works also reported the same finding, in which AAEM removal only by acid-washing produce less reaction water with total bio-oil yield remain unchanged, indicating that organic fraction was increased slightly, resulting in heavier bio-oil. There are two possibilities exist; (i) AAEM species (especially divalent Ca and Mg) could be bound in the form of carboxylates, joining and acting as stabilising 3-D cross-linked of lignin or between lignin and holocellulose in biomass structures. When introduced to acid, the cations were replaced by H^+, resulting in disintegration (structure relaxation) and lower the degree of these AAEM-related crosslink (Chaiwat, Hasegawa, Kori & Mae, 2008). This would facilitate the releasing of large lignin fragments during pyrolysis. This reaction result in the increasing of anhydrosugars (principally levoglucosan and anhydropentoses) and lignin-derived oligometric compounds yields in bio-oil, and decrease the chance of reactions to form water and light organic compounds; (ii) Water-soluble AAEMs species consisting roughly 70 % of total AAEM content, and well dispersed in the wood structure. Since AAEM also catalysing water-forming reactions during pyrolysis, thus, their removal did not significantly affect the water formation. The first possibility is more likely important to occur during pyrolysis. In addition, acid-washing also has proven to give nearly doubling of sugars yields, while water washing only resulted in limited increasing of sugars. Mourant et al. concluded washing pre-treatment produce higher bio-oil viscosity as compared to untreated biomass, and the viscosity of bio-oil would increase drastically over-time in acid washed-biomass as compared to water washed-biomass. The viscosity has been proven to be sensitive to the present of heavy components in bio-oil, instead of AAEM content in biomass feedstock.

2.4.2 Impregnation Method

The present of mineral matter in biomass also can be changed by the addition of metal ions or metal salts via physical adsorption on the surface of demineralised biomass particles. Richards and Zheng (1991) reported in their publication that cation K^+, Li^+ and Ca^+ induced high char and low tar yields, in which the tar yield was very low in levoglucosan. Nevertheless, of all of ions investigated, transition metals impregnated feedstock promoted in enhancing levoglucosan yield. In addition to cation, their report

also considers on anion effect. Chlorides (particularly copper and iron chlorides) assisted in improving levoglucosan yield. Sulphates (especially $FeSO_4$), as well, at low level was sufficient to catalyst the formation of both levoglucosan and levoglucosenone.

Eom et al. (2012) conducted the experiments by impregnated feedstock with inorganic metal chlorides for the aim to study the effect of different concentrations of inorganic metal on primary thermal degradation. Based on their study, they found that lower molecular compounds such as glycolaldehyde, acetic acid, acetol and butanedial in pyrolytic liquid were increased as the K content increased. Their result also consistent with formation route as suggested by Shen, Gu and Bridgwater (2010), in which, at higher level of K, the formation of acetic acid (mainly formed from O-acetyl group) would be enhanced via dehydration and subsequent rehydration of glycolaldehyde. Eom, Kim, Kim, et al. also reported the yields of levoglucosan, furans and pyrans remain decreasing with the increasing in K concentration. Similar pattern of levoglucosan yield also was obtained when level of Ca concentration in sample was increased. However, their result contradict with finding reported by Kleen and Gellerstedt (1995). As compared to both K and Ca impregnated samples, Mg (transition metal) impregnated sample solely gave a different pattern in levoglucosan yield in pyrolytic oil, in which levoglucosan yield was observed to be gradually enhanced, and in the meantime suppresses glycolaldehyde formation.

2.5   Bio-oil

Bio-oil or crude pyrolysis liquid is a synthetic fuel that is extracted from biomass to liquid via thermochemical conversion technologies. Bio-oil also synonyms with the names of pyrolysis oil, pyrolysis liquid, bio-crude oil, wood liquid, wood oil, liquid smoke, wood distillates, pyroligneous acid and liquid wood (Mohan et al., 2006).

Bio-oil is a free-flowing organic liquid fraction, comprised of highly oxygenated compound, and having dark red-brown to almost black liquid colour. The colour level of bio-oil is dependent upon the chemical composition of feedstock and the amount of fine char present in the oil (Venderbosch & Prins, 2011; Mohan et al., 2006). Tar product of pyrolysis is included in bio-oil. Bio-oil is produced from hot volatiles resulting from pyrolysis reaction at high temperature along with short reactor time, and further experiencing rapid cooling or quenching. This process produces condensate.

Bio-oil is not a product of thermodynamic equilibrium during pyrolysis but is produced with short reactor times and rapid cooling or quenching from the pyrolysis temperatures (Zhang, Chang, Wang & Xu, 2007). This process produces a condensate that is also not at thermodynamic equilibrium at storage temperatures (Zhang et al., 2007). The chemical composition of the bio-oil tends to change toward thermodynamic equilibrium during storage (Zhang et al., 2007). Pyrolysis oil can be used as a liquid fuel, which can be used as a replacement for natural gas as well as coal and provides many advantages; wood pyrolysis oil does not contribute to CO_2 emission, low sulphur content that reduce sulphur emission, carbon monoxide and hydrocarbon emissions are usually low (Vigouroux, 2001). Bio-oil is acidic, unstable, viscous liquids containing solids and a large amount of chemically dissolved water (Ran Xu, 2010). Heating value, density, and viscosity of pyrolysis liquid vary with water and additives (Chiaramonti, Oasmaa & Solantausta, 2007). Bio-oil varies considerably and depends on many factors such as feedstock species, feedstock moisture content, process parameters, reactor, recovery-unit design and scale of operation (Zhang, 1996).

Pyrolysis liquid is formed by rapidly and simultaneously depolymerising and fragmenting cellulose, hemicelluloses and lignin with a rapid increase in temperature. Rapid quenching then 'freezes in' the intermediate products of the fast degradation of these three components. Rapid quenching traps many products that would further react (degrade, cleave or condensate with other molecules) if the residence time at high temperature was extended. Bio-oil contains many reactive species, which contribute to unusual attributes.

2.5.1 Bio-oil Nature

Fast pyrolysis bio-oil liquid has been produced in the laboratory from numerous biomass feedstock. The physical properties of bio-oil result from the chemical composition of the biomass feedstock, and it is significantly differ from that of petroleum-derived oils (Czernik & Bridgwater, 2004). Bio-oil is multicomponent mixtures which comprise quite a lot of water, more or less solid particles and hundreds of organic compounds that belong to alcohols, acids, sugar, aldehydes, esters, ethers, ketones, furans, phenols, nitrogen compounds and multifunctional compounds (Lu et al., 2009), as well as, lignin-derived oligomers (Xiu & Shahbazi, 2012) with all these compounds can be classified as aliphatic hydrocarbons (alkanes, alkenes), aromatics hydrocarbons

with a single ring (benzene, toluene and alkylated derivatives) and polycyclic aromatic hydrocarbons (PAHs) with more than one single ring, phenolics and other oxygenated compounds (carboxylic acids, carbonyls, alcohols and furans) (Wang et al., 2010). Bio-oil compounds has different size molecules which derived primarily from depolymerisation and fragmentation reactions of three key biomass components; cellulose, hemicellulose and lignin. Hence, the elemental compositions of bio-oil resemble that of biomass (Mohan et al., 2006). Table 2.2 shows the distribution of some compound detected by GC-MS analysis for *Pterocarpus Indicus* (hardwood type) (Luo, Wang, Liao, Zhou, Gu & Cen, 2004). Research conducted by Adam, Blazso, Meszaros, Stocker, Nilsen, Bouzga, Hustad, Gronli and Oye (2005) on spruce wood also exhibits many similar results with those in Table 2.2. Most of the compounds are in low concentrations (Lu et al., 2009). The molecular weights of these compounds vary significantly, as low as 18 for water to as high as 5000 or more for pyrolytic lignin. The average molecular weight varies in the range of 370 – 1000 g/mol (Lu et al., 2009).

Bio-oil is highly polar compounds (esters, ethers and phenolics) and non-polar compounds (hexane and other hydrocarbons) where these compounds are not completely mutual soluble (Lu et al., 2009). Bio-oil can be considered as microemulsions which water and water soluble molecules form the continuous phase, water insoluble materials are dispersed as micelles in bio-oil and some multipolar compounds act as emulsifiers to stabilise the structures (Radlein, 2002). Fractionation is widely used to separate bio-oil into groups of compounds to facilitate analysis and quantification of compounds (Oasmaa & Kuoppala, 2003; Garcia-Perez et al., 2007). However, complete chemical characterization of bio-oil is almost impossible mainly due to the presence of pyrolytic lignin (Meier, 1999). The pyrolytic lignin is derived from the partial cracking of lignin molecules, and they cannot be determined by gas chromatography or high-performance liquid chromatography. Analysis of pyrolytic lignin shows that they are constituted by oligomers (mainly tetramers) and their basic units are very similar to milled wood lignin (Lu et al., 2009). Owing to the presence of large amounts of oxygenated components, the oil has a polar nature and immiscible with hydrocarbon fuels (Venderbosch & Prins, 2011). However, bio-oil is miscible with both ethanol and methanol (Mohan et al., 2006). Bio-oil can be stored, pumped and transported in a similar manner of that conventional petroleum-based product, and can be combusted directly in boiler, gas turbines and diesel engine for heat and power applications (Czernik & Bridgwater, 2004).

Table 2.2 Relative content of main compounds in organic composition of bio-oil produced from *Pterocarpus Indicus*

Compound	Relative content (%)
Furfural	9.06
Acetoxyacetone, 1-hydroxyl	1.21
Furfural, 5-methyl	1.82
Phenol	2.55
2-Cyclopentane-1-one, 3-methyl	1.58
Benzaldehyde, 2-hydroxyl	2.70
Phenol, 2-methyl	5.04
Phenol, 4-methyl	0.51
Phenol, 2-methoxyl	0.27
Phenol, 2,4-dimethyl	9.62
Phenol, 4-ethyl	2.18
Phenol, 2-methoxy-5-methyl	4.15
Phenol, 2-methoxy-4-methyl	0.55
Benzene, 1,2,4-trimethoxyl	3.80
Phenol, 2,6-dimethyl-4-(1-propenyl)	4.25
1,2-Benzenedicarboxylic acid, diisooctyl ester	1.80
2-Furanone	5.70
Levoglucosan	6.75
Phenol, 2,6-dimethoxy-4-propenyl	3.14
Furanone, 5-methyl	0.49
Acetophenone, 1-(4-hydroxy-3-methoxy)	2.94
Vanillin	6.35
Benzaldehyde, 3,5-dimethyl-4-hydroxyl	4.54
Cinnamic aldehyde, 3,5-demethoxy-4-hydroxyl	2.19

Source: Luo et al. (2004)

2.5.2 Bio-oil Properties

The typical physical properties data for wood derived bio-oil as compared to conventional fuels are listed in Table 2.3. Light fuel oil in table consists mainly aliphatic and aromatic hydrocarbons ($C_9 – C_{25}$) that are immiscible with highly polar pyrolysis liquids (Chiaramonti et al., 2007). The explanations of these properties were discussed below. The application of bio-oil is so far limited by these undesired properties, unless it can be burned directly as a substitute fuel oil in various static applications such as boilers and furnaces (Bridgwater & Peacocke, 2000). Despite of these frailty of fuel properties,

bio-oil also has some promising properties, such as less toxicity, good lubricant and greater biodegradation than petroleum fuel (Zhang, Liu, Yin & Mei, 2013).

Table 2.3   Typical physical properties of wood pyrolysis liquids and minerals oils

Physical properties	Pyrolysis liquids	Light fuel oil	Heavy fuel oil
Moisture content (wt. %)	20 – 30	0.0025	0.1
Solids (wt. %)	<0.5	0	0.2 – 1.0
pH	2 – 3	Neutral	N/A
Elemental composition (wt. %)			
C	32 – 48	86	85.6
H	7 – 8.5	13.6	10.3
O	44 – 60	0	0.6
N	<0.4	0.2	0.6
S	<0.05	<0.18	2.5
Vanadium, ppm	0.5	<0.05	100
Sodium, ppm	38	<0.01	20
Calcium, ppm	100	N/A	1
Potassium, ppm	220	<0.02	1
Chloride, ppm	80	N/A	3
Ash	<0.2	0.01	0.03
LHV (MJ/kg)	13 – 18	40.3	40.7
Stability	Unstable	Stable	Stable
Viscosity, cSt	13 – 35 at 40 °C	3.0 – 7.5 at 40 °C	351 at 50 °C
Distillability	Not distillable	160 – 400 °C	95 – 195 °C

Source: Chiaramonti et al. (2007)

2.5.2.1   Water Content

Water is the most abundant single component in bio-oils (Lu et al., 2009). Their present is affected by feedstock moisture and yield of organics in bio-oil (Oasmaa, Elliott & Muller, 2009). Some water in bio-oil is in the form of aldehyde hydrates, which much of it probably hydrogen bonded to polar (oxygenated) organic compounds (Lu et al., 2009). Water content in bio-oil varies over a wide range of 20 – 30 % (Chiaramonti et al., 2007), which represent a serious drawback for many potential applications (Venderbosch & Prins, 2011). Water in bio-oil results from the original moisture in the feedstock and as a product of both the hydration reactions (mainly dehydration of hemicellulose, called pyrolytic water (Azeez et al., 2010)) and reaction water (resulted from catalytic cracking (Fahmi et al., 2008) which occurring during fast pyrolysis process, as well as,

condensation reaction (ageing during storage) (Fahmi et al., 2008; Lu et al., 2009; Ran Xu, 2010). Pyrolytic and reaction waters are estimated by subtracting the initial moisture content of feedstock from the total water content of the liquid product.

The presence of water has both positive and negative effects on the oil properties. It present reduces oil stability and lowers its heating value, especially LHV and flame temperature, which limits its application as a fuel oil substitution (Venderbosch & Prins, 2011). In addition, water in oil also leads to the increase in ignition delay and in certain cases contribute to the decrease of combustion rate compared to hydrocarbon fuels. On the other hand, it improves bio-oil flowing characteristics by reduces the viscosity, which is beneficial for atomisation and combustion of the bio-oil in the engine (Zhang et al., 2007). Shihadeh (2002) compared the bio-oil of National Renewable Energy Laboratory (NREL) to those of Renewable Fuels and Chemicals from Non-Food Biomass (ENSYN) and found that additional thermal cracking improved it chemical and vaporisation characteristics. NREL oil gave the better performance and ignition which derived from bio-oil lower water content and lower molecular weight. Water presence also provide a more uniform temperature profile in the cylinder of a diesel engine and lower NO_x emissions (Czernik & Bridgwater, 2004).

Bio-oil has limited solubility with water (Lu et al., 2009). With the increase in water content, the microemulsion structure will destroy and bio-oil tends to separate into an aqueous phase and heavier organic phase. Once this kind of phase separation takes place, it will bring great trouble to the bio-oil utilizations. To maintain homogeneity, the upper limit of the water content is determined by the chemical compositions of bio-oils which are usually in the range of 30 – 35 wt. % (Radlein., 2002). In order to prevent phase separation and control water in bio-oils at favourable level, the original moisture in feedstock required to be below than 10 wt. % (Lu et al., 2009).

Water is hard to remove from bio-oil (Lu et al., 2009). It cannot be removed by conventional methods like distillation (Bridgwater, 1999), since the heated oil tend to polymerised. Thus, careful control of moisture control of the bio-oil prior to pyrolysis as mentioned above is important for assuring high-quality bio-oil (Venderbosch & Prins, 2011). Selective condensation also may reduce the water content of one or more fractions but it leads to possible loss of low molecular weight volatiles components (Bridgwater, 1999).

2.5.2.2 Solid Content

Solid content is measured as the amount of solvent insoluble materials (Lu et al., 2009). Solids in bio-oil present mainly char particles and other materials such as fluidised bed materials used in pyrolysis process (Lu et al., 2009). Cyclone separators are commonly installed in pyrolysis system which sets to get rid of solids in pyrolysis vapour, but they are only efficient in separating large particles with the size larger than 10 µm. Many fine particles that escaped from separation will be condensed with pyrolysis vapour in bio-oil liquid. Solid content in bio-oil can reach as high as 3 wt. % and the particles size typically varies in the range of 1 – 200 µm with most particles being below 10 µm (Lu et al., 2009). Solid particles in bio-oil contribute to negative effect to the combustion and storage of bio-oils (Oasmaa & Czernik, 1999) by; (i) fine char particles tends to agglomerate slowly and settle at the bottom of the vessel, (ii) solids increase the apparent viscosity of bio-oil which leads to difficulties in pumping and atomization, (iii) solids will cause erosion and blockage to the fuel injection systems, (iv) char particles will act as a catalysts to accelerate the ageing reactions of bio-oil, resulting in the increase in viscosity and even in phase separation with solid absorbed with pyrolytic lignin to form gummy tars, and (v) char particles will lead to form slow burning carbonaceous cenospheres and consequently unburned particles in the flue gas (Oasmaa & Czernik, 1999).

2.5.2.3 Acidity and Corrosiveness

Bio-oil contain substantial amounts of carboxylic acids, such as formic, acetic and propanoic acids, which results in a pH of 2 – 3 (Zhang et al., 2007; Ran Xu, 2010). Acidity makes bio-oil very corrosive to common construction materials like aluminium, copper and carbon steel, and can affect some sealing materials (Czernik & Bridgwater, 2004). Corrosiveness behaviour extremely severe at elevated temperature and increased in water content. Thus, the storage of bio-oil should be in acid-proof materials like stainless-steel or poly-olefin (Venderbosch & Prins, 2011), and need to be upgraded before using bio-oil as transportation fuel (Zhang et al., 2007).

2.5.2.4 Oxygen Content

The oxygen content in the bio-oil is usually 44 - 60 wt. % (Chiaramonti et al., 2007). This oxygen is present in more than 300 compounds, which the distribution of oxygen in these compounds mostly depends on the type of biomass used as a feedstock

and severity of the process (temperature, residence time and heating rate) (Czernik & Bridgwater, 2004). Oxygen is present almost all in organic compounds in bio-oil (Lu et al., 2009). Because of their complex compositions, bio-oil shows a wide range of boiling point temperature, where during the distillation, the slow heating induces the polymerization of some reactive components, and bio-oil starts boiling below 100 °C, while stopping at 250 – 280 °C, leaving 35 – 50 wt. % as solid residues. Therefore, bio-oil cannot be used in the instance of complete evaporation before combustion (Zhang et al., 2007). The amount of oxygen content present in oil component is the primary issue that distinguishes in the properties and behaviour between biomass pyrolysis oil and hydrocarbon fuel (Ran Xu, 2010). The high oxygen content contributes to low energy density (heating value) compared to conventional fuel by 50 % immiscibility with hydrocarbon fuel (Zhang et al., 2007; Ran Xu, 2010). Organic oxygen content in oil also leads to thermal instability which hinders the storage stability of bio-oil (Czernik & Bridgwater, 2004; Lu et al., 2009). The oxygen content in bio-oil can be reduced or removed by means convert the oxygen into CO, CO_2 or H_2O during pyrolysis process. There are two methods of removing oxygen in bio-oil; (i) typical catalytic hydrotreating with hydrogen or hydrogen and carbon monoxide under high pressure, (ii) utilising cracking catalysts (zeolites and molecular sieves) under atmospheric pressure without hydrogen (Wang et al., 2010).

2.5.2.5   Ash Content

The amount of ash content can be assessed as the amount of residue when bio-oil is heated to the temperature of 850 °C overnight with the present of oxygen (Lu et al., 2009). Ash content in bio-oil depends on the properties of the original biomass composition and pyrolysis systems, especially at cyclone and hot filtration system (Ran Xu, 2010). Most pyrolysis system only employed cyclone as char and ash removal system, however, some fine char inevitably carried over which resulting in catalysing secondary cracking in vapour phase, and eventually result in bio-oil instability. Thus, installation of two-staged char removal system which include hot filter downstream to cyclone can provide better efficiency in char separation. During pyrolysis process, most inorganic compounds in biomass isolate in char particles, thus, the ash content in char can be 3 – 8 times higher than those of the feedstock (Lu et al., 2009). If ash content in bio-oil higher than 0.1 %, it can cause erosion, corrosion and kicking problems in engines and

valves and even deterioration (Zhang et al., 2007). Moreover, ash in bio-oil can enhance the undesired ageing of the oil (Ran Xu, 2010). Alkali metals such as sodium, potassium and vanadium in ash are problematic components of the ash which they are responsible for high temperature corrosion and deposition, while calcium is responsible for hard deposits (Zhang et al., 2007). Metals in ashes also are believed to cause the same effect as alkali metals (Lu et al., 2009).

2.5.2.6   Heating Value

Typically, lower heating value (LHV) of the bio-oil is the range of 13 – 18 MJ/kg which the values depending on the type of feedstock and production processes (Chiaramonti et al., 2007). The LHV of bio-oil is around 40 – 45 wt. % of that exhibited by hydrocarbon fuel and in term of volume basis, the LHV is estimated about 60 % as compared to heating value of conventional fuels (Czernik & Bridgwater, 2004) due to the water presence, high oxygen content and high bio-oil density. A typical LHV of bio-oil based on dry matter is 19 - 22 MJ/kg for hardwood, 18 – 21 MJ/kg for softwood and bio-oil with water content of 25 wt. % has typical LHV around 15 – 16 MJ/kg (Oasmaa, Koponen, Levander & Tapola, 1997). Usually the bio-oil of oil plants have a higher heating value compared with those of straw, wood or agriculture residues (Zhang et al., 2007). Beis, Ona and Kockar (2002) conducted pyrolysis experiments on a sample of safflower seed and obtained bio-oil with a heating value of 41.0 MJ/kg and a maximum yield of 44 %. Ozcimen and Karaosmanoglu (2004) produced bio-oil from rapeseed cake in a fixed bed with a heating value of 36.4 MJ/kg and a yield of 59.7 %. However, taking wood and agricultural residues as raw materials, the bio-oil have a heating value of about 20 MJ/kg and a yield up to 70-80 %.

2.5.2.7   Stability

Stability is an important property for bio-oil which its change characteristics over time (Venderbosch & Prins, 2011). Chemical reactions of bio-oil product from fast pyrolysis process is thermodynamically non-equilibrium reaction. The short residence times at high temperature zone followed by rapid thermal quenching results in a liquid product that is also not at equilibrium condition. Many components in oil will take part in diverse reactions that leads to oil's instability which can be describe as follows (Ran Xu, 2010):

Stability during storage

Chemical reaction may take place during bio-oil storage, including the reactions between various organics components present in bio-oil. The most unstable fraction is aldehydes, which it reacts with water to form hydrates, with phenolics to form resin and water, with alcohols to form hemiacetals, acetals and water, with protein to form dimmers, and with each other to form oligomers and resins. In addition, acids in bio-oil react with alcohols to form esters and water, merceptans react to forms dimer, olefins polymerise to form oligomers and polymer. Furthermore, oxidation of bio-oils by oxygen present in air, contribute to form more acids and reactive peroxides that catalyse the repolymerisation of unsaturated components (Lu et al., 2009). Other than that, char and ash also act as catalyst to accelerate ageing reactions and as a result of all these reactions, the properties of bio-oil will change with time. The changes lead to the increase in viscosity and water content, as well as, it tendency to separate (watery phase and organic phase) due to insoluble large molecules form from the polymerisation reactions (Oasmaa & Kuoppala, 2003; Ran Xu, 2010). Fratini, Bonini, Oasmaa, Solantausta and Teiseira (2006) concluded that the fundamental process in ageing related to phase separation was the results from the aggregation of pyrolytic lignin, where the process continued until the heaviest lignin-rich fraction separated out from the bio-oil matrix to form viscous sludge. According to Fahmi et al. (2008), bio-oil derived feedstock with higher lignin content will be undergone for a greater changes. This statement agreed with Mourant et al. (2011). The chemical changes involve during ageing was the increase in high molecular mass lignin materials, decrease in aldehydes, ketones and lignin monomers. The physical changes involve the increase in viscosity, water content, density and flash point, and a decrease in heating value (Oasmaa & Kuoppala, 2003).

Stability at high temperature

At elevated temperature, ageing reactions can be observed as four stages; thickening, phase separation, gummy formation from the pyrolytic lignin at temperature around 140 °C and char formation from the gummy phase at higher temperature (Oasmaa et al., 1997). At room temperature the ageing of bio-oil occurs over periods of month or years, depending on the type of feedstock and its initial quality. However, at elevated temperatures the polymerization reactions are enhanced significantly. Chaala, Ba, Garcia-Perez and Roy (2004) conducted a research to observe the effect of temperature on bio-

oil properties. The result gave a significant acceleration of oil ageing at a temperature of 80 °C or higher, where it shows the increasing in molecular weight for maintaining the bio-oil for a week at 80 °C was equivalent to maintain the sample for a year at room temperature. Therefore, it is recommended to avoid long bio-oil storage at temperature above 50 °C (Venderbosch & Prins, 2011).

2.5.2.8 Viscosity and Aging

Viscosity of a fluid is a measure of a resistance of the liquid to flow (Oasmaa et al., 1997). Viscosity plays an important role in the design and operations of the fuel injection systems, as well as, in atomisation quality and subsequent combustion properties of the fuel (Lu et al., 2009). The viscosity of bio-oil can vary over a wide range of depending on the water content and the amount of light components in the oil (Venderbosch & Prins, 2011). Viscosity of oil can be reduced by increase the temperature, which makes the oil flow much faster than petroleum-derived oil, so that even very viscous bio-oil can be easily pumped after a moderate preheating. However, at the temperature above 80 °C, the bio-oil properties would be totally changed due to acceleration of ageing reactions (Boucher, Chaala, Pakdel & Roy, 2000). A viscosity also can be reduced with the addition of polar solvents such as methanol or acetone. However, the oil viscosity is observed to be increasing with time if they were stored or handled at high temperature, with exposure to light and the presence of O_2 (Dickerson & Soria, 2013). It is believed due to the chemical reactions that occur between various compounds present in oil, where lead to the formation of larger molecules and also reaction of oil components with oxygen in air (Czernik & Bridgwater, 2004). Fahmi et al. (2008) reported, in bio-oil derived non-woody feedstock, levoglucosan content in bio-oil was increasing as ageing occurred at the expense of hydroxyacetaldehyde, resulted in the re-polymerisation. However, bio-oil derived woody feedstock behaves contrary and do not exhibit the same changes, possibly due to unsuited conditions for lower molecular weight in oil to reform larger molecular weight compounds, in which levoglucosan is one of such compounds (Fahmi et al., 2008).

2.5.2.9 Distillation

Bio-oil show a very wide range of boiling temperature due to various their chemical compositions. Besides water and volatile organic components, pyrolytic oil also

contains substantial amounts of non-volatiles materials such as sugars and oligometric phenolics (Oasmaa & Czernik, 1999). Thus, the slow heating of oil during distillation resulted in polymerisation of some reactive components and consequently, the oil starts boiling below 100 °C and distillation ends at 250 – 280 °C, with eventually leaving 35 – 50 °C of the polymerised materials as residue (Oasmaa & Czernik, 1999; Lu et al., 2009). Therefore, bio-oils cannot be used for applications that require complete evaporation before combustion.

2.5.2.10   Homogeneity

The homogeneity of bio-oil liquid is connected with the complex solubility and reactivity of a high number of compounds in liquid (Oasmaa et al., 1997). Normally, most bio-oil appears as homogenous solution (Lu et al., 2009). These kinds of bio-oil produced from many types' biomass materials which contain a few extractives (soluble materials) and will not undergo for phase separation due to dispersion of small amount of extractive in bio-oil matrix (Lu et al., 2009). However, for some biomass containing substantial amount of extractives, inhomogeneity of bio-oil is unavoidable. Oasmaa, Kuoppala, Gus and Solantausta (2003) recommended that extractive in bio-oil can be removed by letting the bio-oil to separate into two phase where the top phase is the frothy bio-oil enriched extractive and bottom phase is bio-oil with typical characteristics. Harinan (2004) conducted the analysis of the phase fraction of wood pyrolysis liquids and result showed that the top phase contains approximately the extractives (26 – 50 %), pyrolytic lignin (20 – 40 %) and water-soluble compound (20 – 40 %). Homogeneity of pyrolytic oil can be checked by analysing water content from different depths of the liquid (Oasmaa, Elliott & Muller, 2009). Even though most bio-oil is macroscopic single-phase liquid, in fact they still possess microscopic multiphase structure as discussed above.

2.6   Bio-oil Application

Bio-oil has the potential for multiple applications when used directly. These applications can range from a variety of combined heat and power, and the extraction of selected chemical products. Possibilities for bio-oil applications are given in Figure 2.12.
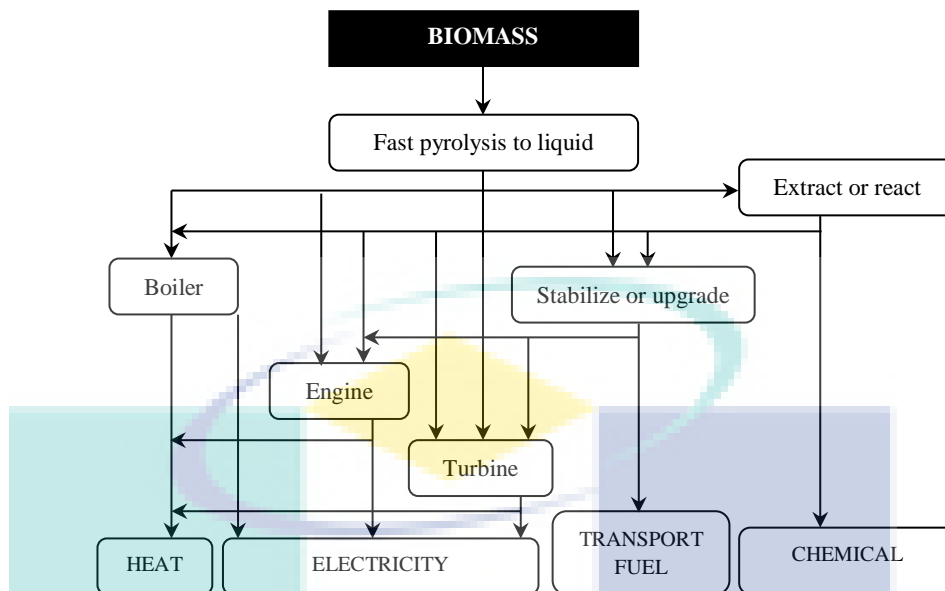
Figure 2.12   Bio-oil applications

Source: Czernik and Bridgwater (2004)

2.6.1   Heat and Power Generation

Bio-oil has higher energy density that of the original biomass and can be readily stored and transported, attracts special attentions. The properties of bio-oil result in several significant problems during its use as a fuel in standard equipment, such as boilers, engines and gas turbines constructed for combustion petroleum-derived fuel. Poor volatility, high viscosity, coking, and corrosiveness are probably the most challenging and have so far limited the range of bio-oil applications (Czernik & Bridgwater, 2004). It is necessary to conduct large-scale and long-duration tests on boilers, engines and gas turbines before accepting pyrolysis liquid as commercial fuel. These tests will require a substantial supply of liquids with specified properties established by the producers and users (Oasmaa & Peacocke, 2001).

2.6.2   Chemical Products

Bio-oil can also be used for the production of chemicals. For many centuries, wood pyrolysis liquid was a major source of chemicals, such as methanol, acetic acid, turpentine, tars and so on. At present, most of these compounds can be produced at a lower cost from other feedstock derived from natural gas, crude oil, or coal (Czernik & Bridgwater, 2004). Hundreds of the components of bio-oil are determined, and reclaiming one or more kinds of small and valuable chemicals arouses great interest among scholars

and businessmen. There are many substances that can be extracted from bio-oil, such as phenols used in the resins industry; volatile organic acids in the formation of de-icers; levoglucosan; hydroxyacetaldehyde; and some additives applied in the pharmaceutical, fibre synthesising or fertilizing industry; and flavouring agents in food products (Zhang et al., 2007). Among of many chemical extracted from bio-oil, levoglucosan is regard as an important product which has a potential application in the production of biodegradable plastics, and in the synthesis of high value specialty chemicals such as pharmaceuticals using chiral catalysts incorporating levoglucosan-based ligands (Longley, 1993).

2.6.3 Transportation Fuel

Biomass is considered to be a promising resource of global fuel production due to the diminishing supply of fossil fuel and increasing in environmental concern. As compared to fossil fuel, biomass energy for example bio-oil, has a great potential to be alternative source energy to substitute fossil fuel due to its advantages on reproducibility and resources universality (Xu, Jiang, Chen & Sun, 2010) and environmental protection. However, as a promising alternative energy source, direct application of bio-oil is limited due to present of ash content, high viscosity, high oxygen content, low heating value, thermal instability and high corrosiveness (Xiu & Shahbazi, 2012; Zhang et al., 2013) which lead to a series of problems in bio-oil applications. Thus, in order to improve bio-oil properties for practical application of liquid fuel, upgrading the quality of bio-oil is always necessary. However, the process of bio-oil upgrading is very difficult due to the complexity of bio-oil contents (Zhang et al., 2013) and it characteristics which differ with the feedstock compositions and pyrolysis process conditions. Although research on biomass fast pyrolysis for bio-oil production has been aroused extensively in recent years, there are still a lot of unknown mechanisms and process that have to be clarified before bio-oil can be used widely.

To serve as alternative fuel, final product of bio-oil is necessarily evaluated by its low O/C and high H/C ratios, where it indicates a higher quality liquid product (Dickerson & Soria, 2013). The suitability of bio-oil as hydrocarbon can be measured and compared in Van Krevelen diagram as shown in Figure 2.13.
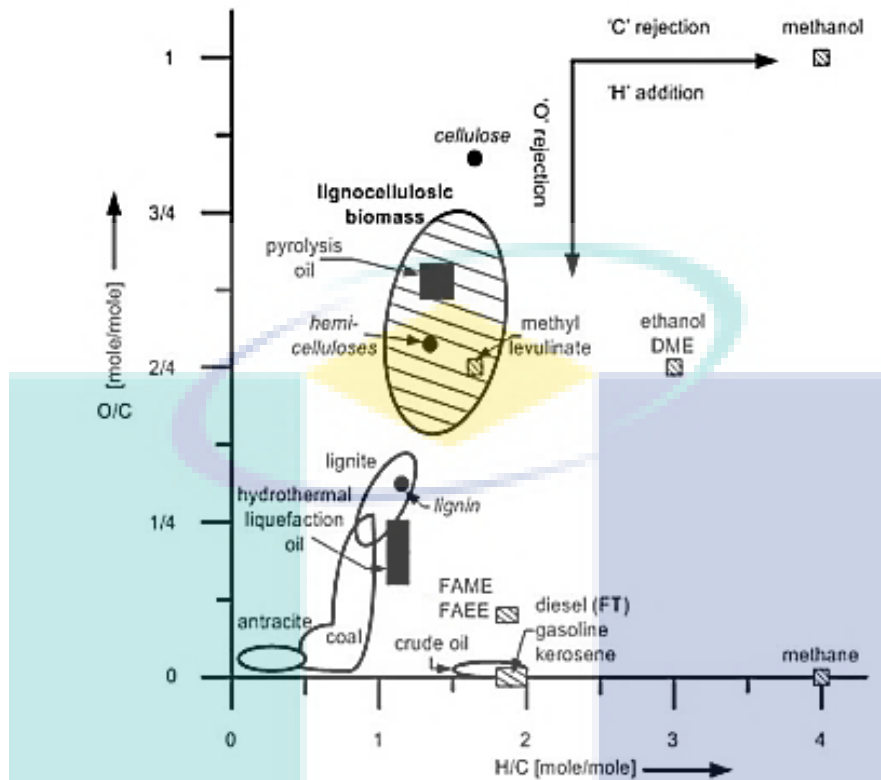
Figure 2.13   Van Krevelen Diagram with other products
Source: Kersten et al. (2007)

This diagram is used widely as an indicator to study the evolution and evaluate the suitability of oil samples and coals as ideal hydrocarbon product (Wildschut, 2009). 'Ideal hydrocarbon' in this diagram indicates the targeted ratios that should be achieved in order to serve and transform potential oil sample into transportation fuel, in which, ideal hydrocarbon possess value of oxygen content close to zero and H/C ratio ranging 1.5 to 2.0. Typical pyrolysis bio-oil lies within the range of H/C and O/C equal to 1.7 and 0.6, respectively (Wildschut, 2009). Other products such as methanol has a ratios value (H/C, O/C) = (4,1), methane is (4,0), and oils from high pressure thermal of biomass is (1.2, 0.13 – 0.25).

There are two ways to upgrade the quality of bio-oil; (i) improve or changing pyrolysis reaction chemically by manipulate the feedstock' composition and/or conducting pyrolysis in the presence of catalyst (Mohan et al., 2006), and (ii) modify the chemistry of bio-oil produced. At present, there are numerous researches have been

conducted to upgrade the quality value of bio-oil, including emulsification, catalytic cracking or hydrodeoxygenation.

2.7   Response Surface Methodology (RSM)

Response surface methodology (RSM) is a useful methodology derived from the combination of both specific mathematics and statistic manner. In addition, Montgomery (2012) defined that RSM is a collection of mathematical statistical techniques that are useful for the modelling and the analysis problems in which a response is influenced by several variables of factors, and the objective is to optimize this response. All the variables or factors are assumed continuous and controllable with negligible error whereas the response is assumed to be a random variable (Montgomery, 2012).

To assist the researcher in resolving problems related to optimum product design, procedure improvement or optimum system, RSM is the best way to provide a feasible 50 analysis and resolution program as the characteristic of an industrial system has been significantly affected. In most RSM problems, the form of the relationship between the response and the factors is unknown. Thus, the first step in RSM is to find a suitable approximation for the true functional relationship between response and the set of factors. If the response is well-modelled by linear function of the factors, then the approximating function is the first order model whereas if there is curvature in the optimum region, then polynomial of higher degree such as the second order model must be used (Montgomery, 2012).

RSM is a beneficial technique in obtaining the optimum experimental design and operational conditions for various industrial applications such as electronics, engineering, agriculture, chemical, biotechnology and food science (Chang & Shaw, 2009). There were several designs classed in RSM including Box-Behnken design (BBD), central composite design (CCD), hybrid design and 3-Level Factorial. However, all factorial designs do not have the property of being rotatable. 2k complete factorial designs are all rotatable, but 3k factorials are not. In order a design to be rotatable, the design points should construct a regular geometric figure such as a cube. Rotatable designs have the property of equal precision regardless of distance, which means that the standard deviation of the fitted value is the same for any distance from the centre of the design. This is a desirable property since it is not usually known which direction from the centre

point will be of the later interest. Rotatable designs make the fitted values precise without being affected by the direction, only by the distance from the centre point (Michael, John & Christopher, 2011). Fortunately, there are classes of designs to be used as alternatives to 3k factorial designs which do not have the property of being rotatable.

Two special classes of designs serving as alternatives to 3k factorial designs are central composite designs and Box-Behnken designs. Both of these designs are fractions of the 3k factorials, but they can be made rotatable and they make more efficient use of the experimental runs than 3k factorials. Efficiency is achieved by reducing the number of factor-level combinations from the one required using complete or fractional factorial experiments. Between these two designs, CCD is one of the favourable design in application of optimising fast pyrolysis process variables for the production of bio-oil from eucalyptus wood (Kumar et al., 2010), palm shell (Abnisa et al., 2011) and red oak (Ellens & Brown, 2012).

Kumar et al. (2010) pyrolysed 20 g samples of eucalyptus wood in a batch reactor with catalysts achieving a maximum bio-oil yield of 60.5 wt. % with a fast heating rate, pyrolysis temperature of 450 C, and particles sized between 2,000 and 5,000 µm. Abnisa et al. (2011) pyrolysed 150 g samples of palm shell waste in a fixed-bed reactor achieving a maximum bio-oil yield of 46.4 wt. % at 500 °C of temperature, 2 L/min of N_2 flow rate, 2000 lm of particles size and 60 min of reaction time. Ellens and Brown (2012) achieved maximum bio-oil yield more than 70 wt. % are scale free-fall pyrolysis reactor when operating with heater set point near 575 °C, feeding red oak particles less than 300 µm at 2 kg/h. Sweep gas flow rate did not significantly influence bio-oil yields over the $1 - 5$ L/min range tested.

2.8   Summary

Fast pyrolysis operating conditions play a significant role in defining the yield and composition of bio-oil product. The process parameters are often reported in literatures are temperature, N_2 flow rate, retention times, feed particles size and feeding rates. Although many studies have been conducted to determine the effect of these parameters on bio-oil production from pyrolysis of different biomass such as eucalyptus wood (Heidari et al., 2014), waste furniture (Heo, Park, Park, et al., 2010), palm kernel cake (Kim, Koo, Ryu, Lee, Kim, Lee, Kim & Choi, 2013), palm shell (Abnisa et al., 2011) and

so on, in different pyrolysis reactors, the study of red meranti sawdust as biomass feedstock has not yet been reported, unless study reported by Mazlan et al. (2015). Mazlan et al. performed fast pyrolysis experiment of meranti sawdust in fixed bed drop-type reactor, by study the influence of pyrolysis temperature on pyrolytic products. Based on their report, Mazlan et al. (2015) achieved maximum yield of bio-oil about 33.7 wt. % at 600 °C. Optimum temperature obtained by Mazlan et al. (2015) was high as compared to pyrolysis of other lignocellulose biomass, in which, most biomass were produced maximum bio-oil yield in a range between 450 and 500 °C of temperature such as studied conducted by Heidari et al. (2014), Heo, Park, Park, et al. (2010), Heo, Park, Yim, et al. (2010) and Kim et al., (2013). Hence, for the practical application, higher optimum temperature is not favourable since it requires higher operating cost for bio-oil production. Furthermore, the effect of other parameters process such as N_2 flow rate, retention time and feed particles size are not be found in this report. However, for the large scale of bio-oil production, the effect of these parameters are essential to be investigated and optimised. Therefore, for this purpose, a set of fast pyrolysis experiments will be carried out in fluidised bed reactor according to OFAT approach to examine the influences of individual parameters process on pyrolytic products yield, and further, determine the optimum parameter process to obtain maximum bio-oil production. One of the applications of bio-oil is as transportation fuel substitution but the information with regards to this point is less reported in literature. Therefore, in this work, the suitability of bio-oil for fuel application will be assessed and tabulated in Van Krevelen Diagram.

In OFAT approach, the experiments were conducted mainly to investigate the individual effect of process parameter and this method cannot be manipulated to represent the combined effect of all process variables. The application of statistical experimental design such CCD in RSM is used to optimise and demonstrate combine effect of process variables, as well as, serve for prediction and verification of model equation. Several studies have been conducted regarding to the application of CCD in optimising bio-oil yield such as Kumar et al. (2010) investigated process parameter such as feed particle size, temperature, presence of catalyst, and heating rate on the yield of bio-oil from pyrolysis of eucalyptus wood, Abnisa et al. (2011) reported the combined effect of four process parameters such as temperature, N_2 flow rate, feed size and reaction time on bio-oil yield from palm shell, Ellens and Brown (2012) identified optimum conditions such as heater set-point temperature, biomass particle size and sweep gas flow rate for

maximising bio-oil production from red oak. Though, optimisation of process parameters on bio-oil yield from red meranti never been reported in any literature. Thus, a complete set of experiments according to CCD in RSM approach will be employed to maximise bio-oil production from red meranti sawdust. Process variables involve in this study are temperature, N_2 flow rate and retention time. Furthermore, a universal model of RMS as fast pyrolysis feedstock also will be developed.

Apart of fast pyrolysis operating conditions, the composition of biomass also important in determining the bio-oil production. In this study, the study scope only focus on the effect of AAEM concentration in feedstock. Many studies have been conducted to study this effect such as Jendoubi et al (2011) studied the repartition of inorganic in the products formed in the fast pyrolysis process of beech sawdust, Mourant et al (2011) investigated the changes in bio-oil composition and properties with the extend of the AAEM removal from malle wood prior to pyrolysis, Eom et al. (2011) studied the catalytic effects of inorganics on thermal degradation of woody biomass, and Hu, Jiang, Wang, Su, Sun, Xu, He and Xiang (2015) evaluated the effect of AAEM on yield and properties of biomass at different temperature (500 °C, 700 °C and 900 °C). However, the information on how the washing technique changes the strength of molecular bond and its effect on the thermal degradation of biomass has not yet been reported. For that purpose, this study will be carried out by analysing biomass using TGA and FTIR prior to pyrolysis process in order to study the relationship between the effect of washing on both the molecular bonds strength and thermal degradation of feedstock. Fast pyrolysis experiments also will be conducted at the temperature range of 350 to 600 °C to investigate the amount of bio-oil yield for each treatment and further, by this finding, a more practical washing method will be suggested by taking into consideration on the chemical involved for treatment.

Impregnated method is one of the treatments on biomass that can change the characteristic of biomass and improve bio-oil quality. Among studies that have been conducted on this topic were the investigation on the catalytic effect of cations in impregnated eucalyptus (Eibner et al., 2015), the influences of impregnated metal in beech wood to conversion of biomass constituent (Collard et al., 2012). the influence of pyrolysis condition and transition metal salt on product yield (Jiang, Song, Cheng, Chen, Zhang, Zhang, Hu, Li & Li, 2015). However, the effect of impregnation method to both

thermal degradation behaviour and the strength of molecular bond in biomass could not be found in literatures. Furthermore, the catalysing effect of this method to enhance pyrolysis process at lower temperature also never been reported in any literature. Therefore, in this work, impregnated RMS will be analysed using TGA and FTIR to assess the thermal degradation behaviour and the changes in molecular strength of impregnated RMS, respectively. Through TGA analysis, the maximum degradation temperature also will be assessed to evaluate either the impregnated method can enhance pyrolysis process at lower temperature or not. In order to determine the amount of bio-oil yield as a function of temperature, fast pyrolysis experiments will be carried out at a temperature range of 350 to 600 °C. Amount of levoglucosan yield in bio-oil also will be analysed by GC-MS to determine and confirm the effectiveness of this method to increase its production.

CHAPTER 3

METHODOLOGY

3.1 Introduction

This chapter describes the methods and materials used in the present study which involving the production of bio-oil extracted from pyrolysis of RMS using fast pyrolysis process technology. There are four mains of fast pyrolysis experimental work carried out, in which, each experimental work has its own objective as shown in research methodology chart in Figure 3.1. As shown in Figure 3.1, each block of process starting from feedstock preparation until bio-oil characterisation is labelled according to the number of objective study.

3.1.1 Pyrolysis Apparatus

This research is focusing for liquid bio-oil production and therefore, the system of fast pyrolysis process with bench-scale fluidised bed reactor was employed to conduct the experiment. The schematic diagram of the fast pyrolysis set-up is illustrated in Figure 3.2 and pyrolysis system engaged in this study is shown in Figure 3.3. The reactor used in this study is made from stainless steel pipe (tubular furnace, LT Furnace brand) with opening diameter of 60 mm and height of 300 mm.

In this research, the sweeping gas of N_2 was employed as fluidising gas in pyrolysis system for maintaining pyrolysis atmosphere without oxygen. During pyrolysis process, N_2 was delivered into the reactor and passed through the process to reduce the residence time of vapour.
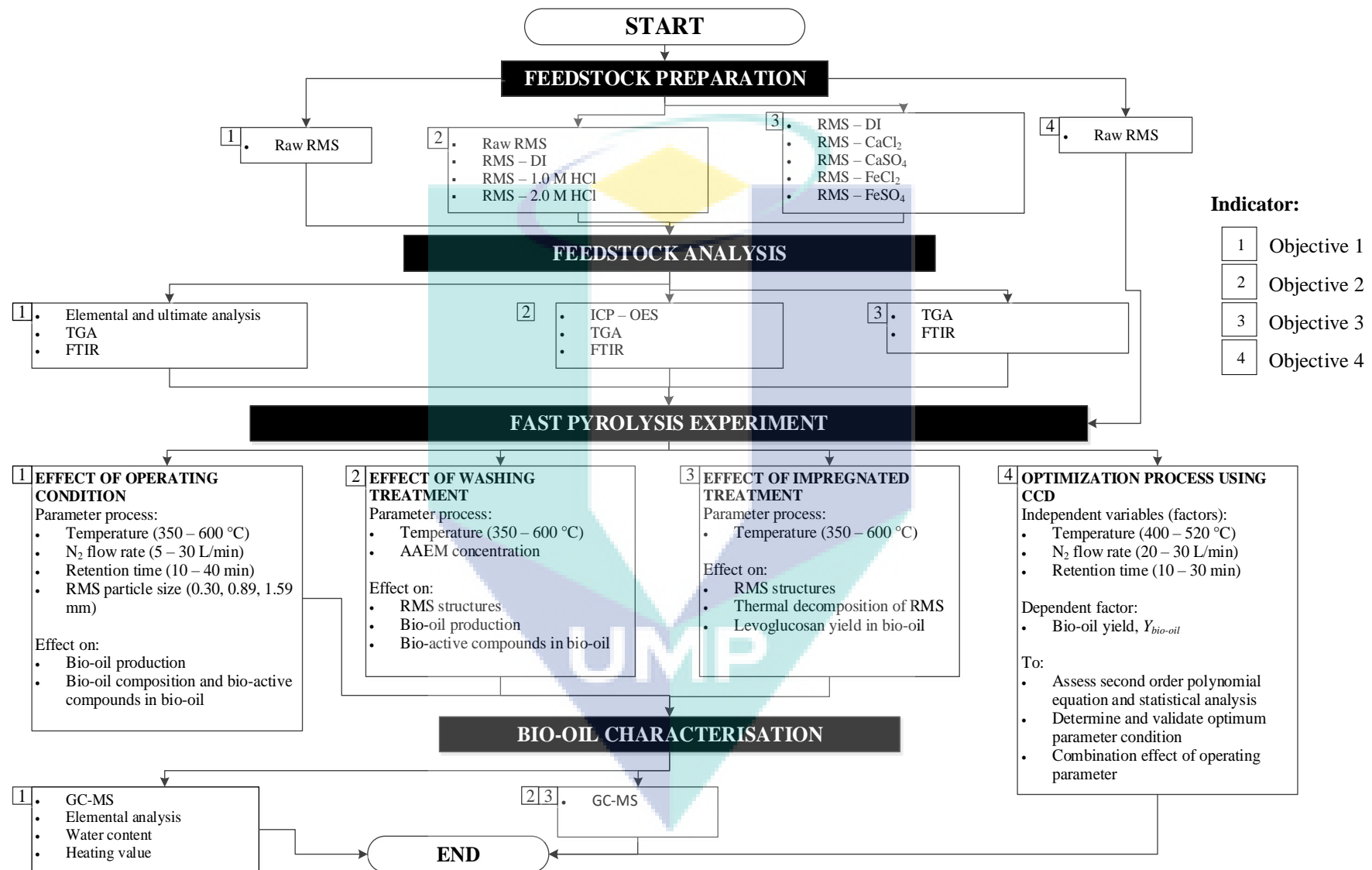
Figure 3.1   Research methodology chart

Prior to experiment, 50.0 ± 0.10 g of RMS was inserted into tabular furnace reactor. Furnace temperature was set to 105 °C at temperature controller and run for 30 min with the head of reactor opened, in order to allow evaporation of residual initial moisture in RMS and, further, minimise water content in bio-oil. After 30 min., the head of reactor was closed with cap and N_2 was flowed into the reactor at desired flow rate. Temperature of furnace, then, was set to desire operating temperature with a constant heating rate of 50 °C/min. Fast pyrolysis process started and run in which the retention time of RMS was varied according to experimental design. During pyrolysis process, pyrolysis vapour with entrained char were swept out from the furnace tube and passed through the cyclone, in which, larger and heavier particles of solid (char) product was separated and collected in the bottle, CC, below the cyclone. After passing through the cyclone, the mixtures of hot pyrolysis products (pyrolysis vapour and fine char particles) were cooled down by water as coolant agent in two units of condenser. Below these condensers, condensable vapour was collected as bio-oil in bio-oil collectors, named BC1, BC2 and BC3.
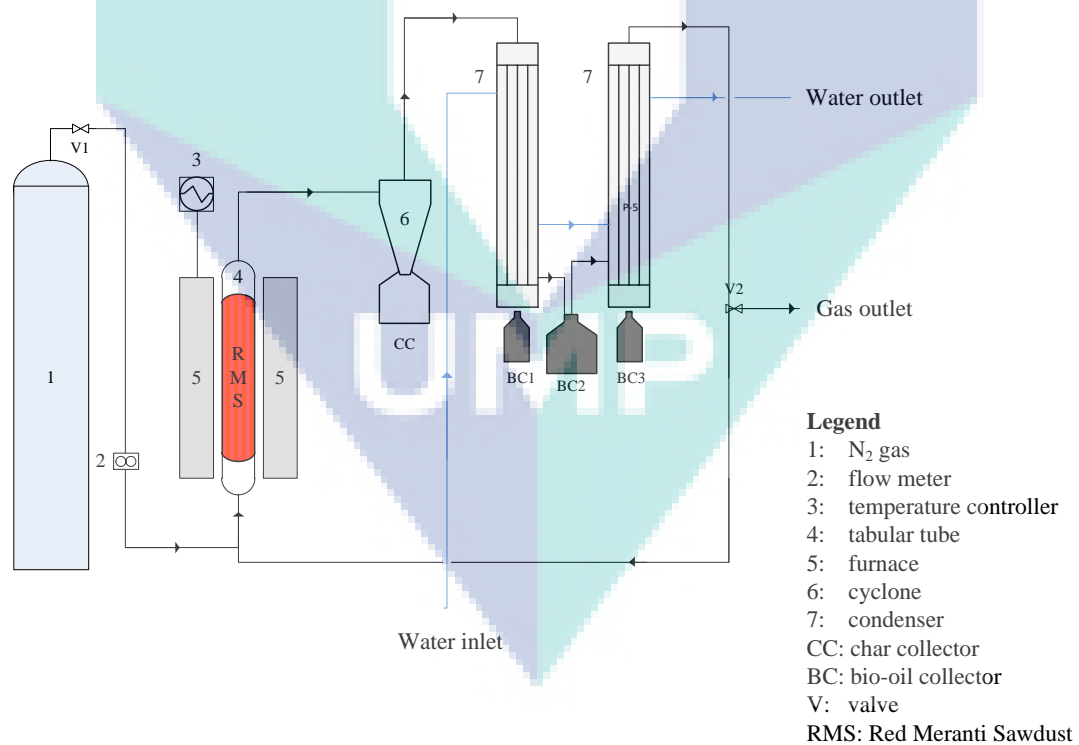
Figure 3.2   Schematic diagram of the fast pyrolysis set-up
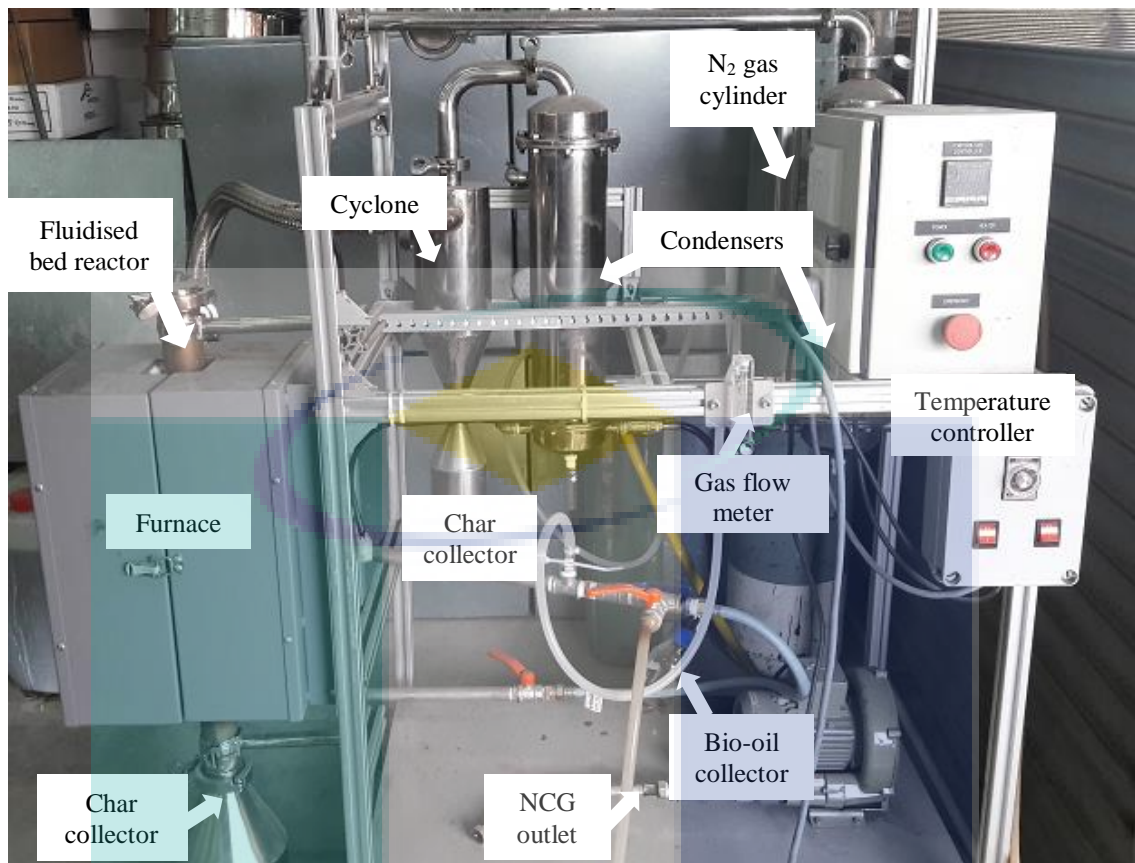
Figure 3.3   Fast pyrolysis experimental set up

To ensure the results obtained were reliable and verifiable, each experiment was performed and repeated three times with the experimental error around $\pm$ 5 wt. % and the average value was used for analysis.

3.1.2   Red Meranti Sawdust Analysis

In this study, the RMS was used as pyrolysis feedstock. The RMS was supplied by Sen Peng Sawmill Gambang, Pahang. This biomass was collected in form of sawdust resulted from the waste of wooden products processing. Before being used as feedstock for fast pyrolysis experiments, the characteristics of feedstock sample was initially analysed to evaluate its suitability for oil production through thermo-chemical conversion method (Onay, 2007).

3.1.2.1   Physicochemical Analysis

The chemistry of pyrolysis process and the products are strongly influenced by the physicochemical properties of feedstock. Therefore, determination of this properties on feedstock prior to pyrolysis process is crucial. The analyses involved to determine

physicochemical properties of RMS include proximate and ultimate analyses, AAEM concentrations and heating values.

The proximate analysis is the analysis to determine moisture content, volatile content, fixed carbon and ash content of particular biomass fuel. This analysis provides a fair idea of the percentage of the major pyrolysis products (char and volatiles), in which the weight of volatiles may be expected to be lost due to complete pyrolysis process, and all the volatile matter is released (Krishna Prasad, 1985).

The ultimate analysis gives the value of chemical composition of biomass in weight percentage of carbon, hydrogen, oxygen, and nitrogen, as well as, sulphur ("Biomass Fuel Analysis For Energy Crop (Closed-Loop) and Wood Derived Fuel/Yardwaste (Open-Loop)," 2015). Typically, ultimate analysis of various types of wood elements (dry weight basis) shows the proportion approximately; C, 49 – 50 %; H, 6 %; O, 44 – 45 % and N, 0.1 – 1 %, and remaining is some small amounts of minerals such as Ca, K and Mg that are found in wood ash. The ash content is commonly in the range of 0.2 – 1 % (Vigouroux, 2001). The detailed of feedstock analysis is listed in Table 3.1.

3.1.2.2   Thermal Decomposition Analysis

Temperature is one of the important factors that influence the pyrolytic products yield. In order to determine the ideal range of RMS feedstock decomposition reaction temperatures, thermogravimetric analysis (TGA) were carried out using thermogravimetric analyser (Brand METTLER TOLEDO, Model TGA DSC 1). TGA is a method of thermal analysis which provides a semi-quantitative analysis of thermal degradation of materials during thermo-chemical conversion under various atmospheres (Uzun et al., 2007). The results of TGA experiments are expressed as a function of conversion X, as shown in Equation 3.1 and differential rate of conversion, dX/dt is obtained from DTG at different heating rates (Park et al., 2008).

Table 3.1   Methods for feedstock analyses

Analysis	Method	Description
Proximate analysis (wt. %):	ASTM E870 - 82(2013)	Standard Test Methods for Analysis of Wood Fuels (Meier, 2013)
Moisture	ASTM E871	Dry in oven at 105 °C overnight. Sample is weighted before and after drying.
Volatiles	ASTM E872	1 g of biomass is placed in dry crucible with the lid on and heated in a muffle furnace at a temperature of 950 °C for a period of 7 minutes. Volatile matter is determined as the mass lost during the process.
Ash	ASTM D1102	Biomass is heated to 600 °C in furnace for 6 hours. Remaining ash is weighted.
Fixed carbon	ASTM D3172	Obtained by subtracting the percentages of volatile matter, moisture content and ash from 100 wt. % (Uzun et al., 2007).
Elemental analysis (wt. %):	ASTM D3176	Standard procedures/ an automatic elemental analyser
C, H, N, S	Elemental analysis	Elemental analyser
O	-	Obtained by subtracting the percentages of C, H, S, N from 100 wt. %.
HV (MJ/kg)		HHV is calculated using the Dulong-type equation which modified by Mott and Spooner and LHV is calculated through equation proposed by Oasmaa. HHV (MJ/kg) = 0.336C + 1.418H – (0.153 – 0.000720O)O + 0.0941S (Buckley, 1991) LHV (MJ/kg) = HHV – (0.218 x H) (Abnisa et al., 2011)

$$X = \frac{W_0 - W}{W_0 - W_\infty}$$

<div align="right">3.1</div>

Where W_0 is the initial mass of the sample, W is the mass of pyrolysed sample, and W_∞ is the final residue mass.

For this analysis, a few milligrams of sample with particles size below than 200 µm was taken and heated up to 900 °C at heating rates of 10 °C/min. To maintain inert atmosphere during TGA analysis, N_2 was purged and kept flowing at 30 mL/min of flow rate.

Next, for fast pyrolysis experiments on feedstock, the temperature range was selected based on the range of temperature resulted from TGA.

3.1.2.3 Functional Group Analysis

The functional group of RMS samples were analysed using Fourier Transform Infrared Spectroscopy (FTIR) with the method of ATR. FTIR is an analytical technique that relies on light in the infrared portion of the electromagnetic spectrum to characterise materials. FT-IR is generally a qualitative tool that is particularly beneficial in identifying the presence of specific functional groups ("Cornerstone Analytical Libraries," 2017).

In this study, FTIR analyses were carried out to examine the changes in chemical structures in RMS after treatment. Prior to analysis, RMS samples were dried in oven for 24 hours at 105 °C and grounded in mortar. The scan region ranged from 4000 to 400 cm^{-1} with a resolution of 4 cm^{-1} was applied in this analysis.

3.1.3 Bio-oil Characterisation

Bio-oil properties are important characteristics where it determines the suitability of their application. For this research, their properties are vital in targeting the compatibility of their usage as transportation fuel. The bio-oils properties were determined by the methods as presented in Table 3.2.

The bio-oil samples were collected in the bio-oil collectors and weighted to determine its yield. The bio-oils yield were calculated using the Equation 3.2 (Abnisa et al., 2011). The example of calculation is attached in APPENDIX C.

$$Yield\ (wt.\ \%)=\frac{Liquid\ product\ (g)}{Feedstock\ (g)}\times100\%$$

3.2

Before further analysis, bio-oils were kept in a dark fridge at 4 °C (Garcia-Perez et al., 2008) to prevent ageing reaction. There are three bio-oil collectors used in this study, BC1, BC2 and BC3. Thus, for water content and ultimate analyses, all of collected bio-oils were mixed well to avoid any physical phase separation.

For bio-oil compounds determination, the samples were taken only at the optimal operating parameters which produce maximum yield of bio-oil. The analysis of bio-oil

compounds were determined according to GC-MS analysis, where the area % of a GC-MS chromatogramme can be considered a good approximation because it identifies and quantifies the amounts of various chemical compounds in bio-oil (Park et al., 2008). In this study, both qualitative and quantitative analyses of bio-oil were performed according to 6890 GC METHOD with an HP-5MS (30 m x 250 µm x 0.25 µm) capillary column and with helium as carrier gas. The mass spectra obtained by GC-MS were interpreted through an automatic NIST Mass Spectral Library search programme. Only compounds with the result of qualitative analysis (Qual) more than 50 % were reported in this study.

Table 3.2   Analytical methods for wood-based pyrolysis liquids

Properties	Method	Description
Water content (wt. %)	Karl-Fischer titration according to ASTM E203	Suitable method for determining moisture in sample containing aldehydes and ketones (Oasmaa et al., 1997).
C, H, N, S content (wt. %)		In this analysis, sample compositions of feedstock are simultaneously determined as gases products (carbon dioxide, water vapour and nitrogen). Brand: Elementar Model: Vario Macro Cube
O	-	Obtained by subtracting the percentages of C, H, S, N from 100 wt %
HV (MJ/kg)		The different of high heating value (HHV) and lower heating value (LHV) is equal to the heat of vaporization of water formed by combustion of the fuel. HHV is calculated using the Dulong-type equation which modified by Mott and Spooner and LHV is calculated through equation proposed by Oasmaa. HHV (MJ/kg) = 0.336C + 1.418H – (0.153 – 0.000720O)O + 0.0941S (Buckley, 1991) LHV (MJ/kg) = HHV – (0.218 x H) (Abnisa et al., 2011)
Bio-oil Compounds	GC-MS	Brand : AGILENT Model : 7890A

3.2 Study of Fast Pyrolysis Conditions

Pyrolysis operating conditions play an important role on pyrolytic products distribution and properties. For instances, lower process temperature and longer vapour residence time favour the production of charcoal, high temperatures and longer residence times increase conversion biomass to NCG, and moderate temperatures (around 400 – 550 °C) and short vapour residence time (< 2 s) are optimum for liquid production (Naik

et al., 2010). Therefore, by designing the desired product type, the pyrolysis process is carried out by controlling the process parameters. Since this study is focussed on the production of bio-oil, the fast pyrolysis process method has been selected and the process parameters involved are studied. In addition, bio-oil extracted from RMS also is characterised and discussed at the following subsection.

3.2.1 Red Meranti Sawdust Preparation

For this experiment, RMS feedstock was separated by four sieves with mesh sizes of 0.60, 1.18, 2.00 and 4.00 mm with arithmetic sizes for each particles size range were 0.30 mm (less than 0.6 mm), 0.89 mm (0.60 to 1.18 mm), 1.59 mm (1.18 to 2.00 mm), 3.00 mm (2.00 – 4.00 mm) and larger than 4.00 mm. However, particles retained at sieve mesh size 2.00 mm was neglected for further study due to very small sample amount (approximately 3 % of a bulk sawdust sample). Result of particles size of RMS is attached in APPENDIX A and its particles distribution is shown in Figure 3.4. Image of separated feedstock subjected to pyrolysis process is shown in Figure 3.5. After separation, the feedstock was dried in oven (model RF115) at 105 °C for a few hours duration to minimise the initial moisture. Targetted moisture content for experiment was less than 10 wt. % in order to minimise water content in bio-oil product.
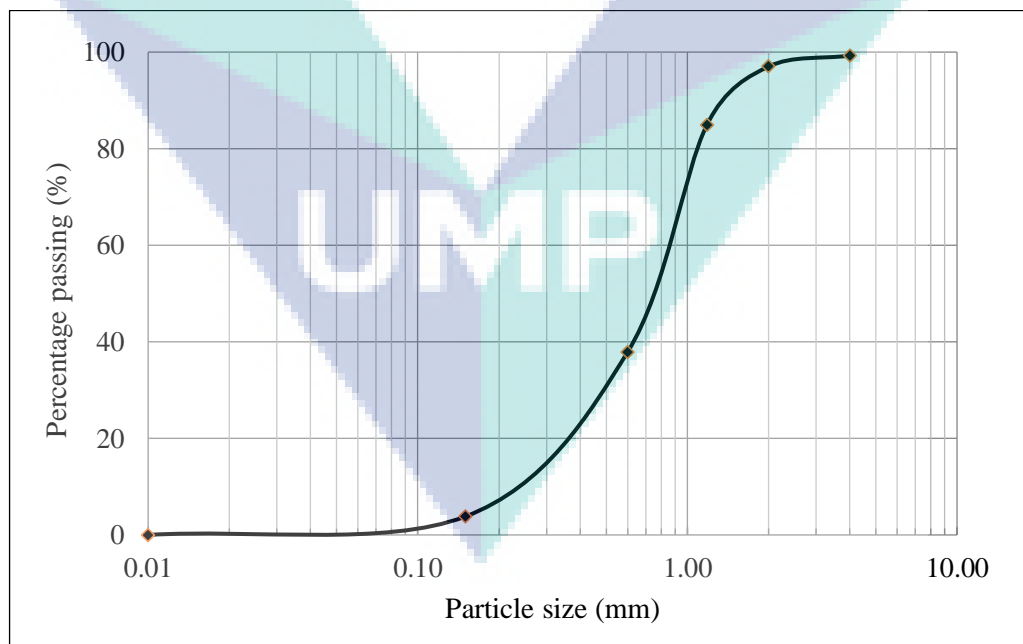
Figure 3.4   Particles size distribution graph of red meranti sawdust
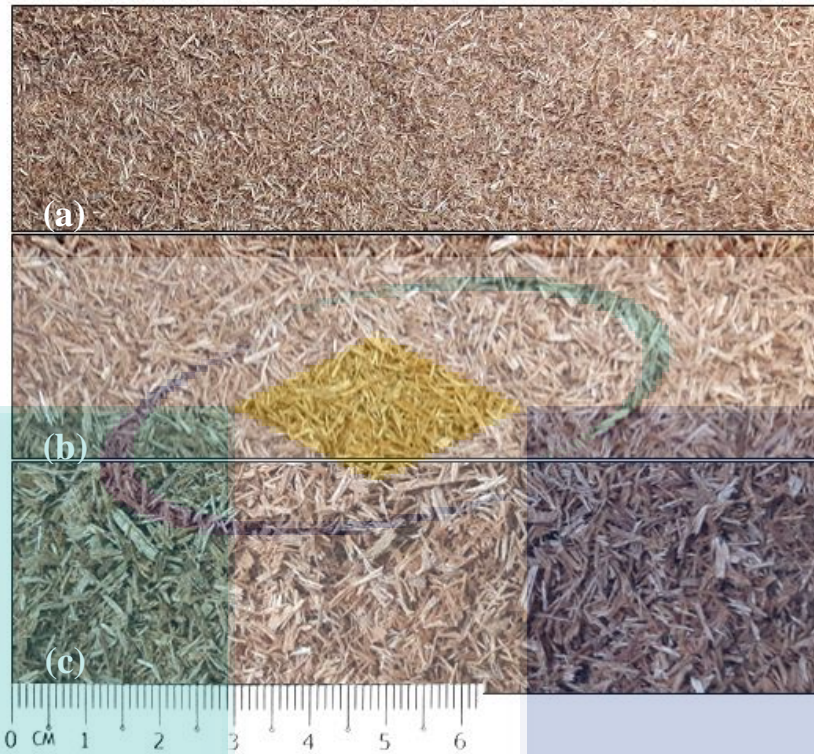
Figure 3.5   Separated feed particles size (a) less than 0.06 mm, (b) 0.06 – 1.18 mm, and (c) 1.18 – 2.00 mm

3.2.2   Fast Pyrolysis Experiment

This study was conducted to produce maximum yield of bio-oil from RMS and investigate the influence of individual parameter of fast pyrolysis process over bio-oil production. The scope of pyrolysis operating parameter studied include temperature (°C), sweeping N_2 flow rate (L/min), retention time (min) and feed particles size (mm) of RMS, in which, these parameters were measured as independent variables, while bio-oil yield was observed as dependent variable. During experiment, particular parameter (independent variable) studied was varied, while other variables were maintained constant at specific value, in which, the range values of parameters studied were taken from the previous reports of pyrolysis studies of others lignocellulosic biomass such as Heidari et al. (2014), Ngo et al. (2013) and Heo, Park, Park, et al. (2010). The experimental work for this study was conducted at process conditions as listed in Table 3.3.

Table 3.3   Fast pyrolysis operating condition

Run	Parameter process			
	Temperature (°C)	Gas flow rate (L/min)	Retention time (min)	Arithmetic mean of feed size (mm)
1	350	20	20	0.30
2	400	20	20	0.30
3	450	20	20	0.30
4	500	20	20	0.30
5	550	20	20	0.30
6	600	20	20	0.30
7	450	5	20	0.30
8	450	10	20	0.30
9	450	15	20	0.30
10	450	20	20	0.30
11	450	25	20	0.30
12	450	30	20	0.30
13	450	25	10	0.30
14	450	25	20	0.30
15	450	25	30	0.30
16	450	25	40	0.30
17	450	25	20	0.30
18	450	25	20	0.89
19	450	25	20	1.59

3.3   Study the Effect of Washing Treatment

Previous literatures reported that, mineral matter also known as alkali and alkaline earth metal (AAEM) content in biomass contributes to significant effect towards thermal decomposition behaviour and reducing bio-oil product yield, as well as, downgrading its quality. Based on the result obtained and discussed in Subchapter 4.2, it indicated that the quantity and quality of bio-oil product from pyrolysis of raw RMS was not satisfied. One of the reasons contributing to these effects is the presence of AAEM species in RMS feedstock. Therefore, to ameliorate this outcome, AAEM in feedstock must be removed as much as possible prior to subject to pyrolysis process. One of the practical methods to remove AAEM species is by washing method, which, either by water washing or acid washing. Thus, this study was conducted to investigate the effect of washing treatment to RMS structure and identify which washing treatment can offer better AAEM removal in

RMS. Furthermore, pyrolysis experiments also were carried out in order to examine to what extent the removal of AAEM is able to produce higher bio-oil yield and improve bio-oil 'organic' compound yield. In addition, washing method represents somewhat costly step if the ultimate goal of product (for example fermentation sugars) is relatively low value. For example, if the pyrolysis process is aim to produce anhydrosugars, DI water washing is sufficient to be applied. Thus, depending on targetted product and cost incurred, one can evaluate and consider which treatment is the best to prevail.

3.3.1 Feedstock Preparation

In this study, RMS feedstock with particles size $\leq$ 2.00 mm was chosen as pyrolysis feedstock. Preparation of RMS is described as below. To determine the concentration of AAEM remains in RMS and the efficiency of AAEM removal, approximately 0.20 g of demineralised samples were taken, digested and treated for ICP-OES analysis.

3.3.1.1 Raw Feedstock Sawdust

Raw RMS feedstock was sieved and prepared by drying in oven overnight at 105 °C to minimise its moisture content.

3.3.1.2 Demineralised Feedstock

Demineralisation is the process to remove all naturally occurring inorganic mineral matters from wood particles, where its presence contributes to high ash content in liquid product and promote the catalytic effect during conversion process which lead to increasing in char formation. In this study, demineralised feedstock was prepared by washing it with; (i) 1.0 M or 2.0 M HCl (37 wt. % HCl in H_2O), or (ii) deionised water. Preparation of HCl solution is attached in APPENDIX B. Before introduced to pyrolysis process, demineralised feedstock was filtered using a 30 µm stainless steel mesh and remaining solid retained on filter were dried in oven (Model: RF115) overnight at 105 °C to remove moisture content.

Acid wash

The acid-washed RMS feedstock was prepared by immersing in diluted HCl to remove AAEM content in feedstock. The total volume of liquid used for the

demineralising process was 10 mL for per gram of biomass, in which the feedstock was immersed and stirred at 50 rpm for 2 hours at room temperature either in 1.0 M or 2.0 M HCl (100 mL). The samples were repeatedly rinsed with deionised water until the effluent achieved neutrality.

Water wash

The water-washed RMS feedstock was treated by placing into the beaker, in which for every 1 g of biomass, 10 mL of deionised water was added. The mixture was stirred for 2 hours at 50 rpm at room temperature (25 ± 3 °C).

3.3.2 Fast Pyrolysis Experiment

The pyrolysis process was carried out in fluidised bed reactor as the same manner as described in Subchapter 3.1.1. In this experiment, fast pyrolysis experiment was operated at following conditions:

i)   Temperature (°C)   = 350, 400, 450, 500, 550 and 600
ii) N_2 flow rate (L/min)   = 25
iii)   Retention time (min)   = 20
iv)   Average feed particle size (mm) = ≤ 2.00

In this experimental work, fast pyrolysis temperature and AAEM concentration in RMS were considered as independent variables, whereas amount of pyrolytic products yield was measured as dependent variable.

3.4 Study the Influence of Impregnated Red Meranti Sawdust

This study was performed to investigate either the metal salt addition is able to enhance decomposition process or not, and at the same time, examine the catalytic effect of impregnated RMS towards bio-oil yield and the amount of anhydrosugars especially levoglucosan compound in bio-oil yield.

3.4.1 Feedstock Preparation

In this study, demineralised RMS - DI water feedstock and impregnated RMS with particles size of ≤ 2.00 mm were selected as pyrolysis feedstock. Preparation of these feedstock are described in next subchapter.

3.4.1.1   Control Feedstock

According to Scott et al. (2001), washing with DI water is more than sufficient to be applied for thermal conversion of cellulose for the aim to increase anhydrosugars yield. Thus, demineralised RMS – DI water was selected as a control and a benchmark for comparison. Demineralised RMS was prepared by immersing for every 1 g of raw RMS in 10 mL of deionised water and stirred for 2 hours at 50 rpm at room temperature (25 ± 3 °C).

3.4.1.2   Impregnated Feedstock Preparation

Impregnation is a physical adsorption on the surface of biomass particles. In this study, 0.1 M of alkali metal salts [$CaCl_2$ (≥ 99 %, anhydrous, granular) or $CaSO_4$ (≥ 98 %, dehydrate, granular)] or transition metal salts [$FeCl_2$ (≥ 99 %, tetrahydrate, granular) or $FeSO_4$ (≥ 99 %, heptahydrate, granular)] was added to RMS in order to investigate the influence of metal salt to extracted liquid oil. These chemicals were purchased from Chemolab Supplies and had been chosen because of its water-soluble properties. Metal salt solutions were prepared using the Equation 3.3 and Equation 3.4 (Koenig, n.d.). Example of preparation is attached in APPENDIX B. Prior to impregnation process, RMS feedstock was washed with DI water to reduce indigenous inorganic (AAEM) content, filtered and dried in oven. Then, demineralised RMS – DI water were immersed into respective chloride or sulphate metal salt solution with a ratio of salt solution to RMS was 20 mL to per gram of RMS. The mixtures were stirred with rotation of stirrer was 50 rpm for 24 hours at room temperature, as shown in Figure 3.6. Then, impregnated RMS were washed with distilled water to remove any metal ions which do not bound to RMS (Collard et al., 2012; Mayer, Apfelbacher & Hornung, 2012), filtered and dried in the oven at 105 °C overnight to achieve moisture content less than 10 wt. % (Mayer et al., 2012; Eom et al., 2012).

$$Concentration\ (M) = \frac{Amount\ (in\ mol)}{Volume\ (in\ L)} \qquad 3.3$$

$$Amount\ (in\ mol) = \frac{Amount\ (in\ g)}{Molar\ mass\ (in\ g/mol)} \qquad 3.4$$

Figure 3.6　　Impregnated RMS preparation

3.4.2　Pyrolysis Experiment

In this work, fast pyrolysis process was operated at following operating conditions:

i)　　Temperature (°C)　　　　　　= 350, 400, 450, 500, 550 and 600
ii)　　N_2 flow rate (L/min)　　　= 25
iii)　　Retention time (min)　　　= 20
iv)　　Average feed particle size (mm) = ≤ 2.00

Fast pyrolysis temperature and impregnated feedstock were set as independent variables, and amount of pyrolysis products yield were considered as dependent variable.

3.5　Pyrolysis Process Optimisation using Experimental Design of Central Composite Design (CCD)

The experimental study in Subchapter 3.2 were conducted mainly to investigate the individual effect of operating parameter towards bio-oil yield. However, this classical approach cannot be manipulated to represent the optimum process parameter and do not depict the combined effect of all process variables towards bio-oil yield. In addition, this method leads to time and cost consuming to complete a number of experiments. Thus, to solve such concerns, these limitations can be eliminated by using statistical experimental design, for instance response surface methodology (RSM).

In this study, standard RSM design based on central composite design (CCD) was put into practice to find the optimum process variables associated to maximising bio-oil

yield. CCD is considered as the most successful factorial design (Ghafoori, 2013). Besides optimising process variables, CCD also is used to minimising number of conducted experiments, illustrate combined effect of variables toward bio-oil yield, and serve for prediction and verification of model equation.

3.5.1 Red Meranti Sawdust Preparation

In this part, optimisation process was carried out on raw RMS. Raw RMS was chosen to represent its broad species and provides an optimum range of variables for bio-oil production. In this study, RMS with particles size ≤ 2.00 mm was selected as fast pyrolysis feedstock since it is the optimum particles size for better heating transfer rate for the production of bio-oil (Garcia-Perez et al., 2008).

Prior to pyrolysis process, RMS was dried in oven (model RF115) overnight at 105 °C to minimise its moisture content. The pyrolysis experiments were run in the same manner as describe in Subchapter 3.1.1.

3.5.2 Experimental Design of Central Composite Design (CCD)

There are few steps involve in optimisation process. First, determine a mathematical relationship between the response and the factors as given in Equation 3.5. Second step, estimate the coefficient in mathematical model and predict the response. In CCD, model used for predicting is typically a quadratic equation or second-order model and can be written as shown in Equation 3.6. Last step, check the adequacy of the model. One of the methods is testing the lack-of-fit. The lack-of-fit is a measure of a model failure in representing data in the experimental domain.

$$Y = f(X_1, X_2, X_3,..., X_n)$$
3.5

Where Y is the response, f is the unknown function of response, $X_1, X_2, X_3, ..., X_n$ are the factors and n is the number of independent factors.

$$Y = \beta o + \sum_{i=1}^{n} \beta i \times Xi + \sum_{i=1}^{n} \beta_{ii} \times X_i^2 + \sum_{i=1}^{n} \sum_{j>1}^{n} \beta_{ij} \times X_i X_j$$
3.6

Where Y is the predicted response, β_o, β_i, β_{ii} and β_{ij} are regression coefficient for the constant, linear, quadratic and interaction coefficients respectively. X_i and X_j are the coded independent factors.

In application of CCD, there were three operating parameters involve which were considered as independent variables (factors); temperature (A), N_2 flow rate (B) and retention time (C). The bio-oil yield (Y_B) was considered as the dependent factor (process response). The particles size in this study was fixed to size ≤ 2.00 mm. The factors were coded at five levels; -1 (minimum), 0 (center), +1 (maximum), $-\alpha$ and $+\alpha$. The α values was determined using Equation 3.7. By substituting the value of n = 3 into Equation 3.7 the value of alpha was presented at -1.68 and +1.68. Table 3.4 shows the ranges of factors and levels applied in this study. Range of factors used in this study were selected from previous OFAT study in subchapter 3.3.

$$\alpha = [2^n]^{1/4} \qquad\qquad 3.7$$

Where n is the number of factor (Box & Wilson, 1951).

Table 3.4   Independent variables and their code levels for bio-oil production of fast pyrolysis process

Independent variable	Unit	Symbol	Coded level				
			$-\alpha$	-1	0	+1	$+\alpha$
Temperature	°C	A	359.1	400	460	520	560.9
N_2 flow rate	L/min	B	16.6	20	25	30	33.4
Reaction time	min	C	3.2	10	20	30	36.8

To support the RSM data in CCD, the total numbers of 20 experiments were conducted where number of experiments were generated by Equation 3.8. Table 3.5 shows the complete design matrixes of experiments, in which, the pyrolysis process was carried out upon the factors value in this design.

$$N = 2^n + 2n + n_c \qquad\qquad 3.8$$

Where n is the number of variable and n_c is the replicate number of experiments. $2n$ refer the standard factorial with its origin at the centre, $2n$ points fixed axially at a distance and n_c replicate test at the centre.

A statistical software, Design-Expert 10.0.1 was used for the regression analysis and the coefficient estimation of the response function. The statistical significance of the model equation was analysed by the analysis of variance (ANOVA). The three-dimensional (3D) surface and the two-dimensional (2D) contour plots were developed while holding a variable constant in the quadratic model. The experimental and predicted values were compared to validate the model. The optimal operating conditions to maximise bio-oil yield were also determines using a numerical technique built in the software.

Table 3.5   Experimental design matrix

Run	Factor		
	A: Temperature (°C)	B: N$_2$ flow rate (L/min)	C: Retention time (min)
1	460	25	20
2	460	25	20
3	520	20	15
4	520	30	15
5	400	30	15
6	400	20	25
7	460	25	20
8	520	30	25
9	400	20	15
10	359	25	20
11	460	25	20
12	400	30	25
13	460	25	28
14	460	33	20
15	520	20	25
16	460	17	20
17	460	25	20
18	460	25	12
19	460	25	20
20	561	25	20

CHAPTER 4

RESULT AND DISCUSSION

4.1 Introduction

This chapter is written to present the finding and discuss the results obtained from experimental work conducted as mentioned in Chapter 3.

4.2 Study of Fast Pyrolysis Condition to Bio-oil Yield

Pyrolysis product distribution is determined by pyrolysis process conditions. Since the purpose of the study is to optimise bio-oil production, the four process parameters such as temperature, N_2 flow rate, retention time and feedstock particles size were selected and studied based on OFAT approach. Effect of individual parameter is discussed and result obtained is used as preliminary framework for the next study objective.

4.2.1 Red Meranti Analysis

In this study, raw RMS was used as pyrolysis feedstock to determine the effect of fast pyrolysis operating conditions to both bio-oil yield and composition. Analysis of RMS is presented and discussed below.

4.2.1.1 Physicochemical Analyses

Physicochemical analysis is a vital analysis to determine the nature of the interaction within a sample by taking into account their relationship involving both physical properties and composition. Result of physicochemical analysis of RMS is presented in Table 4.1.

Table 4.1   Physicochemical properties of RMS

Properties	
Proximate analysis[a] (wt. %)	
Moisture	5.95
Volatiles	78.61
Fixed carbon[c]	15.19
Ash	0.25
Alkali and Alkaline Earth Metal (ppm)	
K	397.5
Na	67.5
Ca	227.5
Mg	97.5
Elemental analysis[b] (wt. %)	
C	42.10
H	7.88
O[c]	49.75
N	0.24
S	0.03
O/C	0.89
H/C	2.24
Molar formula	$CH_{2.24}O_{0.89}N_{0.01}$
HHV[d] (MJ/kg)	19.49
LHV[e] (MJ/kg)	17.77
Density (kg/m^3)	0.55

[a] As received
[b] On dry ash free basis
[c] By difference
[d] By calculation using Dulong-type equation
[e] By calculation proposed by Oasmaa

As shown in Table 4.1, RMS has $CH_{2.24}O_{0.89}N_{0.01}$ of empirical formula. This formula is consistent with other plant biomass which typically has chemical formula range of $C_{3.3-4.9}H_{5.1-7.2}O_{2.0-3.1}$ (Tillman, 1991). In proximate analysis result, RMS consists volatiles matter and ash about 78.61 wt. % and 0.25 wt. %, respectively, indicating that RMS is suitable for thermo-chemical conversion of biomass to biofuel. According to Bridgwater (1991), high volatiles matter content of biomass with low ash and sulphur content is the main criterion for pyrolysis conversion. This is because, this volatiles matter has tendency to be converted to bio-oil after rapid cooling. In term of AAEM content, similar like other lignocellulose biomass, RMS also contains AAEM species which serve as nutrient for plant growth. However, total AAEM concentration in RMS is quite lower, about 0.24 % of RMS as compared to other typical plant as reported by Eom et al. (2012), indicating that the amount of bio-oil yield will be less affected by AAEM presence. In term of calorific value, RMS has higher heating value (HHV) about 19.49 MJ/kg,

showing that HHV of RMS is almost similar with HHV of other lignocellulosic biomass (Hamelinck, Van Hooijdonk & Faaij, 2005).

4.2.1.2   Thermal Analysis of Red Meranti

The TGA and DTG results of RMS is presented in Figure 4.1(a) and (b), respectively.
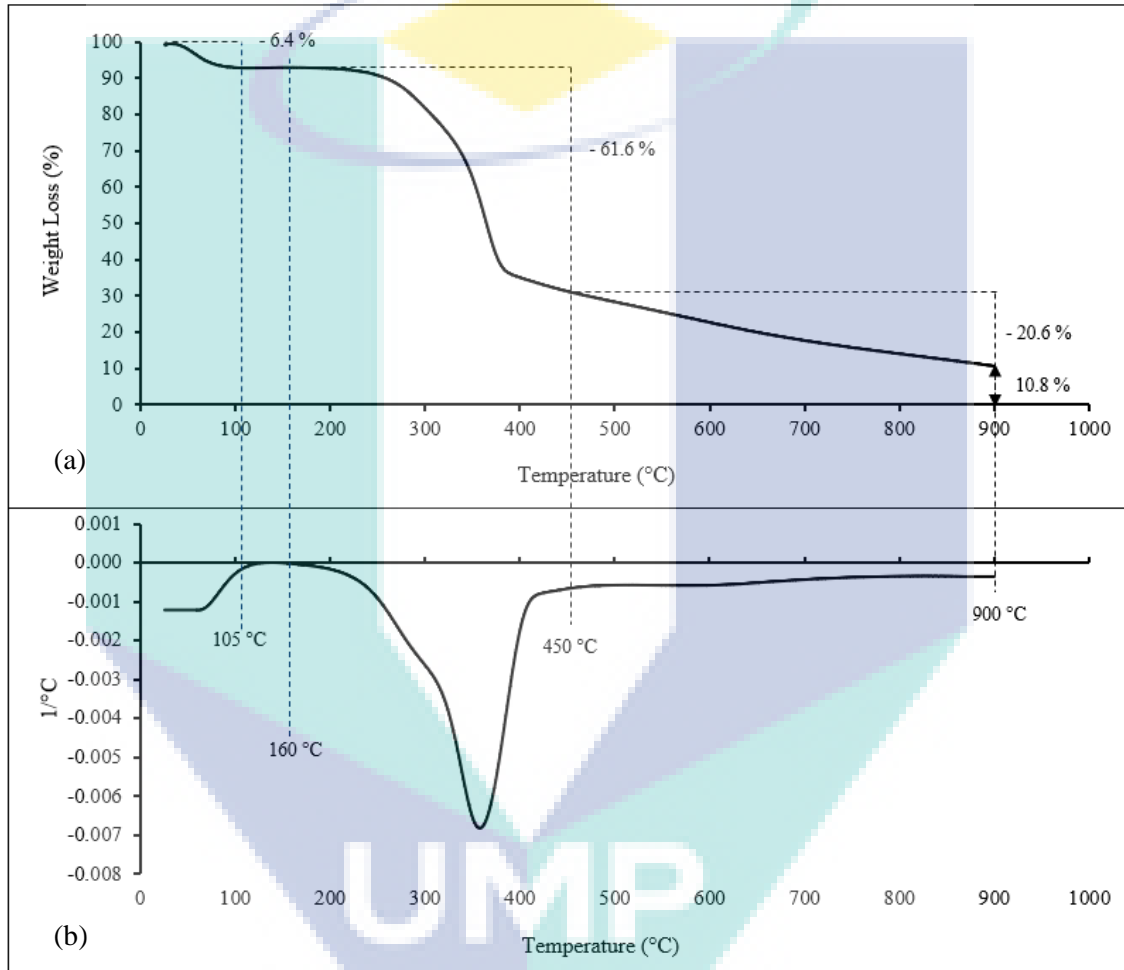
Figure 4.1   Thermo-gravimetric analysis of RMS at 10 °C/min of heating rate in N_2 atmosphere (a) TGA, and (b) DTG

Figure 4.1(a) shows the percentage of RMS weight loss as a function of temperature in N_2 atmosphere at 10 °C/min of heating rate in TGA. Three main stages of weight loss were observed during thermal decomposition of RMS. The initial minor weight loss occurred before 105 °C, This is attributed to evaporation of moisture as bound water on the surface and pores of the sample (Park et al., 2008). The decomposition of RMS constituents commenced at 160 °C, and this point is the starting temperature where RMS underwent important weight loss with the major decomposition occurred between

250 °C and 450 °C. The trend of this behaviour is associated with thermal decomposition combination with started by lignin, followed by hemicellulose and cellulose components in RMS. Lignin start to decompose slowly at 160 °C, followed by hemicellulose and cellulose which have decomposition temperature ranges from 220 to 400 °C and from 300 to 450 °C, respectively (Venderbosch & Prins, 2011). After 450 °C, decomposition rate of RMS was relatively constant until final temperature of 900 °C. Throughout this range of temperature, only decomposition of lignin took place. This is supported by the fact that lignin decomposed with small intensity over wide range of thermal decomposition temperature between 160 and 900 °C (Venderbosch & Prins, 2011; Akhtar & NorAishah, 2012).

Figure 4.1(b) represents the differential rate of weight loss, *dx/dT* versus temperature which gathered from differential thermogravimetric analysis (DTG). In Figure 4.1(b), it clearly can be seen that the decomposition of RMS largely occurred between 220 and 450 °C, with two peaks were observed. The first peak had a unresolved shoulder around 300 °C, associated with decomposition of hemicellulose and second peak also the main peak at 357 °C, attributed to decomposition of cellulose (Park et al., 2008). The trend of thermal decomposition rate of RMS is identically showing the same pattern as Japanese larch, which served as feedstock in experiment conducted by Park et al. (2008).

4.2.1.3 Functional Group Analysis

The functional group of RMS is shown in IR spectra in Figure 4.2 and typical functional group is listed in Table 4.2.

It can be observed that the spectrum of RMS has a main peak which is strong broad O-H stretching (3200 – 3400 cm^{-1}), C–H stretching in methyl and methylene groups (2800 – 3000 cm^{-1}), C–C in dienes group (1600 cm^{-1}) and a strong broad superposition with sharp absorptions in the region of 1000 cm^{-1}.
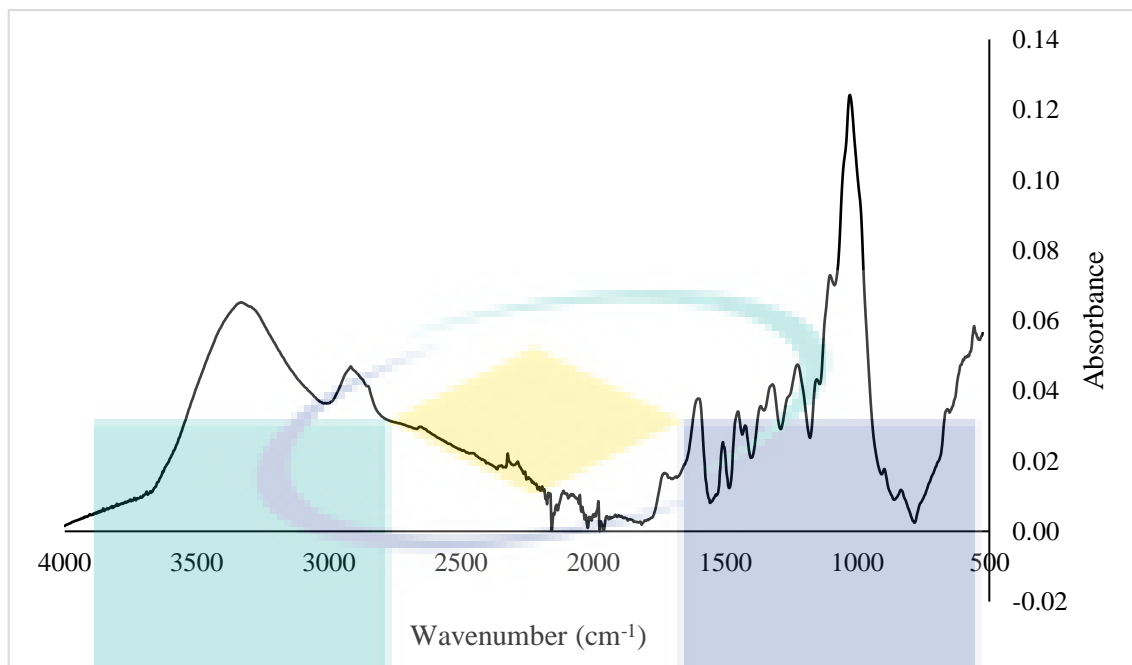
Figure 4.2   IR spectra of RMS

Table 4.2   Main functional group of RMS

Wavenumber	Bond	Types of bond	Appearance
3200 - 3400	O-H	alcohol, phenols	broad
2925	C-H	alkyl	medium to strong
2070 - 2250	C-C	C≡C	weak
1600	C-C	with C=O, conjugated C-C	strong
1500	C=C	aromatic C=C	weak to strong
1450	C=C	aromatic C=C	weak to strong
1250 - 1300	C-O	carboxylic acids	medium to strong
1220 - 1260	C-O	ether	strong
1020 - 1220	C-N	aliphatic amines	strong
700 - 400	C-C	aromatic hydrogen	

4.2.2   Fast Pyrolysis Experiment

Example of pyrolytic product yield calculation is shown in APPENDIX C and completed result of pyrolytic products is attached in APPENDIX D in Table D1. Effect of fast pyrolysis process conditions toward product distributions especially bio-oil are presented and discussed at the following subsection.

4.2.2.1 Effect on Bio-oil Yield

In order to investigate the effect of individual pyrolysis operating parameter on bio-oil production from RMS, several experimental works were carried out at different conditions as listed in Table 3.3.

Effect of temperature

Pyrolysis temperature is the most influential parameter affecting bio-oil yield (Uzun et al., 2007; Heo, Park, Yim, et al., 2010). Thus, to obtain a more precise temperature for maximum yield of bio-oil, thermal decomposition experiments of RMS were carried out at different temperatures starting from 350 to 600 °C, in inert atmosphere by applying N_2 as pyrolysis medium.

Figure 4.3 shows bio-oil yield including char and NCG products distribution at different pyrolysis process temperatures. As presented in Figure 4.3, at 350 °C, char formation was the highest and bio oil yields was the lowest. Solid collected from the furnace showed that large components of RMS, still not yet fully decomposed, indicating that incomplete pyrolysis had occurred on RMS which led to form more char. Hemicellulose and cellulose decompose at the temperature ranges from 220 to 400 °C and from 300 to 450 °C, respectively (Venderbosch & Prins, 2011). Hence, at 350 °C, only small portion of these components were decomposed and released volatiles, while the rest was collected as char.

However, as temperature was increased up to 450 °C, char formation decreased and bio-oil yield increased. The pattern of results indicate that RMS was increasingly pyrolysed and releasing more vapour containing more condensable compound. At the temperature between 450 and 500 °C, bio-oil production achieved maximum yield about 52.5 %. This range of temperature is the most optimum temperature in which large fraction of RMS components had been pyrolysed and converted to vapour, and finally condensed as bio-oil. This result coincides with the findings of other researchers such as Heidari et al. (2014), Heo, Park, Park, et al. (2010), Heo, Park, Yim, et al. (2010), Kim et al. (2013) and Garcia-Perez et al. (2008) which reported the highest bio-oil yield at this temperature range when pyrolysed lignocellulose biomass in different reactor. However, for comparison with the same type of feedstock, Mazlan et al. (2015) obtained maximum bio-oil yield of 33.7 % at a higher temperature, namely 600 °C.

After 500 °C, both bio-oil and char produced gradually decreased, while NCG released increased significantly, until final pyrolysis temperature of 600 °C. This is attributed to greater thermal decomposition, which led to the reactions of secondary cracking and fragmentation on unstable pyrolysis vapour. These reactions eventually resulted in releasing higher NCG product. Char yield gradually decreased due to decomposition of lignin component was still occurred in RMS biomass.
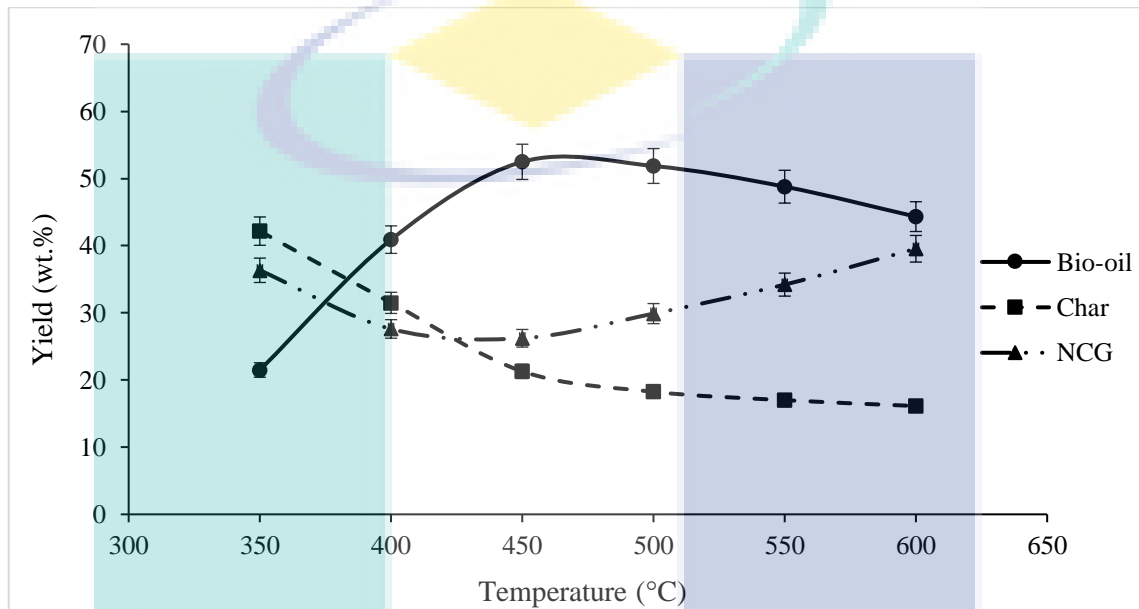
Figure 4.3   Products distribution as a function of pyrolysis temperature at 20 L/min of N_2 flow rate, 20 min of retention time and 0.3 mm of RMS particles size

The whole pattern of the graph is supported by the fact, at lower temperature, heat transfer between biomass particles is slower. This condition lead to the production of high quantity of char (Boroson et al., 1989), where the process is almost identical to conventional pyrolysis process. In addition of that, each component of biomass possesses a certain decomposition temperature, therefore, component that has not yet reaching the decomposition temperature will form a char. However, when lignocellulose biomass is pyrolysed at higher degree of temperature, more and more biomass fraction undergo greater primary thermal decomposition (Heidari et al., 2014) which lead to release more hot pyrolysis volatiles by char. The pattern of the bio-oil production is continued until it achieving optimum temperature. Higher than optimum temperature, the bio-oil yield is gradually decreasing. This trend is caused by higher heat transfer rate and greater thermal decomposition which lead to secondary cracking conversion and primary fragmentation of heavy-molecular-weight product in pyrolysis vapour which eventually results in releasing much higher NCG volume (Vigouroux, 2001; Heidari et al., 2014). Although

decomposition of lignin is still occurred, the lignin-derived bio-oil yield is still insignificant (Heo, Park, Yim, et al., 2010), and lignin itself mostly yields char.

Effect of nitrogen gas flow rate

With the aim of highest liquid producing, the need of short vapour residence time is also vital as its part of the important features of fast pyrolysis process, in order to minimise secondary reactions occur on produced volatiles (Boroson et al., 1989). The short vapour residence time is accomplished by controlling the rate of inflow of inert sweeping gas into the pyrolysis reactor. Accordingly, to estimate the optimum sweeping gas, the experimental work was carried out by running the experiment at N_2 flow rate in the range from 5 to 30 L/min.

As shown in Figure 4.4, when N_2 flow rate was set to 5 L/min, it can be observed that the amount of bio-oil yield was relatively low, while char formation and NCG released were high. This is because, at this flow rate, N_2 was too slow to sweep the vapour out from the pyrolysis reactor. This condition led to longer vapour residence time in reactor which eventually permits to secondary reactions occurred on pyrolysis vapour, and further resulted in secondary char formation and increased the amount of NCG released. When the flow rate of N_2 was increased up to 25 L/min, bio-oil yield increased rapidly, opposite with the amount of NCG released, while char formation gradually decreased. The pattern of graph indicates that, as the flow rate of sweeping gas is increased up to optimum flow rate, shorter vapour residence time can be achieved and primary product of pyrolysis can be prevented from undergoing secondary reactions. Collected bio-oil attained highest yield about 56.3 % at the 25 L/min of N_2 flow rate. Therefore, the 25 L/min is the optimal flow rate and by the definition of vapour residence time in Subchapter 2.3.1.2, the N_2 flow rate meets the need of less than 2 s of vapour residence time in pyrolysis reactor. Then, when the flow rate of N_2 was increased highly more than 25 L/min, bio-oil yield started to decrease, while NCG released increased and char formation insignificantly changed. This is attributed to higher movement of fluidising gas has interrupted the heat transfer between RMS particles and this condition led to too short vapour residence time for volatiles to cool down in condenser, which eventually resulted in lowering bio-oil yield and increasing NCG released containing more volatiles components.
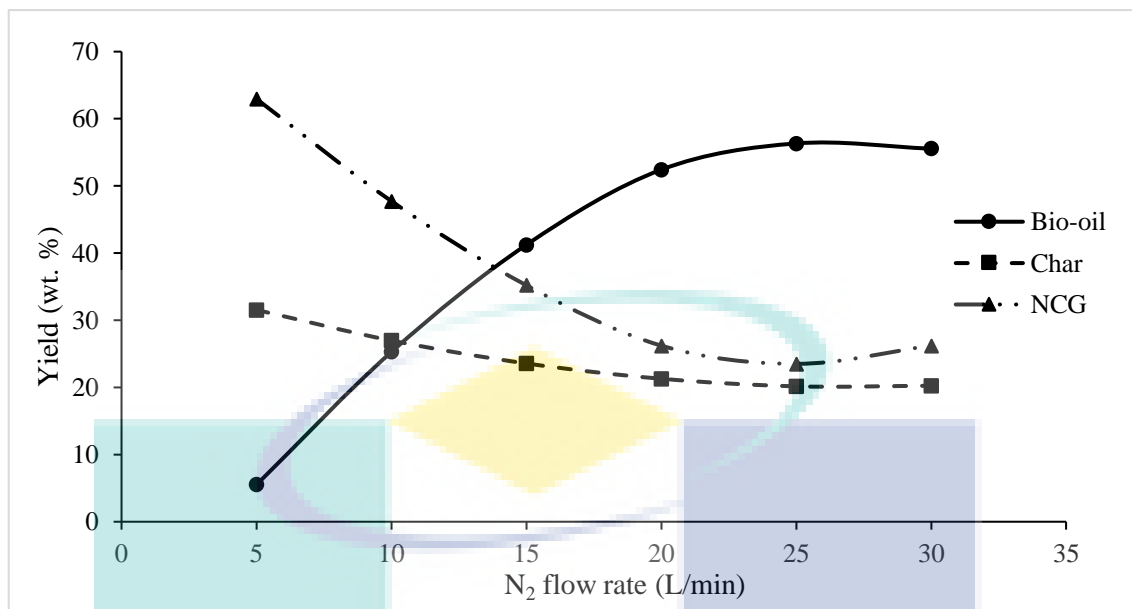
Figure 4.4   Products distribution as a function of sweeping N_2 flow rate at 450 °C of temperature, 20 min of retention time and 0.3 mm of RMS particles size

         Result obtained from this experiment exhibits almost similar trend with result gathered by Choi et al. (2012) and Heidari et al. (2014). Flow rate of inert gas flow in reactor determines vapour residence time, fluidisation condition and heat transfer characteristics. At lower gas flow rate, vapour residence time is longer than needed, thus, secondary reactions such as cracking, depolymerisation and recondensation tend to occur on pyrolysis vapour. This reactions eventually lessen the yield of bio-oil and increase in NCG product (Heo, Park, Park, et al., 2010). When the flow rate of gas is increased until optimum flow rate is reached, the shorter the vapour residence time can be achieved. According to Choi et al., higher N_2 flow rate supports and enhances mixing between feed particles due to high bubbling motion and further, promotes shorter vapour residence time, which consequently, favours for higher liquid yield and probability for secondary cracking occurs on primary products in pyrolysis vapour can be minimised. On the other hand, when the flow rate of N_2 gas is too high, bubbling motion also will be high. This situation leads to lower in both solid mixing and heat transfer efficiency, and eventually results in lower yield of bio-oil (Choi et al., 2012; Heidari et al., 2014).

Effect of retention time

         To study the effect of retention time of RMS in pyrolysis reactor towards pyrolysis products, the experiment was conducted with retention time of RMS feedstock in

fluidised bed reactor varied as stated in Table 3.3 and result obtained is presented in Figure 4.5.
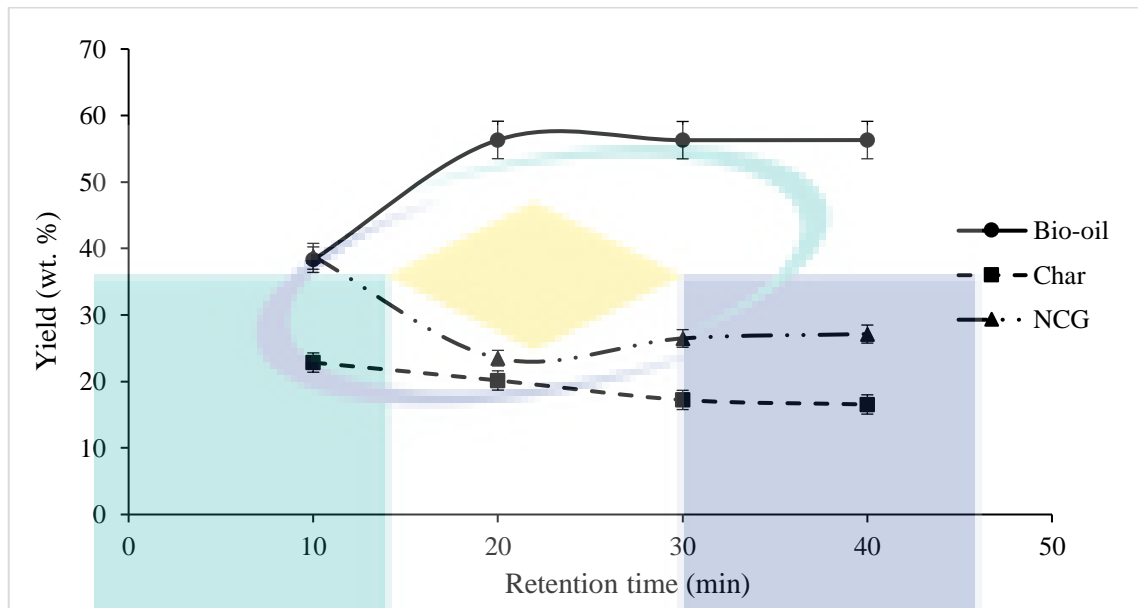
Figure 4.5   Products distribution as a function of retention time at 450 °C of temperature, 25 L/min of N_2 flow rate and 0.3 mm of RMS particles size

By referring to Figure 4.5, RMS fraction was completely pyrolysed at optimum retention time of 20 min, with the production of bio-oil was 56.3 %. When retention time was increased up to 40 min, bio-oil yield insignificantly changed, while char formation decreased and NCG released increased gradually. Through observation on collected char, when retention time shorter than 20 min, some fraction of RMS still did not fully pyrolysed. This is due to insufficient reaction time available for RMS to heat up and transfer the heat between and within RMS particles, which eventually led to incomplete decomposition. Same finding also reported by Ngo et al. (2013). However, when longer retention time was provided, RMS completely decomposed but on the other hand, in term of operation, it would increase operating cost and consumes unneeded time. Furthermore, bio-oil yield could be decreased due to secondary reactions of cracking and repolymerisation which occur on unstable pyrolysis vapour, with finally lead to release more NCG and form more char (Boroson et al., 1989).

Effect of particle size, D_p

Feed particles size is another factor that can influence liquid yield. Hence, this study was conducted to evaluate its effect. In this study, the effect of three particles sizes

of RMS with arithmetic average size of 0.30, 0.89 and 1.59 mm on product yield were studied and compared.

Result of this pyrolysis experiment is presented in Figure 4.6. As shown in Figure 4.6, as the particles size was increased from 0.30 to 0.89 mm, and next to 1.59 mm, amount of bio-oil yield decreased slightly from 56.3 to 55.0 %, and next to 54.4 %. This result suggests that feed particles size insignificantly affecting the bio-oil yield due to the size of feed particles was smaller than 2.00 mm, which still allowing efficient heat transfer within RMS fraction to decompose to produce bio-oil. However, as the size of particles was increased, heat transfer efficiency within RMS became slower due to heat residence distance from surface to centre of particles is longer. This condition led to imperfect pyrolysis condition and caused incomplete decomposition, which eventually resulted in increasing char formation and decreasing bio-oil yield, as observed in Figure 4.6.
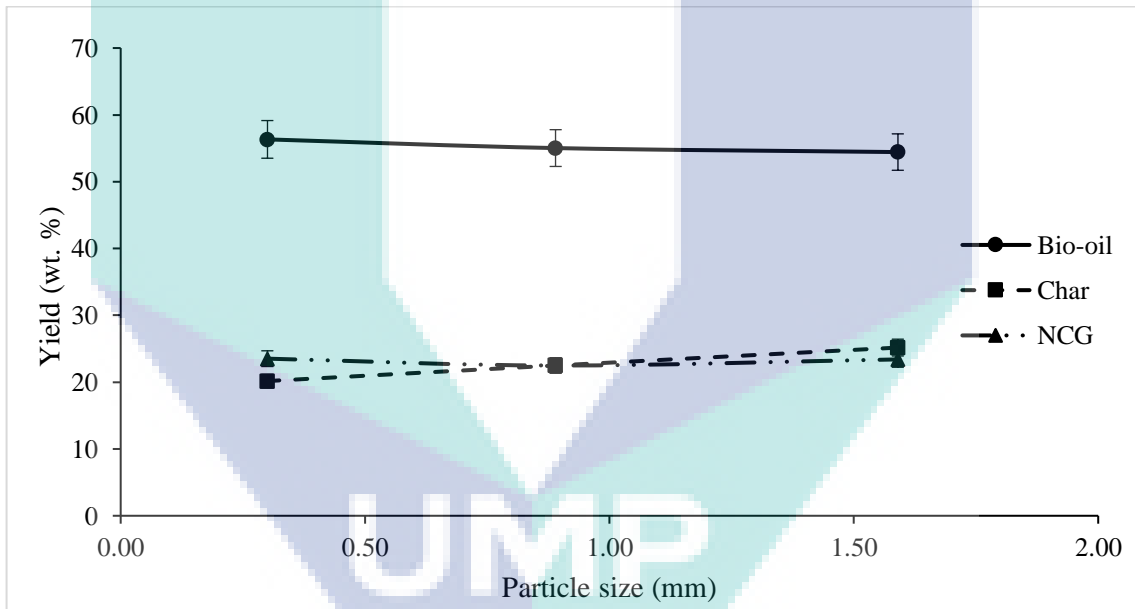
Figure 4.6   Products distribution as a function of RMS particles size at 450 °C of temperature, 25 L/min of N_2 flow rate and 20 min of retention time

Larger particle requires more time to heat by intra-particle conduction (Uzun et al., 2007), where eventually lead to slower heating rate and incomplete thermal decomposition, and thereby increase in char and less in vapour yields (Park et al., 2009). Thus, for the higher yield of bio-oil, smaller size of biomass is much needed, in which, the smaller the particles size, the higher the surface area per unit weight is provided to promote better heat transfer (Neves et al., 2011). However, too smaller particles size also is not recommended because this smaller size will drives higher heat transfer coefficient

and as a result, increases the gases yield (Islam & Ani, 1998). Thus, the optimum feed particle size for more efficient heating transfer rate is smaller than 2 mm (Garcia-Perez et al., 2008).

4.2.2.2   Effect on Bio-oil Composition

In terms of operating parameter of pyrolysis, previous studies reported only two operating parameters affecting the quality of extracted bio-oil, while the other parameters do not have a significant impact (Wang et al., 2010) and thus, their effect are not discussed here. These parameters are temperature and biomass particles size. The results of the experimental work are discussed below.

Effect of Temperature

Pyrolysis temperature is the most important operating parameter affecting the yield of bio-oil and apart of the yield, temperature also plays a role in determining the chemical properties of extracted bio-oil. Thus, the bio-oil obtained (Run 1 to Run 6 as listed in Table 3.3) at every pyrolysis reaction temperature were taken for both elemental and compounds analyses.

Bio-oil yield as indicated in Figure 4.3 is an actual yield where the initial moisture content of liquid product which free from initial water content in RMS because water in RMS is considered already been removed during heating at 105 °C overnight and 30 min in pyrolysis reactor before pyrolysis process started. Even though RMS was initially water free, some portion of water was still produced during pyrolysis process (Akhtar & NorAishah, 2012) and it cannot be avoided. Figure 4.7 shows in detailed the content of organic liquid and water produced at wide range of temperature. As shown in Figure 4.7, water content in bio-oils varied as the temperature was increased. At the temperature range from 350 to 450 °C, water in bio-oil was significantly increased. This is due to dehydration reaction occurred on biomass, with the major contribution of water (pyrolytic water) produced was believed especially by dehydration of hemicellulosic component in RMS. This result agrees with Azeez et al. (2010) which reported that amount of pyrolytic water produced is high as the hemicellulose component in biomass high. Apart of pyrolytic water, reaction water was also produced during pyrolysis process, attributed to the intra-particle cracking and/or condensation reactions occurred due to the presence of AAEM content in RMS (Mourant et al., 2011). When the temperature was increased up

to 600 °C, water content still gradually increased but insignificantly, also attributed to pyrolytic water formed during dehydration of remaining carbohydrates (Di Blasi et al., 2008; Azeez et al., 2010) and reaction water (catalytic cracking by AAEM) (Fahmi et al., 2008; Mourant et al., 2011).
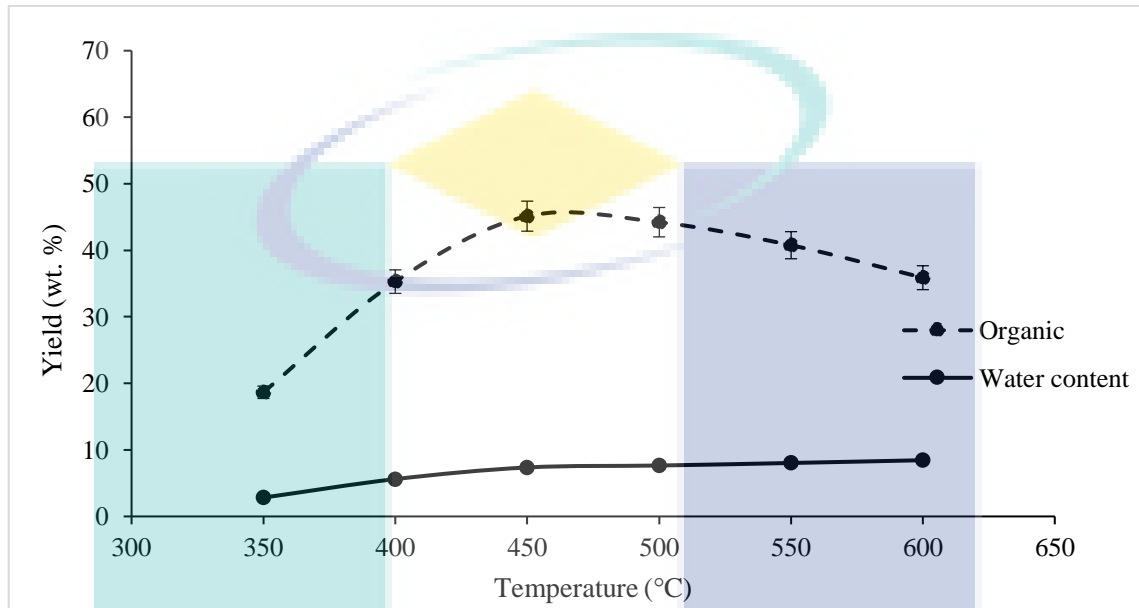
Figure 4.7   Organic liquid and water content in bio-oil as a function of pyrolysis temperature at 25 L/min of N_2 flow rate, 20 min of retention time and 0.3 mm of RMS particles size

Apart of water content, elemental analysis of bio-oil also shown some changes with increasing temperature. These changes are listed in Table 4.3. Calorific value of bio-oil exhibited an increasing within the ranges between 20.91 and 23.00 MJ/kg for HHV and 19.22 to 21.33 MJ/kg for LHV. HHV is a gross heating value, while LHV is the net heating value (Garcia-Perez et al., 2008). The heating values obtained in this study are very close to those reported for other bio-oil with the range from 19 to 22 MJ/kg for dry hardwood (Oasmaa et al., 1997). As compared to RMS, all extracted bio-oil have higher HHV than RMS, indicating that potential energy of biomass can be improved by thermal-chemical conversion.

Table 4.3   Elemental analysis of RMS and bio-oil as a function of pyrolysis temperature

Composition	RMS	Temperature (°C)					
		350	400	450	500	550	600
C	42.099	45.75	46.05	46.97	47.56	49.75	50.44
H	7.88	7.73	7.66	7.48	7.86	7.89	7.67
N	0.235	1.58	2.39	2.98	3.99	3.42	3.32
O^b	49.754	44.95	43.87	42.47	40.56	38.90	38.54
S	0.03	0.02	0.03	0.01	0.03	0.04	0.03
H/C	2.24	2.04	2.04	1.92	1.98	1.92	1.80
O/C	0.89	0.55	0.71	0.68	0.64	0.59	0.57
HHV^a	19.492	20.91	21.01	21.19	22.11	23.05	23.00
LHV^b	17.77	19.23	19.34	19.56	20.39	21.33	21.33
Water content (wt. %)	5.95	13.17	13.72	14.02	14.75	16.46	19.06
Molar formula	$CH_{2.24}O_{0.89}N_{0.005}$	$CH_{2.04}O_{0.55}$	$CH_{2.04}O_{0.71}$	$CH_{1.92}O_{0.68}$	$CH_{1.98}O_{0.64}$	$CH_{1.92}O_{0.59}$	$CH_{1.8}O_{0.57}$

[a] By calculation using Dulong-type equation
[b] By calculation proposed by Oasmaa
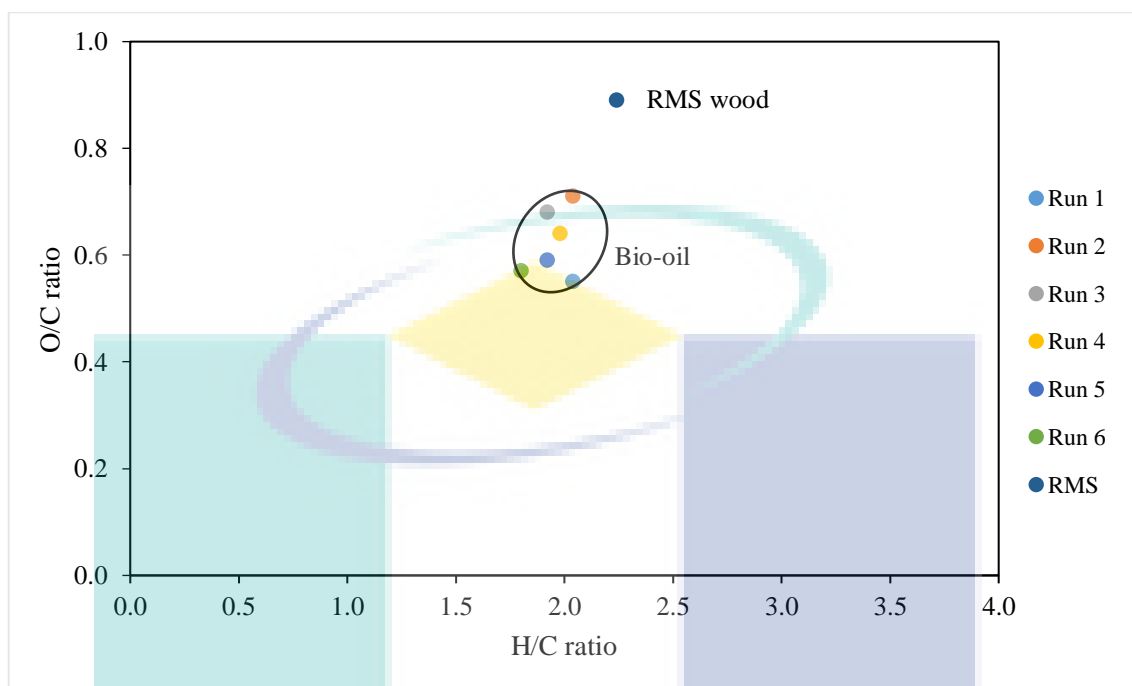
Figure 4.8   Van Krevelen diagram of bio-oil

Besides calorific values, H/C and O/C of bio-oil also showed some changes within the range from 1.92 to 2.04 and 0.55 to 0.71, respectively. The values of these ratios are plotted in Van Krevelen diagram in Figure 4.8. The H/C ratio of bio-oil produced in this work are quite high, almost approaching the value for ideal hydrocarbon. However, high oxygen amount in bio-oil have become a barrier and further treatments such as catalytic cracking or hydrodeoxygenation are needed to eliminate oxygen largely, so that the final product of bio-oil achieves low O/C.

The point of plotted H/C and O/C ratios of bio-oil gathered in this study have similar finding with Kersten et al. (2007) where the plotted points were lying within the point around 1.7 for H/C and 0.6 for O/C (Kersten et al., 2007; Wildschut, 2009). Even though bio-oil produced in this study is not suitable for transportation fuel, bio-oil is still having potential to used directly for heat and power generation in boilers, turbines, and kilns.

Effect of Particle Size

Apart of temperature, biomass particles size also has an influence on bio-oil quality, in aspect of the formation of water during pyrolysis, called 'pyrolytic water'

(Garcia-Perez et al., 2008). The relationship between pyrolytic water formed as a function of feed particle size obtained in this experimental work is presented in Figure 4.9.

As observed in Figure 4.9, it could clearly be seen that amount of pyrolytic water formed during pyrolysis increased as particles size was increased, indicating that feed particles size significantly produced important amount of water in bio-oil. This is because, as particles size of biomass was increased, the volatiles released inside biomass had to travel through the shell of the char formed. This hot surface of char, then, could catalyse dehydration of some primary products in volatiles which eventually increase the amount of water content in liquid. Therefore, the larger the particle size, the greater the amount of water could be produced.
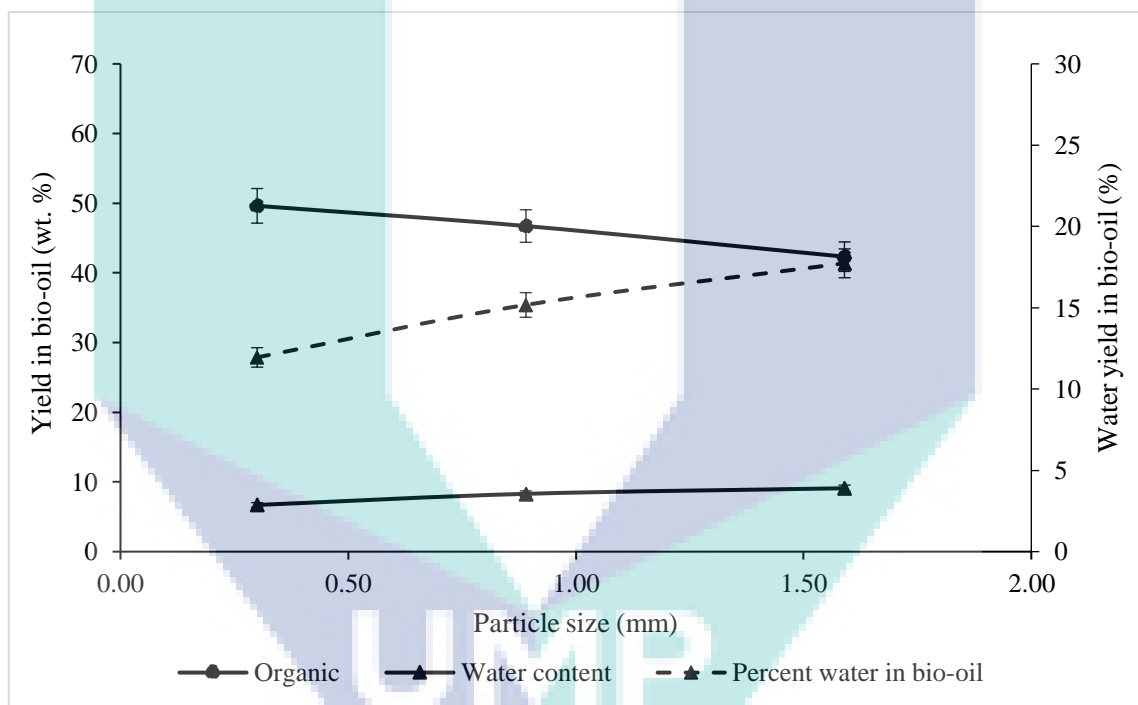
Figure 4.9   Organic liquid and water content in bio-oil as a function of RMS particles size at 450 °C of temperature, 25 L/min of N_2 flow rate and 20 min of retention time

This result agrees with study conducted by Shen et al. (2009). According to the authors, water produced in bio-oil were changing mainly at the average range of particles size between 0.3 and 2.00 mm. However, little changes were observed when particles size were larger than 2.00 mm. Even though this study was limited to particles size smaller than 2.00 mm, the trend of pyrolytic water formation for these small particles were similar to those reported by Scott et al. (1999) and Garcia-Perez et al. (2008).

4.2.3 Bio-oil Compound Characterisation

Table 4.4 shows relative percentage area of bio-oil compound obtained through the experiment of Run 17. Approximately 84.91 % of the total area was identified and quantified by GC-MS analysis. Bio-oil compounds as listed in Table 4.4 is grouped according to their source. Phenolic compounds is originally derived from lignin (Fahmi et al., 2007) and (Tröger et al., 2013), aldehyde, alcohol, ketone and acid compounds are mostly product of hemicellulose (Azeez et al., 2010), anhydrosugar and furan compounds are cellulose derivative (Azeez et al., 2010).

As listed in Table 4.4, the major compound of bio-oil is dominated by phenolic compounds about 40.80 area %, followed by aldehyde, alcohol, ketone and acid compounds about 29.86 area % and anhydrosugar compounds about 12.82 area % with levoglucosan yield only 8.97 area %. Interestingly, bio-oil extracted from RMS is composed of compound with having molecular weight in range from 110.00 to 200.00 g/mol with no lower molecular weight less than 100.00 g/mol such as HAA, acetaldehyde, acetic acid detected. This result is quite differ from the compounds such as listed in Table 2.2 and other findings by Azeez et al. (2010) and Eom et al. (2011). This can be attributed to the low concentration of AAEM (K, Na, Ca and Mg) content in RMS with the total AAEM concentration was only 0.28 wt. % f or 2350 mg/kg (as listed in Table 4.1). During pyrolysis, this lower level of AAEM predominated repolymerisation reaction, rather than fragmentation, resulted in higher molecular weight compounds formation. This statement is in line with Fahmi et al. (2007). Fragmentation reaction, on the other hand, is the reaction catalyst by higher AAEM content which occurred on monomers resulting in producing lower molecular weight compound (Fahmi et al., 2007).

As listed in Table 4.4, it can be seen that amount of levoglucosan (in anhydrosugars) yield in extracted bio-oil is quite low, namely 8.97 area %. This is because, levoglucosan is a product of cellulose and levoglucosan is produced largely at temperature around 300 °C. However, as temperature is increased, levoglucosan production will be decreased. Thus, since typical cellulose (including cellulose in RMS) decompose at the temperature range between 300 and 450 °C, then the amount of levoglucosan produced in bio-oil was proportionate to the quantity of remaining decomposition of cellulose. Moreover, the production of bio-oil was conducted at temperature of 450 °C, in which at this temperature, the formed levoglucosan was

vaporised and decomposed to form furans and acid (Sinha et al., 2000), and dehydrate to form other sugar product (Azeez et al., 2010). This is the reason why furans and D-allose compounds were produced and their content were 1.43 area % and 3.85 area %, respectively.

Table 4.4   Relative percent area of the main compounds identified in bio-oil

Compound	Area Percent	Molecular weight	Chemical Formula
Phenolic			
Phenol, 2,4-dimethyl-	7.62	122.16	$C_8H_{10}O$
Phenol, 2-methoxy-4-methyl-	4.33	138.16	$C_8H_{10}O_2$
2-Methoxy-4-vinylphenol	7.72	150.18	$C_9H_{10}O_2$
Phenol, 2,6-dimethoxy-	3.94	154.16	$C_8H_{10}O_3$
Vanillin	1.36	152.15	$C_8H_8O_3$
Phenol, 2-methoxy-4-(1-propenyl)-, (Z)-	2.15	164.20	$C_{10}H_{12}O_2$
Phenol, 2-methoxy-4-propyl-	1.03	166.22	$C_{10}H_{14}O_2$
Phenol, 2,6-dimethoxy-4-(2-propenyl)-	11.32	194.23	$C_{11}H_{14}O_3$
Ethanone, 1-(4-hydroxy-3,5-dimethoxyphenyl)-	1.32	196.20	$C_{10}H_{12}O_4$
Aldehyde, ketone, acid and alcohol			
3-Cyclobutene-1,2-dione, 3,4-dihydroxy-	5.15	114.06	$C_4H_2O_4$
1,2-Benzenediol	5.95	110.11	$C_6H_6O_2$
1,2-Benzenediol, 3-methoxy-	1.43	140.14	$C_7H_8O_3$
1,2-Benzenediol, 4-methyl-	1.21	124.14	$C_7H_8O_2$
4-Fluoro-3-methylanizole	1.32	140.16	C_8H_9FO
1,2,3-Benzenetriol	1.95	126.11	$C_6H_6O_3$
1-(4-Hydroxymethylphenyl)ethanone	0.63	150.17	$C_9H_{10}O_2$
5-tert-Butylpyrogallol	0.25	182.22	$C_{10}H_{14}O_3$
Homovanillyl alcohol	1.43	168.19	$C_9H_{12}O_3$
4-Methyl-2,5-dimethoxybenzaldehyde	1.82	180.20	$C_{10}H_{12}O_3$
Benzaldehyde, 4-hydroxy-3,5-dimethoxy-	7.33	182.17	$C_9H_{10}O_4$
3,4-Dimethoxy-6-amino toluene	1.25	167.21	$C_9H_{13}NO_2$
Benzeneacetic acid, 4-hydroxy-3-methoxy-, methyl ester	0.13	196.20	$C_{10}H_{12}O_4$
Anhydrosugar			
1,6-Anhydro-.beta.-D-glucopyranose (levoglucosan)	8.97	162.14	$C_6H_{10}O_5$
D-Allose	3.85	180.16	$C_6H_{12}O_6$
Furan			
2-Furancarboxaldehyde, 5-(hydroxymethyl)-	1.43	126.11	$C_6H_6O_3$

4.2.4 Summary

Through this study, it has been confirmed that RMS has a potential as renewable energy resource to produce bio-oil using fast pyrolysis process technology. For optimising bio-oil production, determination the whole parameter for fast pyrolysis process is crucial. In this study, it was found that highest bio-oil was obtained about 56.33 % at 450 °C of temperature, 25 L/min of N_2 flow rate and 20 min of retention time. For bio-oil characterisation, in term of composition, bio-oil containing higher oxygen content, and in term of compound, bio-oil containing high phenolic compounds. Even though bio-oil produced in this study is not suitable for transportation fuel due to high oxygen content, bio-oil is still having other potential application which can used directly for heat and power generation, as well as, can be extracted to recover useful chemical such as phenolic and anhydrosugar compounds for resin and pharmaceutical industries.

4.3 Study the Effect of Washing Treatment

In this study, raw RMS feedstock was washed by DI water or HCl solutions prior to pyrolysis process. Different washing solution was employed in order to determine which solution allows the removal of AAEM in RMS as much as possible, and further, determine detailed thermal decomposition mechanism via TGA, as well as, assess the changes in RMS chemical bond via FTIR. To evaluate the pattern of pyrolytic product distributions, raw RMS along with demineralised RMS were subjected to pyrolysis experiment at different temperature (350 to 600 °C). In addition of that, with targeting higher bio-oil yield as compared to cost incurred in the process, one of the treatment solutions is suggested to be applied. For bio-active compounds of extracted bio-oil characterisation, bio-oil yield at 450 °C of operating temperature for raw- and demineralised-RMS were taken and subjected to GC-MS analysis to observe to what extend the washing treatment can improve bio-oil 'organic' content production, especially in enhancing anhydrosugars yield.

4.3.1 Red Meranti Sawdust Analysis

To determine the effect of AAEM content on yield and quality of bio-oil, AAEM concentrations in raw- and demineralised-RMS were firstly analysed using ICP-OES. In addition, TGA also was performed to discern visually the changes of thermal

decomposition behaviour of each RMS feedstock. Result of these analyses are presented below.

4.3.1.1 Alkali and Alkaline Earth Metal Analysis

AAEM content and demineralisation efficiency of RMS samples before and after washing treatment with DI water and mild HCl acid solutions are listed in Table 4.5.

Table 4.5   ICP-OES analysis of AAEM in raw- and demineralised-RMS

Sample	Metal concentration (mg/kg)				Total AAEM (Mass %)	Demineralisation efficiency (%)			
	K	Na	Ca	Mg		K	Na	Ca	Mg
Raw RMS	1327.5	554.5	315.0	153.5	0.24	-	-	-	-
RMS – DI water	397.5	67.5	227.5	97.5	0.08	70.1	87.8	27.8	36.5
RMS – 1.0M HCl	67.5	53.5	18.0	18.0	0.02	94.9	90.4	94.3	88.3
RMS – 2.0M HCl	23.0	16.5	12.5	12.0	0.01	98.3	97.0	96.0	92.2

Potassium is by far the most abundant AAEM species in RMS. After DI water washing, large fraction of K and Na were successfully removed with observed removal efficiency between 70 % and 90 % as compared to Ca and Mg contents which only less than 40 % can be removed. This result indicates that the majority of K and Na had been dissolved in water, and indirectly suggests that K and Na were present in the form of water-soluble constituents. With regard to different degree concentration of HCl washing, large amounts of Ca and Mg in sample achieved higher removal, which the declining of AAEM concentration was related to acidity level of washing agent, in which, the stronger the acidity, the larger the removal of AAEM achieved. By comparing to their reduction by water washing, it indicates that the most of Ca and Mg were presence in the form of water-insoluble constituents. The different degree of AAEM removal transpired is due to the form of AAEMs present and the way it is bound to cell constituent and its depth from the cell lumen. Thus, some of these species are easy to remove by water washing, and the rest requires acid washing technique for greater AAEM removal (Mourant et al., 2011).

4.3.1.2 Thermal Analysis of Red Meranti Sawdust

Thermal decomposition behaviour of raw- and demineralised-RMS samples are presented in TGA and DTG graph in Figure 4.10, and summary of pyrolysis properties are listed in Table 4.6. Yield of pyrolytic products listed in Table 4.6 are taken at 550 °C

by taking into consideration that at this point of temperature, large fraction of RMS biomass had been pyrolysed.
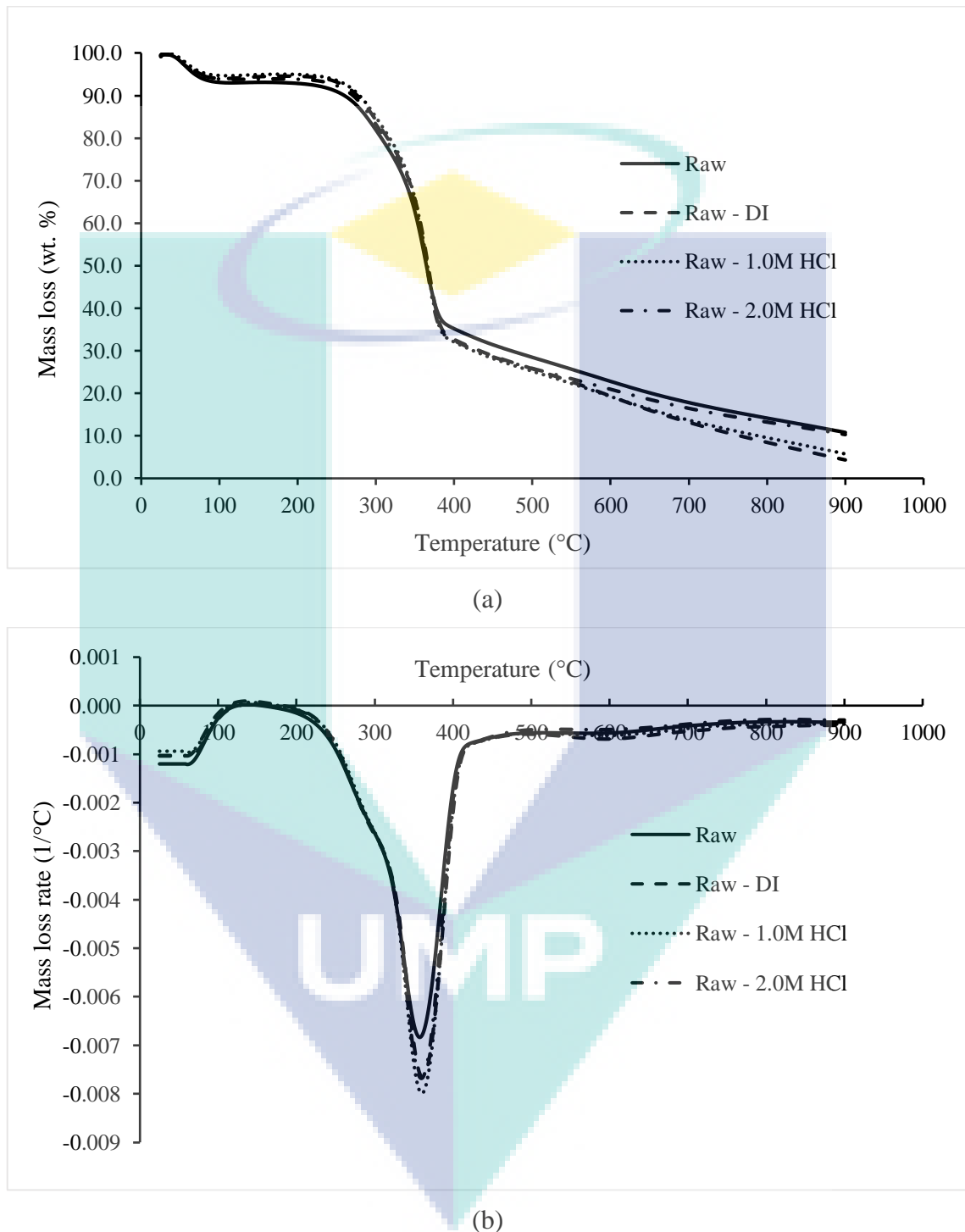

(a)

(b)

Figure 4.10   (a) TGA and (b) DTG profile of raw, acid- and water-washed RMS at heating rate of 10 °C/min in N_2 atmosphere

As shown in Figure 4.10 and refer to the information in Table 4.6, it can be seen that, maximum temperature rate of all demineralised RMS were higher about 3 to 4 °C

than raw RMS. The main reason that degradation of raw RMS was the lowest is attributed to catalysing effect of higher AAEM concentration in RMS which promotes lower thermal decomposition temperature by accelerating char formation. This explanation has been proved through observation in Figure 4.10 (a). As shown in Figure 4.10 (a), noted that raw RMS was initially producing the char at the 380 °C of temperature, while other demineralised RMS were still continuing important weight lost to release volatiles. This finding is consistent with the point that AAEM presence in biomass acted as natural catalyst and it possessed the ability to reduce temperature of degradation reaction (Fahmi et al., 2008). Apart from that, demineralised RMS possessed higher thermal stability for conversion, in which, this properties is explained by higher activation energy, similar as reported by Daniel, Jones, Brydson and Ross (2007) who evaluated activation energy of pre-treated biomass.

With regards to pyrolytic products yield, emission of volatiles during thermal degradation was improved by washing treatment. Demineralisation of RMS with 1.0 M HCl released more volatile about 72.39 %, followed by RMS - 2.0 M HCl about 70.44 %, RMS - DI water about 70.34 %, and raw RMS about 67.39 %. In addition of that, demineralisation also reduced char formation. In sequence, char yield decreased in the following order, raw RMS > RMS - 2.0 M HCl > RMS – DI water > RMS - 1.0 M HCl. By comparing volatiles released and char residues obtained in TGA, it obviously can be seen that the production of both products are contradicting to each other, indicating that pyrolytic products by various washing treatment of RMS were closely associated with difference concentration of AAEM in biomass. It can be concluded that, the lowest the concentration of AAEM, the highest the volatiles released and the least the char produced. This result agrees with previous literature reported by Nik-Azar et al., (1996), Fahmi et al. (2008), and NorAishah (2012).

Table 4.6   Pyrolysis properties of raw- and demineralised-RMS in TGA and DTG in N_2 at heating rate of 10 °C/min

Sample	Yield at 550 °C (wt. %)			Temperature at max rate (°C)	Degradation rate (1/°C)
	Moisture content	Volatiles	Char		
Raw RMS	6.95	67.39	25.66	357	-0.00684
RMS – DI water	6.96	70.34	22.71	361	-0.00766
RMS – 1.0 M HCl	5.31	72.39	22.3	360	-0.00799
RMS – 2.0 M HCl	6.14	70.44	23.42	359	-0.00768

In term of degradation rate, decomposition of demineralised RMS was better than raw RMS. Maximum degradation rate achieved the highest by RMS - 1.0 M HCl about -0.0079 as compared to raw RMS, was the lowest about -0.0068. Therefore, from the result in Figure 4.10 and summary in Table 4.6, it can be concluded that demineralised RMS provide better degradation behaviour than raw RMS.

4.3.1.3   Functional Group Analysis

For functional group analysis, only three samples of raw- and demineralised-RMS were selected for this analysis. They are raw RMS, RMS - DI water and RMS - 1.0 M HCl. Result of FTIR spectra for these samples are shown in Figure 4.11.
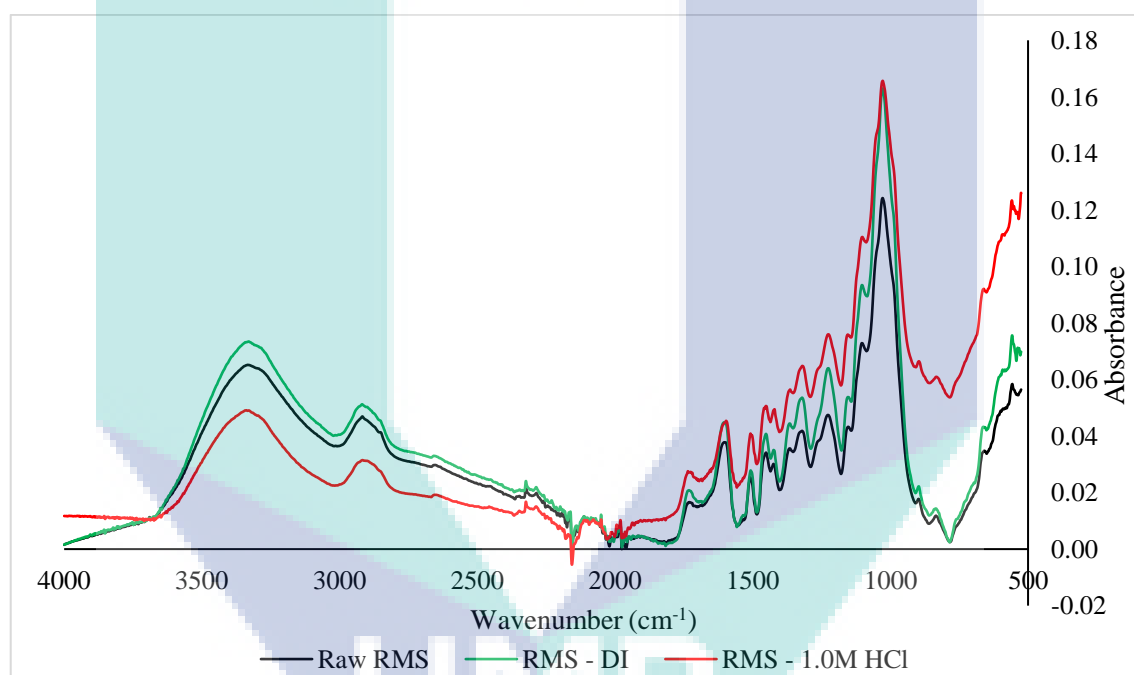
Figure 4.11   FTIR spectra of raw- and demineralised-RMS

As shown in Figure 4.11, in term of wavenumber, it can be observed that wavenumber of IR spectra's peak does not show significant changes to demineralised samples as compared to raw RMS. This imply that the demineralised process on RMS did not affecting the chemical structure of pure samples of RMS, where the functional group of samples are still uninterrupted. However, by comparing the intensity of absorbance, it clearly can be seen that the intensity of the absorbance of demineralised samples were changed, proving that the bond strength in RMS molecules has been altered. According to Michael Biewer (2011), intensity of light absorbed is related to the dipole of the bond, in which, the greater the dipole, the greater the absorbance intensity. Thus,

this result suggests that demineralised process has an influence on the strength of chemical bonds in feedstock.

Compare the IR spectres of raw RMS and demineralised RMS - DI water. It can be observed that absorbance intensity of RMS - DI water is higher, illustrating that bonding between molecules in RMS - DI water was stronger than raw RMS. This is due to the addition of water as polar molecules in RMS, where by this addition, the interaction between dipole-dipole in RMS and water had created very strong intermolecular forces. This argument is supported by the fact that molecular bond in wood are connected by three types of bond, and one of them are dipole-dipole bonds which makes the attraction between polar molecules in wood and other polar molecules became stronger (Vick, 2007). This result is confirmed by DTG profile in Figure 4.10 (b) for RMS - DI water, where, this sample demanded for higher energy of temperature (361 °C) than raw RMS (357 °C) to achieve maximum degradation.

Consider the IR spectres for raw RMS and demineralised RMS - 1.0 M HCl. It can be observed that the absorbance intensity of RMS - 1.0 M HCl was lower at the wavenumber over than 2200 cm^{-1} which suggests that molecular chemical bonds of C-H and O-H in demineralised RMS - 1.0 M HCl became weaker than raw RMS, while other bonds became stronger which leading to the intensity of absorbance at the wavenumber below than 2000 cm^{-1} was higher. Consequently, making the energy for overall temperature decomposition was higher than the original sample of RMS, and this argument is confirmed by maximum degradation temperature which shift from 357 °C for raw RMS to 360 °C for RMS – 1.0 M HCl.

4.3.2   Fast Pyrolysis Experiment

Results of pyrolysis experiments regarding the effect of AAEM content in raw and demineralised RMS to bio-oil yield and composition is attached in APPENDIX D in Table D2 and is discussed below. In this work, the fast pyrolysis experiment for demineralised RMS - 2.0 M HCl was not performed because from the result in Table 4.6, this feedstock does not show significant changes in volatiles released as compared to other demineralised RMS. Furthermore, by considering the cost of chemical involved, the washing treatment process of this feedstock itself is not profitable.

4.3.2.1   Effect on Bio-oil Yield

Figure 4.12 shows pyrolytic product distributions of raw and demineralised RMS at different temperature. As comparison, at the 350 °C of temperature, it can be seen that the amount of bio-oil yield did not showed significant changes between each other, while char formations were slightly lower for raw RMS as compared to demineralised RMS feedstock. This condition is attributed to higher AAEM concentration in raw which played a role as catalyst to accelerate the conversion process of biomass to volatiles at lower temperature. Similar result AAEM also obtained by Fahmi et al. (2008), and Akhtar and NorAishah (2012) which reported that AAEM in raw biomass possess as natural catalyst which able to increase thermal decomposition of biomass at lower temperature.

As temperatures was increased up to 400 °C, bio-oil production had intensified and increased significantly for all types of RMS, indicating that large RMS fractions had been pyrolysed and converted to bio-oil. At this point, bio-oil yield was the lowest, whilst char formation was the highest for raw RMS as compared to demineralised RMS, designating that bio-oil production had begun to be suppressed by AAEM species in biomass in order to promote char formation. This pattern of result coincides with review reported by Akhtar and NorAishah (2012), with stated that inorganics species speed up dehydration and charring reactions during both primary and secondary reactions, which eventually increased char formation.

When pyrolysis process was run at 450 °C of temperature, bio-oil yield for demineralised RMS increased up to 2.3 wt. % than raw RMS and achieved highest yield about 57.3 wt. % for 1.0 M HCl acid washing RMS, followed by RMS - DI water. After this point of temperature, amount of bio-oil yield started to decrease gradually until final temperature at 600 °C, indicating that secondary reactions i.e. cracking reaction on unstable pyrolysis vapour, and charring or dehydration reaction on pores of primary char, had commenced and occurred on primary products especially in raw RMS, resulted in releasing more NCG product and formation of secondary char, respectively. Secondary reactions commonly occur at 600 °C of temperature, but in this study, raw RMS was the first experienced notable loss in bio-oil yield at lower temperature, which the effect is the most attributed to the presence of higher concentration of AAEM in raw RMS as compared to other demineralised RMS. The pattern of result obtained agrees and

consistent with finding reported by Nik-Azar et al. (1996) and literature reviewed by Akhtar and NorAishah (2012). According to Nik-Azar et al., acid wash wood produce more bio-oil at any given temperature than origin wood, and according to Akhtar and NorAishah (2012), AAEM present in biomass lead to decreasing in liquid yield, and tend to promote char and gaseous formation. Fahmi et al., 2008 also reported similar finding.

From the whole pattern of the chart, it is noted that, demineralisation process by 1.0 M HCl washing method was the most applicable technic to remove much AAEM content without substantial changes to RMS structure and further, increased the amount of bio-oil yield. However, by considering the cost incurred in the process, it can be suggested that DI water washing is the most preferred method in a manner to minimise the cost of chemical involved, and in meantime, demineralised RMS with DI water also give higher yield of bio-oil and the lower yield of char formation as compared to others. This finding indirectly supports the suggestion by Scott et al. (2000) which mentioned that water washing is sufficient to put into practice for the aim of levoglucosan yield.
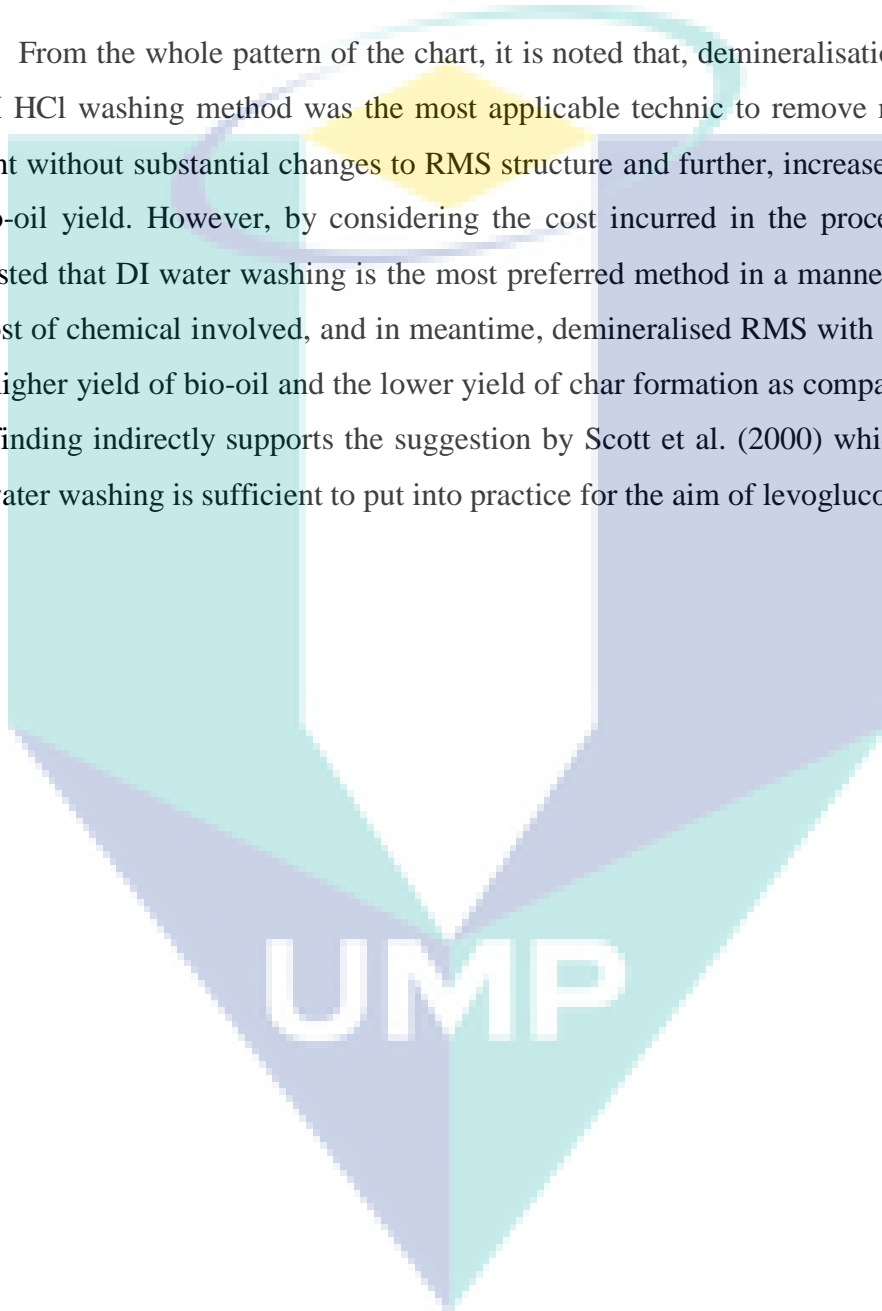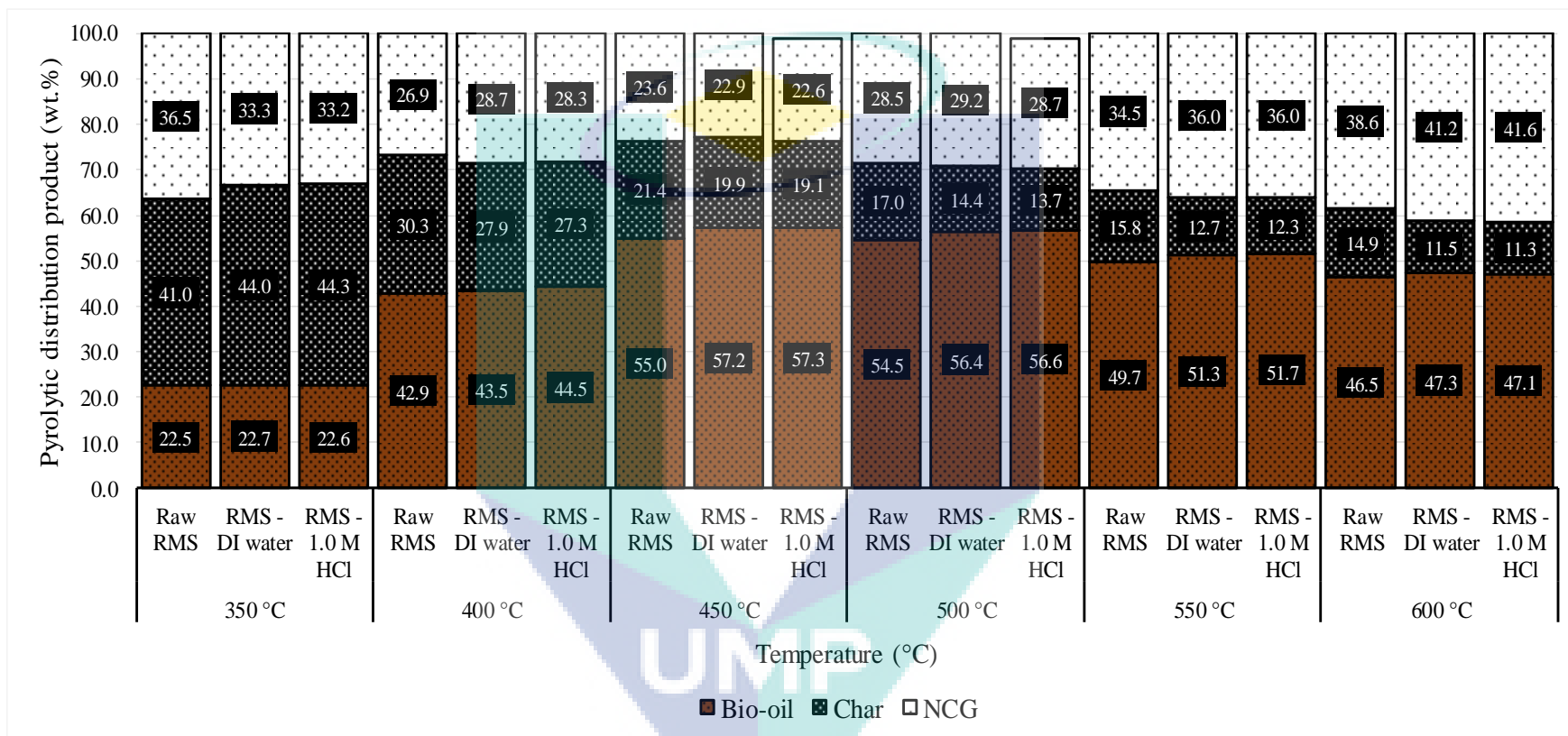
Figure 4.12   Pyrolytic product distribution of raw- and demineralised-RMS as a function of temperature at 25 L/min of N_2 flowrate, 20 min of retention time and ≤ 2.00 mm of RMS particles size

4.3.2.2   Effect on Bio-oil Composition

The influence of total AAEM concentration in raw- and demineralised - RMS feedstock on pyrolytic products yield are shown in Figure 4.13. Pyrolytic water is also included in bio-oil and the actual amount of water in bio-oil is presented in Figure 4.14.

Figure 4.13   Yield of pyrolytic products as a function of AAEM concentration in raw- and demineralised-RMS at 450 ˚C of pyrolysis temperature, 25 L/min of N_2 flowrate, 20 min of retention time and ≤ 2.00 mm of RMS particles size

As shown in Figure 4.13, it can be seen that the amount of bio-oil yield between raw- and demineralised-RMS yield was insignificantly affected by the total concentration of AAEM in RMS feedstock, where the changes in bio-oil yield between raw RMS and demineralised RMS - 1.0 M HCl is only 2.33 wt. %. This attributed to lower total concentration of AAEM in raw RMS, which gave the changes of total bio-oil production between raw- and demineralised-RMS less noticeable.
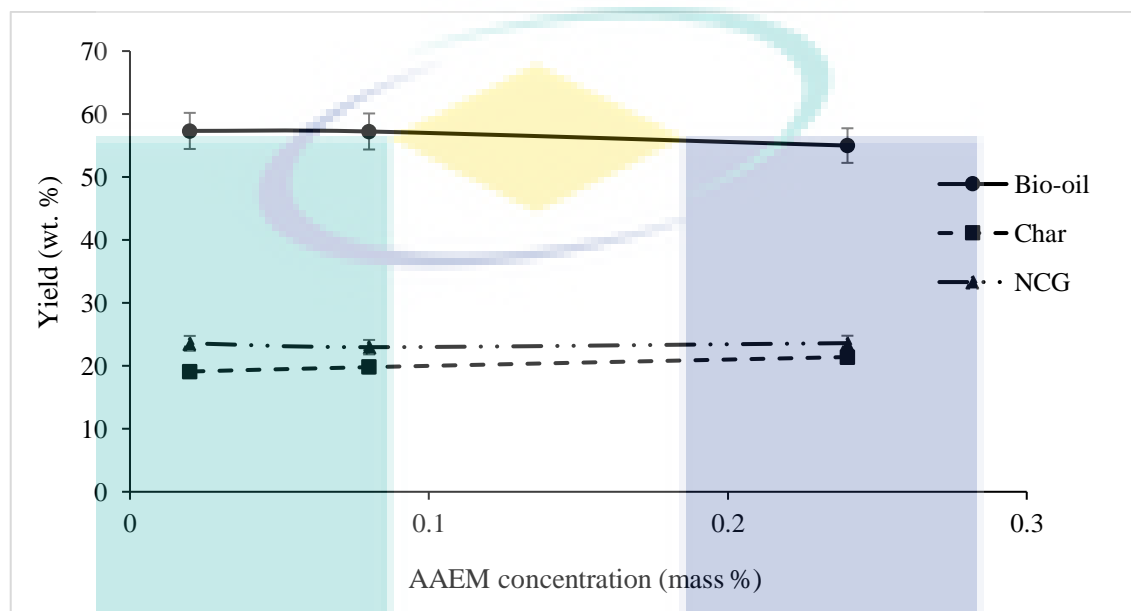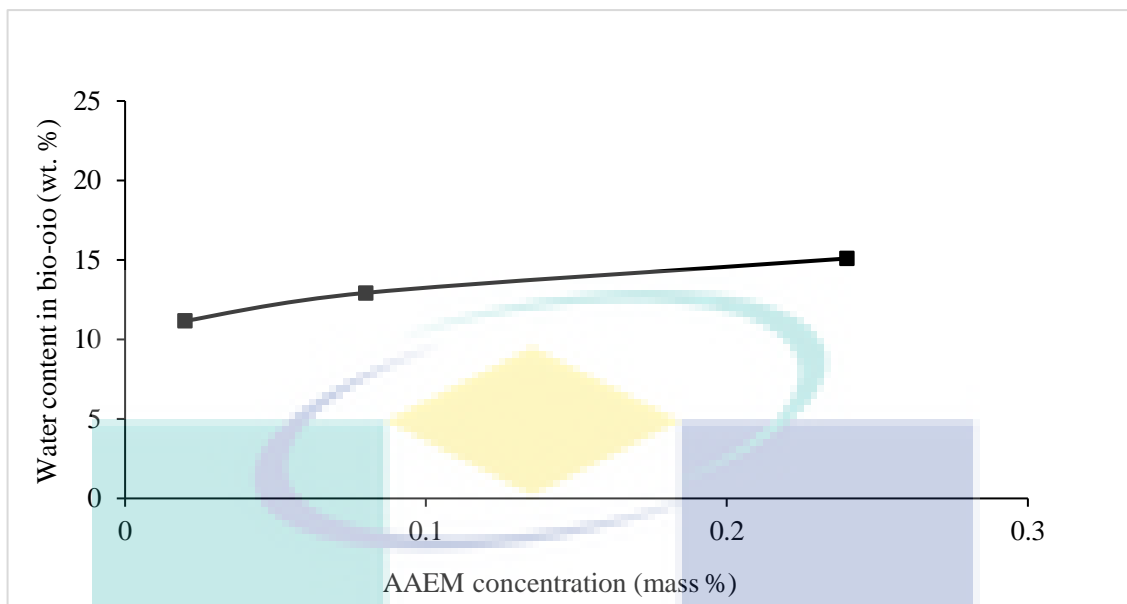
Figure 4.14   Water content in bio-oil as a function of AAEM concentration in raw- and demineralised-RMS at 450 ˚C of pyrolysis temperature, 25 L/min of N_2 flowrate, 20 min of retention time and ≤ 2.00 mm of RMS particles size

In term of water yield in bio-oil as shown in Figure 4.14, it can be seen that water content in bio-oil increased as the concentration of AAEM content increased. This result indicates that AAEM presence in feedstock was very sensitive even at lower concentration because AAEM acted as natural catalyst in accelerating cracking reaction, which eventually resulted in increasing water produced.

Water washing achieved removal of AAEM almost 66.39 % and by this removal, water content in bio-oil reduced about 2.16 %. For acid washing, AAEM in RMS almost completely removed and produced bio-oil with the reduction of water generated during pyrolysis about 3.93 %. At this point, water produced in bio-oil was considered only resulted from dehydration reaction, which no more catalytic cracking by AAEM. This result demonstrates that the more AAEM is eliminated from feedstock, then, the less water content produced in bio-oil. During pyrolysis, apart from initial moisture, water in bio-oil also resulted from both pyrolytic water (dehydration of hemicellulose) (Azeez et al., 2010), and reaction water (catalytic cracking by AAEM) (Fahmi et al., 2008). In this study, initial moisture was neglected by assuming that all initial moisture had been removed prior conducting pyrolysis process. Thus, by combining the data gathered in Figure 4.13 and Figure 4.14, only the removal of AAEM species through acid-washing led to a reduction in reaction water yield with the overall bio-oil yield (that includes the

114

pyrolytic water) remained unchanged. It thus appears that the yield of bio-oil 'organic' fraction was increased slightly by the acid-washing of RMS.

4.3.3   Bio-oil Compound Characterisation

Although bio-oil yield shown insignificant changes with the removal of AAEM species through washing treatment, however, the production of organic compounds in bio-oil is clearly experiencing changes in the number of compounds yield and the variety of compounds produced. Bio-oil compounds of raw- and demineralised - RMS are listed in Table 4.7 to Table 4.9 based on group compound according to their origin. Anhydrosugar and furan compounds are products of cellulose (Azeez et al., 2010), aldehyde, alcohol, ketone and acid compounds are mostly derived from hemicellulose (Azeez et al., 2010), and phenolic compound is mainly from lignin (Fahmi et al., 2007) and (Tröger et al., 2013). Some of the same compounds detected by GC-MS in all samples are simplified in Figure 4.15 to observe any changes in the amount of bio-active compounds yield in bio-oil at different degree of AAEM concentration in RMS. Total compound detected by GC-MS in raw RMS, RMS - DI water and RMS - 1.0 M HCl are 84.91 area %, 84.28 area % and 87.86 area %, respectively.

Table 4.7   Bio-oil compounds of RMS

Compound	Area Percent	Molecular weight	Chemical Formula
Phenolic			
Phenol, 2,4-dimethyl-	7.62	122.16	$C_8H_{10}O$
Phenol, 2-methoxy-4-methyl-	4.33	138.16	$C_8H_{10}O_2$
2-Methoxy-4-vinylphenol	7.72	150.18	$C_9H_{10}O_2$
Phenol, 2,6-dimethoxy-	3.94	154.16	$C_8H_{10}O_3$
Vanillin	1.36	152.15	$C_8H_8O_3$
Phenol, 2-methoxy-4-(1-propenyl)-, (Z)-	2.15	164.20	$C_{10}H_{12}O_2$
Phenol, 2-methoxy-4-propyl-	1.03	166.22	$C_{10}H_{14}O_2$
Phenol, 2,6-dimethoxy-4-(2-propenyl)-	11.32	194.23	$C_{11}H_{14}O_3$
Ethanone, 1-(4-hydroxy-3,5-dimethoxyphenyl)-	1.32	196.20	$C_{10}H_{12}O_4$
Aldehyde, ketone, acid and alcohol			
3-Cyclobutene-1,2-dione, 3,4-dihydroxy-	5.15	114.06	$C_4H_2O_4$
1,2-Benzenediol	5.95	110.11	$C_6H_6O_2$
1,2-Benzenediol, 3-methoxy-	1.43	140.14	$C_7H_8O_3$
1,2-Benzenediol, 4-methyl-	1.21	124.14	$C_7H_8O_2$
4-Fluoro-3-methylanizole	1.32	140.16	C_8H_9FO
1,2,3-Benzenetriol	1.95	126.11	$C_6H_6O_3$
1-(4-Hydroxymethylphenyl)ethanone	0.63	150.17	$C_9H_{10}O_2$
5-tert-Butylpyrogallol	0.25	182.22	$C_{10}H_{14}O_3$
Homovanillyl alcohol	1.43	168.19	$C_9H_{12}O_3$
4-Methyl-2,5-dimethoxybenzaldehyde	1.82	180.20	$C_{10}H_{12}O_3$
Benzaldehyde, 4-hydroxy-3,5-dimethoxy-	7.33	182.17	$C_9H_{10}O_4$
3,4-Dimethoxy-6-amino toluene	1.25	167.21	$C_9H_{13}NO_2$
Benzeneacetic acid, 4-hydroxy-3-methoxy-, methyl ester	0.13	196.20	$C_{10}H_{12}O_4$
Anhydrosugar			
1,6-Anhydro-.beta.-D-glucopyranose (levoglucosan)	8.97	162.14	$C_6H_{10}O_5$
D-Allose	3.85	180.16	$C_6H_{12}O_6$
Furan			
2-Furancarboxaldehyde, 5-(hydroxymethyl)-	1.43	126.11	$C_6H_6O_3$

Table 4.8   Bio-oil compounds of demineralised RMS - DI water

Compound	Percent Area	Molecular weight	Chemical Formula
Phenolic			
Phenol, 2,4-dimethyl-	0.53	122.17	$C_8H_{10}O$
Phenol, 2-methoxy-4-methyl-	4.80	138.17	$C_8H_{10}O_2$
Phenol, 4-ethyl-2-methoxy-	1.25	152.19	$C_9H_{12}O_2$
2-Methoxy-4-vinylphenol	7.72	150.18	$C_9H_{10}O_2$
Phenol, 2,6-dimethoxy-	3.47	154.16	$C_8H_{10}O_3$
Vanillin	1.95	152.15	$C_8H_8O_3$
Phenol, 2-methoxy-4-(1-propenyl)-, (Z)-	2.90	164.20	$C_{10}H_{12}O_2$
Phenol, 2-methoxy-4-propyl-	1.43	166.22	$C_{10}H_{14}O_2$
Ethanone, 1-(4-hydroxy-3-methoxyphenyl)-	0.95	166.18	$C_9H_{10}O_3$
Phenol, 2,6-dimethoxy-4-(2-propenyl)-	14.19	194.23	$C_{11}H_{14}O_3$
Ethanone, 1-(4-hydroxy-3,5-dimethoxyphenyl)-	1.67	196.20	$C_{10}H_{12}O_4$
Aldehyde, ketone, acid and alcohol			
1,2-Benzenediol	1.30	110.11	$C_6H_6O_2$
1,2-Benzenediol, 3-methoxy-	1.06	140.14	$C_7H_8O_3$
1,2-Benzenediol, 4-methyl-	0.41	124.14	$C_7H_8O_2$
1,2,3-Benzenetriol	1.60	126.11	$C_6H_6O_3$
5-tert-Butylpyrogallol	0.65	182.22	$C_{10}H_{14}O_3$
Homovanillyl alcohol	1.08	168.19	$C_9H_{12}O_3$
4-Methyl-2,5-dimethoxybenzaldehyde	2.22	180.20	$C_{10}H_{12}O_3$
Benzaldehyde, 4-hydroxy-3,5-dimethoxy-	5.95	182.17	$C_9H_{10}O_4$
1-Nitro-1-deoxy-d-glycero-l-mannoheptitol	1.97	241.20	$C_7H_{15}NO_8$
3,5-Dimethoxy-4-hydroxyphenylacetic acid	1.92	212.20	$C_{10}H_{12}O_5$
3,5-Dimethoxy-4-hydroxycinnamaldehyde	3.30	208.21	$C_{11}H_{12}O_4$
Benzeneacetic acid, 4-hydroxy-3-methoxy-, methyl ester	0.49	196.20	$C_{10}H_{12}O_4$
Dibenz[a,c]cycloheptane, 2,3,7-trimethoxy-	0.23	284.36	$C_{18}H_{20}O_3$
4-Methoxy-4',5'-methylenedioxybiphenyl-2-carboxylic acid	1.89	272.26	$C_{15}H_{12}O_5$
Dibenzo[e,g]benzimidazole, 2-(2-furyl)-3-methyl-	0.45	298.35	$C_{20}H_{14}N_2O$
Anhydrosugar			
1,6-Anhydro-.beta.-D-glucopyranose (levoglucosan)	10.34	162.14	$C_6H_{10}O_5$
D-Allose	5.80	180.16	$C_6H_{12}O_6$
Furan			
2-Furancarboxaldehyde, 5-(hydroxymethyl)-	1.17	126.11	$C_6H_6O_3$

Table 4.9   Bio-oil compounds of demineralised RMS - 1.0 M HCl

Compound	Area Percent	Molecular weight	Chemical Formula
Phenolic			
Phenol, 2,4-dimethyl-	0.53	122.17	$C_8H_{10}O$
Phenol, 4-ethyl-2-methoxy-	1.25	152.19	$C_9H_{12}O_2$
2-Methoxy-4-vinylphenol	7.93	150.18	$C_9H_{10}O_2$
Phenol, 2,6-dimethoxy-	4.12	154.16	$C_8H_{10}O_3$
Vanillin	2.42	152.15	$C_8H_8O_3$
Phenol, 2-methoxy-4-(1-propenyl)-, (Z)-	3.13	164.20	$C_{10}H_{12}O_2$
Phenol, 2-methoxy-4-propyl-	1.80	166.22	$C_{10}H_{14}O_2$
Ethanone, 1-(4-hydroxy-3-methoxyphenyl)-	1.55	166.18	$C_9H_{10}O_3$
Phenol, 2,6-dimethoxy-4-(2-propenyl)-	15.22	194.23	$C_{11}H_{14}O_3$
Ethanone, 1-(4-hydroxy-3,5-dimethoxyphenyl)-	2.14	196.20	$C_{10}H_{12}O_4$
Aldehyde, ketone, acid and alcohol			
1,2-Benzenediol	2.32	110.11	$C_6H_6O_2$
1,2-Benzenediol, 3-methoxy-	1.28	140.14	$C_7H_8O_3$
1,2-Benzenediol, 4-methyl-	0.33	124.14	$C_7H_8O_2$
5-tert-Butylpyrogallol	1.22	182.22	$C_{10}H_{14}O_3$
Homovanillyl alcohol	3.48	168.19	$C_9H_{12}O_3$
4-Methyl-2,5-dimethoxybenzaldehyde	4.00	180.20	$C_{10}H_{12}O_3$
Benzaldehyde, 4-hydroxy-3,5-dimethoxy-	5.95	182.17	$C_9H_{10}O_4$
1-Nitro-1-deoxy-d-glycero-l-mannoheptitol	2.96	241.20	$C_7H_{15}NO_8$
3,5-Dimethoxy-4-hydroxycinnamaldehyde	3.77	208.21	$C_{11}H_{12}O_4$
Benzeneacetic acid, 4-hydroxy-3-methoxy-, methyl ester	0.49	196.20	$C_{10}H_{12}O_4$
Dibenz[a,c]cycloheptane, 2,3,7-trimethoxy-	0.58	284.36	$C_{18}H_{20}O_3$
4-Methoxy-4',5'-methylenedioxybiphenyl-2-carboxylic acid	2.09	272.26	$C_{15}H_{12}O_5$
Dibenzo[e,g]benzimidazole, 2-(2-furyl)-3-methyl-	0.73	298.35	$C_{20}H_{14}N_2O$
Anhydrosugar			
1,6-Anhydro-.beta.-D-glucopyranose (levoglucosan)	12.53	162.14	$C_6H_{10}O_5$
D-Allose	3.80	180.16	$C_6H_{12}O_6$
Furan			
2-Furancarboxaldehyde, 5-(hydroxymethyl)-	2.25	126.11	$C_6H_6O_3$
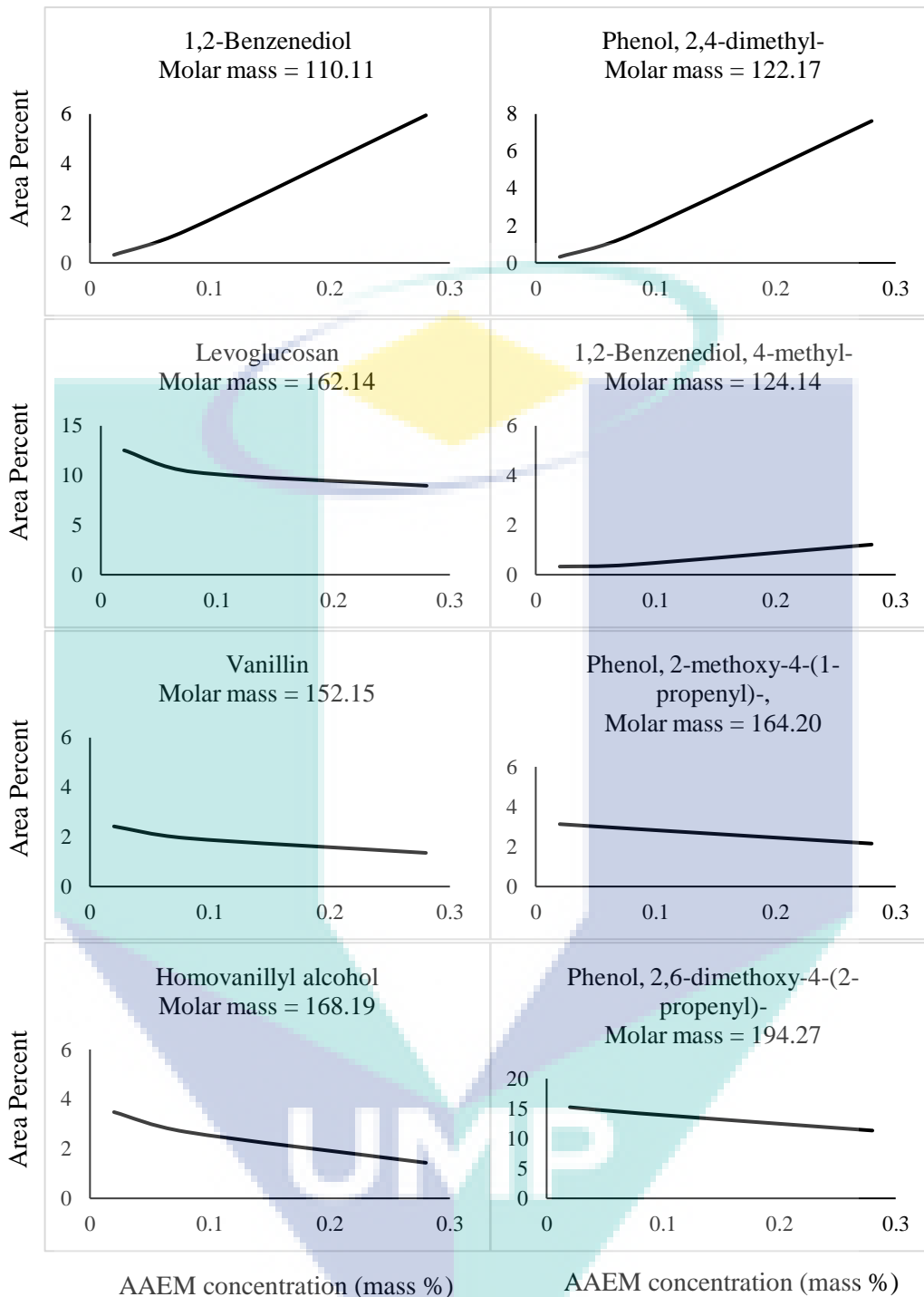
Figure 4.15   Area percent of organic compounds as a function of AAEM content in raw- and demineralised-RMS feedstock

By referring and comparing the data of bio-oil compounds in Table 4.7 to Table 4.9, it can be noted that bio-oil extracted from raw RMS is composed of molecular weight of compounds less than 200 g/mol, differed from the bio-oil extracted from demineralised RMS, which having higher molecular compounds heavier than 200 g/mol. Furthermore, as shown in Figure 4.15, it is noteworthy that lower molecular compound (150 g/mol) in

bio-oil samples decreased, while heavier molecular weight increased as the AAEM content in RMS feedstock decreased. Thus, it has been proven that the removal of AAEM species from RMS feedstock resulted in lowering the production of lower molecular weight compounds and increasing in higher molecular weight compounds. This is because, during pyrolysis, higher level of AAEM in feedstock acted as catalyst in primary fragmentation which eventually resulted in producing lower molecular weight compounds in bio-oil. However, at lower level of AAEM, depolymerisation reaction was predominated on decomposition of RMS fractions and eventually, resulted in higher molecular weight compounds (Fahmi et al., 2007). This result also almost comparable with study reported by Mourant et al. (2011)

In term of levoglucosan yield in extracted bio-oil, when the AAEM species were removed especially by acid washing, levoglucosan yield remarkably increased as expected. The highest in levoglucosan yield is derived from acid washing. This may attributed to the presence of H^+ in acid which acted as ion exchanger in replacing cation in RMS structure, which eventually resulted in disintegration (structure relaxation) and lowered the degree of these AAEM-related crosslink, as suggested by Chaiwat et al., (2008). This reaction led to the increasing anhydrosugars specially levoglucosan yield in bio-oil.

4.3.4 Summary

Washing is an effective method for removal of AAEM. RMS washing with HCl 1.0 M has been proven to get rid of almost 97% AAEM content in RMS sample, while washing with DI water, can get rid of only 70%. From bio-oil production experiments, it can be confirmed that the method of washing does not make a difference to the amount of bio-oil, but in terms of its composition, extracted bio-oil contains higher organic fraction as the lower of AAEM concentrations in feedstock. Thus, to increase useful organic chemical products including anhydrosugars and phenolic compounds, washing with DI water is the most preferable and cost effective.

4.4 Study the Influence of Impregnated Red Meranti Sawdust

Study of the effect of impregnated RMS was conducted to investigate how far the addition of inorganic metal salts in RMS can enhance pyrolysis process performance and evaluate either it can improve bio-oil compound in term of anhydrosugars yields or not.

4.4.1 Red Meranti Sawdust Analysis

In this study, alkaline earth metal salt ($CaCl_2$ or $CaSO_4$) or transition metal salt ($FeCl_2$ or $FeSO_4$) solution was prepared and mixed with RMS to assess the effect of impregnation method in RMS towards thermal decomposition behaviour and levoglucosan yield in bio-oil compounds. Prior to pyrolysis process, impregnated RMS feedstock samples were subjected to TGA and FTIR analyses and their results are listed and discussed below.

4.4.1.1 Thermal Analysis of Red Meranti Sawdust

Thermal decomposition of impregnated RMS as compared to control sample are shown in TGA and DTG profiles in Figure 4.16 (a) and (b), respectively. Pyrolysis properties are gathered from DTG profiles and are summarised in Table 4.10, in which, the yield of pyrolytic products is calculated at the point of 550 °C.

As observed in Figure 4.16(b) and summary in Table 4.6, temperature at maximum degradation rate for all impregnated RMS (except impregnated $CaSO_4$) were lower than control RMS. In sequence, temperature at maximum degradation rate in descending order is as follows; RMS - $CaSO_4$ > RMS control > RMS - $FeCl_2$ > RMS - $CaCl_2$ > $FeSO_4$. This result indicates that impregnated treatment of biomass with $FeCl_2$, $CaCl_2$ and $FeSO_4$ offered the lower thermal decomposition temperature, hence, enabled to save the cost of pyrolysis operating temperature.

By comparing all those impregnated samples, it clearly can be observed that maximum degradation rate of RMS - $FeSO_4$ shifted from 361 °C for the RMS control to 314 °C for RMS - $FeSO_4$, thus, can save the cost of energy intensity about 13.02 %. This result reveals that $FeSO_4$ had a capability as catalyst to enhance cracking reaction of biomass at lower temperature as compared to other impregnated and control feedstocks. Typically, hemicellulose and cellulose decompose at the temperature ranges from 220 to 400 °C and from 300 to 450 °C (Venderbosch & Prins, 2011), respectively. By comparing DTG graph patterns for both RMS control and RMS - $FeSO_4$, it obviously can be seen that decomposition curve had been shifted to left side, indicating that molecular bonds of these components especially cellulose had been weakened and this reaction resulted in lowering decomposition temperature. This result has been confirmed with GC-MS analysis of bio-oil compounds in Figure 4.19, indicating that bio-oil extracted from RMS

impregnated with FeSO$_4$ produced higher levoglucosan compound, resulted from decomposition of cellulose at temperature around 300°C. For lignin component of this feedstock, decomposition of lignin occurred slowly at a temperature between 160 and 900 °C (Venderbosch & Prins, 2011). From the DTA profile, it can be seen that the decomposition of lignin did not showed a significant difference within this range of temperature after impregnated treatment. This profile indicates that the lignin's molecular bonds do not much affected by this treatment.

However, despite of having a low decomposition temperature, the decomposition rate of RMS impregnated FeSO$_4$ was relatively slow, -0.00603/°C as compared to control, -0.00766. Highest decomposition rate was achieved by RMS impregnated CaSO$_4$ about -0.00826. As shown in Table 4.10, temperature for maximum degradation of RMS impregnated CaSO$_4$ are comparable with control. This result indicates that, maximum bio-oil yield only can be achieved by RMS impregnated CaSO$_4$ as compared to other feedstocks. Refer to Figure 4.16(b), it can be noticed that sample of RMS impregnated CaSO$_4$ was still continuing significant weight loss at temperature 400 °C, meanwhile, other samples were started producing char. This is attributed to the strength of molecular bonds of lignin had been weakened by impregnated with CaSO$_4$. This result is confirmed with analysis of bio-oil compounds (Figure 4.19) produced through pyrolysis process, which indicates that bio-oil derived lignin was the highest in this feedstock.
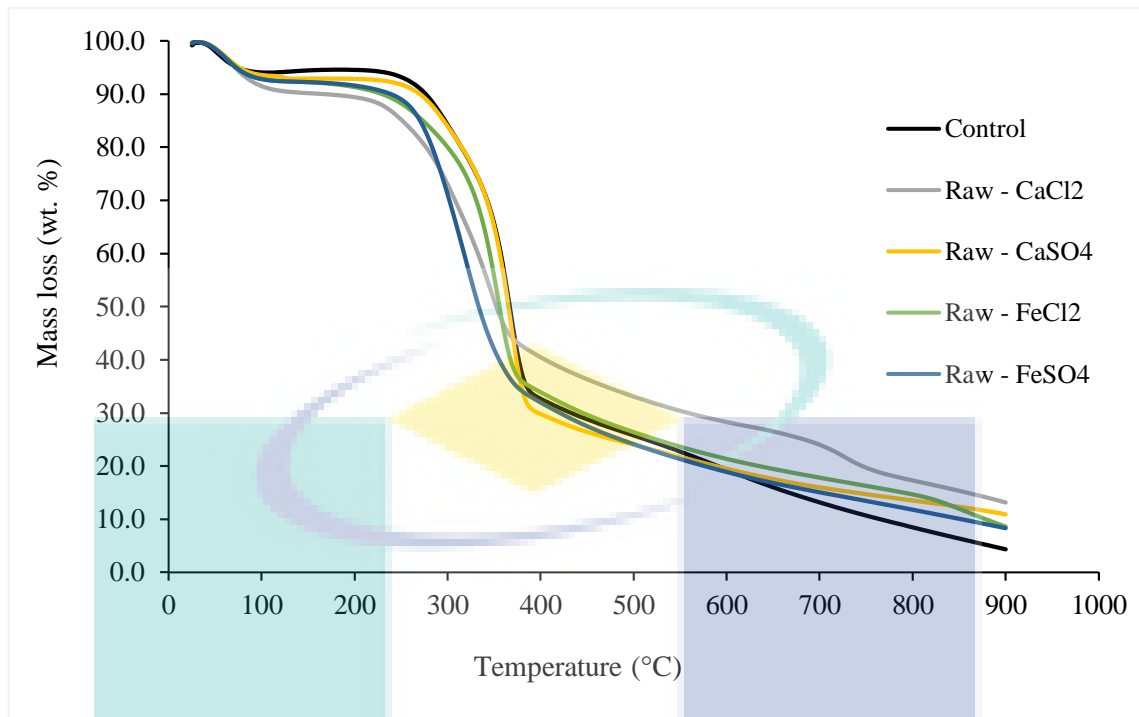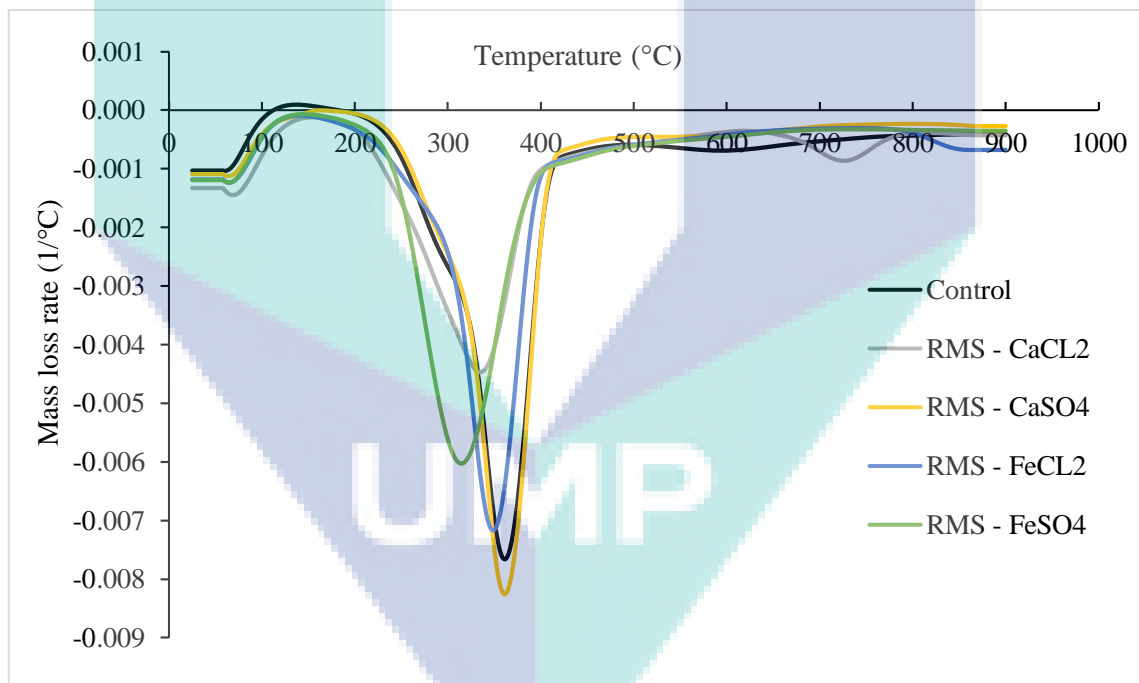
Figure 4.16   (a) TGA and (b) DTG profiles of control- and impregnated-RMS at 10 °C/min of heating rate in N_2 atmosphere

Table 4.10   Pyrolysis properties of control- and impregnated-RMS in TGA and DTG in N_2 at 10 °C/min of heating rate

Sample	Yield at 550 °C (wt. %)			Temperature at max rate (°C)	Degradation rate (1/°C)
	Moisture content	Volatiles	Char		
Control	6.96	70.34	22.71	361	-0.00766
RMS - CaCl$_2$	8.49	61.12	30.39	335	-0.00447
RMS - CaSO$_4$	6.13	72.13	21.73	361	-0.00826
RMS - FeCl$_2$	6.87	69.49	23.64	348	-0.00717
RMS - FeSO$_4$	6.85	71.84	21.31	314	-0.00603

4.4.1.2   Chemical Structure Analysis

This analysis is conducted to examine how far the process of impregnation has changed the chemical structure of feedstock. Due to having lower maximum thermal degradation temperature as compared to other samples (refer to DTG profile in Figure 4.16(b)), then, only the samples of RMS - CaCl$_2$ and RMS - FeSO$_4$ were selected for this analysis. Control RMS also was chosen for comparison. Result of analysis is presented in Figure 4.17.
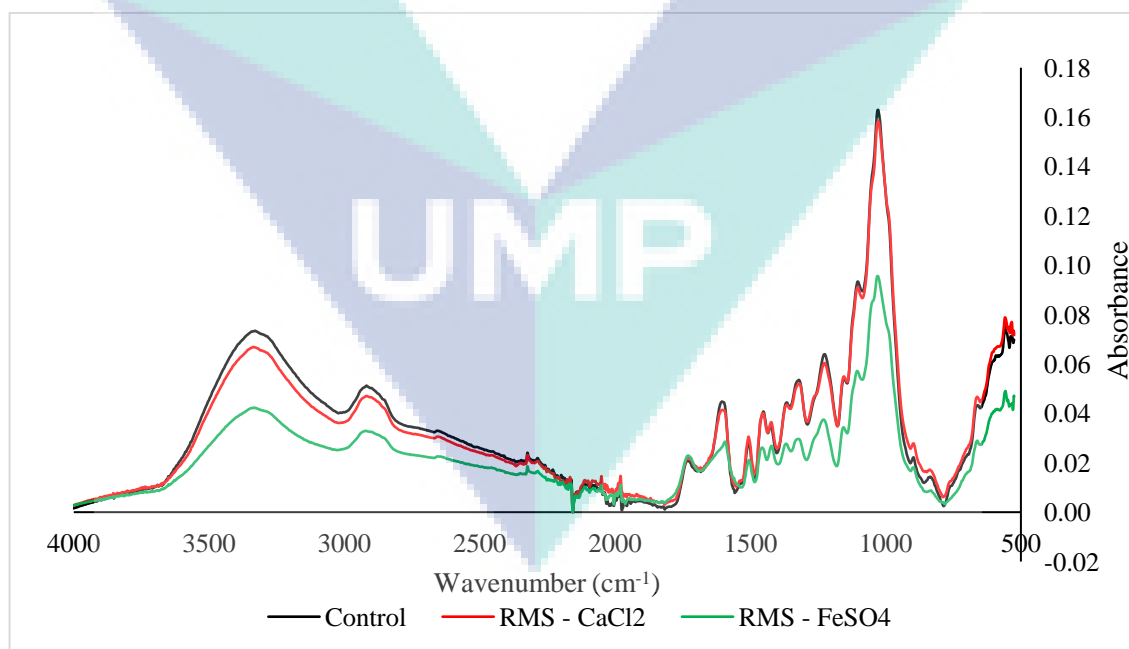
Figure 4.17   FTIR spectra of control- and impregnated-RMS

As shown in Figure 4.17, it is examined that functional group of impregnated samples did not changed with impregnation process. This can be explained by the peak of wavenumber was still the same for impregnation RMS as compared to control RMS, indicating that organic element in samples was not disrupted by it treatment. Nonetheless, the intensity of absorbance illustrates a difference for each sample. By comparing these samples, it apparently can be seen that $FeSO_4$ impregnated RMS had lower absorbance intensity as compared to other samples. As mention earlier, absorbance intensity is closely related to dipole of molecule, where, the greater the dipole of bond, the more intensity of light absorbed. Thus, this analysis confirms that the molecular bonds within the RMS had been weakened by impregnation of $FeSO_4$ in RMS. Additionally, result of this analysis also verify DTG profile of RMS - $FeSO_4$ in Figure 4.16(b), explaining that RMS impregnated $FeSO_4$ debilitated bonds in RMS, thus, enhanced degradation process at lower temperature.

4.4.2 Fast Pyrolysis Experiment

The fast pyrolysis experiment was conducted on all impregnated RMSs in order to determine the amount of bio-oil yield. Bio-oil compounds of each impregnated RMS also was evaluated to assess whether impregnation method enables to promote bio-oil compound in term of anhydrosugars yield, or otherwise. Result of the experiments are discussing as below.

4.4.2.1 Effect on Bio-oil Yield

According to TGA conducted previously, it can be seen decomposition behaviour of impregnated RMS was differ from one another, and the exact amount of pyrolytic products yield, especially bio-oil was inaccessible. Thus, this experiment was conducted to collect the data on pyrolytic product distributions for specific impregnated RMS at different operating temperatures. Result of this experiment is attached in APPENDIX D in Table D3 and simplified in Figure 4.18.

As shown in Figure 4.18, when pyrolysis experiment was run at temperature of 350 °C, all impregnated RMSs produced higher bio-oil yield than control RMS. This is attributed to the presence of inorganic salt in RMS which responsible in expediting decomposition rate. This argument is allied with TGA result, in which, at lower temperature than 350 °C, all impregnated RMS underwent important weight loss than

control. Through experiment, it can be observed that RMS - FeSO$_4$ produced highest bio-oil yield about 34.9 %, followed by RMS - CaCl$_2$ about 28.9 %, RMS - FeCl$_2$ about 27.8 %, RMS - CaSO$_4$ about 25.2 % and control RMS about 22.5 %. At this temperature, by comparing this result and DTG profile in Figure 4.16(b), the conclusion can be made that large fraction of both cellulose and hemicellulose components in RMS - FeSO$_4$, followed by RMS - CaCl$_2$ greatly decomposed while in other feedstock, decomposition only occurred mostly on hemicellulose component with a small fraction of cellulose. This such decomposition trend is obtained due to the present of FeSO$_4$ or CaCl$_2$ in RMS in the RMS which played a role in weakening the molecular bond of cellulose component, making the decomposition temperature decreased and this can be seen from the DTG profile where the maximum decomposition temperature for the RMS - FeSO$_4$ and RMS - CaCl$_2$ samples had shifted from 361 to 314 °C and 361 to 335 °C, respectively. Thus, this result reveals that FeSO$_4$ is the most suitable catalyst to enhance thermal decomposition process of lignocellulose biomass at lower temperature.

As the temperature was increased up to 400 °C, the bio-oil production increased almost twice as the large fraction of RMS had been broken down. However, for samples of RMS - FeSO$_4$ and RMS - CaCl$_2$, bio-oil production was quite slow as compared to other. This is because, at this temperature, typically, hemicellulose and cellulose decomposed rapidly, yet, for these two samples, large fraction of cellulose component had been decomposed earlier at 350 °C, leaving the amount of remaining cellulose to decompose at this temperature has been decreased.

When temperature was increased up to 450 °C, bio-oil yield for all feedstock continuing increased and achieved maximum yield about 58.3 % for RMS - CaSO$_4$, 57.2 % for RMS - FeSO$_4$, 57.2 % for control, 57.1 % for RMS - FeCl$_2$, and 51.3 % for RMS - CaCl$_2$. This is the optimum temperature for highest bio-oil yield for all feedstock. Sequences the amount of bio-oil yield for all these samples is in-line with summary in Table 4.10, in which, the more the volatiles are released, the more the bio-oil will be produced.
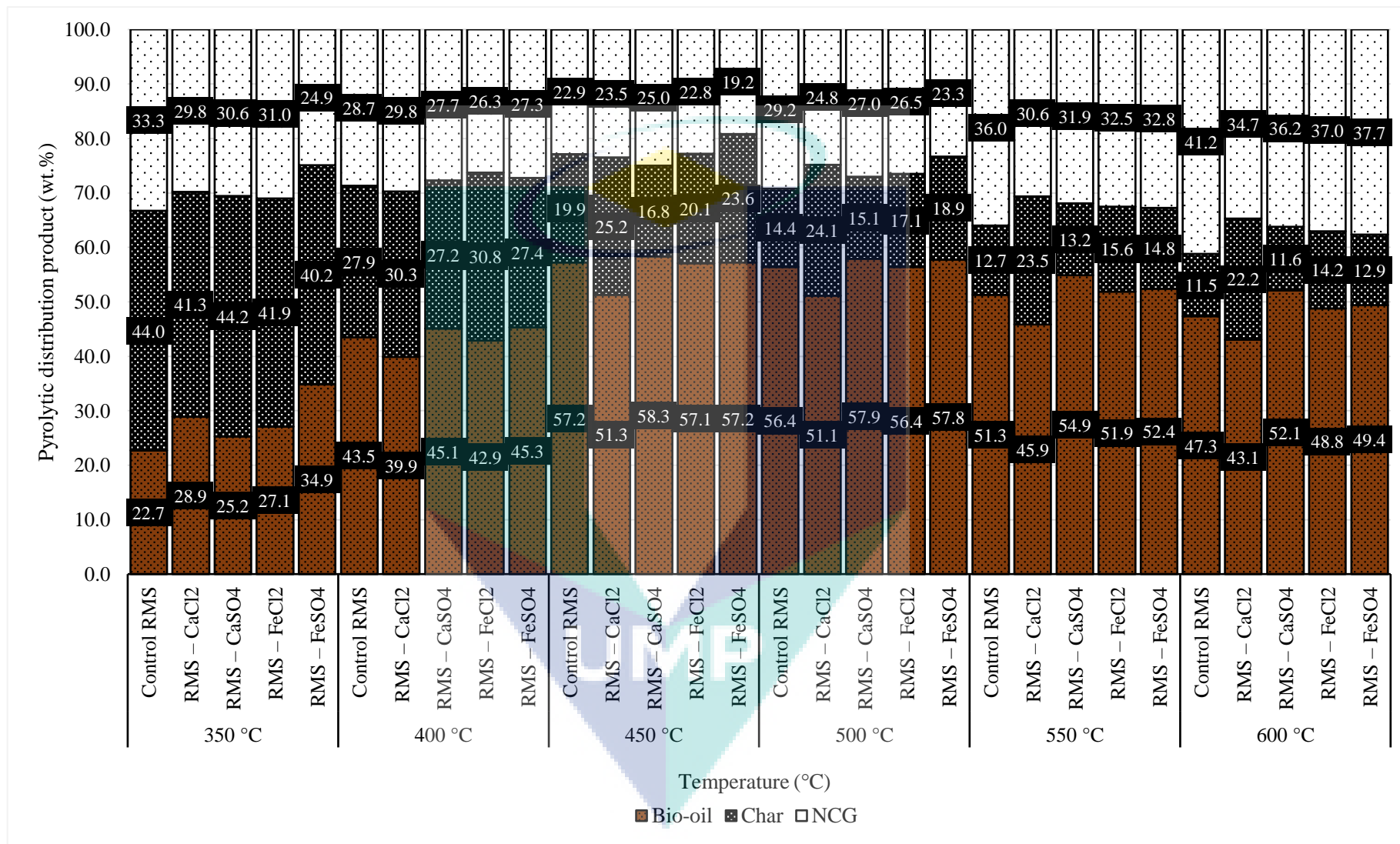
Figure 4.18   Pyrolytic product distribution of control- and impregnated-RMS as a function of temperature at 25 L/min of N_2 flowrate, 20 min of retention time and ≤ 2.00 mm of RMS particles size

After the 450 °C of temperature and up to 600 °C, bio-oil yield of control- and impregnated-RMS gradually decreased. This is attributed to fragmentation and secondary cracking reactions occurred on unstable volatiles by releasing more NCG volume.

4.4.2.2 Effect on Bio-oil Compound

Impregnation process on sample do not only affects the distribution of yield, but also affects the resulting bio-oil components. Result of bio-oil compounds gathered from GC-MS analysis is attached in APPENDIX D in Tables D1 to D4, and classified in bar chart in Figure 4.19. Anhydrosugar and furan compounds are products of cellulose (Azeez et al., 2010), aldehyde, alcohol, ketone and acid compounds are majorly derived from hemicellulose component derivatives (Azeez et al., 2010), and phenolic compound is mainly the lignin derived compound (Fahmi et al., 2007) and (Tröger et al., 2013). All the samples of bio-oil were taken from the experiment conducted at 450 °C. Since the focus of this study is more on levoglucosan yield, thus, in this part, discussion of anhydrosugar compounds especially levoglucosan yield is stressed and discussed further.

As shown in Figure 4.19, amount of anhydrosugar (sum of levoglucosan and D-Allose) compounds in bio-oil were varies and higher in impregnated RMS than control RMS, with descending orders are RMS - $FeSO_4$ > RMS - $CaCl_2$ > RMS - $FeCl_2$ > RMS - $CaSO_4$ > control RMS. This result indicated that the impregnation process catalysed and promoted the production of anhydrosugars in bio-oil as compared to control sample. This is attributed to the catalysing effect of either cation or anion presence in RMS induced levoglucosan yield, thus, showing that impregnated treatment enabled to improve levoglucosan production.
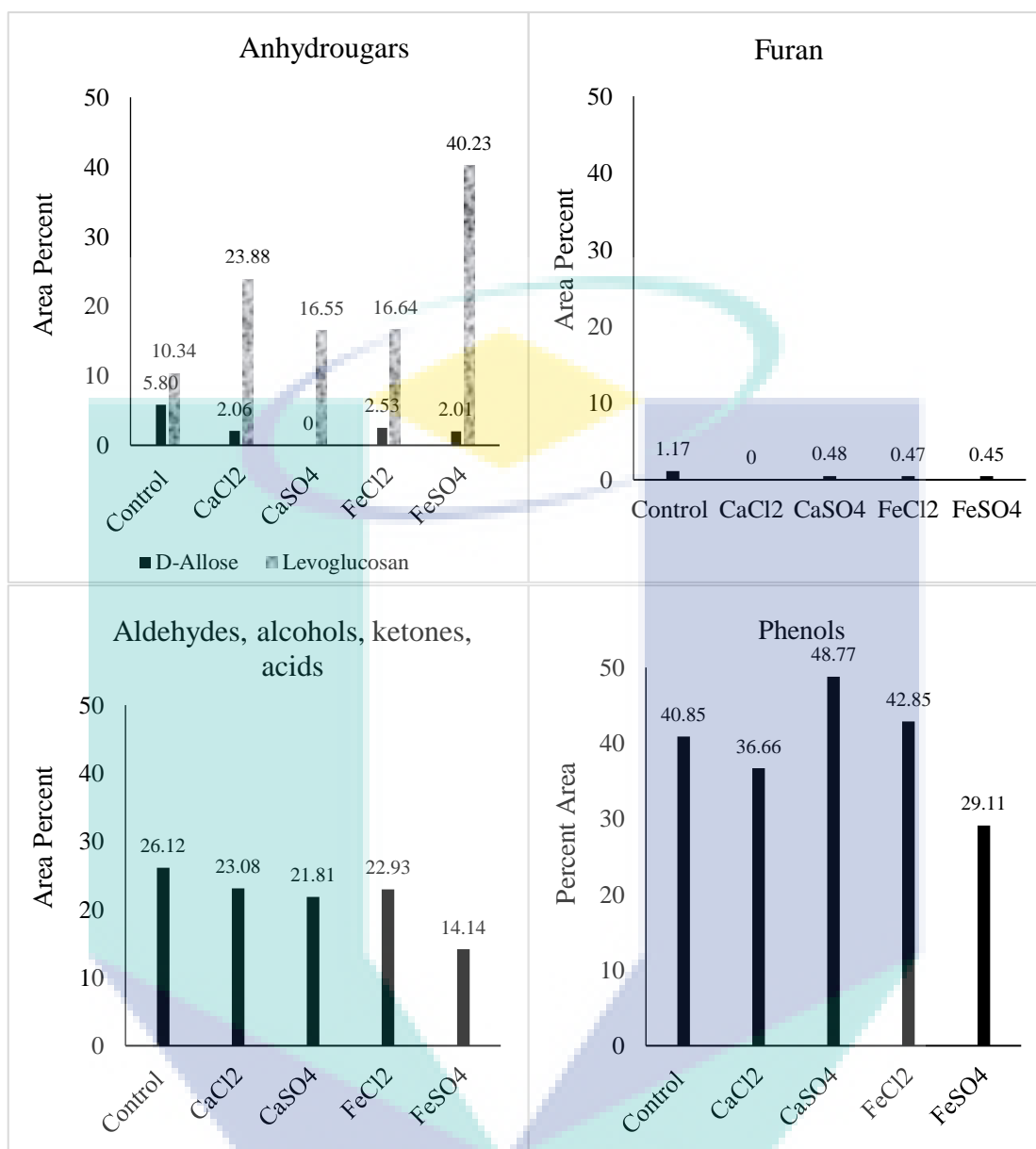
Figure 4.19 Comparison of bio-oil compound

Comparing all those samples, it can be noted that bio-oil extracted from RMS impregnated $FeSO_4$ contains highest anhydrosugar compounds about 42.24 area % (include levoglucosan compound about 40.23 area %), showing that total anhydrosugars yield almost three-fold increased than control, followed by RMS impregnated $CaCl_2$ which produces about 25.94 area % of anhydrosugars yield (consist levoglucosan 23.88 area %), where the amount increased almost double than control RMS. This result is attributed to the presence of transition metal cation, Fe^{2+} which acted as catalyst by providing a surface for reactions to occur and forms weak bonds to the reacting species (RMS), especially in cellulose component. This argument is supported by FTIR analysis

in Figure 4.11 which reveals that chemical bond structure had been decreased in this sample, and through GC-MS analysis in Figure 4.19, it has been proved that high levoglucosan yield indicates that cellulose bonds had been weakened and decomposed largely at lower temperature around 300 °C. Hence, by impregnated RMS with transition ion, Fe^{2+}, the levoglucosan yield in this study is in-line with levoglucosan yield in bio-oil extracted from other impregnated lignocellulose biomass with transition metal salt studied by Eom et al. (2012), and Richards and Zheng (1991). For impregnated RMS – $CaCl_2$, the production of levoglucosan yield in bio-oil was higher than control RMS due to the presence of anion Cl^- in RMS, which altered a number of cellulose chemical structure by lowering its strength (Figure 4.17). This alteration leads to lower decomposition temperature (Table 4.10) and induced levoglucosan yield (Figure 4.19). The pattern of levoglucosan yield is agreed with studied reported by Richards and Zheng (1991).

According to Shafizadeh et al. (1979), the lower the temperature, the higher the levoglucosan production. By linking the production of anhydrosugars and decomposition temperature pattern (both in DTG graphs in (b) and bio-oil yield in Figure 4.18), it can be observed that the amount of anhydrosugar production is closely related to how much cellulose decomposition occurred at lower temperature. Refer to Figure 4.18 for bio-oil yield at temperature 350 °C, although decomposition of control RMS and impregnated feedstocks (other than RMS - $FeSO_4$) also occurred at lower temperature and yield the bio-oil, decomposition of these feedstock mostly occurred on hemicellulose component rather than cellulose, and with regards to the content of bio-oil, the compounds produced predominantly derived from hemicellulose (aldehydes, alcohols, ketones, and acids). This argument is agreed with result obtained in Figure 4.19, which shows that the number of aldehydes, alcohols, ketones, and acids were high in control RMS and low in RMS - $FeSO_4$. Levoglucosan is a primary product which formed through transglycosylation of cellulose conversion which occurred around 300 °C (Azeez et al., 2010) and the amount of levoglucosan produced is lower at higher temperature (Shafizadeh et al., 1979). Without impregnation treatment, typically, cellulose will decompose at 300 – 450 °C, in which in at this range of temperature, the production of high levoglucosan in bio-oil is somewhat impossible. Moreover, at this temperature, levoglucosan tend to vaporizes and decomposes with increasing temperature (Sinha et al., 2000) which ultimately leads to the formation of furan and acids (Azeez et al., 2010). Therefore, for the purposes of high

levoglucosan yield in bio-oil, decomposition of cellulose at low temperatures should be achieved as much as possible.

The above statements explain the reason why RMS impregnated $FeSO_4$ feedstock produced higher yield of levoglucosan compound as compared to other samples. The presence of ferrous ion as transition metal, accompanied with SO_4^{2-} anion in RMS, driven the weakening bonds between molecules in cellulose component, and thereby, reduced the temperature required for cellulose decomposition. Thus, much cellulose decomposition had been achieved at lower temperature, and in turn, increased levoglucosan production. This result reveals that, as long as the maximum temperature rate of feedstock can be reduced, then the more levoglucosan can be produced from cellulose. Through this experiment, it has been identified that $FeSO_4$ can be used as impregnated agent to lower the operating temperature, thus, save the cost on energy intensity. In addition, by conducting fast pyrolysis process at lower temperature (in this study, 314 °C of temperature), evaporation of levoglucosan to produce furans (via secondary reaction of unstable volatile at high temperature) can be avoided.

4.4.3 Summary

Impregnated treatment of RMS with $FeSO_4$ has a capability to enhance thermal degradation process of feedstock at lower temperature due to catalytic effect of $FeSO_4$ weakened molecular bonds in RMS chemical structure, especially in cellulose component, which eventually resulted in production of bio-oil with higher levoglucosan compound. From a number of analyses and experimental work conducted in this study, it reveals that impregnated treatment of RMS with $FeSO_4$ is relatively has a technical and economic viable for producing bio-oil rich-levoglucosan. This is because, (i) in-term of feedstock production, RMS can be obtained at low cost as it abundantly available as forestry residue, and (ii) in-term of bio-oil production, catalysing effect of $FeSO_4$ in RMS is capable to enhance thermal decomposition at lower temperature, hence, save the intensity energy used for fast pyrolysis process. Furthermore, by lowering thermal decomposition temperature of feedstock, levoglucosan production in extracted bio-oil can be increased and possibility for levoglucosan undergo secondary reaction can be avoided.

4.5   Pyrolysis Process Optimisation using Central Composite Design

In this study, a three factor and a five level CCD combined with RSM along with quadratic programming were applied to find the optimum process parameters associated to maximise bio-oil yield. Temperature (A), N_2 flow rate (B) and retention time (C) were the three independent variables (factors) studied. The bio-oil yield (Y_B) was considered as the dependent factor (process response). The variable is coded at five levels between -1.68 and +1.68. The critical range of the factor was selected based on a result of preliminary experiments conducted in Subchapter 4.2.

4.5.1   Statistical Analysis

In this study, a total number of 20 experiments were conducted and used for model prediction. Table 4.11 lists design matrix of experiment and actual and predicted values for bio-oil yield, Y_B by developed quadratic model.

Table 4.11   Experimental design matrix and result of actual and predicted response

Run	Factor			Response	
	A	B	C	Actual	Predicted
1	460	25	20	56.6	55.5
2	460	25	20	55.2	55.5
3	520	20	15	43.9	42.9
4	520	30	15	48.3	47.1
5	400	30	15	49.3	48.1
6	400	20	25	40.2	41.0
7	460	25	20	55.8	55.5
8	520	30	25	49.3	50.1
9	400	20	15	39.8	38.6
10	359	25	20	34.7	35.2
11	460	25	20	56.3	55.5
12	400	30	25	43.9	44.4
13	460	25	28	56.4	54.5
14	460	33	20	56.4	54.5
15	520	20	25	51.1	51.9
16	460	17	20	43.2	43.4
17	460	25	20	55.3	55.5
18	460	25	12	53.8	55.5
19	460	25	20	53.8	55.5
20	561	25	20	43.4	43.6

In analysis part, analysis of variance (ANOVA) was used to determine appropriate model and result, the experimental data are best fitted into a quadratic equation. The quadratic model equation of predicted bio-oil yield, Y_B of RMS thermal conversion in term of actual factors is given in Equation 4.1.

$$Y_B = -440.431 + 1.499A + 9.89B + 1.059C - 0.004AB + 0.005AC - 0.060BC - 0.002A^2 - 0.125B^2 - 0.046C^2 \qquad 4.1$$

Where Y_B is the yield of bio-oil (%), A is the temperature (°C), B is the N_2 flow rate (L/min) and C is the retention time (min).

The quadratic model equation can be recalculated considering only the significant factors. The statistical significance of the second order polynomial model to predict the yield of bio-oil was tested by the ANOVA. The result of the ANOVA is presented in Table 4.12.

The significance of each coefficient in Equation 4.1 was determined by Fisher's F-test and values of probability > F. As shown in Table 4.12, the Model F-value of 37.98 implies that the model is significant. There is only a 0.01% chance that Model F-value this large could occurred because of noise. Values of 'Prob > F" shows a small probability value ($P < 0.0001$) indicates that the model was highly significant. The lack-of-fit value F-value of 3.60 implies the lack-of-fit is not significant relative to the pure error, indicates that the model was fit. Another evidence to check the fit of the model is by validating R^2 coefficient. R^2 value of the model was 0.9716, indicating the reliability of the second-order polynomial equation. Besides that, adequate precision was 19.0245, that's greater than 4, showing that the model can be used to navigate the design space define by the CCD. Adequate precision is a measurement of a range in predicted response relative to its associated error, i.e., a signal to noise ratio. The normality of the data could be checked through the normal probability plot of the residuals. If the points on the plot lie on a straight line, the residuals are normally distributed as confirmed in Figure 4.20. In addition, a high correlation between the data of predicted yields according to Equation 4.1 and actual yield through experimental work as shown in Figure 4.21 indicates their low discrepancies between these data.

Table 4.12   Analysis of variance (ANOVA) for bio-oil yield

Source	Sum of Squares	df	Mean Square	F Value	p-value Prob > F	
Model	779.3204	9	86.59116	37.976	1.46E-06	significant
A-Temperature	84.80354	1	84.80354	37.19201	0.000116	significant
B-N_2 flow rate	50.3675	1	50.3675	22.08951	0.000842	significant
C-Retention time	24.16916	1	24.16916	10.59979	0.008636	significant
AB	14.045	1	14.045	6.159669	0.032439	significant
AC	21.78	1	21.78	9.551982	0.011432	significant
BC	18	1	18	7.8942	0.018486	significant
A^2	468.2478	1	468.2478	205.3579	5.42E-08	significant
B^2	141.8082	1	141.8082	62.19236	1.33E-05	significant
C^2	18.70635	1	18.70635	8.203983	0.016834	significant
Residual	22.80155	10	2.280155			
Lack of Fit	17.84155	5	3.56831	3.597087	0.093169	not significant
Pure Error	4.96	5	0.992			
Cor Total	802.122	19				

R-squared		=	0.971573	
Adjusted R-Squared		=	0.94599	
Predicted R-Squared		=	0.822147	
Adequate Precision		=	19.02453	
C.V. %		=	3.10	

Normal Plot of Residuals
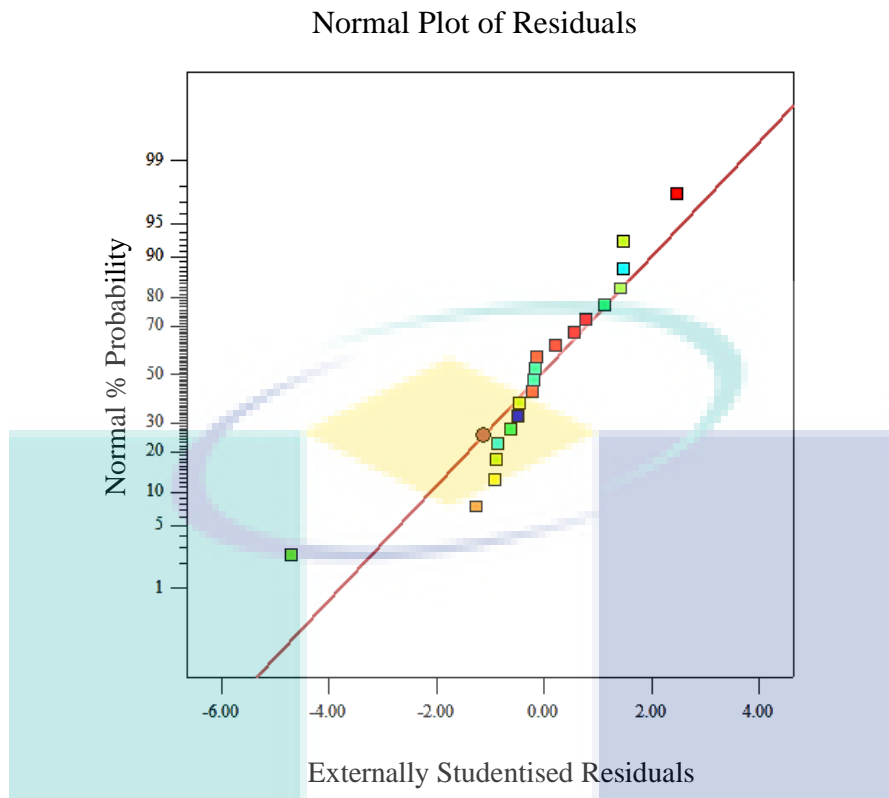
Figure 4.20   Normal probability plot of the internally studentised residuals
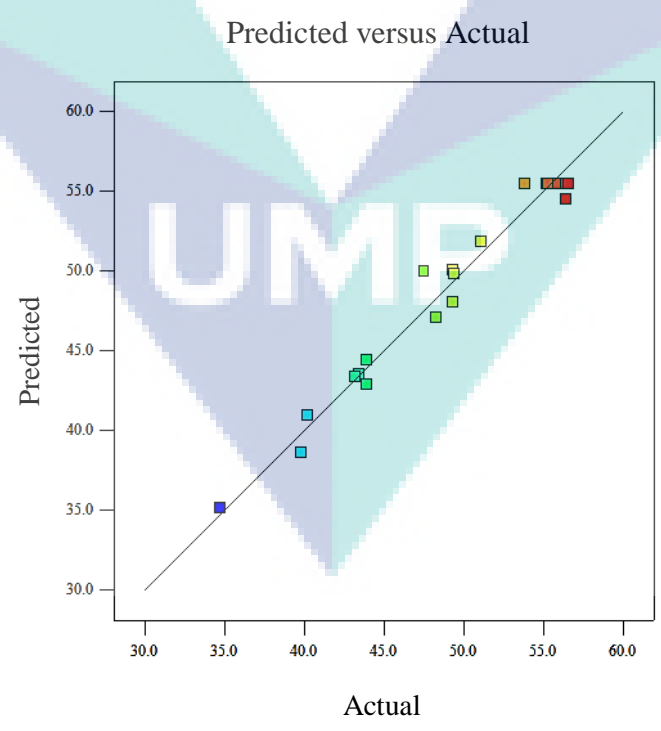
Predicted versus Actual

Figure 4.21   Comparison plot between predicted and actual yield of bio-oil

4.5.2 Interaction Effect of Independent Variables

In order to study the interaction effect between the variables (temperature, N_2 flow rate and retention time of RMS), 3D response surface and 2D contour curves based on quadratic model were plotted as illustrated in Figure 4.22 toFigure 4.24. As seen in those figures and comparing with ANOVA in Table 4.12, all the interaction between the factors significantly affect bio-oil yield, which give the 'Prob > F' lower than 0.0500.

As shown in Figure 4.22, increasing temperature and N_2 flow rate result in enhancing bio-oil production up to an optimum operating temperature and sweeping gas flow rate, and after this point, bio-oil production decreased slightly. At lower temperature, large fraction of RMS component containing holocellulose (cellulose and hemicellulose) was still not fully decomposed to release volatile. Hemicellulose and cellulose have decomposition temperatures around 220 to 400 °C and 300 to 450 °C, respectively. Thus, as temperature was increased, volatile yield also increase proportionate to the amount of decomposition of holocellulose component. After optimum temperature, bio-oil yield decreased since there was no further decomposition occurred on holocellulose component except on lignin, in which, the decomposition of lignin occurs very slowly. Moreover, secondary cracking also occurred on unstable volatile, resulting in reduced bio-oil yield. However, despite having high volatile release at optimum temperatures, bio-oil production still will be stunted in the absence of sweeping gas, in which, sweeping gas is responsible for removing volatile from the reactor. In this experiment, N_2 was not only used to provide inert atmosphere for pyrolysis process, but also used to sweep the volatile out from pyrolysis reactor. At lower N_2 flow rate, vapour residence time in reactor was longer and this condition resulted in secondary reaction (repolymerisation and recondensation) on primary product (volatile) to form secondary char, which eventually lead to decreasing in bio-oil yield. Typically, vapour residence time for higher bio-oil yield must be less than 2 s. Thus, optimum N_2 flow rate in this study was 25 L/min, which comply short vapour residence time in maximising bio-oil yield.
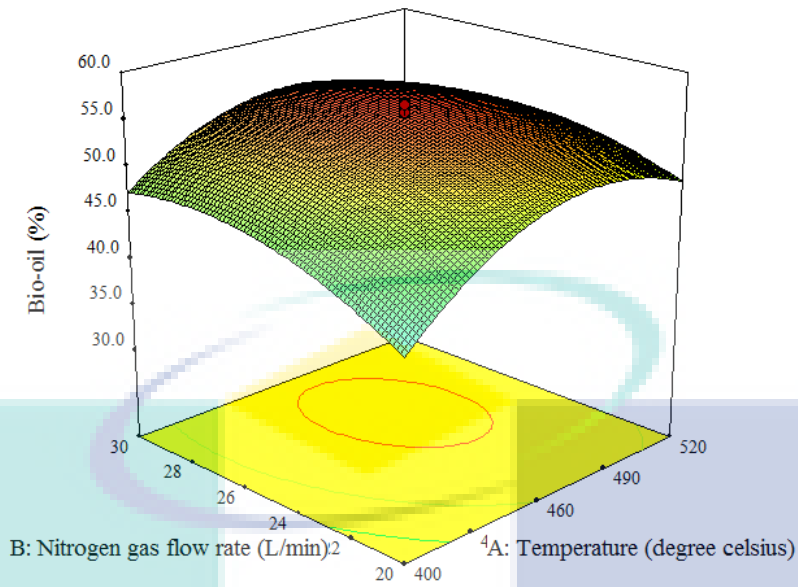
Figure 4.22   Combination effect of N$_2$ flow rate and pyrolysis temperature towards bio-oil yield at retention time of 20 min and particle size ≤ 2.00 mm

Combination effect of temperature and retention time of RMS in reactor is shown in Figure 4.23. The higher the operating temperature, the more the RMS fraction was pyrolyed and the more bio-oil can be recovered from volatile released. Optimum temperature for highest bio-oil yield was 480°C and after this point, bio-oil yield starts to decrease slightly due to secondary reaction occurred on primary product. However, to accomplish the maximum yield, enough retention time of RMS in reactor was needed for completing pyrolysis process. Too short retention time lead to incomplete pyrolysis, while too long lead to the increasing of operating cost. Thus, optimum retention time for the yield bio-oil of 56.6 was 24 min.
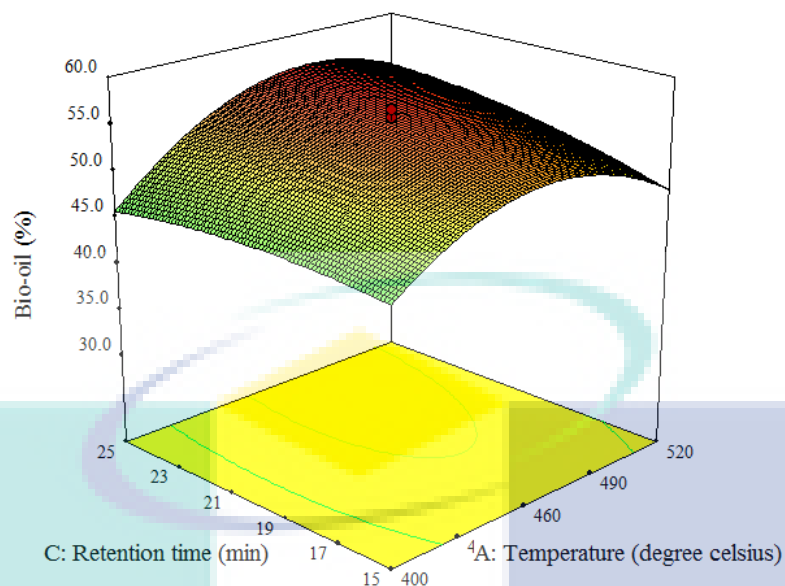
Figure 4.23   Combination effect of retention time and temperature towards bio-oil yield at 25 L/min of N_2 flow rate and ≤ 2.00 mm of RMS particles size

Combination effect of N_2 flow rate and retention time also significantly affect bio-oil yield. Response surface of these variables illustrated in Figure 4.24. Increasing N_2 flow rate resulted in enhancing bio-oil yield because N_2 is responsible for removing the volatiles released out of the reactor to the condenser for cooling, and subsequently produced bio-oil. However, to produce significant amount of bio-oil, retention time of RMS inside the reactor must be enough to complete pyrolysis process on RMS fraction. However, even though the N_2 flow rate is at an optimum level, if pyrolysis was still carried out for a long retention time, bio-oil yield did not show changes as no further biomass conversion occurred on RMS. In this case, secondary cracking on bio-oil did not occurred because operating temperature was conducted below than 500 °C.
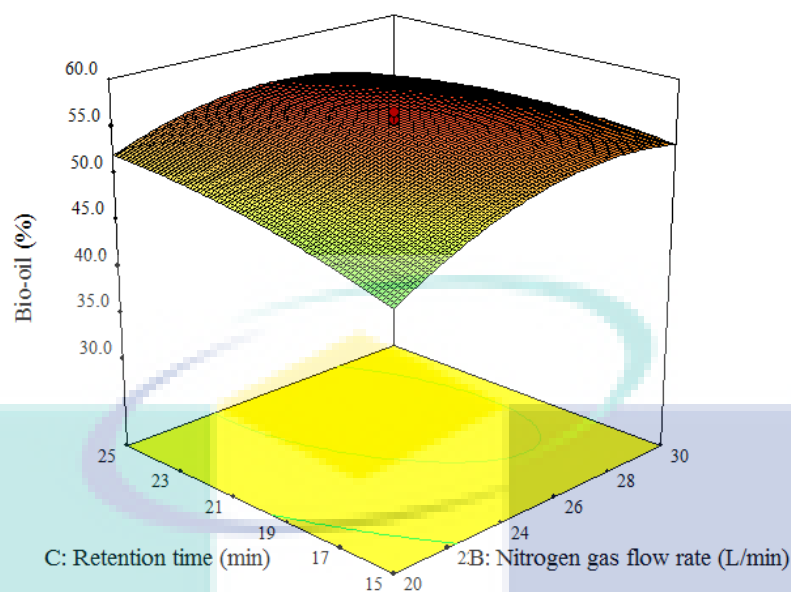
Figure 4.24   Combination effect of retention time and N_2 flow rate towards bio-oil yield at 460 °C of operating temperature and ≤ 2.00 mm of RMS particles size

4.5.3   Determination and Experimental Validation of Optimum Process Variables

RSM was used to determine the optimum values of the three independent variables to produce maximum yield of bio-oil. The optimisation of experimental conditions was carried out by maximising bio-oil yield at defined optimisation criteria for the factors as listed in Table 3.4. Therefore, the optimum operating conditions were found using the numerical technique built in Design-Expert 10.0.1 according to developed model. The numerical optimisation searches the design space using the developed model in the analysis to find factor setting that meet the goal of maximising bio-oil yield. Based on this model, the optimum values of variables to obtain the maximum 56.5 % of bio-oil yield from RMS with particles size ≤ 2.00 mm were at 480 °C of temperature, 25 L/min of N_2 flow rate and 24 min of retention time of. The experimental work was carried out according to optimum values in order to confirm the model adequacy and the validity of the optimisation procedure. Table 4.13 shows the yield of bio-oil using optimum process variable value. From the table, the result obtained from experiment and predicted model was in close agreement where only small error detected and this indeed confirm and validate the accuracy of the model approach.

Table 4.13   Verification experiments at operational conditions

Description	Response, Y_B
Model value, %	56.5
Experimental value, %	55.3
Error, %	2.11
Standard deviation	0.83

4.5.4   Summary

For optimisation of bio-oil production of RMS, CCD in RSM approach was applied to find the optimum process variables and investigate the combined effect of all process variables. Through ANOVA analysis, the experimental data are best fitted into a quadratic equation with the model equation of predicted bio-oil yield, Y_B of RMS in term of actual factors is:

$$Y_B = -440.431 + 1.499A + 9.89B + 1.059C - 0.004AB + 0.005AC - 0.060BC - 0.002A^2 - 0.125B^2 - 0.046C^2$$

From experimental work conducted based on optimum values in this model, the result obtained was in close agreement with predicted model, in which, the error only 2.11 %, thus, confirm the model approach.

Therefore, for the economical process for bio-oil production from RMS with particles size less than 2.00 mm, this model equation can be used as guidelines for optimising bio-oil production.

CHAPTER 5

CONCLUSION

5.1   Introduction

This chapter concludes the objective of the study in fast pyrolysis process of RMS for bio-oil production and to make sure all the objectives were achieved.

5.2   General Conclusion

In this research, there are four objective studies involved. First objective is to evaluate the effect of fast pyrolysis process condition of RMS feedstock to both bio-oil production and its characteristics in term of its composition and compound. There are four operating parameters involved including temperature, N_2 flow rate, retention time and feedstock particles size. In this experiment, OFAT approach was used to access optimum fast pyrolysis operating conditions for maximum bio-oil yield. Through pyrolysis experiment, it was identified that bio-oil achieved maximum yield about 56.3 % at optimum 450 °C of temperature, 25 L/min of N_2 flow rate, 20 min of retention time and 0.3 mm of RMS particles size. Among of these parameters, temperature was the most influential parameter, while feed particles size was insignificantly affecting the amount of bio-oil yield. In Van Krevelen diagram, bio-oil has the ratios of H/C and O/C within the ranges from 1.92 to 2.04 and 0.55 to 0.71, respectively. In term of bio-oil component, bio-oil consists large fractions of phenolic compounds. Levoglucosan yield in this bio-oil was 8.97 % area. Overall, the first objective was accomplished where the effect of pyrolysis conditions to bio-oil production have evaluated and its characteristics have been characterised.

Second objective is to determine the effect of washing treatment on AAEM concentration and RMS structure to bio-oil production, and characterise the bio-active

compounds in bio-oil. In this study, RMS with particles size less than 2 mm was washed with either by DI water or HCl solution at different concentration of 1.0 M and 2.0 M to remove AAEM species in RMS. Washing treatment did not affect RMS chemical structure, however, increased chemical bonds. DI water washing and HCl acid washing with concentration of 1.0 M and 2.0 M capable to remove about 66 %, 93 % and 97 %, of AAEM in RMS, respectively. In fast pyrolysis experiment, the optimum temperature for all feedstock was 450 °C with the highest bio-oil yield obtained by demineralised RMS - 1.0 M HCl, followed by RMS - DI water and last, raw RMS with the yield about 57.3 %, 57.2 % and 55.0 %, respectively. For bio-oil characterisation, raw RMS produced large range of lower molecular weight compounds, with no compounds having molecular weight larger than 200 g/mol. As AAEM content had been reduced in RMS, lower molecular weight compounds were getting less, while heavier molecule weight were getting higher and new heavier compounds were produced. Overall, the second objective was achieved where the effect of washing treatment on AAEM concentration and RMS structure to bio-oil production have been determined and extracted bio-oil compound have been characterised.

For third objective, fast pyrolysis experiments were conducted on impregnated RMS in order to evaluate how far the impregnation treatment affect RMS structures and enhance the decomposition process at lower temperature, as well as, improve the yield of levoglucosan in bio-oil compound. In this study, $CaCl_2$, $CaSO_4$, $FeCl_2$ or $FeSO_4$ solution was mixed with RMS. For comparison, demineralised RMS - DI water was served as control. Among these feedstock, RMS - $FeSO_4$ enhanced the decomposition process at lower temperature with the maximum degradation temperature of this sample was shifted from 361 °C of control sample to 314 °C of RMS – $FeSO_4$ due to the strength of RMS bonds had been weakened by $FeSO_4$. In fast pyrolysis experimental work, the 450 °C of temperature was the optimum temperature of all feedstock. In term of bio-oil compounds, bio-oil was composed of various compounds in large molecular weight range. Levoglucosan yield in bio-oil was the highest in the sample of RMS – $FeSO_4$ about 40.23 % area. This outcome reveals that levoglucosan yield can be increased, provided, much cellulose component can be decomposed at lower temperature. Overall, the third objective was achieved where $FeSO_4$ is capable reduce the strength of chemical bonds, and further, enhances the decomposition process at lower temperature as well as, improves the levoglucosan yield in bio-oil compound.

Last objective is to develop an optimisation model for bio-oil production from RMS as a function of specific close-range operating parameters as variables using RSM approach by CCD to generate results. Range of factors used in this study were selected from OFAT study in objective one. Independent variables (factors) in this study were temperature, N_2 flow rate and retention time. Feed particles size was constant. Dependent variable (process response) was bio-oil yield, $Y_{bio-oil}$. In ANOVA analysis, the experimental data are best fitted into a quadratic equation. Model equation of predicted bio-oil yield, Y_B of RMS thermal conversion in term of actual factors is:

$$Y_B = -440.431 + 1.499A + 9.89B + 1.059C - 0.004AB + 0.005AC - 0.060BC - 0.002A^2 - 0.125B^2 - 0.046C^2$$

Optimisation of bio-oil yield was obtained at 480 °C of temperature, 25 L/min of N_2 flow rate of and 24 min of retention time of, with the yield about 56.6 %. Through experimental work conducted based on optimum values, the result obtained was in close agreement with predicted model, which the error only 2.11 %. This indeed confirm and validate the accuracy of the model approach. Overall, the last objective was accomplished where the optimisation model for bio-oil production using RSM with CCD was developed.

Overall findings, it can be concluded that red meranti wood has a potential to be exploited as renewable energy source for the production of bio-oil through fast pyrolysis process technology. By these studies, the optimisation process for bio-oil production and characterisation of extracted bio-oil had been evaluated. Thus, since red meranti is abundantly available as forestry residue and hold potential for sustainable energy resource, its conversion to bio-oil via fast pyrolysis process is regards as technical and economic viability.

5.3   Recommendation for Future Study

Since bio-oil has multiple application and its extracted chemical product has similarity with end-product of fossil fuel, then, research and technology development for the production of bio-oil to replace fossil fuel is very important. Therefore, this study was conducted to evaluate the potential of red meranti wood, which is forestry residue, to produce bio-oil. From the study, it is found that red meranti wood has a huge potential to be exploited to produce bio-oil. However, this study is limited due to time and financial

constraints. Therefore, in the future study, it is proposed that several studies be made further to gain comprehensive understanding and enhance the knowledge about the production bio-oil from red meranti wood or other lignocellulose biomass waste through fast pyrolysis method.

1) Examine the bio-oil production patterns and make comparisons of bio-oil produced from red meranti with other lignocellulose waste sources. With this proposed study, the government's campaign of waste to wealth product is fully realised.

2) Testing the potential of bio-oil produced by applying it directly to a laboratory boiler or heater.

3) Examine the reaction mechanism that occurs within the current biomass chemical structure and after impregnated treatment is carried out. This is because, from this study, it is found that impregnated with $FeSO_4$ has successfully lowered the temperature of cellulose decomposition and further enhances the production of levoglucosan in bio-oil.

5.4   List of Publication

1) Effect of Fast Pyrolysis Operation Conditions on Bio-oil Production of Red Meranti Sawdust. International Conference on Air Quality & Environmental Sustainability (ICAQES 2017)

2) Optimisation of Fast Pyrolysis Conditions of Red Meranti Sawdust on Bio-oil Yield. International Conference on Air Quality & Environmental Sustainability (ICAQES 2017)

3) Effect of Fast Pyrolysis Operating Conditions on Product Yield of Red Meranti Sawdust. International Research Journal of Engineering and Technology. Vol.: 4. Issue: 9.

REFERENCES

Abdullah, N., & Gerhauser, H. (2008). Bio-oil derived from empty fruit bunches. *Fuel*, *87*, 2606–2613. https://doi.org/10.1016/j.fuel.2008.02.011

Abnisa, F., Wan Daud, W.M., & Sahu, J. (2011). Optimization and characterization studies on bio-oil production from palm shell by pyrolysis using response surface methodology. *Biomass and Bioenergy*, *35*(8), 3604–3616. https://doi.org/10.1016/j.biombioe.2011.05.011

Açıkalın, K., Karaca, F., & Bolat, E. (2012). Pyrolysis of pistachio shell: Effects of pyrolysis conditions and analysis of products. *Fuel*, *95*, 169–177. https://doi.org/10.1016/j.fuel.2011.09.037

Adam, J., Blazso, M., Meszaros, E., Stocker, M., Nilsen, M.H., Bouzga, A., Hustad, J.E., Gronli, M., & Oye, G. (2005). Pyrolysis of biomass in the presence of Al-MCM-41 type catalysts. *Fuel*, *84*, 1494–1502. https://doi.org/10.1016/j.fuel.2005.02.006

Agblevor, F.A., Besler, S., & Wiselogel, A.E. (1995). Fast Pyrolysis of Stored Biomass Feedstocks. *Energy & Fuels*, *9*(3), 635–640. https://doi.org/10.1021/ef00052a010

Akhtar, J., & NorAishah, S.A. (2012). A review on operating parameters for optimum liquid oil yield in biomass pyrolysis. *Renewable and Sustainable Energy Reviews*, *16*(7), 5101–5109. https://doi.org/10.1016/j.rser.2012.05.033

Azeez, A.M., Meier, D., Odermatt, J., & Willner, T. (2010). Fast pyrolysis of African and European lignocellulosic biomasses using Py-GC/MS and fluidized bed reactor. *Energy and Fuels*, *24*(3), 2078–2085. https://doi.org/10.1021/ef9012856

Balat, M., Balat, M., Kirtay, E., & Balat, H. (2009). Main routes for the thermo-conversion of biomass into fuels and chemicals. Part 1: Pyrolysis systems. *Energy Conversion and Management*, *50*(12), 3147–3157. https://doi.org/10.1016/j.enconman.2009.08.014

Ballesteros, I., Ballesteros, M., Cara, C., Saez, F., Castro, E., Manzanares, P., Negro, M.J., & Oliva, J.M. (2011). Effect of water extraction on sugars recovery from steam exploded olive tree pruning. *Bioresource Technology*, *102*(11), 6611–6616. https://doi.org/10.1016/j.biortech.2011.03.077

Beis, S.H., Onay, O., & Kockar, O.M. (2002). Fixed-bed pyrolysis of safflower seed: influence of pyrolysis parameters on product yields and compositions. *Renewable Energy*, *26*, 21–32.

Biewer, M.C. (2011). Structure Determination. Retrieved September 5, 2017, from http://www.utdallas.edu/~biewerm/9H-analytical.pdf

Biomass Fuel Analysis For Energy Crop (Closed-Loop) and Wood Derived Fuel/Yardwaste (Open-Loop). (2015). Retrieved April 9, 2015, from http://www.treepower.org/fuels/analysis.html

Blanco López, M.C., Blanco, C.G., Martínez-Alonso, A., & Tascón, J.M.D. (2002). Composition of gases released during olive stones pyrolysis. *Journal of Analytical and Applied Pyrolysis*, *65*(2), 313–322. https://doi.org/10.1016/S0165-2370(02)00008-6

Boroson, M.L., Howard, J.B., Longwell, J. P., & Peters, W.A. (1989). Product yields and kinetics from the vapor phase cracking of wood pyrolysis tars. *AIChE Journal*, *35*(1), 120–128. https://doi.org/10.1002/aic.690350113

Boucher, M.E., Chaala, A., Pakdel, H. & Roy, C. (2000). Bio-oils obtained by vacuum pyrolysis of softwood bark as a l,iquid fuel for gas turbines. Part II: Stability and ageing of bio-oil and its blends with methanol and a pyrolytic aqueous phase. *Biomass and Bioenergy*, *19*(5), 351–361. https://doi.org/10.1016/S0961-9534(00)00044-1

Box, G.E.P., & Wilson, K.B. (1951). On the Experimental Attainment of Optimum Conditions. *Journal of the Royal Statistical Society. Series B (Methodological)*, *13*(1), 1–45.

Bridgwater, A.V., & Bridge, S.A. (1991). A Review of Biomass Pyrolysis and Pyrolysis Technologies. In *Biomass Pyrolysis Liquids. Upgrading and Utilisation* (pp. 11–92). https://doi.org/10.1007/978-94-011-3844-4_2

Bridgwater, A.V., & Peacocke, G.V.C. (1994). Engineering Developments in Fast Pyrolysis for Bio-oil. In *Proceeding Biomass Pyrolysis Oil Properties and Combustion Meeting, NREL* (pp. 110–127).

Bridgwater, A.V., Meier, D., & Radlein, D. (1999). An overview of fast pyrolysis of biomass. *Organic Geochemistry*, *30*(12), 1479–1493. https://doi.org/10.1016/S0146-6380(99)00120-5

Bridgwater, A.V. (1999). Principles and practice of biomass fast pyrolysis processes for liquids. *Journal of Analytical and Applied Pyrolysis*, *51*(1), 3–22. https://doi.org/10.1016/S0165-2370(99)00005-4

Bridgwater, A.V., & Peacocke, G.V.C. (2000). Fast pyrolysis processes for biomass. *Renewable and Sustainable Energy Reviews*, *4*, 1–73.

Bridgwater, A.V. (2012). Review of fast pyrolysis of biomass and product upgrading. *Biomass and Bioenergy*, *38*, 68–94. https://doi.org/10.1016/j.biombioe.2011.01.048

Buckley, T. J. (1991). Calculation of higher heating values of biomass materials and waste components from elemental analyses. *Resources, Conservation and Recycling*, *5*(4), 329–341.

Butler, E., Devlin, G., Meier, D., & McDonnell, K. (2011). A review of recent laboratory research and commercial developments in fast pyrolysis and upgrading. *Renewable and Sustainable Energy Reviews*, *15*(8), 4171–4186. https://doi.org/10.1016/j.rser.2011.07.035

Chaala, A., Ba, T., Garcia-Perez, M., & Roy, C. (2004). Colloidal properties of bio-oils obtained by vacuum pyrolysis of softwood bark: Aging and thermal stability. *Energy and Fuels*, *18*(5), 1535–1542. https://doi.org/10.1021/ef030156v

Chaiwat, W., Hasegawa, I., Kori, J., & Mae, K. (2008). Examination of degree of cross-linking for cellulose precursors pretreated with acid/hot water at low temperature. *Industrial and Engineering Chemistry Research*, *47*(16), 5948–5956. https://doi.org/10.1021/ie800080u

Chang, S.W., & Shaw, J.F. (2009). Biocatalysis for the production of carbohydrate esters. *New Biotechnology*, *26*(3–4), 109–116. https://doi.org/10.1016/j.nbt.2009.07.003

Chiaramonti, D., Oasmaa, A., & Solantausta, Y. (2007). Power generation using fast pyrolysis liquids from biomass. *Renewable and Sustainable Energy Reviews*, *11*(6), 1056–1086. https://doi.org/10.1016/j.rser.2005.07.008

Choi, H.S., Choi, Y.S., & Park, H.C. (2012). Fast pyrolysis characteristics of lignocellulosic biomass with varying reaction conditions. *Renewable Energy*, *42*, 131–135. https://doi.org/10.1016/j.renene.2011.08.049

Cindy, P.C.F., & David, J.L. (1993). Potential Applications and Markets for Biomass-Derived Levoglucosan. In *Advances in Thermochemical Biomass Conversion* (pp. 1484–1494).

Clark, J.H. (2007). Green chemistry for the second generation biorefinery—sustainable chemical manufacturing based on biomass. *JOURNAL OF CHEMICAL TECHNOLOGY & BIOTECHNOLOGY*, *82*(7), 603–609.

Collard, F.X., Blin, J., Bensakhria, A., & Valette, J. (2012). Influence of impregnated metal on the pyrolysis conversion of biomass constituents. *Journal of Analytical and Applied Pyrolysis*, *95*, 213–226. https://doi.org/10.1016/j.jaap.2012.02.009

Collard, F.X., & Blin, J. (2014). A review on pyrolysis of biomass constituents: Mechanisms and composition of the products obtained from the conversion of cellulose, hemicelluloses and lignin. *Renewable and Sustainable Energy Reviews*, *38*, 594–608. https://doi.org/10.1016/j.rser.2014.06.013

Cornerstone Analytical Libraries. (2017). Retrieved November 24, 2017, from http://www.cornerstoneanalytical.com/infrared-spectroscopy/

Coulson, M. (2006). Pyrolysis of Parennial Grasses from Southern Europe. *Pyne Newsletter*, 6–7.

Czernik, S., & Bridgwater, A.V. (2004). Overview of applications of biomass fast pyrolysis oil. *Energy and Fuels*, *18*(2), 590–598. https://doi.org/10.1021/ef034067u

Demirbaş, A. (2000). Mechanisms of liquefaction and pyrolysis reactions of biomass. *Energy Conversion and Management*, *41*(6), 633–646. https://doi.org/10.1016/S0196-8904(99)00130-2

Demirbas, A., & Arin, G. (2002). An Overview of Biomass Pyrolysis. *Energy Sources*, *24*(5), 471–482. https://doi.org/10.1080/00908310252889979

Demirbas, A. (2004). Effect of initial moisture content on the yields of oily products from pyrolysis of biomass. *Journal of Analytical and Applied Pyrolysis*, *71*(2), 803–815. https://doi.org/10.1016/j.jaap.2003.10.008

Demirbaş, A. (2005). Relationship between Initial Moisture Content and the Liquid Yield from Pyrolysis of Sawdust. *Energy Sources*, *27*(9), 823–830. https://doi.org/10.1080/00908310490479042

Di Blasi, C. (2002). Modeling intra- and extra-particle processes of wood fast pyrolysis. *AIChE Journal*, *48*(10), 2386–2397.

Di Blasi, C., Carmen, B., & Antonio, G. (2007). Effects of Diammonium Phosphate on the Yields and Composition of Products from Wood Pyrolysis. *Industrial & Engineering Chemistry Research*, *46*(2), 430–438.

Di Blasi, C., Branca, C., & Galgano, A. (2008). Thermal and catalytic decomposition of wood impregnated with sulfur- and phosphorus-containing ammonium salts. *Polymer Degradation and Stability*, *93*(2), 335–346. https://doi.org/10.1016/j.polymdegradstab.2007.12.003

Dickerson, T., & Soria, J. (2013). Catalytic Fast Pyrolysis: A Review. *Energies*, *6*(1), 514–538. https://doi.org/10.3390/en6010514

Diebold, J.P., & Bridgwater, A.V. (1997). Overview of Fast Pyrolysis of Biomass for the Production of Liquid Fuels. In *Developments in Thermochemical Biomass Conversion* (pp. 5–23). Springer Netherlands. https://doi.org/10.1007/978-94-009-1559-6_1

Eibner, S., Broust, F., Blin, J., & Julbe, A. (2015). Catalytic effect of metal nitrate salts during pyrolysis of impregnated biomass. *Journal of Analytical and Applied Pyrolysis*, *113*, 143–152. https://doi.org/10.1016/j.jaap.2014.11.024

Ellens, C.J., & Brown, R.C. (2012). Optimization of a free-fall reactor for the production of fast pyrolysis bio-oil. *Bioresource Technology*, *103*(1), 374–380. https://doi.org/10.1016/j.biortech.2011.09.087

Eom, I.Y., Kim, K.H., Kim, J.Y., Lee, S.M., Yeo, H.M., Choi, I.G., & Choi, J.W. (2011). Characterization of primary thermal degradation features of lignocellulosic biomass after removal of inorganic metals by diverse solvents. *Bioresource Technology*, *102*(3), 3437–3444. https://doi.org/10.1016/j.biortech.2010.10.056

Eom, I-Y., Kim, J-Y., Kim, T-S., Lee, S-M., Choi, D., Choi, I-G., & Choi, J.-W. (2012). Effect of essential inorganic metals on primary thermal degradation of lignocellulosic biomass. *Bioresource Technology*, *104*, 687–694. https://doi.org/10.1016/j.biortech.2011.10.035

Eric Meier. (2015). *WOOD! Identifying and Using Hundreds of Woods Worldwide*. The Wood Database.

Fahmi, R., Bridgwater, A.V., Darvell, L.I., Jones, J. M., Yates, N., Thain, S., & Donnison, I. S. (2007). The effect of alkali metals on combustion and pyrolysis of Lolium and Festuca grasses, switchgrass and willow. *Fuel*, *86*(10–11), 1560–1569. https://doi.org/10.1016/j.fuel.2006.11.030

Fahmi, R., Bridgwater, A.V., Donnison, I., Yates, N., & Jones, J.M. (2008). The effect of lignin and inorganic species in biomass on pyrolysis oil yields, quality and stability. *Fuel*, *87*(7), 1230–1240. https://doi.org/10.1016/j.fuel.2007.07.026

Fisher, T., Hajaligol, M., Waymack, B., & Kellogg, D. (2002). Pyrolysis behavior and kinetics of biomass derived materials. *Journal of Analytical and Applied Pyrolysis*, *62*(2), 331–349. https://doi.org/10.1016/S0165-2370(01)00129-2

Fratini, E., Bonini, M., Oasmaa, A., Solantausta, Y., Teiseira, J., & Baglioni, P. (2006). SANS analysis of the microstructural evolution during the ageing of pyrolysis oils from biomass. *American Chemical Society*, *22*, 306–312.

Gani, A., & Naruse, I. (2007). Effect of cellulose and lignin content on pyrolysis and combustion characteristics for several types of biomass. *Renewable Energy*, *32*(4), 649–661. https://doi.org/10.1016/j.renene.2006.02.017

Garca-Pèrez, M., Chaala, A., & Roy, C. (2002). Vacuum pyrolysis of sugarcane bagasse. *Journal of Analytical and Applied Pyrolysis*, *65*(2), 111–136. https://doi.org/10.1016/S0165-2370(01)00184-X

Garcia-Perez, M., Chaala, A., Pakdel, H., Kretschmer, D., & Roy, C. (2007). Characterization of bio-oils in chemical families. *Biomass and Bioenergy*, *31*(4), 222–242. Retrieved from http://www.sciencedirect.com/science/article/pii/S0961953406001838

Garcia-Perez, M., Adams, T.T., Goodrum, J.W., Geller, D.P., & Das, K. C. (2007). Production and Fuel Properties of Pine Chip Bio-oil / Biodiesel Blends. *Energy*, (10), 2363–2372.

Garcia-Perez, M., Wang, X.S., Shen, J., Rhodes, M.J., Tian, F., Lee, W., Wu, H., & Li, C. (2008). Fast Pyrolysis of Oil Mallee Woody Biomass: Effect of Temperature on the Yield and Quality of Pyrolysis Products. *Industrial & Engineering Chemistry Research*, *47*(6), 1846–1854. https://doi.org/10.1021/ie071497p

Ghafoori, S. (2013). *Modeling, Simulation and Optimization of Advanced Oxidation Processes for Treatment of Polymeric*. Thesis of Doctor of Philosophy, Program of Chemical Engineering, Toronto, Ontario, Canada.

Goh, C.S., Tan, K.T., Lee, K.T., & Bhatia, S. (2010). Bio-ethanol from lignocellulose: Status, perspectives and challenges in Malaysia. *Bioresource Technology*, *101*(13), 4834–4841. https://doi.org/10.1016/j.biortech.2009.08.080

Gupta, A.K., & Lilley, D.G. (2003). Thermal Destruction of Wastes and Plastics. In *Plastics and Environment* (pp. 629–696). Wiley-Interscience.

Hamelinck, C.N., Van Hooijdonk, G., & Faaij, A.P.C. (2005). Ethanol from lignocellulosic biomass: Techno-economic performance in short-, middle- and long-term. *Biomass and Bioenergy*, *28*(4), 384–410. https://doi.org/10.1016/j.biombioe.2004.09.002

Harinen, S. (2004). *Analysis of the top phase fraction of wood pyrolysis liquids*. University of Jyväskylä.

Heidari, A., Stahl, R., Younesi, H., Rashidi, A., Troeger, N., & Ghoreyshi, A.A. (2014). Effect of process conditions on product yield and composition of fast pyrolysis of Eucalyptus grandis in fluidized bed reactor. *Journal of Industrial and Engineering Chemistry*, *20*(4), 2594–2602. https://doi.org/10.1016/j.jiec.2013.10.046

Heo, H.S., Park, H.J., Yim, J., Sohn, J. M., Park, J., Kim, S., Ryu, C., Jeon, J., & Park, Y. (2010). Influence of operation variables on fast pyrolysis of Miscanthus sinensis var. purpurascens. *Bioresource Technology*, *101*(10), 3672–3677. https://doi.org/10.1016/j.biortech.2009.12.078

Heo, H.S., Park, H.J., Park, Y., Ryu, C., Suh, D.J., Suh, Y., Yim, J., & Kim, S. (2010). Bio-oil production from fast pyrolysis of waste furniture sawdust in a fluidized bed. *Bioresource Technology*, *101 Suppl*(1), S91-6. https://doi.org/10.1016/j.biortech.2009.06.003

Hu, S., Jiang, L., Wang, Y., Su, S., Sun, L., Xu, B., He, L., & Xiang, J. (2015). Effects of inherent alkali and alkaline earth metallic species on biomass pyrolysis at different temperatures. *Bioresource Technology*, *192*, 23–30. https://doi.org/10.1016/j.biortech.2015.05.042

Ingram, L., Mohan, D., Bricka, M., Steele, P., Strobel, D., Crocker, D., Mitchell, B., Mohammad, J., Cantrell, K., & Pittman, C. U. (2008). Pyrolysis of wood and bark in an auger reactor: Physical properties and chemical analysis of the produced bio-oils. *Energy and Fuels*, *22*(1), 614–625. https://doi.org/10.1021/ef700335k

Isahak, W.N.R.W., Hisham, M.W.M., Yarmo, M.A., & Yun Hin, T. (2012). A review on bio-oil production from biomass by using pyrolysis method. *Renewable and Sustainable Energy Reviews*, *16*(8), 5910–5923. https://doi.org/10.1016/j.rser.2012.05.039

Islam, M.N., & Ani, F.N. (1998). Pyrolytic oil from fluidised bed pyrolysis of oil palm shell and its characterisation. *Renewable Energy 06*, *17*, 73–84.

Jendoubi, N., Broust, F., Commandre, J.M., Mauviel, G., Sardin, M., & Lédé, J. (2011). Inorganics distribution in bio oils and char produced by biomass fast pyrolysis: The key role of aerosols. *Journal of Analytical and Applied Pyrolysis*, *92*(1), 59–67. https://doi.org/10.1016/j.jaap.2011.04.007

Jiang, H., Song, L., Cheng, Z., Chen, J., Zhang, L., Zhang, M., Hu, M., Li, J., & Li, J. (2015). Influence of pyrolysis condition and transition metal salt on the product yield and characterization via Huadian oil shale pyrolysis. *Journal of Analytical and Applied Pyrolysis*, *112*, 230–236. https://doi.org/10.1016/j.jaap.2015.01.020

Kan, T., Strezov, & Evans, T.J. (2016). Lignocellulosic biomass pyrolysis: A review of product properties and effects of pyrolysis parameters. *Renewable and Sustainable Energy Reviews*, *57*, 126–1140. https://doi.org/10.1016/j.rser.2015.12.185

Kang, B.S., Lee, K.H., Park, H.J., Park, Y.K., & Kim, J.S. (2006). Fast pyrolysis of radiata pine in a bench scale plant with a fluidized bed: Influence of a char separation system and reaction conditions on the production of bio-oil. *Journal of Analytical and Applied Pyrolysis*, *76*(1–2), 32–37. https://doi.org/10.1016/j.jaap.2005.06.012

Kersten, S.R.A., Van Swaaij, W.P.M., Lefferts, L., & Seshan, K. (2007). Chapter 6. Options for Catalysis in the Thermochemical Conversion of Biomass into Fuels. In *Catalysis for Renewables: from feedstock to Energy Production*. Wiley-VCH.

Kim, S.W., Koo, B.S., Ryu, J.W., Lee, J.S., Kim, C.J., Lee, D.H., Kim, G.R., & Choi, S. (2013). Bio-oil from the pyrolysis of palm and Jatropha wastes in a fluidized bed. *Fuel Processing Technology*, *108*, 118–124. https://doi.org/10.1016/j.fuproc.2012.05.002

Kleen, M., & Gellerstedt, G. (1995). Influence of inorganic species on the formation of polysaccharide and lignin degradation products in the analytical pyrolysis of pulps. *Journal of Analytical and Applied Pyrolysis*, *35*(1), 15–41. https://doi.org/10.1016/0165-2370(95)00893-J

Koenig, J. A. (n.d.). Amount and Concentration : Making and Diluting Solutions. Retrieved December 30, 2015, from http://www.mathcentre.ac.uk/resources/uploaded/module2textbooklike.pdf

Krishna Prasad K., Sangen, E., & Visser, P. (1985). Woodburning Cookstoves. In *Advances in Heat Transfer* (pp. 159–310).

Larson, D. (2008). Biofuel production technologies: Status, prospects and implications for trade and development. *United Nations Conference on Trade and Development*, 1–41.

Lédé, J., Broust, F., Ndiaye, F.T., & Ferrer, M. (2007). Properties of bio-oils produced by biomass fast pyrolysis in a cyclone reactor. *Fuel*, *86*(12–13), 1800–1810. https://doi.org/10.1016/j.fuel.2006.12.024

Lehto, J., Oasmaa, A., Solantausta, Y., Kytö, M., & Chiaramonti, D. (2013). Fuel oil quality and combustion of fast pyrolysis bio-oils. *VTT Publications*, (87), 79. https://doi.org/http://dx.doi.org/10.1016/j.apenergy.2013.11.040

Liew, W.H., Hassim, M.H., & Ng, D.K.S. (2014). Review of evolution, technology and sustainability assessments of biofuel production. *Journal of Cleaner Production*. https://doi.org/10.1016/j.jclepro.2014.01.006

Lu, Q., Li, W-Z., & Zhu, X-F. (2009). Overview of fuel properties of biomass fast pyrolysis oils. *Energy Conversion and Management*, *50*(5), 1376–1383. https://doi.org/10.1016/j.enconman.2009.01.001

Lu, Q., Yang, X-C., Dong, C-Q., Zhang, Z-F., Zhang, X-M., & Zhu, X-F. (2011). Influence of pyrolysis temperature and time on the cellulose fast pyrolysis products: Analytical Py-GC/MS study. *Journal of Analytical and Applied Pyrolysis*, *92*(2), 430–438. Retrieved from http://www.sciencedirect.com/science/article/pii/S0165237011001495

Luo, Z., Wang, S., Liao, Y., Zhou, J., Gu, Y., & Cen, K. (2004). Research on biomass fast pyrolysis for liquid fuel. *Biomass and Bioenergy*, *26*(5), 455–462. https://doi.org/10.1016/j.biombioe.2003.04.001

Lv, D., Xu, M., Liu, X., Zhan, Z., Li, Z., & Yao, H. (2010). Effect of cellulose, lignin, alkali and alkaline earth metallic species on biomass pyrolysis and gasification. *Fuel Processing Technology*, *91*(8), 903–909. https://doi.org/10.1016/j.fuproc.2009.09.014

Malaysia Energy Centre. (2002). Retrieved June 24, 2015, from www.ptm.org.my

Mamleeva, V., Bourbigot, S., Le Bras, M., & Yvon, J. (2009). The facts and hypotheses relating to the phenomenological model of cellulose pyrolysis: Interdependence of the steps. *J. Anal. Appl. Pyrolysis*, *84*(1), 1–17.

Mayer, Z.A., Apfelbacher, A., & Hornung, A. (2012). Effect of sample preparation on the thermal degradation of metal-added biomass. *Journal of Analytical and Applied Pyrolysis*, *94*, 170–176. https://doi.org/10.1016/j.jaap.2011.12.008

153

Mazlan, M.A.F., Uemura, Y., Osman, N.B., & Yusup, S. (2015). Fast pyrolysis of hardwood residues using a fixed bed drop-type pyrolyzer. *Energy Conversion and Management*, *98*, 208–214. https://doi.org/10.1016/j.enconman.2015.03.102

McGrath, T.E., Chan, W.G., & Hajaligol, M.R. (2003). Low temperature mechanism for the formation of polycyclic aromatic hydrocarbons from the pyrolysis of cellulose. *Journal of Analytical and Applied Pyrolysis*, *66*(1–2), 51–70. https://doi.org/10.1016/S0165-2370(02)00105-5

Meier, D. (1999). New methods for chemical and physical characterization and round robin testing. In *Fast Pyrolysis of Bomass: A Handbook*. Newburry: CPL Press.

Meier, S. (2013). Elemental Analysis of Wood Fuels NYSERDA's Promise to New Yorkers: NYSERDA provides resources, expertise and objective information so New Yorkers can make confident, informed energy decisions . *NYSERDA Report 13-13*, (June).

Mekhilef, S., Saidur, R., Safari, A., & Mustaffa, W.E.S.B. (2011). Biomass energy in Malaysia: Current state and prospects. *Renewable and Sustainable Energy Reviews*, *15*(7), 3360–3370. https://doi.org/10.1016/j.rser.2011.04.016

Michael, L.B., Jack, B.H., John, P.L. and William, A.P. (1989). Heterogeneous cracking of wood pyrolysis tars over fresh wood char surfaces. *Energy Fuels*, *3*(6), 735–740.

Michael, H.K., John, N., Christopher, J., & Nachtsheim, W.W. (2011). *No Title* (4th editio). McGraw-Hill Education.

Mofijur, M., Masjuki, H.H., Kalam, M.A., Hazrat, M.A., Liaquat, A.M., Shahabuddin, M., & Varman, M. (2012). Prospects of biodiesel from Jatropha in Malaysia. *Renewable and Sustainable Energy Reviews*, *16*(7), 5007–5020. https://doi.org/10.1016/j.rser.2012.05.010

Mohan, D., Pittman, C.U., & Steele, P.H. (2006). Pyrolysis of Wood/Biomass for Bio-oil: A Critical Review. *Energy & Fuels*, *20*(3), 848–889. https://doi.org/10.1021/ef0502397

Montgomery, D.C. (2012). Design and Analysis of Experiments (8th Editio). John-Wiley & Sons. Inc. Tempe, Arizona.

Morf, P., Hasler, P., & Nussbaumer, T. (2002). Mechanisms and kinetics of homogeneous secondary reactions of tar from continuous pyrolysis of wood chips. *Fuel*, *81*(7), 843–853. Retrieved from http://www.sciencedirect.com/science/article/pii/S0016236101002162

Mourant, D., Wang, Z., He, M., Wang, X.S., Garcia-Perez, M., Ling, K., & Li, C-Z. (2011). Mallee wood fast pyrolysis: Effects of alkali and alkaline earth metallic species on the yield and composition of bio-oil. *Fuel*, *90*(9), 2915–2922. https://doi.org/10.1016/j.fuel.2011.04.033

Mszros, E., Vrhegyi, G., Jakab, E., & Marosvlgyi, B. (2004). Thermogravimetric and Reaction Kinetic Analysis of Biomass Samples from an Energy Plantation Thermogravimetric and Reaction Kinetic Analysis of Biomass Samples from an Energy Plantation. *Review Literature And Arts Of The Americas*, (10), 497–507. https://doi.org/10.1021/ef034030

Mullen, C.A., & Boateng, A.A. (2011). Characterization of water insoluble solids isolated from various biomass fast pyrolysis oils. *Journal of Analytical and Applied Pyrolysis*, *90*(2), 197–203. Retrieved from http://www.sciencedirect.com/science/article/pii/S0165237010001798

Naik, S.N., Goud, V.V., Rout, P.K., & Dalai, A.K. (2010). Production of first and second generation biofuels: A comprehensive review. *Renewable and Sustainable Energy Reviews*, *14*(2), 578–597. https://doi.org/10.1016/j.rser.2009.10.003

Nanda, S., Kozinski, J.A., & Dalai, A. K. (2016). Lignocellulosic biomass: A review of conversion technologies and fuel products. *Current Biochemical Engineering*, *3*(1), 24–36. https://doi.org/10.2174/2213385203666150219232000

Neves, D., Thunman, H., Matos, A., Tarelho, L., & Gómez-Barea, A. (2011). Characterization and prediction of biomass pyrolysis products. *Progress in Energy and Combustion Science*, *37*(5), 611–630. https://doi.org/10.1016/j.pecs.2011.01.001

Ngo, T-A., Kim, J., & Kim, S-S. (2013). Fast pyrolysis of palm kernel cake using a fluidized bed reactor: Design of experiment and characteristics of bio-oil. *Journal of Industrial and Engineering Chemistry*, *19*(1), 137–143. https://doi.org/10.1016/j.jiec.2012.07.015

Nigam, P.S., & Singh, A. (2011). Production of liquid biofuels from renewable resources. *Progress in Energy and Combustion Science*, *37*(1), 52–68. https://doi.org/10.1016/j.pecs.2010.01.003

Nik-Azar, M., Hajaligol, M.R., Sorahbi, M., & Dabir, B. (1996). Mineral matter effects in rapid pyrolysis of beech wood. *Fuel Processing Technology*, *3820*(96), 7–17.

Nowakowski, D.J., Bridgwater, A.V., Elliott, D.C., Meier, D., & de Wild, P. (2010). Lignin fast pyrolysis: Results from an international collaboration. *Journal of Analytical and Applied Pyrolysis*, *88*(1), 53–72. https://doi.org/10.1016/j.jaap.2010.02.009

Nowakowski, D.J., Jones, J.M., Brydson, R.M.D., & Ross, A.B. (2007). Potassium catalysis in the pyrolysis behaviour of short rotation willow coppice. *Fuel*, *86*(15), 2389–2402. https://doi.org/10.1016/j.fuel.2007.01.026

Nurbakhsh Said. (1989). *Thermal Decomposition of Charring Materials*. Michigan State University.

Oasmaa, A., Leppamaki, E., Koponen, P., Levander, J., & Tapola, E. (1997). Physical characterisation of biomass-based pyrolysis liquids application of standard fuel oil analyses. *VTT Publications*, (306). https://doi.org/10.1016/S0140-6701(98)97220-4

Oasmaa, A., & Czernik, S. (1999). Fuel oil quality of biomass pyrolysis oil - State of the art for the end users. *Energy & Fuels*, *13*(4), 914–921. https://doi.org/10.1021/ef980272b

Oasmaa, A., & Peacocke, C. (2001). A guide to physical property characterisation of biomass-derived fast pyrolysis liquids. *VTT Publications*, (450), 2–65.

Oasmaa, A., Kuoppala, E., Gust, S., & Solantausta, Y. (2003). Fast pyrolysis of forestry residue. 1. Effect of extractives on phase separation of pyrolysis liquids. *Energy and Fuels*, *17*(1), 1–12. https://doi.org/10.1021/ef020088x

Oasmaa, A., Kuoppala, E., & Solantausta, Y. (2003). Fast pyrolysis of forestry residue. 2. Physicochemical composition of product liquid. *Energy and Fuels*, *17*(2), 433–443. https://doi.org/10.1021/ef020206g

Oasmaa, A., & Kuoppala, E. (2003). Fast Pyrolysis of Forestry Residue. 3. Storage Stability of Liquid Fuel. *Energy & Fuels*, *17*(4), 1075–1084.

Oasmaa, A., Elliott, D.C., & Muller, S. (2009). Quality control in fast pyrolysis bio-oil production and use. *Environmental Progress and Sustainable Energy*, *28*(3), 404–409. https://doi.org/10.1002/ep.10382

Onay, O. (2007). Influence of pyrolysis temperature and heating rate on the production of bio-oil and char from safflower seed by pyrolysis, using a well-swept fixed-bed reactor. *Fuel Processing Technology*, *88*(5), 523–531. https://doi.org/10.1016/j.fuproc.2007.01.001

Ong, H.C., Mahlia, T.M.I., & Masjuki, H.H. (2011). A review on energy scenario and sustainable energy in Malaysia. *Renewable and Sustainable Energy Reviews*, *15*(1), 639–647. https://doi.org/10.1016/j.rser.2010.09.043

Ortega, J.V., Renehan, A.M., Liberatore, M.W., & Herring, A.M. (2011). Physical and chemical characteristics of aging pyrolysis oils produced from hardwood and softwood feedstocks. *Journal of Analytical and Applied Pyrolysis*, *91*(1), 190–198. https://doi.org/10.1016/j.jaap.2011.02.007

Ozcimen, D., & Karaosmanoglu, F. (2004). Production and characterization of bio-oil and biochar from rapeseed cake. *Renewable Energy*, *29*(5), 779–787.

Park, H.J., Dong, J-I., Jeon, J-K., Park, Y-K., Yoo, K-S., Kim, S-S., Kim, J., & Kim, S. (2008). Effects of the operating parameters on the production of bio-oil in the fast pyrolysis of Japanese larch. *Chemical Engineering Journal*, *143*(1–3), 124–132. https://doi.org/10.1016/j.cej.2007.12.031

Park, H.J., Park, Y-K., Dong, J-I., Kim, J-S., Jeon, J-K., Kim, S-S., Kim, J., Song, B., Park, J., & Lee, K-J. (2009). Pyrolysis characteristics of Oriental white oak: Kinetic study and fast pyrolysis in a fluidized bed with an improved reaction system. *Fuel Processing Technology*, *90*(2), 186–195. https://doi.org/10.1016/j.fuproc.2008.08.017

Part 1: Literature Review and Model Simulations. (2005). In *Biomass Fast Pyrolysis in a Fluidized Bed: Product Cleaning by In-situ Filtration* (pp. 8773–8785).

Radlein, D. (2002). Study of levoglucosan production – a review biomass. In *A Handbook: Fast pyrolysis of biomass. Vol. 2*. Newburry: CPL Press.

Ran Xu. (2010). *Development of advanced technologies for biomass pyrolysis*. (Doctoral Desertation). The University of Western Ontario, London, Ontario.

Rath, J., Wolfinger, M.G., & Stainer, G. (2003). Heat of Wood Pyrolysis. *Fuel*, *82*(1), 81–91.

Raveendran, K., Ganesh, A., & Khilart, K.C. (1995). Influence of mineral matter pyrolysis characteristics on biomass, *74*(12), 1812–1822.

Richards, G. N. and Zheng, G. (1991). Influence of Metal Ion and Salts on the Products from Pyrolysis of Wood: Application to Thermochamical Processing of Newspring and Biomass. *J. Anal. Appl. Pyrolysis*, *21*(1–2), 133–146.

Rowell, R.M. (1984). The Chemistry of Solid Wood.

Scheirs, J., Camino, G., & Tumiatti, W. (2001). Overview of water evolution during the thermal degradation of cellulose. *European Polymer Journal*, *37*(5), 933–942. https://doi.org/10.1016/S0014-3057(00)00211-1

Scott, D.S., Piskorz, J. (1984). The Continuous Flash Pyrolysis of Biomass. *J. Chem. Eng*, *62*(3), 404–412.

Scott, D.S., Majerski, P., Piskorz, J., & Radlein, D. (1999). A second look at fast pyrolysis of biomass—the RTI process. *Journal of Analytical and Applied Pyrolysis*, *51*(1–2), 23–37. https://doi.org/10.1016/S0165-2370(99)00006-6

Scott, D.S., Paterson, L., Piskorz, J., & Radlein, D. (2000). Pretreatment of poplar wood for fast pyrolysis: Rate of cation removal. *Journal of Analytical and Applied Pyrolysis*, *57*(2), 169–176. https://doi.org/10.1016/S0165-2370(00)00108-X

Shafizadeh, F. (1982). Introduction to pyrolysis of biomass. *Journal of Analytical and Applied Pyrolysis*, *3*(4), 283–305.

Shafizadeh, F., Furneaux, R.H., Cochran, T.G., Scholl, J.P., & Sakai, Y. (1979). Production of levoglucosan and glucose from pyrolysis of cellulosic materials. *Journal of Applied Polymer Science*, *23*(12), 3525–3539. https://doi.org/10.1002/app.1979.070231209

Sharma, R.K., Wooten, J.B., Baliga, V.L., Lin, X., Geoffrey Chan, W., & Hajaligol, M. R. (2004). Characterization of chars from pyrolysis of lignin. *Fuel*, *83*(11–12), 1469–1482. https://doi.org/10.1016/j.fuel.2003.11.015

Shen, J., Wang, X-S., Garcia-Perez, M., Mourant, D., Rhodes, M.J., & Li, C-Z. (2009). Effects of particle size on the fast pyrolysis of oil mallee woody biomass. *Fuel*, *88*(10), 1810–1817. https://doi.org/10.1016/j.fuel.2009.05.001

Shen, D.K., Gu, S., & Bridgwater, A.V. (2010). Study on the pyrolytic behaviour of xylan-based hemicellulose using TG-FTIR and Py-GC-FTIR. *Journal of Analytical and Applied Pyrolysis*, *87*(2), 199–206. https://doi.org/10.1016/j.jaap.2009.12.001

Shihadeh A., & H. S. (2002). Impact of Biomass Pyrolysis Oil Process Conditions on Ignition Delay in Compression Ignition Engines. *Energy & Fuels*, *16*(3), 552–561.

Sinha, S., Jhalani, A., Ravi, M. R., & Ray, A. (2000). Modelling of Pyrolysis in Wood : A Review. *Journal of Solar Energy Sosiety of India (SESI)*, *10 (1)*, 41–62.

Sudo, S., Takahashi, F., & Tekeuchi, M. (1989). *Chemical Properties of Biomass*. (A. H. C. W. Kitani, O, Ed.). New York: Gordon and Breach Science.

The Japan Institute of Energy. (2010). Bahagian 7: Situasi biojisim di negara- negara Asia. In *The Asian Biomass Handbook: A Guide for Biomass Production and Utilization* (pp. 200–243).

Tillman, D. A. (1991). *The Combustion of Solid Fuels and Wastes*. ACADEMIC PRESS. INC.

Timber Wood Supply. (2017). Retrieved November 23, 2017, from http://timberwoodsupplymalaysia.com.my/

Tröger, N., Richter, D., & Stahl, R. (2013). Effect of feedstock composition on product yields and energy recovery rates of fast pyrolysis products from different straw types. *Journal of Analytical and Applied Pyrolysis*, *100*, 158–165. https://doi.org/10.1016/j.jaap.2012.12.012

Uzun, B.B., Pütün, A.E., & Pütün, E. (2007). Composition of products obtained via fast pyrolysis of olive-oil residue: Effect of pyrolysis temperature. *Journal of Analytical and Applied Pyrolysis*, *79*(1–2 SPEC. ISS.), 147–153. https://doi.org/10.1016/j.jaap.2006.12.005

Vaca Garcia, C. (2008). Biomaterials. In J. C. and F. Deswarte (Ed.), *Introduction to Chemicals from Biomass*. John-Wiley and Sons, Ltd.

Vamvuka, D. (2011). Bio-oil, solid and gaseous biofuels from biomass pyrolysis processes - An overview. *International Journal of Energy Research*, *35*(10), 835–862.

Van de Velden, M., Baeyens, J., Brems, A., Janssens, B., & Dewil, R. (2010). Fundamentals, kinetics and endothermicity of the biomass pyrolysis reaction. *Renewable Energy*, *35*(1), 232–242. Retrieved from http://www.sciencedirect.com/science/article/pii/S0960148109001803

Várhegyi, G., Grønli, M.G., & Di Blasi, C. (2004). Effects of Sample Origin, Extraction, and Hot-Water Washing on the Devolatilization Kinetics of Chestnut Wood. *Industrial & Engineering Chemistry Research*, *43*(10), 2356–2367. https://doi.org/10.1021/ie034168f

Venderbosch, R.H., & Prins, W. (2011). Fast Pyrolysis. In *Wiley Series in Renewable Resource : Thermochemical Processing of Biomass : Conversion into Fuels, Chemicals and Power*. (pp. 124–156). John Wiley and Sons, Ltd.

Vick, C.B. (2007). Adhesive Bonding of Wood Materials. In U. S. Department ofAgriculture (Ed.), *The Encyclopedia of Wood* (p. 2). Skyhorse Publishing, Inc. Delaware corporation.

Vigouroux, R.Z. (2001). *Pyrolysis of Biomass*. Faculty of Mississipi State University.

Wang, X., Kersten, S.R.A., Prins, W., Van Swaaij, & Wim, P.M. (2005). Biomass Pyrolysis in a Fluidized Bed Reactor. Part 2: Experimental Validation of Model Results. *Ind. Eng. Chem. Res.*, *44*(23), 8786–8795. https://doi.org/10.1021/ie050486y

Wang, K., Zhang, J., Shanks, B.H., & Brown, R.C. (2015). The deleterious effect of inorganic salts on hydrocarbon yields from catalytic pyrolysis of lignocellulosic biomass and its mitigation. *Applied Energy*, *148*, 115–120. https://doi.org/10.1016/j.apenergy.2015.03.034

Wang, P., Zhan, S., Yu, H., Xue, X., & Hong, N. (2010). The effects of temperature and catalysts on the pyrolysis of industrial wastes (herb residue). *Bioresource Technology*, *101*(9), 3236–3241. https://doi.org/10.1016/j.biortech.2009.12.082

Water and Energy Consumer Association of Malaysia. (2009). Retrieved June 24, 2015, from www.ptm.org.my/cabd/pdf/GreenTechnologyWaterEnergySector.pdf

Wei, L., Xu, S., Zhang, L., Zhang, H., Liu, C., Zhu, H., & Liu, S. (2006). Characteristics of fast pyrolysis of biomass in a free fall reactor. *Fuel Processing Technology*, *87*(10), 863–871. https://doi.org/10.1016/j.fuproc.2006.06.002

Wildschut, J. (2009). Chapter 1: An Introduction to the Hydroprocessing of Biomass Derived Pyrolysis oil. In *Pyrolysis oil upgrading to transportation fuels by catalytic hydrotreatment.* (pp. 5–9). University of Groningen. Retrieved from http://www.rug.nl/research/portal

Xiu, S., & Shahbazi, A. (2012). Bio-oil production and upgrading research: A review. *Renewable and Sustainable Energy Reviews*, *16*(7), 4406–4414. https://doi.org/10.1016/j.rser.2012.04.028

Xu, J., Jiang, J., Chen, J., & Sun, Y. (2010). Biofuel production from catalytic cracking of woody oils. *Bioresource Technology*, *101*(14), 5586–5591. https://doi.org/10.1016/j.biortech.2010.01.148

Yang, H., Yan, R., Chen, H., Lee, D.H., & Zheng, C. (2007). Characteristics of hemicellulose, cellulose and lignin pyrolysis. *Fuel*, *86*(12–13), 1781–1788. https://doi.org/10.1016/j.fuel.2006.12.013

Zafar, S. (2011). Biomass Energy in Malaysia. Retrieved April 23, 2015, from http://cleantechsolutions.wordpress.com/2011/07/15

Zafar, S. (2015). Biomass Resources in Malaysia. Retrieved June 26, 2015, from http://www.bioenergyconsult.com/biomass-energy-malaysia/

Zaror, C.A., & Pyle, D.L. (1982). The pyrolysis of biomass: A general review. *Proceedings of the Indian Academy of Science (Engg. Sci.)*, *5*(December), 269–285.

Zhang, L., Liu, R., Yin, R., & Mei, Y. (2013). Upgrading of bio-oil from biomass fast pyrolysis in China: A review. *Renewable and Sustainable Energy Reviews*, *24*, 66–72. https://doi.org/10.1016/j.rser.2013.03.027

Zhang, J. (1996). *Pyrolysis of Biomass*. Thesis of Master Degree of Science, Chemical Engineering, Mississippi State University.

Zhang, Q., Chang, J., Wang, T., & Xu, Y. (2007). Review of biomass pyrolysis oil properties and upgrading research. *Energy Conversion and Management*, *48*(1), 87–92. https://doi.org/10.1016/j.enconman.2006.05.010

APPENDIX A

Particles size distribution

Table A1:   Particles size analysis

Sieve Size (mm)	Particle size (mm)	Mass of Sawdust (g)	Percent mass retained (%)	Percent cumulative retained (%)	Percent Passing (%)
4.00	> 4.00	1.46	0.73	0.73	99.27
2.00	2.00 - 4.01	4.53	2.27	3.00	97.01
1.18	1.18 - 2.00	24.27	12.14	15.13	84.87
0.60	0.6 - 1.18	94.00	47.00	62.13	37.87
0.15	0.15 - 0.06	68.13	34.07	96.20	3.81
0.01	0.00 - 0.15	7.60	3.80	100.00	0.01
		199.99	100.00		

APPENDIX B

Preparation of diluted 1.0 and 2.0 Molar of HCl from 37% w/w of HCl

From chemical and physical data:

Density of 37% w/w $HCl_{(aq)}$ =		1.19 kg L^{-1} @ 1.19 g mL^{-1}
Molecular weight of HCl	=	36.5 g mol^{-1}

Percent concentration to molar conversion:

% w/w to w/v of HCl	=	37% HCl x 1.19 g mL^{-1}
	=	0.44 g mL^{-1} HCl
w/v to mol/v	=	0.44 g mL^{-1} / 36.5 g mol^{-1}
	=	0.012 mol mL^{-1}
	=	12 mol L^{-1}

Concentrated 37% of HCl is equivalent to 12 M @ mol L^{-1}. Therefore, diluted 1.0 M and 2.0 M of HCl from concentrated HCl was prepared by:

- 1 M HCl: add 1 mol/12 M = 83 mL concentration HCl to 1L of distilled water or 8.3 mL to 100 mL.
- 2 M HCl: add 2 mol/12 M = 167 mL concentration HCl to 1L of distilled water or 16.7 mL to 100 mL.

Preparation of metal salts solution

        Metal salt solutions were prepared based on the example below. Amount of metal salt dissolved in distilled water was calculated using the Eq. (3.1) and (3.2) (Koenig, n.d.), and was listed in Table B1.

Example:

Preparation 0.1 Molar of bentonite:

$$Concentration\ (M) = \frac{Amount\ (in\ mol)}{Volume\ (in\ L)} \qquad (3.1)$$

$$Amount\ (in\ mol) = 0.1\ M\ x\ 1L\ =\ 0.1\ mol\ of\ bentonite$$

Molecular mass of bentonite = 360.31 g/mol

$$Amount\ (in\ mol) = \frac{Amount\ (in\ g)}{Molar\ mass\ (in\ g/mol)} \qquad (3.2)$$

$$Amount\ (in\ g) = 0.1\ mol\ x\ 360.31\ g/mol\ =\ 36.01\ g$$

        Therefore, 0.1 M solution was prepared by mixed 36.01 g of bentonite with around 800 ml of distilled water in volumetric flask. Once bentonite was dissolved completely, distilled water was added until the solution achieves the final volume of 1000 ml.

Table B1:   Amount of metal salt (in g) dissolved for 0.1 M solution preparation

No.	Chemical	Chemical composition	Molecular mass ($g\ mol^{-1}$)	Mass of chemical dissolved (g)
1.	$CaCl_2$ anhydrous	$CaCl_2$	110.99	11.10
2.	$CaSO_4$ dihydrate	$CaSO_4.2H_2O$	172.17	17.22
3.	$FeCl_2$ tetrahydrate	$FeCl_2.4H_2O$	198.81	19.89
4.	$FeSO_4$ heptahydrate	$FeSO_4.7H_2O$	278.01	27.80

APPENDIX C

Pyrolytic product calculation

$$Yield\ (wt.\ \%) = \frac{Liquid\ product\ (g)}{Feedstock\ (g)} \times 100\%$$

Example Run 1: RMS weight subjected to pyrolysis process = 50.00 ± 0.10 g

i)   Bio-oil yield (wt. %):

$$Averange\ bio-oil\ yield\ (g) = \frac{11.01 + 10.44 + 10.78\ (g)}{3} \times 100\ \%$$
$$= 10.74\ g$$

$$Bio-oil\ yield\ (wt.\%) = \frac{10.74\ (g)}{50.00\ (g)} \times 100\ wt.\% = 21.48\ wt.\%$$

ii)   Char yield (wt. %):

$$Averange\ char\ yield\ (g)\quad = \frac{20.85 + 21.11 + 21.30\ (g)}{3} \times 100\ \%$$
$$= 21.09\ g$$

$$Char\ yield\ (wt.\%) = \frac{21.09\ (g)}{50.00\ (g)} \times 100\ wt.\% = 42.13\ wt.\%$$

iii)   Gases released (wt. %):

$$Gases\ released\ (wt.\%) = 100 - bio-oil\ yield - char\ yield$$
$$= 100 - 21.48 - 42.13$$
$$= 36.34\ wt.\%$$

165

APPENDIX D

Result of pyrolytic product yield

Table D1: Fast pyrolysis condition experiment

Run	Temperature (°C)	Gas flow rate (L/min)	Retention time (min)	Average feed size (mm)	Bio-oil (wt.%)	Char (wt.%)	NCG (wt.%)
	Parameter process				**Pyrolytic product**		
1	350	20	20	0.30	21.48 ± 0.57	42.18 ± 0.45	36.34
2	400	20	20	0.30	40.90 ± 1.07	31.49 ± 1.31	27.61
3	450	20	20	0.30	52.42 ± 0.71	21.31 ± 0.82	26.22
4	500	20	20	0.30	51.87 ± 0.54	18.25 ± 0.74	29.89
5	550	20	20	0.30	48.79 ± 1.19	17.00 ± 0.69	34.21
6	600	20	20	0.30	44.33 ± 1.17	16.13 ± 0.40	39.55
7	450	5	20	0.30	5.50 ± 0.22	31.54 ± 0.62	62.96
8	450	10	20	0.30	25.28 ± 0.73	26.98 ± 0.82	47.74
9	450	15	20	0.30	41.23 ± 1.35	23.57 ± 0.85	35.21
10	450	20	20	0.30	52.42 ± 0.71	21.31 ± 0.82	26.27
11	450	25	20	0.30	56.33 ± 1.10	20.16 ± 0.49	23.51
12	450	30	20	0.30	55.55 ± 1.22	20.25 ± 0.39	26.21
13	450	25	10	0.30	38.32 ± 0.75	22.85 ± 0.58	38.83
14	450	25	20	0.30	56.33 ± 1.10	20.16 ± 0.49	23.51
15	450	25	30	0.30	56.29 ± 0.92	17.23 ± 0.72	26.48
16	450	25	40	0.30	56.31 ± 0.81	16.55 ± 0.52	27.14
17	450	25	20	0.30	56.33 ± 1.10	20.16 ± 0.49	23.51
18	450	25	20	0.89	55.03 ± 1.94	22.49 ± 0.80	22.49
19	450	25	20	1.59	51.43 ± 1.40	25.17 ± 0.74	23.40

Table D2: Fast pyrolysis experiment of raw and washed RMS feedstock

Temperature (°C)	Feedstock								
	Raw RMS			RMS - DI water			RMS - 1.0 M HCl		
	Bio-oil (wt.%)	Char (wt.%)	NCG (wt.%)	Bio-oil (wt.%)	Char (wt.%)	NCG (wt.%)	Bio-oil (wt.%)	Char (wt.%)	NCG (wt.%)
350	22.51 ± 0.76	40.99 ± 1.66	36.5	22.72 ± 0.94	43.98 ± 1.80	33.3	22.57 ± 0.90	44.29 ± 0.70	33.15
400	42.88 ± 1.22	30.25 ± 1.32	26.87	43.5 ± 1.34	27.85 ± 1.26	28.65	44.46 ± 0.56	27.27 ± 0.96	28.27
450	54.99 ± 1.30	21.43 ± 1.02	23.59	57.23 ± 1.48	19.87 ± 0.64	22.91	57.32 ± 0.68	19.11 ± 0.90	22.57
500	54.52 ± 1.18	17.03 ± 0.72	28.45	56.41 ± 1.24	14.35 ± 0.64	29.24	56.57 ± 1.08	13.73 ± 0.44	28.69
550	49.73 ± 0.70	15.79 ± 0.68	34.48	51.25 ± 1.64	12.73 ± 0.70	36.03	51.71 ± 0.94	12.34 ± 0.36	35.95
600	46.47 ± 0.58	14.93 ± 0.52	38.59	47.33 ± 1.56	11.45 ± 0.46	41.23	47.11 ± 0.66	11.32 ± 0.42	41.57

Table D3:   Fast pyrolysis experiment of raw and impregnated RMS feedstock

Temperature (°C)	Control			RMS - $CaCl_2$			RMS - $CaSO_4$			RMS - $FeCl_2$			RMS - $FeSO_4$		
	Bio-oil (wt.%)	Char (wt.%)	NCG (wt.%)	Bio-oil (wt.%)	Char (wt.%)	NCG (wt.%)	Bio-oil (wt.%)	Char (wt.%)	NCG (wt.%)	Bio-oil (wt.%)	Char (wt.%)	NCG (wt.%)	Bio-oil (wt.%)	Char (wt.%)	NCG (wt.%)
350	22.72 ± 0.94	43.98 ± 1.80	33.3	28.87 ± 0.81	41.30 ± 1.03	29.83	25.24 ± 1.12	44.21 ± 1.26	34.55	27.07 ± 1.09	41.90 ± 1.28	31.03	34.85 ± 1.00	40.21 ± 0.68	20.95
400	43.5 ± 1.34	27.85 ± 1.26	28.65	39.90 ± 0.75	30.33 ± 2.01	29.77	45.08 ± 1.15	27.21 ± 1.02	25.71	42.90 ± 1.19	30.83 ± 0.92	26.27	45.34 ± 1.06	27.41 ± 1.21	27.25
450	57.23 ± 1.48	19.87 ± 0.64	22.91	51.31 ± 1.20	25.21 ± 0.89	23.47	58.25 ± 0.99	16.79 ± 0.73	24.35	57.08 ± 1.15	20.13 ± 0.88	22.79	57.21 ± 1.07	23.63 ± 1.08	19.15
500	56.41 ± 1.24	14.35 ± 0.64	29.24	51.09 ± 1.63	24.11 ± 1.19	24.81	57.88 ± 1.01	15.13 ± 0.67	26.99	56.38 ± 0.68	17.13 ± 0.69	26.49	57.79 ± 0.88	18.87 ± 0.84	23.34
550	51.25 ± 1.64	12.73 ± 0.70	36.03	45.86 ± 1.44	23.51 ± 0.94	30.63	54.90 ± 1.62	13.18 ± 0.52	34.25	51.89 ± 1.52	15.62 ± 0.71	32.49	52.43 ± 0.76	14.80 ± 0.68	32.77
600	47.33 ± 1.56	11.45 ± 0.46	41.23	43.07 ± 1.26	22.23 ± 0.86	34.71	52.13 ± 1.64	11.63 ± 0.52	40.17	48.77 ± 0.98	14.21 ± 0.39	38.02	49.41 ± 2.00	12.91 ± 0.64	37.69

Bio-oil compound of impregnated RMS

Table E1:   Bio-oil compounds of RMS – CaCl$_2$

Compound	Percent Area	Molecular weight	Chemical Formula
Phenolic			
Phenol, 2-methoxy-	2.40	124.14	C$_7$H$_8$O$_2$
2-Methoxy-5-methylphenol	5.24	138.16	C$_8$H$_{10}$O$_2$
Phenol, 2,6-dimethoxy-	2.95	154.16	C$_8$H$_{10}$O$_3$
Vanillin	1.32	152.15	C$_8$H$_8$O$_3$
Phenol, 2-methoxy-4-(1-propenyl)-,(Z)-	2.58	164.20	C$_{10}$H$_{12}$O$_2$
Phenol, 2-methoxy-4-propyl-	0.9	166.22	C$_{10}$H$_{14}$O$_2$
Ethanone, 1-(3-hydroxy-4-methoxyphenyl)-	1.1	166.17	C$_9$H$_{10}$O$_3$
Phenol, 2,6-dimethoxy-4-(2-propenyl)-	15.8	194.23	C$_{11}$H$_{14}$O$_3$
Ethanone, 1-(4-hydroxy-3,5-dimethoxyphenyl)-	1.75	196.20	C$_{10}$H$_{12}$O$_4$
1-Butanone, 1-(2,4,6-trihydroxy-3-methylphenyl)-	2.62	210.23	C$_{11}$H$_{14}$O$_4$
Aldehyde, ketone, acid and alcohol			
4-Fluoro-3-methylanizole	1.07	140.16	C$_8$H$_9$FO
Benzoic acid, 4-hydroxy-3-methoxy-	6.72	168.15	C$_8$H$_8$O$_4$
1,1'-Biphenyl, 2-ethyl-	1.04	182.26	C$_{14}$H$_{14}$
Homovanillyl alcohol	1.09	168.19	C$_9$H$_{12}$O$_3$
2,3,5,6-Tetrafluoroanisole	2.03	180.10	C$_7$H$_4$F$_4$O
Benzaldehyde, 4-hydroxy-3,5-dimethoxy-	9.14	182.17	C$_9$H$_{10}$O$_4$
2-Propenal, 3-(4-hydroxy-3-methoxyphenyl)-	0.48	178.19	C$_{10}$H$_{10}$O$_3$
Diphenylmethane	0.1	168.23	C$_{13}$H$_{12}$
3,5-Dimethoxy-4-hydroxycinnamaldehyde	0.3	208.21	C$_{11}$H$_{12}$O$_4$
Phenylacetylformic acid, 4-hydroxy-3-methoxy-	0.15	210.23	C$_{11}$H$_{14}$O$_4$
Benzoic acid, 3-nitro-	0.1	167.12	C$_7$H$_5$NO$_4$
2-[p-(Adamantyl-1)phenoxy]ethanol	0.86	272.39	C$_{18}$H$_{24}$O$_2$
Anhydrosugar			
.beta.-D-Glucopyranose, 1,6-anhydro-	23.88	162.14	C$_6$H$_{10}$O$_5$
D-Allose	2.06	180.16	C$_6$H$_{12}$O$_6$

Table E2:   Bio-oil compounds of RMS - $CaSO_4$

Compound	Percent Area	Molecular weight	Chemical Formula
Phenolic			
Phenol, 2-methoxy-	2.41	124.14	$C_7H_8O_2$
Creosol	4.9	138.16	$C_8H_{10}O_2$
2-Methoxy-4-vinylphenol	2.4	150.18	$C_9H_{10}O_2$
Phenol, 2,6-dimethoxy-	2.41	154.16	$C_8H_{10}O_3$
Vanillin	1.14	152.15	$C_8H_8O_3$
Phenol, 2-methoxy-4-(1-propenyl)-	2.26	164.20	$C_{10}H_{12}O_2$
Phenol, 2-methoxy-4-propyl-	1.86	166.22	$C_{10}H_{14}O_2$
Ethanone, 1-(3-hydroxy-4-methoxyphenyl)-	0.87	166.17	$C_9H_{10}O_3$
Phenol, 2,6-dimethoxy-4-(2-propenyl)-	27.32	194.23	C11H14O3
2-Pentanone, 1-(2,4,6-trihydroxyphenyl)	3.2	210.23	$C_{11}H_{14}O_4$
Aldehyde, ketone, acid and alcohol			
3-Cyclobutene-1,2-dione, 3,4-dihydroxy-	2.22	114.06	$C_4H_2O_4$
4-Fluoro-3-methylanizole	0.75	140.16	C_8H_9FO
Benzoic acid, 4-hydroxy-3-methoxy-	6.81	168.15	$C_8H_8O_4$
1,1'-Biphenyl, 2-ethyl-	0.89	182.26	$C_{14}H_{14}$
Homovanillyl alcohol	1.15	168.19	$C_9H_{12}O_3$
2,3,5,6-Tetrafluoroanisole	2.56	180.10	$C_7H_4F_4O$
Benzaldehyde, 4-hydroxy-3,5-dimethoxy-	6.01	182.17	$C_9H_{10}O_4$
8-Methoxy-[1,2,4]triazolo[4,3-a]pyridine-3-thiol	0.95	181.22	$C_7H_7N_3OS$
3,5-Dimethoxy-4-hydroxycinnamaldehyde	0.25	208.21	$C_{11}H_{12}O_4$
Ethyl homovanillate	0.22	210.23	$C_{11}H_{14}O_4$
Anhydrosugar			
1,6-anhydro-.beta.-D-Glucopyranose,	16.55	162.14	$C_6H_{10}O_5$
Furan			
5-Acetyl-2-furanmethanol	0.48	140.14	$C_7H_8O_3$

Table E3:   Bio-oil compounds of RMS - FeCl$_2$

Compound	Percent Area	Molecular weight	Chemical Formula
Phenolic			
Phenol, 2-methoxy-	1.95	124.14	C$_7$H$_8$O$_2$
2-Methoxy-4-vinylphenol	6.719	150.18	C$_9$H$_{10}$O$_2$
Phenol, 2,6-dimethoxy-	3.4713	154.16	C$_8$H$_{10}$O$_3$
Vanillin	1.9529	152.15	C$_8$H$_8$O$_3$
Creosol	5.95	138.16	C$_8$H$_{10}$O$_2$
Phenol, 2-methoxy-4-(1-propenyl)-, (Z)-	4.5072	164.20	C$_{10}$H$_{12}$O$_2$
Phenol, 2,6-dimethoxy-	1.43	154.16	C$_8$H$_{10}$O$_3$
Vanillin	0.87	152.15	C$_8$H$_8$O$_3$
Phenol, 2-methoxy-4-propyl-	1.48	166.22	C$_{10}$H$_{14}$O$_2$
Phenol, 2,6-dimethoxy-4-(2-propenyl)-	13.72	194.23	C$_{11}$H$_{14}$O$_3$
Ethanone, 1-(4-hydroxy-3,5-dimethoxyphenyl)-	0.8	196.20	C$_{10}$H$_{12}$O$_4$
Aldehyde, ketone, acid and alcohol			
3-Cyclobutene-1,2-dione, 3,4-dihydroxy-	1.22	114.06	C$_4$H$_2$O$_4$
1,2-Benzenediol	2.2982	110.11	C$_6$H$_6$O$_2$
1-(4-Hydroxymethylphenyl)ethanone	0.55	150.17	C$_9$H$_{10}$O$_2$
1,2,3-Trimethoxybenzene	3.93	168.19	C$_9$H$_{12}$O$_3$
1-Oxaspiro[2.5]octane, 2,4,4-trimethyl-8-methylene-	0.67	166.26	C$_{11}$H$_{18}$O
3-Isopropyl-1-methyl-4-methylamino-pyrrole-2,5-dione	0.28	182.22	C$_9$H$_{14}$N$_2$O$_2$
Homovanillyl alcohol	0.69	168.19	C$_9$H$_{12}$O$_3$
1-Nitro-1-deoxy-d-glycero-l-mannoheptitol	1.9743	241.20	C$_7$H$_{15}$NO$_8$
2,3,5,6-Tetrafluoroanisole	2.1	180.10	C$_7$H$_4$F$_4$O
4-Methoxy-4',5'-methylenedioxybiphenyl-2-carboxylic acid	1.8902	272.26	C$_{15}$H$_{12}$O$_5$
Dibenzo[e,g]benzimidazole, 2-(2-furyl)-3-methyl-	0.4461	298.35	C$_{20}$H$_{14}$N$_2$O
Benzaldehyde, 4-hydroxy-3,5-dimethoxy-	4.52	182.17	C$_9$H$_{10}$O$_4$
2-Propenal, 3-(4-hydroxy-3-methoxyphenyl)-	0.37	178.19	C$_{10}$H$_{10}$O$_3$
3,4-Dimethoxy-6-amino toluene	1.66	167.21	C$_9$H$_{13}$NO$_2$
Thiazolo[3,2-a]pyridinium, 2,3-dihydro-8-hydroxy-2,5-dimethyl-, hydroxide, inner salt	0.33	182.26	C$_9$H$_{12}$NOS
Anhydrosugar			
1,6-anhydro- beta.-D-Glucopyranose,	16.64	162.14	C$_6$H$_{10}$O$_5$
D-Allose	2.35	180.16	C$_6$H$_{12}$O$_6$
Furan			
5-Acetyl-2-furanmethanol	1.47	140.14	C$_7$H$_8$O$_3$

Table E4:   Bio-oil compounds of RMS - FeSO$_4$

Compound	Percent Area	Molecular weight	Chemical Formula
Phenolic			
Creosol	4.32	138.16	$C_8H_{10}O_2$
Phenol, 2,6-dimethoxy-	1.23	154.16	$C_8H_{10}O_3$
Vanillin	1.01	152.15	$C_8H_8O_3$
Phenol, 2-methoxy-4-(1-propenyl)-,(Z)-	1.54	164.20	$C_{10}H_{12}O_2$
Phenol, 2-methoxy-4-propyl-	1.57	166.22	$C_{10}H_{14}O_2$
Ethanone, 1-(3-hydroxy-4-methoxyphenyl)-	0.82	166.17	$C_9H_{10}O_3$
Phenol, 2,6-dimethoxy-4-(2-propenyl)-	16.74	194.23	$C_{11}H_{14}O_3$
1-Butanone, 1-(2,4,6-trihydroxy-3-methylphenyl)-	1.88	210.23	$C_{11}H_{14}O_4$
Aldehyde, ketone, acid and alcohol			
3-Cyclobutene-1,2-dione, 3,4-dihydroxy-	0.2	114.06	$C_4H_2O_4$
1-(4-Hydroxymethylphenyl)ethanone	0.7	150.17	$C_9H_{10}O_2$
3-Amino-4-methoxybenzoic acid	0.37	166.15	$C_8H_8NO_3$
Homovanillyl alcohol	0.83	168.19	$C_9H_{12}O_3$
2,3,5,6-Tetrafluoroanisole	1.94	180.10	$C_7H_4F_4O$
Benzaldehyde,4-hydroxy-3,5-dimethoxy-	8.31	182.17	$C_9H_{10}O_4$
2-Propenal, 3-(4-hydroxy-3-methoxyphenyl)-	0.78	178.19	$C_{10}H_{10}O3$
3,5-Dimethoxy-4-hydroxycinnamaldehyde	0.34	208.21	$C_{11}H_{12}O_4$
4-Methoxy-4',5'-methylenedioxybiphenyl-2-carboxylic acid	0.67	272.25	$C_{15}H_{12}O_5$
Anhydrosugar			
1,6-anhydro-.beta.-D-Glucopyranose,	40.23	162.14	$C_6H_{10}O_5$
D-Allose	2.01	180.16	$C_6H_{12}O_6$
Furan			
2-Furanmethanol	0.45	98.10	$C_5H_6O_2$